Genomics link obesity and type 2 diabetes to Alzheimer's disease to unveil novel biological insights

César Cunha[1], Mario Garcia-Ureña[1], Raquel Martínez[1], María José Romero-Lado[1], Maria Victoria Fernandez[2], Ole A. Andreassen[3,4,5], Rebecca Sims[6], Magda Tsolaki[7], Kristel Sleegers[8,9], Mikko Hiltunen[10], Gaël Nicolas[11], Pascual Sánchez-Juan[12,13], Martin Ingelsson[14-16], Vilmantas Giedraitis[17], Roberta Ghidoni[18], Henne Holstege[19-23], Cornelia van Duijn[24,25], Sven van der Lee[19,21,22], Alfredo Ramirez[26-30], Céline Bellenguez[31], Jean-Charles Lambert[31], Ruth Frikke-Schmidt[32,33], EADB, Tuomas O. Kilpeläinen[1], Ruth J.F. Loos[1]

[1]Novo Nordisk Foundation Center for Basic Metabolic Research, University of Copenhagen, Denmark
[2]Ace Alzheimer Center Barcelona, Universitat Internacional de Catalunya (UIC), Barcelona, Spain
[3]Centre for Precision Psychiatry, Institute of Clinical Medicine, University of Oslo, Oslo, Norway
[4]Division of Mental Health and Addiction, Oslo University Hospital, Oslo, Norway
[5]KG Jebsen Centre for Neurodevelopmental disorders, University of Oslo, Oslo, Norway
[6]Division of Psychological Medicine and Clinical Neuroscience, School of Medicine, Cardiff University, Wales, UK
[7]Aristotle University of Thessaloniki, Greece
[8]VIB Center for Molecular Neurology, VIB, Antwerp, Belgium
[9]Department of Biomedical Sciences, University of Antwerp, Antwerp, Belgium
[10]Institute of Biomedicine, University of Eastern Finland, Yliopistoranta 1E, 70211 Kuopio, Finland
[11]Univ Rouen Normandie, Normandie Univ, Inserm U1245 and CHU Rouen, Department of Genetics and Reference Center for Developmental Disorders, Rouen, France.
[12]Alzheimer's Centre Reina Sofia-CIEN Foundation, Madrid, Spain.
[13]CIBERNED, Network Center for Biomedical Research in Neurodegenerative Diseases, National Institute of Health Carlos III, Madrid, Spain
[14]Department of Public Health and Caring Sciences, Molecular Geriatrics, Rudbeck Laboratory, Uppsala University, Uppsala, Sweden
[15]Krembil Brain Institute, University Health Network, Toronto, Ontario, Canada
[16]Tanz Centre for Research in Neurodegenerative Diseases, Departments of Medicine and Laboratory Medicine & Pathobiology, University of Toronto, Toronto, Ontario, Canada
[17]Department of Public Health and Caring Sciences, Clinical Geriatrics, Uppsala University, Uppsala, Sweden
[18]Molecular Markers Laboratory, IRCCS Istituto Centro San Giovanni di Dio Fatebenefratelli, Brescia, Italy
[19]Genomics of Neurodegenerative Diseases and Aging, Human Genetics, Vrije Universiteit Amsterdam,
[20]Amsterdam UMC location VUmc, Amsterdam, The Netherlands
[21]Alzheimer Center Amsterdam, Neurology, Vrije Universiteit Amsterdam, Amsterdam UMC location VUmc, Amsterdam, The Netherlands.
[22]Amsterdam Neuroscience, Neurodegeneration, Amsterdam, The Netherlands
[23]VIB Center for Brain and Disease Research, ON5 Herestraat 49 - box 602, 3000 Leuven, Belgium
Department of Neurosciences, Leuven Brain Institute, KU Leuven, Leuven, Belgium.
[24]Department of Epidemiology, ErasmusMC, Rotterdam, The Netherlands
[25]Nuffield Department of Population Health Oxford University, Oxford, UK
[26]Division of Neurogenetics and Molecular Psychiatry, Department of Psychiatry and Psychotherapy, Faculty of Medicine and University Hospital Cologne, University of Cologne, Cologne, Germany
[27]Department for Cognitive Disorders and Old Age Psychiatry, University Hospital Bonn, Bonn, Germany.
[28]Department of Psychiatry & Glenn Biggs Institute for Alzheimer's and Neurodegenerative Diseases, San Antonio, TX, USA
[29]German Center for Neurodegenerative Diseases (DZNE), Bonn, Germany
[30]CECAD
[31]Université de Lille, Inserm, CHU Lille, Institut Pasteur de Lille, Lille, France.
[32]Department of Clinical Biochemistry, Copenhagen University Hospital - Rigshospitalet, Blegdamsvej 9, 2100 Copenhagen, Denmark
[33]Department of Clinical Medicine, Faculty of Health and Medical Sciences, University of Copenhagen, Blegdamsvej 3B, 2100 Copenhagen, Denmark

KEYWORDS

Alzheimer's disease; Obesity; Type 2 diabetes; Shared genomics

ABSTRACT

Body mass index (BMI), type 2 diabetes (T2D) and associated cardiometabolic features modify Alzheimer's disease (AD) risk, yet shared mechanisms remain poorly understood. Using sex- and age-stratified genotyping data for BMI and T2D, we investigate how these traits converge on shared genetic pathways to AD risk. Employing multi-trait, machine learning and single-cell transcriptomics, we identify sex-specific cardiometabolic liability linked to higher BMI-associated risk in women and T2D-driven risk in men. Variant-level analyses reveal AD risk associates with genetically-driven hypotension and hypoglycaemia. We identify 35 putative effector genes in seven independent loci colocalizing between BMI/T2D and AD, mapping to peripheral immune and metabolic tissues and cell-types. Pathway enrichment identifies druggable targets in calcium and potassium channel signaling. Across 81 approved drugs modulating shared risk genes, levosimendan - a calcium sensitizer for heart failure - inhibits tau oligomerization and emerges as a repurposing candidate. These findings elucidate sex-specific cardiometabolic drivers of AD, identify actionable biological pathways, and reveal drug candidates for AD prevention and treatment.

.

INTRODUCTION

Late-onset Alzheimer's disease (AD) is a devastating disorder that affects patients and families alike. AD is the leading form of dementia[1], an umbrella term encompassing multiple diseases that progressively deteriorate cognition severely enough to impair independence. Globally, over 55 million individuals live with dementia, affecting approximately one in nine individuals over age 65 and one in three over age 85[2]. With the global aging population projected to reach 2.4 billion individuals over 65 years by 2100[3], from 800 million currently[4], the global economic burden of AD is projected to escalate from $2.8 trillion in 2019[5] to $16.9 trillion by 2050[5].

The sex-specific prevalence in AD is striking, with women accounting for two-thirds of cases[6] and exhibiting significantly higher age-adjusted odds of AD than men at older ages[7] independent of their longer life expectancy. This contrasts with other neurodegenerative disorders, such as Parkinson's disease, where men are at twice the risk[8]. Women also show higher susceptibility to APOE4-associated AD risk[9,10], for which current therapeutic approaches are less effective[11]. Addressing modifiable risk factors could prevent 45% of dementia cases, with 12% directly attributable to cardiometabolic factors such as obesity, type 2 diabetes (T2D), high LDL cholesterol, and hypertension[12]. Obesity and T2D are independent modifiable risk factors for dementia and AD[13-16], with their sex-specific prevalence - obesity being more common in women[17] and T2D in men[18] - possibly influencing the sex-specific risk of AD[9].

Midlife overweight and obesity elevate dementia risk by 33% and 63% respectively[19]. Likewise, diabetes elevates dementia risk by 59%[20]. Despite strong epidemiological associations, the molecular bases underlying obesity, T2D, and AD are poorly understood. It is unclear whether epidemiological findings stem from non-linear associations such as age-dependent and disease-stage reverse causation or sex-specific differences[21]. This uncertainty is compounded by the prevalent incorporation of AD-proxies - based on undiagnosed parental cases - in genetic association studies[22-24].

Human genetic data enables systematic decoding of shared biology linking modifiable risk factors to the long preclinical and prodromal curves of AD. We mapped the shared genetic architecture linking obesity, T2D, and AD by integrating genetic correlation, colocalization, phenome-wide association, and protein-protein interaction analyses with deep learning and single-cell transcriptomic approaches to identify actionable biology in effector genes and tissues.

RESULTS

Study design

Our multi-trait analyses used European-ancestry genotyping data from: GIANT consortium meta-analysis (BMI)[25], T2D genomics Initiative meta-analysis (T2D risk[26]), and European Alzheimer & Dementia Biobank (EADB) consortium meta-analysis (AD risk)[27] (**Table 1**). The primary AD meta-analysis (AD1) includes parental proxy cases (self-reported by offsprings, undiagnosed), risking signal dilution from potential misclassification (*e.g.* undiagnosed dementia subtypes or lack of neurodegenerative pathology[27-29]). Hence, we additionally analyzed data excluding AD-proxy cases (AD2) and excluding AD cases, age-matched and non-age-matched controls from the UK Biobank (UKB; AD3) to minimize age-related confounding. The data were provided by the EADB consortium and has recently been made publicly available[30].

To account for potential sex-specific genetic effects associated with BMI and T2D on AD risk, we analyzed sex-stratified genotyping data from the GIANT consortium (BMI)[31] and T2D genomics initiative[32]. We additionally analyzed age-stratified BMI data (under/over age 50)[31]. Age 50 approximates the average age of menopause, a critical period affecting metabolic and hormonal risk factors[31], and marks onset of asymptomatic AD preclinical pathology[33]. Sex-specific AD data is currently not available, which may result in an underestimation of joint sex-specific genetic effects of BMI, T2D, and AD.

Subsequent analyses included: (1) genetic correlations; (2) risk variant identification through multi-trait colocalization; (3) variant-level phenotyping through phenome-wide associations; (4) effector gene mapping through variant-to-gene linkage; (5) effector tissue and cell-type prioritization through multi-omic and deep learning perturbation analyses; (6) mechanistic detailing through enrichment analyses; and (7) genetic-backed drug repurposing identification through gene-drug interaction analyses (**Fig. 1**).

Genetic correlations between BMI and AD, but not T2D and AD, suggest sex and age-specificity

We assessed genetic correlations (r_g) between BMI, T2D, and AD using linkage disequilibrium score regression (**LDSC**; **Fig. 2**; **Table S1**; **Methods**). BMI showed negative genetic correlation with AD risk (r_g= -0.13; p=1x10^{-6}), linking lower BMI variants with higher AD risk. This correlation was significantly stronger in women than men across all AD datasets (p<4x10^{-4}).

Divergent age patterns (≤50y versus >50y) emerged when excluding the UKB. In men, a stronger genetic correlation was observed for AD and BMI >50y versus ≤50y (p<6x10^{-4}). In women, a stronger genetic correlation was observed for AD and BMI ≤50y versus >50y (p<6x10^{-6}). The genetic correlation for BMI ≤50y is significantly stronger for women versus men (p<5x10^{-6}), but non-significant >50y. These sex and age patterns were absent in AD-proxy- and UKB-inclusive data, indicating sex and age-dependent specificity between BMI and clinically diagnosed AD that disappeared when including AD-proxy cases.

No sex differences emerged in the genetic correlation between T2D and AD despite significant correlation in the overall population (r_g= -0.09; p=6x10^{-3}; **Table S1**). However, excluding AD-proxy cases and UKB abolished this correlation, suggesting that the shared T2D and AD architecture may be biased by AD-proxies or reflect broader dementia susceptibility rather than AD-specific biology.

Overall, BMI showed stronger genetic correlation with AD than T2D (**Table S1**). Polygenic BMI risk confers stronger genetic susceptibility to AD in women. Marked age-sensitivity, particularly under 50 years in women, suggests non-linear, age- and sex-dependent mechanisms.

Colocalization analysis identifies unique loci between BMI, T2D and AD specific to sex and age

We identified genome-wide significant AD variants ($p \leq 5x10^{-8}$) concurrently associated with BMI and/or T2D ($p \leq 5x10^{-4}$), yielding 32 unique BMI-AD and 16 T2D-AD overlapped loci (**Table S2; Methods**). Colocalization analyses complemented by locuszoom visual inspection minimized spurious/mediated pleiotropy (**Fig. 3**A), identifying 14 shared causal variants in seven independent loci ($r^2<0.01$; ±500 kb): four shared loci for BMI and AD (BMI-AD), two shared loci for T2D and AD (T2D-AD) and one shared locus for BMI, T2D and AD (BMI-T2D-AD) (**Fig. 3**B; **Methods**). The low percentage of overlapped loci that colocalize reflect a high degree of pleiotropy in the shared genetic architecture of BMI, T2D risk and AD risk.

We mapped each locus to the closest gene for orientation. COX7C and FERMT2 BMI-AD alleles increased both BMI and AD risk. ATP8B3 and NECTIN2-TOMM40 (APOE) increased AD risk linked to lower BMI. T2D-AD and BMI-T2D-AD alleles increased AD risk associated with lower BMI and T2D risk (**Table 2**).

To determine sex-specific effects, we evaluated regional locus structures using locuszoom plots (**Fig. 3**C) and association metrics (p-value, beta) across traits (**Fig. 3**D; **Fig. S1**A-I**; Table S3**). For instance, the COX7C locus is women and age-specific (**Fig. S1**A), exhibiting a locus peak and significant GWAS association from BMI in women ($p=1.6x10^{-5}$) not found in BMI in men (p=0.13). Conversely, the ACE locus is specific to men, showing no locus peak and weak genetic association from T2D GWAS in women (p=0.02), and significantly higher effect size in T2D in men versus women ($p=1.7x10^{-7}$) (**Fig. S1**G; **Table S3**).

Effect sizes remained consistent across AD1 (AD-proxy-inclusive), AD2 (AD-proxy-excluded), and AD3 (UKB-excluded; **Fig. 3**E-G), indicating robustness to case misclassification and improper control age-matching. Overall, stringent colocalization revealed women-predominant BMI-AD associations with age-sensitivity, while ACE T2D-AD effects were specific to men.

Phenome-wide association analyses pinpoint phenotype and sex-specific biology

Phenome-wide association screening (n=1,314 phenotypes) of seven colocalized loci uncovered broad biological links (**Table S4**; **Methods**). BMI-AD variants consistently associate with lower blood pressure (**Fig. 4; Fig. S2**A-J), but show mixed cardiometabolic associations independent of BMI effect direction: COX7C (women-specific) exhibited the standard obesity profile while FERMT2 resembled metabolically healthy obesity (elevated BMI, hematological inflammation markers, but lower blood and pulse pressure)[34,35].

Aligned to the risk increasing allele for AD, T2D-AD and BMI-T2D-AD loci associated with favorable profiles: lower glucose, HbA1c, and GGT (pro-inflammatory liver enzyme), with healthier lipid signatures and blood pressure (**Fig. 4**; **Fig. S2**A-J). BMI loci exhibited women-specific associations (SHBG, age at menarche), absent in men. The men-specific TP53INP1 locus (T2D-AD) associated with Y chromosome mosaic alterations, known to accelerate AD progression in men[36], corroborating sex-specific variant findings. Overall, BMI influences AD risk primarily through underlying cardiometabolic mechanisms, where genetically-driven hypotension and hypoglycemia associate with elevated AD risk.

Variant-to-gene mapping identifies multi-omic functional links to effector genes

To map the colocalized loci between BMI, T2D risk, and AD risk to effector genes, we applied the combined SNP-to-gene (cS2G) approach that ranks genes based on a hierarchy of gene prioritization strategies (**Methods**).

We mapped colocalized loci to effector genes using hierarchical cS2G prioritization variants in the same credible set with the colocalized variant (**Table S5**). Supporting evidence came from nearest transcription start site annotation (closest gene)[37], fine-mapped cis-sQTL data (54 tissues)[38] and plasma pQTL data[39] (**Table 3**; **Table S6**).

We identified 35 unique effector genes across seven loci, of which 10 are novel genes for AD (*i.e.* not previously reported in the literature) and 29 are novel genes for phenotype pairs. To assess whether effector genes incorporate similar functional networks, we performed a protein-protein interaction (PPI) analysis (**Fig. 5; Table S7**). Protein-protein interaction (PPI) analysis (**Fig. 5**; **Table S7**) revealed that the genes in the BMI-T2D-AD locus formed a strong interaction network, suggesting shared mechanistic pathways. Most other loci lacked inter-gene interactions, indicating locus-specific biology. NECTIN2-TOMM40 (APOE) showed strong intra-locus but no cross-loci interactions, suggesting non-APOE may be independent of APOE effects.

Deep-learning and multi-omic analyses implicate peripheral biology in risk loci

We mapped tissue and cell-type associations using AlphaGenome[40] for lead variant effects across functional genomic data-types (**Table S8**; **Fig. S3**; **Methods**), cS2G, splicing QTL (sQTL) and protein QTL (pQTL) functional links (**Table S5-S6**), and GTEx tissue enrichment[38] via ShinyGO[41] (**Fig. S4**; **Methods**). AlphaGenome aligned with cS2G and GTEx sQTLs, mapping risk loci primarily to peripheral immune and cardiometabolic tissues (**Fig. 6**A) with pervasive mesenchymal effects, particularly endothelial and immune cell-types (**Fig. 6**B). Notably, the women-specific COX7C locus induces strong expression changes in gonadal and reproductive tissues not predicted in other loci (**Fig. 6**C).

Peripheral immune niches

GTEx enrichment analyses implicated select loci in immune-related tissues (small intestine, colon, blood, spleen; **Fig. S4**). Single-cell transcriptomic analyses of the immune niches of 17 peripheral tissues[42] revealed prevalent shared risk gene expression across immune cell-types (**Fig. 6**D; **Fig. S5**A-C). While not directly comparable, effector genes showed negligible central nervous system (CNS) microglia expression (**Fig. 7**B-C), the primary AD-enriched CNS cell-type[27], supporting non-CNS immune effects. Despite no overall sex differences in immune-related expression, five genes showed significantly stronger expression in men (FDR 1%): *APOC1*, *NECTIN2*, *ADATA3*, *DOC2A*, and *ACE* (**Fig. S5**D-E; **Methods**). APOE-associated AD risk in women[10,43] contrasts with the significant *APOC1*/*NECTIN2* enriched expression in men, suggesting that men might benefit from protective immune-associated effects from the APOE locus. In contrast, men show higher baseline ACE activity and greater ACE inhibitor response for hypertension[44], suggesting that elevated ACE expression may contribute to specific immune signatures in men linking to hypertension-associated AD mechanisms.

Peripheral cardiometabolic associations

GTEx enrichment extended to metabolic tissues (heart, vasculature, liver, adipose, muscle; **Fig. S4**). COLOCUS analysis evaluated colocalization between metabolic GWAS traits and eQTLs in ±100kb regions around lead variants (**Table 4**; **Fig. S6**; **Table S9**; **Methods**). Extensive colocalization emerged between metabolic GWAS traits and eQTLs in adipose tissue, liver, muscle, and pancreatic islets. We showcase BMI-TMEM219 colocalization in adipose tissue with broad cell-type expression (**Fig. 6**E, G)

and T2D-TP53INP1 colocalization in liver with hepatocyte-specificity (**Fig. 6**F, H). The enhancer-to-gene (E2G) analysis[45] corroborated cS2G associations and validated COLOCUS findings by reporting extensive links to regulatory regions in adipose tissue and hepatocytes using tissue-specific data (**Fig. 6**I; **Table S10**). E2G highlights the still uncharacterized LOC100288123 as a novel liver-specific RNA gene (**Fig. 6**J).

Tissue expression and single-cell profiles reveal CNS regional differences and cell-type specificity

GTEx enrichment implicated brain regions in T2D loci with strong expression and splicing activity (**Fig. S4**, **S7**; **Table S5**). BMI-associated MIR4280 and T2D-associated MIR3150 (**Table S6**) mapped to regulatory activity in nucleus accumbens, cerebellum, cortex, and hippocampus. To examine CNS effects, we analyzed neurotypical GTEx data (13 brain regions), prefrontal cortex (PFC) and hypothalamus single-cell transcriptomics, and middle temporal gyrus (MTG) single-cell profiles from 5 AD donors (**Methods**).

Moderate bulk-level gene expression appeared primarily in cerebellum, cerebellar hemisphere and cortical regions (**Fig. 7**A). PFC excitatory neurons and hypothalamic endothelial cells were the primary expressing cell-types (**Fig. 7**B), contrasting with AD-genetic CNS microglia enrichment[27]. Regional gene expression differed substantially. ACE, an AD drug target[46] and key driver of blood pressure regulation[47], is primarily expressed in hypothalamic endothelial cells but not the PFC (**Fig 7**B, C), linking the renin-angiotensin system to hypothalamic glucose homeostasis and AD risk[48]. Expected pancreatic TMEM219 expression contrasted with minimal expression in heart, vascular muscle, or retina (**Fig. S8**), implicating TMEM219 in CNS-adipose-immune axis regulation of metabolic-immune AD susceptibility. AD MTG neuronal cells expressed select risk genes (COX7C, INTS8, NDUFAF6, DOC2A, KCTD13, YPEL3; **Fig. 7**D), consistent with PFC neurotypical data (**Fig. 7**B).

Overall, CNS expression of BMI, T2D, and AD risk effector genes is limited in both neurotypical and AD brain. These results support a systemic metabolic model of AD susceptibility.

Pathway enrichment indicates novel systemic biology

Pathway enrichment (GO, KEGG, Reactome; **Fig. 8**; **Table S11**; **Methods**) and interactome analyses identified overarching immune and RNA pathways. Pervasive mechanisms included cell cycle, adhesion, autophagy, lipid metabolism, MAPK signaling, DNA/mitochondrial biology and cation channels. BMI-AD loci are uniquely involved in viral biology, T2D-AD loci in renin-angiotensin pathways, and BMI-T2D-AD loci in GTPase, glucagon signaling, and cardiac biology (**Fig. S9**A-C).

The ATP8B3 locus (BMI-AD) enriched for synaptic and endosomal biology (**Fig. 8**A), with ATP8B3 linked to lipid biology and ion channels (**Fig. 8**B). These findings are of particular interest given that TRPML1, a lysosomal calcium channel, has been shown to revert synaptic decline through lysosomal reacidification[49]. ABHD17A localizes to endosomes[50] to regulate postsynaptic activity via PSD-95 depalmitoylation[51] (calcium-NMDA-dependent[52]), modulate RAS-MAPK signaling[53] and calcium-activated potassium channels[54], unifying locus mechanisms. Both calcium channels[55] and depalmitoylases[56,57] are therapeutically interventionable targets.

The ACE locus (T2D-AD) enriched for cardiac and neuropeptide pathways (**Fig. 8**D). The same-locus effector gene *KCNH6* associates with potassium channels (**Fig. 8**E), corroborating cation channels as promising druggable targets. In line, TBX6 shows brain-heart developmental links (**Fig. 8**F), with cardiac pathways represented across multiple loci.

To link systemic and CNS biology, we analyzed secreted protein interactors (Human Protein Atlas; **Table S12**) to identify angiotensinogen (AGT, ACE interactor) and insulin-like growth factor binding protein 3 (IGFBP3, TMEM219 interactor) as potential mediators. AGT (liver/kidney-predominant) regulates renin-angiotensin-mediated blood pressure and emerges as a cardiometabolic therapeutic target[58]. IGFBP3, primarily produced in the liver, is upregulated in AD brain, interacts with humanin to prevent AD-related neuronal death[59], and its knockdown reverses senescence[63,64].

Overall, the broad evidence of molecular mechanisms spanning peripheral and central biological signatures support the systemic involvement of pathways mediating BMI and T2D risk in AD risk.

Genetic-backed drug target discovery reveals novel and repurposing candidates

We evaluated whether effector genes underlie ongoing therapeutic programs (**Table 5**). ACE targets multiple approved drugs and phase 3 trials for cardiometabolic conditions. Additional risk genes are in preclinical development for cancer, liver fibrosis, autoimmune disease, hepatic steatosis, stroke, and mitochondrial disorders.

To identify novel targets of interest, proteomic-based drug targeting using EnrichR-KG (**Methods**) identified 81 approved drugs modulating effector gene expression ($p<0.05$), primarily for cardiovascular disorders (heart failure, hypertension), cancer and neurological conditions (schizophrenia, multiple sclerosis) (**Fig. 8**G; **Table S14**).

We highlight [1] Guanfacine, a drug approved for ADHD and hypertension (**Fig. 8**H), [2] Clozapine, a drug approved for atypical antipsychotic and treatment-resistant schizophrenia (**Fig. 8I**), [3] Levosimendan, a calcium sensitizer[60] approved for heart failure (**Fig. 8**I) shown to rescue cognitive decline in mice and inhibit tau oligomerization, a major AD pathology[61], [4] Tafluprost, a prostaglandin analog approved for open angle glaucoma and ocular hypertension (**Fig. 8**J), [5] INT-747, a farnesoid X receptor agonist with preclinical indications for insulin sensitizing, hypertension, bile acid homeostasis, hepatic and intestinal inflammation, liver fibrosis, and cardiovascular disease[62-64], and [6] A-317491, a P2X2/P2X3 antagonist with preclinical indications for neuropathic pain and chronic inflammation[65] (**Fig. 8**K). Of note, Resmetirom (thyroid hormone receptor-β agonist recently approved for NASH/liver fibrosis[66], **Table S14**) modulates the novel gene SCAMP4, an endocytic trafficking protein.

These findings demonstrate the genetically-backed repurposing potential of approved and pipeline drugs, identify novel targets, and leverage drug mechanisms to uncover risk biology.

DISCUSSION

Obesity and type 2 diabetes are major modifiable risk factors for AD, and their shared genetic architecture has the potential to unveil actionable biology relevant to the long prodromal curve of AD. We identify loci associated with BMI/T2D and AD, of which some demonstrate sex and age-specific associations. Besides brain involvement, peripheral immune and metabolic tissues and cell-types emerge as primary effectors of shared risk mechanisms. We explore multiple drug targeting approaches to expand the breadth of genetically-backed therapeutic options for potential AD prevention.

Our approach primarily reflects the sex-specific and age-stratified risk from variations in BMI and the pathobiology of T2D in AD development. All BMI-AD loci reported here are novel and exhibit consistent sex- and age-specific effects in women. The APOE locus has been linked to T2D-AD[67], but not directly for BMI-AD. We report a novel TP53INP1 lead variant (rs12546365) and male-specific ACE effects,

expanding prior T2D-AD findings[68,67,69]. Further, we identify TAOK2 as the first jointly associated locus with BMI, T2D, and AD.

We find that risk variants linked to lower BMI, and lower risk of T2D are generally linked to higher AD risk, in line with recent clinical evidence that compared people with underweight, normal weight and obesity to the risk of Aβ positivity[70]. Genetics captures lifelong risk and can dissect disease reverse causation, unlike epidemiological studies that often capture the risk profile of comorbidities or risk factors late in adulthood and early in preclinical AD discourse. A critical consideration in our work is the potential for survival bias to confound results at the summary statistics data level. Individuals who develop AD may be depleted of genetic variants that predisposes to higher cardiometabolic risk. These individuals are selectively removed from the population before the age of AD onset, thus enriching AD GWAS for protective cardiometabolic alleles[24]. This could obscure causal relationships, as apparent protective associations could reflect selective survival rather than true biological antagonism. Age-stratified BMI data partially addresses the potential bias, though the lack of necessary information to adjust for these biases at the aggregated summary statistics level could be further mitigated using individual-level data.

AD is often associated with weight loss[71], BMI decrease in older adults is linked to higher risk of AD[72,73] and a common missense variant in APOE (rs429358) has been associated with longitudinal BMI decrease and weight loss[74]. Nonetheless, we find that BMI-AD loci effects are independent of BMI direction but driven by underlying cardiometabolic associations. Genetically-driven low blood pressure and low glucose levels link to elevated AD risk, directly opposing the hypothesis motivating trials of GLP1R agonists for AD, aligning with observed lack of clinical efficacy in recent Phase III trials despite key biomarker engagement[75]. Cross-sectional and longitudinal studies substantiate an increased prevalence of AD and dementia in older individuals with low blood pressure[76-78], but with higher blood pressure in younger individuals[79]. Antihypertensive clinical trials are inconclusive[80] and only recently genetic evidence was linking hypertension to AD in multivariate Mendelian randomization studies[24] whereas multi-trait GWAS failed to identify strong links[81]. Likewise, our findings that low glucose levels link to elevated AD risk align with AD patients showing strong glucose hypometabolism and insulin resistance in the brain[82,83]. As increased fasting plasma glucose levels directly associate with higher brain glucose concentrations[84], our results suggest that lower peripheral glucose levels may potentiate long term cerebral energy deficits.

Cardiometabolic risk research in AD has primarily focused on T2D and AD, but our findings show that BMI-AD biology is more specific to AD while T2D-AD is more ubiquitous, in line with recent observations[15,85]. We find consistent evidence that women are at higher risk from cardiometabolic outcomes associated with variations in BMI and men from cardiometabolic outcomes associated with T2D, in line with recent longitudinal findings[86]. These observations align with higher prevalence of obesity in women[17] and higher susceptibility to AD[6]. Our findings further indicate that women suffer more severe consequences associated with BMI variations driven by APOE, yet current approved drugs are less effective in women and APOE4 carriers[9]. Consistently, T2D and Parkinson's disease (PD) share a stronger correlation compared to T2D and AD[87], with PD being substantially more common in men[8]. For example, women show superior insulin sensitivity compared to men, but insulin resistance is not a relevant phenotype in our loci. On the other hand, clinical trials targeting the male-specific ACE locus (T2D-AD) show that men have significantly higher baseline plasma ACE activity than women and benefit more when taking ACE inhibitors for hypertension[44]. These considerations should prompt the field to examine sex-stratified data for clinical trials targeting genes or pathways evidencing sex-dysmorphic profiles.

Deciphering the genetic architecture and underlying biology of AD has been limited to the brain and its constituent cell-types. While T2D-related loci show brain associations, peripheral immune and metabolic tissues, not brain or microglia, primarily drive BMI and T2D-associated AD risk. This aligns

with recent findings that APOE4 drives immune-related proteomic signatures enriched in circulating immune cells, directly linking AD's primary genetic risk factor to peripheral immunity[88].

Human genetic evidence boosts the likelihood of drugs' clinical success by 2.6-fold[89], with GWAS variants pointing to highly successful drug targets[90]. We identify multiple genetically-backed drug targets with vast repurposing and novel development potential. Even drug targets unrelated to the input cardiometabolic phenotypes are experiencing a substantial repurposing push for neurological disorders, exemplified by immunomodulatory cancer drugs like Lenalidomide currently in clinical trial for AD[91].

Limitations of our work include the current unavailability of sex-specific AD data that may underestimate joint sex-specific genetic effects of BMI, T2D, and AD. The upcoming AD meta-analysis will provide large-scale sex-stratified data, though preliminary results appear underpowered[92]. Moreover, HyPrColoc stringency ensures reliability but may miss other true shared genetic signals. Also, assessing genome-wide significance alone may miss key insights for AD, exemplified by genetic variation linked to GLP1R driving obesity therapeutics but reaching BMI significance only in upcoming GWAS (5M+, unpublished).

Our findings enable informed therapeutics targeting the shared genetic blueprint of BMI, T2D, and cardiometabolic-driven AD risk. Blood pressure interventions warrant more refined sex, age-range and disease stage eligibility criteria. Given prior focus on T2D-AD biology, BMI-related traits may yield outcomes more targeted to AD. The identification of peripheral tissues, not brain, as primary effectors of cardiometabolic risk in AD opens novel research directions for AD risk mitigation via genetically-backed candidates.

METHODS

GWAS summary statistics curation

All BMI and T2D summary statistics (sex-combined and sex-stratified) were originally sourced in the human reference genome GRCh37 (HG19) while the AD1, AD2 and AD3 summary statistics were made available in the human reference genome GRCh38 (HG38). Given that conversion rates are higher from HG19 to HG38[93], we proceeded to liftover the BMI and T2D GWAS data from HG19 to HG38 using the "rtracklayer" R statistical software[94] (version 4.2.2) package from the Bioconductor project[95]. BMI, T2D, AD2 and AD3 summary statistics required reference SNP cluster ID (rsID) annotation. Altogether, a total of ≈52.5 million chromosome positions were annotated using the "BSgenome" R statistical software (version 4.2.2) package from the Bioconductor project[96]. The APOE locus was retained in all analyses, reflecting a methodological consideration specific to our study design. The three AD meta-analyses used here (AD1, AD2, AD3) differ systematically in case ascertainment and control matching strategies. Regional APOE exclusion would result in unpredictable interactions with these pre-existing differences. Further, we aimed to evaluate sex-specific differences in cardiometabolic risk associated with the APOE region given the differential drug responses for women and APOE4 carriers[9]. To address potential APOE dominance concerns, we report: [1] full transparency of APOE findings (NECTIN2-TOMM40 locus), including novel BMI-AD associations with female-specific effects; and [2] protein-protein interaction analyses to assess non-APOE loci independence from APOE biology.

Heritability and genetic correlation

We leveraged LD score regression[97] (LDSC) to estimate narrow-sense heritability (additive genetic effects of common variants) and genetic correlation (GC) between AD, BMI and T2D datasets. We leveraged precalculated LD scores calculated in individuals of European ancestry from the 1000

Genomes Project (*eur_w_ld_chr*). Standard GC data curation and quality control procedures were followed[97,98]. We tested the differences between trait-pair genetic correlation estimates using

$$z = \frac{r_{g1} - r_{g2}}{\sqrt{SE_1^2 + SE_2^2 - 2r \cdot SE_1 \cdot SE_2}}$$

where rg is the genetic correlation for each trait-pair, SE are the standard errors, and r is the genetic correlation coefficient estimate between the different traits in both trait-pairs[101]. The genetic correlation coefficient r between non-AD traits accounts for their underlying genetic similarity. This parameter is key for controlling whether observed differences in genetic correlation estimates (rg) reflect true significant biological differences rather than shared genetic architecture of the traits themselves. For example, when comparing rg estimate differences between BMI.Male-AD1 and BMI.Female-AD1, r represents the genetic correlation between BMI.Male and BMI.Female, effectively quantifying their genetic similarity and correcting for it in statistical testing. We assumed a Bonferroni corrected p-value threshold of ($0.05/27=1.85 \times 10^{-3}$).

Variant discovery

We conducted genetic overlap analyses using Python[99] (version 3.9.13) between AD, BMI and T2D datasets in HG38. We defined the significance thresholds (*p*-value) of 5×10^{-8} for AD datasets and 5×10^{-4} for all BMI and T2D datasets. The use of asymmetric significance thresholds reflects the distinct roles these traits play in the etiology of AD. The biological expectation that variants affecting intermediate or risk-factor phenotypes (BMI, T2D) through additive cascade mechanisms may exert smaller individual effects than those affecting disease endpoints (AD), and therefore may not reach genome-wide significance in individual cross-section GWAS but remain relevant in shared genetic architecture. The GLP1R locus exemplifies this principle: variants linked to GLP1R reach genome-wide significance for T2D[100], but more modest associations in BMI[25]. Yet, therapeutic GLP1R agonists produce substantial body weight reduction[101], demonstrating that variants below genome-wide significance for intermediate or risk-factor phenotypes can have substantial biological and therapeutic relevance. For AD, we applied the standard genome-wide significance threshold to minimize the propagation of systematic biases inherent to the use of AD-proxy phenotypes in all contemporary GWAS[24,102]. We then performed phenotype overlap on chromosome position, including all pair-traits and triangulations. After variant overlap, we performed colocalization analysis was performed HyPrColoc, a Bayesian method for identifying shared genetic associations between traits within genomic regions. HyPrColoc analysis was conducted using GWAS summary statistics, including regression coefficients and standard errors for each variant and trait. The method tests whether multiple traits share causal variants in a genomic region and, when evidence for full colocalization is insufficient, employs a clustering algorithm to identify subsets of traits that colocalize at distinct causal variants. Default parameters were used for the analysis. We adopted a hypothesis-generating approach, without pre-specifying a posterior probability threshold. Instead, we [1] performed HyPrColoc across the full posterior probability distribution, [2] performed sensitivity analyses to assess the robustness of identified colocalization clusters and [3] validated candidate colocalization signals through visual inspection of local Locuszoom plots to confirm signal, LD structure and regional architecture. This approach prioritizes identification of robust candidate signals for hypothesis generation while minimizing the risk of threshold-driven false negatives. Candidate signals identified at lower posterior probabilities but persistent across sensitivity analyses and confirmed via Locuszoom inspection were deemed biologically plausible for further investigation. All analyses were performed using the HyPrColoc R package[103]. The HLA region (chr6:28,510,120-33,480,577) was removed post-analysis. Locuszoom plots were generated using a package that creates regional Manhattan plots leveraging an european linkage disequilibrium reference panel (https://github.com/Geeketics/LocusZooms). We tested the differences between women-specific and men-specific beta-estimates (b_{women}, b_{men}) using:

$$t = \frac{b_{men} - b_{women}}{\sqrt{SE_{men}^2 + SE_{women}^2 - 2r \cdot SE_{men} \cdot SE_{women}}}$$

where SE are the standard errors and r is Spearman rank correlation coefficient across all SNPs across BMI and T2D strata. We assumed a Bonferroni corrected p-value threshold of ($0.05/12=4.2\times10^{-3}$).

Phenome-wide association analysis

Phenome-wide association studies (PheWAS) were conducted using the Association to Function Knowledge Portal (A2F; a2fkp.org) to systematically test genetic variants for associations across a broad spectrum of phenotypes. We analyzed a total of 1,314 distinct phenotypes, encompassing diseases, disorders, and clinical traits derived from electronic health records and biobank data. We screened PheWAS associations for the seven colocalized loci aligned to the risk increasing allele for AD. To account for multiple testing, a statistical significance was determined using a Bonferroni-corrected p-value threshold of 4.3×10^{-5} (0.05/1,314 phenotypes). Results meeting the corrected significance threshold were considered evidence for phenome-wide significant associations.

Variant-to-gene mapping

For establishing connections between genetic variants and their corresponding target genes, we utilized the cS2G methodology[104]. The analysis was conducted using the GRCh37/hg37 genome assembly. The cS2G approach integrates various SNP-to-gene association methods by incorporating functional annotations derived from seven component strategies, listed according to their assigned weights: Exon regions, Promoter sequences, fine-mapped cis-eQTL data from eQTLGen blood studies, fine-mapped cis-eQTL information from GTEx across 54 human tissue types, enhancer-gene associations from EpiMap spanning 833 cellular types, Activity-By-Contact (ABC) methodology covering 167 cellular types, and Cicero analysis for blood/basal conditions. The cS2G framework computes an integrated association score by applying weights to individual strategy scores, thereby identifying the most probable effector gene(s) for each single nucleotide polymorphism (SNP).

AlphaGenome

We performed an in-silico perturbation screen using batch variant scoring from AlphaGenome[40] to predict the functional consequences of colocalized BMI/T2D-AD variants across multiple functional domains. The effect of each colocalized variants was predicted within a 100kb genome window in humans. We used “UBERON” and “CL” ontologies to predict variant effects on up to 116 tissues and 106 cell-types, respectively. The colocalized variants within the APOE region were not considered in this analysis given their overwhelming predicted effects across all data-types. Importantly, neither data-type in AlphaGenome included central nervous system microglia. For each variant, we report the raw scores representing the predicted regulatory effect for each data-type. Raw scores are specific to individual data-types, thus not comparable between different them. We present variant effects by ordering raw scores on magnitude of effect from highest to lowest, thus identifying the tissues and cell-types where predicted variant impacts are strongest. The raw scores are shown as absolute values due to current limitations of deep neural network models in accurately predicting the direction of variant effects[105]. To contextualize the magnitude of variant effects, we report quantile scores which provide a percentile-based ranking of variant effects relative to the background genome (**Table S8**). The quantile score is computed by establishing an empirical background distribution using scores from common variants (minor allele frequency > 0.01 in any GnomAD v3 population) for each data-type. For example, a variant with a quantile score of 0.99 indicates that its predicted regulatory effects in a given tissue or cell-type ranks at the 99th percentile among common variants. Variant effect predictions are evaluated across the following functional scorers:

Data Type	Description	Biosamples	Resolution	Category
Total RNA-seq	Measures RNA expression across all RNA types (polyadenylated, non-polyadenylated, and non-coding RNAs).	285	Single bp	Transcriptomic
PolyA+ RNA-seq	Measures RNA expression of mature polyadenylated transcripts enriched for polyA+ tails.	285	Single bp	Transcriptomic
CAGE	Measures RNA expression at transcription start sites (TSS) using 5' cap capture.	264	Single bp	Transcriptomic
PROCAP	Measures nascent RNA expression at TSS via run-on sequencing with capping.	6	Single bp	Transcriptomic
DNase-seq	Measures chromatin accessibility through DNase I hypersensitive site mapping.	305	Single bp	Epigenomic
ATAC-seq	Measures chromatin accessibility through transposase insertion patterns.	167	Single bp	Epigenomic
ChIP-seq (Histone Modifications)	Measures relative abundance of histone modification marks (24 histone markers).	219	128 bp	Epigenomic
ChIP-seq (Transcription Factors)	Measures DNA-bound transcription factors (43 proteins) via chromatin immunoprecipitation.	163	128 bp	Epigenomic
Splice Sites	Predicts location of donor and acceptor splice sites on both DNA strands with probability scores.	-	Single bp	Splicing
Splice Junctions	Predicts spliced read counts at exon-exon junctions from RNA-seq data.	282	Single bp	Splicing
Splice Usage	Predicts fraction of transcripts using a given splice site from RNA-seq data.	282	Single bp	Splicing

GWAS-eQTL colocalization

We colocalized the lead cross-phenotype colocalized variants (from HyPrColoc) plus its credible sets (± 100kb) with eQTLs in metabolic tissues, including adipose, pancreatic islets, liver and muscle (build 37) using COLOCUS, a platform from HuGeAMP. COLOCUS implements the COLOC Bayesian algorithm, utilizing conditionally independent or fine-mapped signals identified through statistical fine-mapping approaches, with each signal represented by a lead variant and corresponding credible set.

Immune, adipose and liver analyses

We evaluated the individual gene expression and % of cells in the immune compartment of 17 peripheral tissues using the Single Cell Portal[106], including ileum, lung, thoracic lymph node, mesenteric lymph node, bone marrow, skeletal muscle tissue, liver, spleen, omentum, caecum, thymus, duodenum, blood, transverse colon, sigmoid colon, lamina propria and jejunal epithelium[42]. Statistical sex-strata differences were evaluated using a Wilcoxon matched-pairs signed rank test (nonparametric) following the evaluation of data normality using the Anderson-Darling, D'Agostino-Pearson omnibus, Shapiro-Wilk and Kolmogorov-Smirnov normality tests. Outliers in **Fig. S5**D-E were identified using the Robust Regression and Outlier removal Using Nonlinear TukeyBiweight (ROUT) method (Q = 1%) implemented in GraphPad Prism (version 9.0.0). This method applies robust regression with a false discovery rate (FDR) of 1% to identify data points as outliers. We checked the single-cell expression in the human adipose tissue using the adipose tissues knowledge portal[107] and the single-cell expression in the human liver[108] using the liver cell atlas.

Enhancer-to-gene

We adapted the E2G pipeline from Perrin *et al.*[45] to map shared risk variants falling within regulatory genomic regions of human adipose tissue, liver, adipocytes and hepatocytes. The analysis was conducted in hg37. For the adipose tissue and adipocytes, we leveraged promoter capture HiC data from SGBS cells (both pre- and mature adipocytes)[109], RNA-seq, ATAC-seq and ABC-STARE data from SGBS cells (days 0, 4 and 14)[45], human adipose tissue ATAC-seq data from METSIM (10,197 Finnish men)[110] and eQTL data from AdipoExpress (2344 human subcutaneous adipose tissue samples)[111]. We further supplemented E2G with peak annotations from ChIP using the ChIPseeker R package[112], Cis-regulatory element annotations from single-cell epigenetic datasets using the Cis-element Atlas (CATlas)[113], and Roadmap epigenomics data from samples E023 (mesenchymal stem cell (MSC) derived adipocyte cultured cells) and E063 (adipose nuclei)[114]. E023 derives from *in vitro* differentiated MSCs into adipocytes and models adipocyte development. E063 consists of nuclei isolated directly from adult adipose tissue and reflects the native epigenetic state of *in vivo* mature adipocytes. For the liver and hepatocytes, we leveraged promoter capture HiC data from the liver[115], RNA-seq and ATAC-seq data from primary human hepatocytes[116] and eQTL data from the most recent liver eQTL meta-analysis[117]. We further implemented ATAC peak annotations[112] using the *annotatr* and *annotatePeak* R packages and Roadmap epigenomics data from liver samples. We complemented E2G with e/sQTL data from GTEx[118] (version 10).

Brain analysis

We performed single-cell analyses using the Single Cell Portal[105] in the prefrontal cortex[118] (PFC, key AD region[119]) and hypothalamus[119] (key region in obesity, T2D and metabolism[48,120]). We used the Allen Brain Atlas[120] to perform exploratory analyses of the single-cell diversity of the middle temporal gyrus of individuals with AD (MTG 10x SEA-AD; vulnerable AD brain region[121]) (166,868 total nuclei from 5 post-mortem human AD brain specimens, median age of 80)[121].

Enrichment analysis

We performed enrichment analyses in GO Biological Processes, GO Cellular Components, GO Molecular Functions, KEGG and GTEx tissues[38] using ShinyGO[41] (v0.85) and an FRD cutoff of 0.05. The GTEx tissue gene expression profiles dataset contains gene expression data from 17,382 RNA-seq samples of 54 different human tissues (plus 2 cell lines) from 838 postmortem donors. We performed enrichment analyses based on the "Co.Expression GTEx.Tissue Expression.Down,", "Co.Expression GTEx.Tissue Expression.Up." and "Co-expression.GTEx.Tissues.V8.2023" categories.

This analysis evaluates whether shared risk genes are enriched within genes showing elevated or decreased expression in specific tissues. Additionally, we performed an over-representation analysis based on GO terms, KEGG, Reactome and Proteomic Drug Atlas using EnrichR-KG[122]. Of note, the proteomic drug targeting was originally performed on human immortalized cell lines[123].

EADB ACKNOWLEDGMENTS

The EADB consortium groups together 20,464 Alzheimer's disease (AD) cases and 22,244 controls after quality controls from 16 European countries (Austria, Belgium, Bulgaria, Czech Republic, Denmark, Finland, France, Germany, Greece, Italy, Portugal, Spain, Sweden, Switzerland, The Netherlands and the UK). These samples were genotyped in three independent centers (France, Germany and the Netherlands) leading to define three nodes: EADB-France, EADB-Germany and EADB-Netherlands. In addition, EADB also included Australian partners. We thank the numerous participants, researchers, and staff from many studies who collected and contributed to the data. We thank the high performance computing service of the University of Lille. We thank all the CEA-CNRGH staff who contributed to sample preparation and genotyping for their excellent technical assistance. This work was supported by a grant (European Alzheimer DNA BioBank, EADB) from the EU Joint Programme – Neurodegenerative Disease Research (JPND). Inserm UMR1167 is also funded by Inserm, Institut Pasteur de Lille, the Lille Métropole Communauté Urbaine, the French government's LABEX DISTALZ program (development of innovative strategies for a transdisciplinary approach to Alzheimer's disease). The Bulgarian cohort was partially supported by the European Union-NextGenerationEU, through the National Recovery and Resilience Plan of the Republic of Bulgaria, project BG-RRP-2.004-0004-C01, Strategic research and innovation program for development of Medical university - Sofia.

SUPPLEMENTARY AUTHOR INFORMATION

Céline Bellenguez[1], Benjamin Grenier-Boley[1], Sami Heikkinen[2], Pablo García-González[3-5], Atahualapa Castillo-Morales[6], Fahri Küçükali[7,8], Najaf Amin[9], Itziar de Rojas[3,4,10], Victoria Alvarez[11,12], Beatrice Arosio[13,14], Jesper Qvist Thomassen[15], Sverre Bergh[16,17], Merce Boada[3,4], Barbara Borroni[18,19], Paola Bossù[20], María J. Bullido[4,21,22], Ángel Carracedo[23,24], Antonio Daniele[25,26], Alexandre de Mendonça[27], Jürgen Deckert[28], Martin Dichgans[29-31], Srdjan Djurovic[32,33], Oriol Dols-Icardo[4,34], Carole Dufouil[35], Emrah Düzel[36,37], Valentina Escott-Price[38], Tormod Fladby[39,40], Laura Fratiglioni[41,42], Daniela Galimberti[43,44], Jose Maria García-Alberca[4,45], Guillermo Garcia-Ribas[46], Vilmantas Giedraitis[47], Caroline Graff[41,48], Timo Grimmer[49], Edna Grünblatt[50-52], Olivier Hanon[53], Lucrezia Hausner[54], Stefanie Heilmann-Heimbach[55], Jakub Hort[56,57], Frank Jessen[58-60], Ville Leinonen[61,62], Anssi Lipponen[2], Jiao Luo[15, 63], Henna Martiskainen[2], Carlo Masullo[64], Patrizia Mecocci[42,65], Shima Mehrabian[66], Pablo Mir[4,67,68], Susanne Moebus[69], Laura Molina Porcel[70,71], Fermin Moreno[4,72,73], Benedetta Nacmias[74,75], Lucilla Parnetti[76], Pau Pastor[77,78], Jordi Pérez-Tur[4,79,80], Oliver Peters[81,82], Yolande A.L. Pijnenburg[83,84], Gerard Piñol-Ripoll[85,86], Julius Popp[87- 90], Innocenzo Rainero[91], Luis M Real[92,93], Steffi Riedel-Heller[94], Eloy Rodriguez-Rodriguez[4,95], Arvid Rongve[96], Giacomina Rossi[97], Jose Luis Royo[98], Dan Rujescu[99,100], Ingvild Saltvedt[101], María Eugenia Sáez[102], Raquel Sánchez-Valle[103], Florentino Sanchez-Garcia[104], Nicolai Sandau[15], Nikolaos Scarmeas[105,106], Katja Scheffler[107,108], Norbert Scherbaum[109], Anja Schneider[59,110], Geir Selbæk[16,111,112], Davide Seripa[113], Vincenzo Solfrizzi[114,115], Marco Spallazzi[116], Alessio Squassina[117], Eystein Stordal[118], Niccoló Tesi[84,119,120], Betty Tijms[83,84], Latchezar Traykov[66], Lucio Tremolizzo[121,122], Kumar P. Tripathi[123,124], Julie Williams[6,125], Jens Wiltfang[126-128], Dag Aarsland[129-131], Philippe Amouyel[1], Stéphanie Debette[35], Gael Nicolas[132], Sven van der Lee[83,84,133], Henne Holstege[83,84,119,134,135], Maria Victoria Fernandez[3], Magda Toslaki[136], Patrick Gavin Kehoe[137], Kristel Sleegers[7,8], Martin Ingelsson[47,138,139], Roberta Ghidoni[19], Ole A Andreassen[33,140,141], Peter A.

Holmans[125], Pascual Sánchez-Juan[4,142], Rebecca Sims[125], Alfredo Ramirez[59,60,110,123,143], Agustin Ruiz[3,4,144], Mikko Hiltunen[2], Cornelia van Duijn[9,145], Ruth Frikke-Schmidt[15,146], Jean-Charles Lambert[1]

1. Université de Lille, Inserm, CHU Lille, Institut Pasteur de Lille, Lille, France.
2. Institute of Biomedicine, University of Eastern Finland, Yliopistoranta 1E, 70211 Kuopio, Finland
3. Ace Alzheimer Center Barcelona, Universitat Internacional de Catalunya (UIC), Barcelona, Spain
4. Networking Research Center on Neurodegenerative Diseases (CIBERNED), Instituto de Salud Carlos III, Madrid, Spain
5. Doctorate in Biotechnology, Faculty of Pharmacy and Food Sciences, University of Barcelona, Barcelona, Spain.
6. UK Dementia Research Institute, School of Medicine, Cardiff University, Wales, UK
7. VIB Center for Molecular Neurology, VIB, Antwerp, Belgium
8. Department of Biomedical Sciences, University of Antwerp, Antwerp, Belgium
9. Nuffield Department of Population Health, University of Oxford, Oxford, UK
10. Luxembourg Centre for Systems Biomedicine (LCSB), University of Luxembourg, Esch-sur-Alzette, Luxembourg
11. Laboratorio de Genética. Hospital Universitario Central de Asturias, Oviedo, Spain
12. Instituto de Investigación Sanitaria del Principado de Asturias (ISPA)
13. Department of Clinical Sciences and Community Health, University of Milan, Milan, Italy
14. Geriatric Unit, Fondazione IRCCS Ca' Granda Ospedale Maggiore Policlinico, Milan, Italy
15. Department of Clinical Biochemistry, Copenhagen University Hospital - Rigshospitalet, Blegdamsvej 9, 2100 Copenhagen, Denmark
16. The Research Centre for Age-related Functional Decline and Disease, Innlandet Hospital Trust, Ottestad, Norway
17. Norwegian National Centre for Aging and Health, Vestfold Health Trust, Tønsberg, Norway
18. Department of Clinical and Experimental Sciences, University of Brescia, Italy
19. Molecular Markers Laboratory, IRCCS Istituto Centro San Giovanni di Dio Fatebenefratelli, Brescia, Italy
20. Laboratory of Experimental Neuropsychobiology, Clinical Neuroscience and Neurorehabilitation Department, IRCCS Santa Lucia Foundation, Rome, Italy
21. Centro de Biología Molecular Severo Ochoa (UAM-CSIC)
22. Instituto de Investigacion Sanitaria 'Hospital la Paz' (IdIPaz), Madrid, Spain
23. Grupo de Medicina Xenómica, CIBERER, CIMUS. Universidade de Santiago de Compostela, Santiago de Compostela, Spain.
24. Fundación Pública Galega de Medicina Xenómica- IDIS, Santiago de Compostela, Spain.
25. Department of Neuroscience, Università Cattolica del Sacro Cuore, Rome, Italy
26. Neurology Unit, IRCCS Fondazione Policlinico Universitario A. Gemelli, Rome, Italy
27. Faculty of Medicine, University of Lisbon, Portugal
28. Department of Psychiatry, Psychosomatics and Psychotherapy, Center of Mental Health, University Hospital of Würzburg, Germany
29. Institute for Stroke and Dementia Research (ISD), University Hospital, LMU Munich, Munich, Germany.
30. German Center for Neurodegenerative Diseases (DZNE), Munich, Germany
31. Munich Cluster for Systems Neurology (SyNergy), Munich, Germany
32. Department of Medical Genetics, Oslo University Hospital, Oslo, Norway
33. Centre for Precision Psychiatry, Institute of Clinical Medicine, University of Oslo, Oslo, Norway
34. Department of Neurology, Institut de Recerca Sant Pau, Hospital de la Santa Creu i Sant Pau, Universitat Autònoma de Barcelona, Barcelona, Spain.
35. University of Bordeaux, Inserm Bordeaux Population Health Research Center U1219, Bordeaux, France.
36. German Center for Neurodegenerative Diseases (DZNE), Magdeburg, Germany
37. Institute of Cognitive Neurology and Dementia Research (IKND), Otto-von-Guericke University, Magdeburg, Germany
38. UKDRI@ Cardiff, School of Medicine, Cardiff University, Cardiff, UK
39. Institute of Clinical Medicine, Campus Ahus, University of Oslo, Oslo, Norway
40. Department of Neurology, Akershus University Hospital, Lørenskog, Norway
41. Karolinska University Hospital, Theme inflammation and Aging, Sweden
42. Karolinska Institutet, Center for Alzheimer Research, Department NVS, Division of ARC, Stockholm, Sweden
43. Neurodegenerative Diseases Unit, Fondazione IRCCS Ca' Granda, Ospedale Policlinico, Milan, Italy
44. Dept. of Biomedical, Surgical and Dental Sciences, University of Milan, Milan, Italy

45. Alzheimer Research Center & Memory Clinic, Andalusian Institute for Neuroscience, Málaga, Spain.
46. Hospital Universitario Ramon y Cajal, IRYCIS, Madrid
47. Department of Public Health and Caring Sciences, Clinical Geriatrics, Uppsala University, Uppsala, Sweden
48. Karolinska Institutet, Center for Alzheimer Research, Department NVS, Division of Neurogeriatrics, Bioclinicum J10:20, 171 64 Stockholm Sweden
49. Center for Cognitive Disorders, Department of Psychiatry and Psychotherapy, Technical University of Munich, School of Medicine, Munich, Germany
50. Department of Child and Adolescent Psychiatry and Psychotherapy, University Hospital of Psychiatry Zurich, University of Zurich, Zurich, Switzerland
51. Neuroscience Center Zurich, University of Zurich and ETH Zurich, Switzerland
52. Zurich Center for Integrative Human Physiology, University of Zurich, Switzerland
53. Université Paris Cité, EA 4468, APHP, Hospital Broca, Memory Resource and Research Centre of de Paris-Broca-Ile de France, Paris, France
54. Department of Geriatric Psychiatry, Central Institute for Mental Health Mannheim, Faculty Mannheim, University of Heidelberg, Germany
55. Institute of Human Genetics, University of Bonn, School of Medicine & University Hospital Bonn, Bonn, Germany
56. Memory Clinic, Department of Neurology, Charles University, Second Faculty of Medicine and Motol University Hospital, Czech Republic
57. International Clinical Research Center, St. Anne's University Hospital Brno, Brno, Czech Republic
58. Department of Psychiatry and Psychotherapy, Faculty of Medicine and University Hospital Cologne, University of Cologne, Cologne, Germany
59. German Center for Neurodegenerative Diseases (DZNE), Bonn, Germany
60. Cluster of Excellence Cellular Stress Responses in Aging-associated Diseases (CECAD), University of Cologne, Cologne, Germany
61. Department of Neurosurgery, Kuopio University Hospital, Puijonlaaksontie 2 FI-70210 Kuopio, Finland
62. Institute of Clinical Medicine-Neurosurgery, University of Eastern Finland, Kuopio, Finland
63. Novo Nordisk Foundation Center for Basic Metabolic Research, Faculty of Health and Medical Science, University of Copenhagen, Blegdamsvej 3, 2200 Copenhagen
64. Institute of Neurology, Catholic University of the Sacred Heart, Rome, Italy
65. Division of Gerontology and Geriatrics, Department of Medicine and Surgery, University of Perugia, Italy
66. Clinic of Neurology, UH "Alexandrovska", Medical University - Sofia, Sofia, Bulgaria
67. Unidad de Trastornos del Movimiento, Servicio de Neurología y Neurofisiología. Instituto de Biomedicina de Sevilla (IBiS), Hospital Universitario Virgen del Rocío/CSIC/Universidad de Sevilla, Seville, Spain
68. Departamento de Medicina, Facultad de Medicina, Universidad de Sevilla, Seville, Spain
69. Institute for Urban Public Health, University Hospital of University Duisburg-Essen, Essen, Germany.
70. Neurological Tissue Bank - Biobanc- Hospital Clinic -IDIBAPS, Barcelona, Spain
71. Alzheimer's disease and other cognitive disorders Unit. Neurology Department, Hospital Clinic , Barcelona, Spain
72. Department of Neurology. Hospital Universitario Donostia. San Sebastian, Spain
73. Neurosciences Area. Instituto Biodonostia. San Sebastian, Spain
74. Department of Neuroscience, Psychology, Drug Research and Child Health University of Florence, Florence, Italy
75. IRCCS Fondazione Don Carlo Gnocchi, Florence, Italy
76. Centre for Memory Disturbances, Lab of Clinical Neurochemistry, Section of Neurology, University of Perugia, Perugia, Italy
77. Fundació Docència i Recerca MútuaTerrassa, Terrassa, Barcelona, Spain
78. Memory Disorders Unit, Department of Neurology, Hospital Universitari Mutua de Terrassa, Terrassa, Barcelona, Spain
79. Unitat de Genètica Molecular, Institut de Biomedicina de València-CSIC, Valencia, Spain
80. Unidad Mixta de Neurologia Genètica, Instituto de Investigación Sanitaria La Fe, Valencia, Spain.
81. German Center for Neurodegenerative Diseases (DZNE), Berlin, Germany
82. Charité – Universitätsmedizin Berlin, corporate member of Freie Universität Berlin, Humboldt-Universität zu Berlin, and Berlin Institute of Health, Institute of Psychiatry and Psychotherapy, Hindenburgdamm 30, 12203 Berlin, Germany
83. Alzheimer Center Amsterdam, Neurology, Vrije Universiteit Amsterdam, Amsterdam UMC location VUmc, Amsterdam, The Netherlands
84. Amsterdam Neuroscience, Neurodegeneration, Amsterdam, The Netherlands

85. Unitat Trastorns Cognitius, Hospital Universitari Santa Maria de Lleida, Lleida, Spain
86. Institut de Recerca Biomedica de Lleida (IRBLLeida), Lleida, Spain
87. Old Age Psychiatry, Department of Psychiatry, Lausanne University Hospital, Lausanne, Switzerland
88. Department of Geriatric Psychiatry, University Hospital of Psychiatry Zürich, Zürich, Switzerland
89. Institute for Regenerative Medicine, University of Zürich, Switzerland
90. Center for memory disorders and Alzheimer's disease, Klinik für Neurologie Hirslanden, Zürich, CH
91. Department of Neuroscience “Rita Levi Montalcini”, University of Torino, Torino, Italy
92. Centro de Investigación Biomédica en Red de Enfermedades Infecciosas (CIBERINFEC), Instituto de Salud Carlos III, Madrid, Spain
93. Instituto de Biomedicina de Sevilla, IBiS/Hospital Universitario Virgen de Valme /CSIC/ Departamento de Bioquímica Médica, Biología Molecular e Inmunología, Universidad de Sevilla, Sevilla, Spain
94. Institute of Social Medicine, Occupational Health and Public Health, University of Leipzig, 04103 Leipzig, Germany.
95. Neurology Service, Marqués de Valdecilla University Hospital (University of Cantabria and IDIVAL), Santander, Spain.
96. Haugesund Hospital, Department of Research and Innovation, Haugesund, Norway
97. Unit of Neurology V - Neuropathology, Fondazione IRCCS Istituto Neurologico Carlo Besta, Milan, Italy
98. Depatamento de Especialidades Quirúrgicas, Bioquímica e Inmunología. Facultad de Medicina. Universidad de Málaga. Málaga, Spain
99. Department of Psychiatry and Psychotherapy, Medical University Vienna, Vienna, Austria
100. Martin-Luther-University Halle-Wittenberg, University Clinic and Outpatient Clinic for Psychiatry, Psychotherapy and Psychosomatics, Halle (Saale), Germany
101. Department of Neuromedicine and Movement Science, Faculty of Medicine and Health Sciences, Norwegian University of Science and Technology (NTNU), Department of Geriatrics, St. Olav's Hospital, Trondheim University Hospital, Trondheim, Norway
102. CAEBI, Centro Andaluz de Estudios Bioinformáticos, Sevilla, Spain.
103. Alzheimer's disease and other cognitive disorders unit. Service of Neurology. Hospital Clínic of Barcelona. Institut d'Investigacions Biomèdiques August Pi i Sunyer, University of Barcelona, Barcelona, Spain
104. Department of Immunology, Hospital Universitario Doctor Negrín, Las Palmas de Gran Canaria, Las Palmas, Spain.
105. Taub Institute for Research in Alzheimer’s Disease and the Aging Brain, The Gertrude H. Sergievsky Center, Depatment of Neurology, Columbia University, New York, NY
106. 1st Department of Neurology, Aiginition Hospital, National and Kapodistrian University of Athens, Medical School, Greece
107. Department of Neurology and Clinical Neurophysiology, Trondheim University Hospital , Trondheim, Norway
108. Department of Neuromedicine and Movement Science, Norwegian University of Science and Technology (NTNU), Trondheim, Norway
109. Department of Psychiatry and Psychotherapy, LVR-Klinikum Essen, University of Duisburg-Essen, Germany Medical Faculty, Germany
110. Department for Cognitive Disorders and Old Age Psychiatry, University Hospital Bonn, Bonn, Germany.
111. Norwegian National Advisory Unit on Aging and Health, Vestfold Health Trust, Tønsberg, Norway
112. Institute of Health and Society, Faculty of Medicine, University of Oslo, Oslo, Norway
113. Department of Hematology and Stem Cell Transplant, Vito Fazzi Hospital, Lecce, Italy
114. Interdisciplinary Department of Medicine, Geriatric Medicine and Memory Unit, University of Bari “A. Moro, Bari, Italy
115. Academic Division “C. Frugoni” & Hospital Division of Internal and Geriatric Medicine, Policlinico Hospital, Bari, Italy
116. Department of Medicine and Surgery, Unit of Neurology, University-Hospital of Parma, Parma, Italy
117. Department of Biomedical Sciences, Section of Neuroscience and Clinical Pharmacology, University of Cagliari, Cagliari, Italy
118. Namsos Hospital, Namsos, Norway
119. Genomics of Neurodegenerative Diseases and Aging, Human Genetics, Vrije Universiteit Amsterdam, Amsterdam UMC location VUmc, Amsterdam, The Netherlands
120. Delft Bioinformatics Lab, Delft University of Technology, Delft, The Netherlands
121. Neurology Unit, IRCCS "San Gerardo dei Tintori", Monza, Italy
122. School of Medicine and Surgery, University of Milano-Bicocca, Monza, Italy
123. Division of Neurogenetics and Molecular Psychiatry, Department of Psychiatry and Psychotherapy, Faculty of Medicine and University Hospital Cologne, University of Cologne, Cologne, Germany

[124] Estudios en Neurociencias y Sistemas Complejos (ENyS) CONICET-HEC-UNAJ
[125] Division of Psychological Medicine and Clinical Neuroscience, School of Medicine, Cardiff University, Wales, UK
[126] Department of Psychiatry and Psychotherapy, University Medical Center Goettingen, Goettingen, Germany
[127] German Center for Neurodegenerative Diseases (DZNE), Goettingen, Germany
[128] Medical Science Department, iBiMED, Aveiro, Portugal
[129] Department of Old Age Psychiatry, Division of Academic Psychiatry, Institute of Psychiatry, Psychology and Neuroscience, King's College London, United Kingdom
[130] Wolfson Centre for Age Related Diseases, Division of Neuroscience of the Institute of Psychiatry, Psychology and Neuroscience, King's College London, United Kingdom
[131] Stavanger University Hospital, Stavanger, Norway
[132] Univ Rouen Normandie, Normandie Univ, Inserm U1245 and CHU Rouen, Department of Genetics and Reference Center for Developmental Disorders, Rouen, France.
[133] Genomics of Neurodegenerative Diseases and Aging, Human Genetics, Vrije Universiteit Amsterdam, Amsterdam UMC location VUmc, Amsterdam, The Netherlands.
[134] VIB Center for Brain and Disease Research, ON5 Herestraat 49 - box 602, 3000 Leuven, Belgium
[135] Department of Neurosciences, Leuven Brain Institute, KU Leuven, Leuven, Belgium.
[136] Aristotle University of Thessaloniki, Greece
[137] Bristol Medical School, University of Bristol, Bristol, UK
[138] Krembil Brain Institute, University Health Network, Toronto, Ontario, Canada
[139] Tanz Centre for Research in Neurodegenerative Diseases, Departments of Medicine and Laboratory Medicine & Pathobiology, University of Toronto, Toronto, Ontario, Canada
[140] Division of Mental Health and Addiction, Oslo University Hospital, Oslo, Norway
[141] KG Jebsen Centre for Neurodevelopmental disorders, University of Oslo, Oslo, Norway
[142] Alzheimer's Centre Reina Sofia-CIEN Foundation, Madrid, Spain.
[143] Department of Psychiatry & Glenn Biggs Institute for Alzheimer's and Neurodegenerative Diseases, San Antonio, TX, USA
[144] Biggs Institute for Alzheimer's and Neurodegenerative Diseases, University of Texas Health Science Center, San Antonio, Texas, USA.
[145] Department of Epidemiology, ErasmusMC, Rotterdam, The Netherlands
[146] Department of Clinical Medicine, Faculty of Health and Medical Sciences, University of Copenhagen, Blegdamsvej 3B, 2100 Copenhagen, Denmark

REFERENCES

1. WHO. *Global action plan on the public health response to dementia 2017 - 2025*, (2017).
2. Association., A.s. 2024 Alzheimer's disease facts and figures. *Alzheimers Dement* **20**, 3708-3821 (2024).
3. Vollset, S.E. *et al.* Fertility, mortality, migration, and population scenarios for 195 countries and territories from 2017 to 2100: a forecasting analysis for the Global Burden of Disease Study. *Lancet* **396**, 1285-1306 (2020).
4. United Nations Department of Economic and Social Affairs, P.D. World Population Ageing 2023: Challenges and opportunities of population ageing in the least developed countries. (2023).
5. Nandi, A. *et al.* Global and regional projections of the economic burden of Alzheimer's disease and related dementias from 2019 to 2050: A value of statistical life approach. *EClinicalMedicine* **51**, 101580 (2022).
6. Rajan, K.B. *et al.* Population estimate of people with clinical Alzheimer's disease and mild cognitive impairment in the United States (2020-2060). *Alzheimers Dement* **17**, 1966-1975 (2021).
7. Beam, C.R. *et al.* Differences Between Women and Men in Incidence Rates of Dementia and Alzheimer's Disease. *J Alzheimers Dis* **64**, 1077-1083 (2018).
8. Cerri, S., Mus, L. & Blandini, F. Parkinson's Disease in Women and Men: What's the Difference? *J Parkinsons Dis* **9**, 501-515 (2019).
9. Lopez-Lee, C., Torres, E.R.S., Carling, G. & Gan, L. Mechanisms of sex differences in Alzheimer's disease. *Neuron* **112**, 1208-1221 (2024).

10. Juul Rasmussen, I., Rasmussen, K.L., Nordestgaard, B.G., Tybjaerg-Hansen, A. & Frikke-Schmidt, R. Impact of cardiovascular risk factors and genetics on 10-year absolute risk of dementia: risk charts for targeted prevention. *Eur Heart J* **41**, 4024-4033 (2020).
11. van Dyck, C.H. *et al.* Lecanemab in Early Alzheimer's Disease. *N Engl J Med* **388**, 9-21 (2023).
12. Livingston, G. *et al.* Dementia prevention, intervention, and care: 2024 report of the Lancet standing Commission. *Lancet* (2024).
13. Meng, L., Wang, Z., Ji, H.F. & Shen, L. Causal association evaluation of diabetes with Alzheimer's disease and genetic analysis of antidiabetic drugs against Alzheimer's disease. *Cell Biosci* **12**, 28 (2022).
14. Ma, Y., Ajnakina, O., Steptoe, A. & Cadar, D. Higher risk of dementia in English older individuals who are overweight or obese. *Int J Epidemiol* **49**, 1353-1365 (2020).
15. Thomassen, J.Q., Tolstrup, J.S., Benn, M. & Frikke-Schmidt, R. Type-2 diabetes and risk of dementia: observational and Mendelian randomisation studies in 1 million individuals. *Epidemiol Psychiatr Sci* **29**, e118 (2020).
16. Nianogo, R.A. *et al.* Risk Factors Associated With Alzheimer Disease and Related Dementias by Sex and Race and Ethnicity in the US. *JAMA Neurol* **79**, 584-591 (2022).
17. Gonzalez-Muniesa, P. *et al.* Obesity. *Nat Rev Dis Primers* **3**, 17034 (2017).
18. DeFronzo, R.A. *et al.* Type 2 diabetes mellitus. *Nat Rev Dis Primers* **1**, 15019 (2015).
19. Zeng, M. *et al.* Adiposity and dementia among Chinese adults: longitudinal study in the China Health and Retirement Longitudinal Study (CHARLS). *Int J Obes (Lond)* **49**, 706-714 (2025).
20. Cao, F. *et al.* The relationship between diabetes and the dementia risk: a meta-analysis. *Diabetol Metab Syndr* **16**, 101 (2024).
21. Andrews, S.J. *et al.* Causal Associations Between Modifiable Risk Factors and the Alzheimer's Phenome. *Ann Neurol* **89**, 54-65 (2021).
22. Lambert, J.C., Ramirez, A., Grenier-Boley, B. & Bellenguez, C. Step by step: towards a better understanding of the genetic architecture of Alzheimer's disease. *Mol Psychiatry* (2023).
23. Andrews, S.J. *et al.* The complex genetic architecture of Alzheimer's disease: novel insights and future directions. *EBioMedicine* **90**, 104511 (2023).
24. European, A.s. *et al.* Genetic Associations Between Modifiable Risk Factors and Alzheimer Disease. *JAMA Netw Open* **6**, e2313734 (2023).
25. Pulit, S.L. *et al.* Meta-analysis of genome-wide association studies for body fat distribution in 694 649 individuals of European ancestry. *Hum Mol Genet* **28**, 166-174 (2019).
26. Mahajan, A. *et al.* Multi-ancestry genetic study of type 2 diabetes highlights the power of diverse populations for discovery and translation. *Nat Genet* **54**, 560-572 (2022).
27. Bellenguez, C. *et al.* New insights into the genetic etiology of Alzheimer's disease and related dementias. *Nat Genet* **54**, 412-436 (2022).
28. Wu, Y. *et al.* Pervasive biases in proxy genome-wide association studies based on parental history of Alzheimer's disease. *Nat Genet* (2024).
29. Pedersen, E.M., Wimberley, T. & Vilhjalmsson, B.J. A cautionary tale for Alzheimer's disease GWAS by proxy. *Nat Genet* (2024).
30. Nicolas, A. *et al.* Transferability of European-derived Alzheimer's disease polygenic risk scores across multiancestry populations. *Nat Genet* **57**, 1598-1610 (2025).
31. Winkler, T.W. *et al.* The Influence of Age and Sex on Genetic Associations with Adult Body Size and Shape: A Large-Scale Genome-Wide Interaction Study. *PLoS Genet* **11**, e1005378 (2015).
32. Mahajan, A. *et al.* Fine-mapping type 2 diabetes loci to single-variant resolution using high-density imputation and islet-specific epigenome maps. *Nat Genet* **50**, 1505-1513 (2018).
33. Dubois, B. *et al.* Preclinical Alzheimer's disease: Definition, natural history, and diagnostic criteria. *Alzheimers Dement* **12**, 292-323 (2016).
34. Huang, L.O. *et al.* Genome-wide discovery of genetic loci that uncouple excess adiposity from its comorbidities. *Nat Metab* **3**, 228-243 (2021).
35. Huang, L.O., Loos, R.J.F. & Kilpelainen, T.O. Evidence of genetic predisposition for metabolically healthy obesity and metabolically obese normal weight. *Physiol Genomics* **50**, 169-178 (2018).
36. Garcia-Gonzalez, P. *et al.* Mendelian Randomisation Confirms the Role of Y-Chromosome Loss in Alzheimer's Disease Aetiopathogenesis in Men. *Int J Mol Sci* **24**(2023).
37. Mountjoy, E. *et al.* An open approach to systematically prioritize causal variants and genes at all published human GWAS trait-associated loci. *Nature Genetics* **53**, 1527-+ (2021).
38. Aguet, F. *et al.* The GTEx Consortium atlas of genetic regulatory effects across human tissues. *Science* **369**, 1318-1330 (2020).

39. Sun, B.B. *et al.* Plasma proteomic associations with genetics and health in the UK Biobank. *Nature* **622**, 329-338 (2023).
40. Avsec, Ž. *et al.* AlphaGenome: advancing regulatory variant effect prediction with a unified DNA sequence model. *bioRxiv*, 2025.06.25.661532 (2025).
41. Ge, S.X., Jung, D. & Yao, R. ShinyGO: a graphical gene-set enrichment tool for animals and plants. *Bioinformatics* **36**, 2628-2629 (2020).
42. Dominguez Conde, C. *et al.* Cross-tissue immune cell analysis reveals tissue-specific features in humans. *Science* **376**, eabl5197 (2022).
43. Altmann, A., Tian, L., Henderson, V.W., Greicius, M.D. & Alzheimer's Disease Neuroimaging Initiative, I. Sex modifies the APOE-related risk of developing Alzheimer disease. *Ann Neurol* **75**, 563-73 (2014).
44. Liu, S. *et al.* A clinical dose of angiotensin-converting enzyme (ACE) inhibitor and heterozygous ACE deletion exacerbate Alzheimer's disease pathology in mice. *J Biol Chem* **294**, 9760-9770 (2019).
45. Perrin, H.J. *et al.* Chromatin accessibility and gene expression during adipocyte differentiation identify context-dependent effects at cardiometabolic GWAS loci. *PLoS Genet* **17**, e1009865 (2021).
46. Ryan, D.K. *et al.* Genetic Evidence for Protective Effects of Angiotensin-Converting Enzyme Against Alzheimer Disease But Not Other Neurodegenerative Diseases in European Populations. *Neurol Genet* **8**, e200014 (2022).
47. Zheng, W. *et al.* Small molecule angiotensin converting enzyme inhibitors: A medicinal chemistry perspective. *Front Pharmacol* **13**, 968104 (2022).
48. Pan, S., Worker, C.J. & Feng Earley, Y. The hypothalamus as a key regulator of glucose homeostasis: emerging roles of the brain renin-angiotensin system. *Am J Physiol Cell Physiol* **325**, C141-C154 (2023).
49. Burrinha, T. *et al.* Deacidification of endolysosomes by neuronal aging drives synapse loss. *Traffic* **24**, 334-354 (2023).
50. Lin, D.T. & Conibear, E. ABHD17 proteins are novel protein depalmitoylases that regulate N-Ras palmitate turnover and subcellular localization. *Elife* **4**, e11306 (2015).
51. Yokoi, N. *et al.* Identification of PSD-95 Depalmitoylating Enzymes. *J Neurosci* **36**, 6431-44 (2016).
52. Chowdhury, D. *et al.* Ca(2+)/calmodulin binding to PSD-95 mediates homeostatic synaptic scaling down. *EMBO J* **37**, 122-138 (2018).
53. Remsberg, J.R. *et al.* ABHD17 regulation of plasma membrane palmitoylation and N-Ras-dependent cancer growth. *Nat Chem Biol* **17**, 856-864 (2021).
54. McClafferty, H., Runciman, H. & Shipston, M.J. Site-specific deacylation by ABHD17a controls BK channel splice variant activity. *J Biol Chem* **295**, 16487-16496 (2020).
55. Liu, X. *et al.* Calcium channels as pharmacological targets for cancer therapy. *Clin Exp Med* **25**, 94 (2025).
56. Jayaraman, S., Kochiss, A., Alcalay, T.L., Del Rivero Morfin, P.J. & Ben-Johny, M. Engineered depalmitoylases enable selective manipulation of protein localization and function. *Nat Commun* **16**, 3514 (2025).
57. Child, M.A. *et al.* Small-molecule inhibition of a depalmitoylase enhances Toxoplasma host-cell invasion. *Nat Chem Biol* **9**, 651-6 (2013).
58. Daugherty, A., Sawada, H., Sheppard, M.B. & Lu, H.S. Angiotensinogen as a Therapeutic Target for Cardiovascular and Metabolic Diseases. *Arterioscler Thromb Vasc Biol* **44**, 1021-1030 (2024).
59. Naseri, N. & Mofid, M.R. Role of IGFBP-3 in Human Diseases Relying on Different Cell Signaling Pathways. *Adv Biomed Res* **14**, 15 (2025).
60. Papp, Z. *et al.* Levosimendan: molecular mechanisms and clinical implications: consensus of experts on the mechanisms of action of levosimendan. *Int J Cardiol* **159**, 82-7 (2012).
61. Lim, S. *et al.* Levosimendan inhibits disulfide tau oligomerization and ameliorates tau pathology in Tau(P301L)-BiFC mice. *Exp Mol Med* **55**, 612-627 (2023).
62. Ghebremariam, Y.T. *et al.* FXR agonist INT-747 upregulates DDAH expression and enhances insulin sensitivity in high-salt fed Dahl rats. *PLoS One* **8**, e60653 (2013).
63. de Oliveira, M.C. *et al.* Bile acid receptor agonists INT747 and INT777 decrease oestrogen deficiency-related postmenopausal obesity and hepatic steatosis in mice. *Biochim Biophys Acta* **1862**, 2054-2062 (2016).
64. Verbeke, L. *et al.* Obeticholic acid, a farnesoid X receptor agonist, improves portal hypertension by two distinct pathways in cirrhotic rats. *Hepatology* **59**, 2286-98 (2014).

65. Jarvis, M.F. *et al.* A-317491, a novel potent and selective non-nucleotide antagonist of P2X3 and P2X2/3 receptors, reduces chronic inflammatory and neuropathic pain in the rat. *Proc Natl Acad Sci U S A* **99**, 17179-84 (2002).
66. Harrison, S.A. *et al.* A Phase 3, Randomized, Controlled Trial of Resmetirom in NASH with Liver Fibrosis. *N Engl J Med* **390**, 497-509 (2024).
67. Wang, X.F. *et al.* Linking Alzheimer's disease and type 2 diabetes: Novel shared susceptibility genes detected by cFDR approach. *Journal of the Neurological Sciences* **380**, 262-272 (2017).
68. Hardy, J., de Strooper, B. & Escott-Price, V. Diabetes and Alzheimer's disease: shared genetic susceptibility? *Lancet Neurol* **21**, 962-964 (2022).
69. Hong, H. *et al.* Investigating the common genetic architecture and causality of metabolic disorders with neurodegenerative diseases. *Diabetes Obes Metab* (2024).
70. Lee, E.H. *et al.* Different associations between body mass index and Alzheimer's markers depending on metabolic health. *Alzheimers Res Ther* **16**, 194 (2024).
71. Cho, S.H. *et al.* Association of late-life body mass index with the risk of Alzheimer disease: a 10-year nationwide population-based cohort study. *Sci Rep* **12**, 15298 (2022).
72. Kang, S.Y. *et al.* Body mass index trajectories and the risk for Alzheimer's disease among older adults. *Sci Rep* **11**, 3087 (2021).
73. Besser, L.M. *et al.* Body mass index, weight change, and clinical progression in mild cognitive impairment and Alzheimer disease. *Alzheimer Dis Assoc Disord* **28**, 36-43 (2014).
74. Venkatesh, S.S. *et al.* Characterising the genetic architecture of changes in adiposity during adulthood using electronic health records. *Nat Commun* **15**, 5801 (2024).
75. Cummings, J.L. *et al.* evoke and evoke+: design of two large-scale, double-blind, placebo-controlled, phase 3 studies evaluating efficacy, safety, and tolerability of semaglutide in early-stage symptomatic Alzheimer's disease. *Alzheimers Res Ther* **17**, 14 (2025).
76. Morris, M.C. *et al.* The cross-sectional association between blood pressure and Alzheimer's disease in a biracial community population of older persons. *J Gerontol A Biol Sci Med Sci* **55**, M130-6 (2000).
77. Guo, Z., Viitanen, M., Fratiglioni, L. & Winblad, B. Low blood pressure and dementia in elderly people: the Kungsholmen project. *BMJ* **312**, 805-8 (1996).
78. Qiu, C., von Strauss, E., Fastbom, J., Winblad, B. & Fratiglioni, L. Low blood pressure and risk of dementia in the Kungsholmen project: a 6-year follow-up study. *Arch Neurol* **60**, 223-8 (2003).
79. Jung, H. *et al.* Associations of hypertension burden on subsequent dementia: a population-based cohort study. *Sci Rep* **11**, 12291 (2021).
80. Hughes, D. *et al.* Association of Blood Pressure Lowering With Incident Dementia or Cognitive Impairment: A Systematic Review and Meta-analysis. *JAMA* **323**, 1934-1944 (2020).
81. Koskeridis, F. *et al.* Multi-trait association analysis reveals shared genetic loci between Alzheimer's disease and cardiovascular traits. *Nat Commun* **15**, 9827 (2024).
82. Brandon, J.A., Farmer, B.C., Williams, H.C. & Johnson, L.A. APOE and Alzheimer's Disease: Neuroimaging of Metabolic and Cerebrovascular Dysfunction. *Front Aging Neurosci* **10**, 180 (2018).
83. Raut, S. *et al.* Hypometabolism, Alzheimer's Disease, and Possible Therapeutic Targets: An Overview. *Cells* **12**(2023).
84. An, Y. *et al.* Evidence for brain glucose dysregulation in Alzheimer's disease. *Alzheimers Dement* **14**, 318-329 (2018).
85. Jeong, S., Lin, L., Leone, A.P. & Hsu, Y.H. Type 2 diabetes and late-onset Alzheimer's disease and related dementia: A longitudinal cohort study integrating polygenic risk score. *J Alzheimers Dis* **105**, 107-119 (2025).
86. Martin, J., Gordon, E.H., Reid, N., Hubbard, R.E. & Ward, D.D. Sex differences in modifiable dementia risk factors: Findings from the Rush Memory and Aging Project. *Alzheimers Dement* **21**, e70506 (2025).
87. Stinson, S.E. *et al.* Distinct metabolic signatures of Alzheimer's and Parkinson's disease revealed through genetic overlap with metabolic markers. *medRxiv* (2025).
88. Shvetcov, A. *et al.* APOE epsilon4 carriers share immune-related proteomic changes across neurodegenerative diseases. *Nat Med* **31**, 2590-2601 (2025).
89. Minikel, E.V., Painter, J.L., Dong, C.C. & Nelson, M.R. Refining the impact of genetic evidence on clinical success. *Nature* **629**, 624-629 (2024).
90. Plenge, R.M., Scolnick, E.M. & Altshuler, D. Validating therapeutic targets through human genetics. *Nat Rev Drug Discov* **12**, 581-94 (2013).

91. Decourt, B. *et al.* MCLENA-1: A Phase II Clinical Trial for the Assessment of Safety, Tolerability, and Efficacy of Lenalidomide in Patients with Mild Cognitive Impairment Due to Alzheimer's Disease. *Open Access J Clin Trials* **12**, 1-13 (2020).
92. Uffelmann, E. *et al.* Genomic analyses reveal new insights into Alzheimer's disease. *medRxiv*, 2025.10.10.25337470 (2025).
93. Pan, B. *et al.* Similarities and differences between variants called with human reference genome HG19 or HG38. *BMC Bioinformatics* **20**, 101 (2019).
94. R Core, T. R: a Language and Environment for Statistical Computing. (R Foundation for Statistical Computing, 2014).
95. Lawrence, M., Gentleman, R. & Carey, V. rtracklayer: an R package for interfacing with genome browsers. *Bioinformatics* **25**, 1841-2 (2009).
96. Pagès, H. BSgenome: Software infrastructure for efficient representation of full genomes and their SNPs. R package version 1.68.0 edn (2023).
97. Bulik-Sullivan, B.K. *et al.* LD Score regression distinguishes confounding from polygenicity in genome-wide association studies. *Nat Genet* **47**, 291-5 (2015).
98. Foote, I.F. *et al.* The shared genetic architecture of modifiable risk for Alzheimer's disease: a genomic structural equation modelling study. *Neurobiol Aging* **117**, 222-235 (2022).
99. Silaparasetty, N. Python Programming in Jupyter Notebook. In: Machine Learning Concepts with Python and the Jupyter Notebook Environment. (Apress, Berkeley, CA, 2020).
100. Suzuki, K. *et al.* Genetic drivers of heterogeneity in type 2 diabetes pathophysiology. *Nature* **627**, 347-357 (2024).
101. Drucker, D.J. GLP-1-based therapies for diabetes, obesity and beyond. *Nat Rev Drug Discov* (2025).
102. Wu, Y. *et al.* Pervasive biases in proxy GWAS based on parental history of Alzheimer's disease. *bioRxiv*, 2023.10.13.562272 (2023).
103. Foley, C.N. *et al.* A fast and efficient colocalization algorithm for identifying shared genetic risk factors across multiple traits. *Nat Commun* **12**, 764 (2021).
104. Gazal, S. *et al.* Combining SNP-to-gene linking strategies to identify disease genes and assess disease omnigenicity. *Nat Genet* **54**, 827-836 (2022).
105. Sasse, A. *et al.* Benchmarking of deep neural networks for predicting personal gene expression from DNA sequence highlights shortcomings. *Nat Genet* **55**, 2060-2064 (2023).
106. Tarhan, L. *et al.* Single Cell Portal: an interactive home for single-cell genomics data. *bioRxiv* (2023).
107. Zhong, J. *et al.* adiposetissue.org: A knowledge portal integrating clinical and experimental data from human adipose tissue. *Cell Metab* **37**, 566-569 (2025).
108. Guilliams, M. *et al.* Spatial proteogenomics reveals distinct and evolutionarily conserved hepatic macrophage niches. *Cell* **185**, 379-396 e38 (2022).
109. Wachowski, N.A. *et al.* Implicating type 2 diabetes effector genes in relevant metabolic cellular models using promoter-focused Capture-C. *Diabetologia* **67**, 2740-2753 (2024).
110. Laakso, M. *et al.* The Metabolic Syndrome in Men study: a resource for studies of metabolic and cardiovascular diseases. *J Lipid Res* **58**, 481-493 (2017).
111. Brotman, S.M. *et al.* Adipose tissue eQTL meta-analysis highlights the contribution of allelic heterogeneity to gene expression regulation and cardiometabolic traits. *Nat Genet* **57**, 180-192 (2025).
112. Yu, G., Wang, L.G. & He, Q.Y. ChIPseeker: an R/Bioconductor package for ChIP peak annotation, comparison and visualization. *Bioinformatics* **31**, 2382-3 (2015).
113. Zhang, K. *et al.* A single-cell atlas of chromatin accessibility in the human genome. *Cell* **184**, 5985-6001 e19 (2021).
114. Roadmap Epigenomics, C. *et al.* Integrative analysis of 111 reference human epigenomes. *Nature* **518**, 317-30 (2015).
115. Jung, I. *et al.* A compendium of promoter-centered long-range chromatin interactions in the human genome. *Nat Genet* **51**, 1442-1449 (2019).
116. Ma, H. *et al.* The nuclear receptor THRB facilitates differentiation of human PSCs into more mature hepatocytes. *Cell Stem Cell* **29**, 795-809 e11 (2022).
117. Broadaway, K.A. *et al.* Liver eQTL meta-analysis illuminates potential molecular mechanisms of cardiometabolic traits. *Am J Hum Genet* **111**, 1899-1913 (2024).
118. Consortium, G.T. The GTEx Consortium atlas of genetic regulatory effects across human tissues. *Science* **369**, 1318-1330 (2020).
119. Gong, Y. *et al.* Stereo-seq of the prefrontal cortex in aging and Alzheimer's disease. *Nat Commun* **16**, 482 (2025).

120. Argente, J. *et al.* Hypothalamic obesity: from basic mechanisms to clinical perspectives. *Lancet Diabetes Endocrinol* **13**, 57-68 (2025).
121. Chen, S. *et al.* Spatially resolved transcriptomics reveals genes associated with the vulnerability of middle temporal gyrus in Alzheimer's disease. *Acta Neuropathol Commun* **10**, 188 (2022).
122. Evangelista, J.E. *et al.* Enrichr-KG: bridging enrichment analysis across multiple libraries. *Nucleic Acids Res* **51**, W168-W179 (2023).
123. Mitchell, D.C. *et al.* A proteome-wide atlas of drug mechanism of action. *Nat Biotechnol* **41**, 845-857 (2023).

Table 1 | Dataset details.

Dataset	Cases	Controls	Total	Source
AD1	39,106 diagnosed 46,828 proxies	401,577	487.511	EADB consortium meta-analysis[1]
AD2	39,106 diagnosed	401,577	440.683	EADB consortium meta-analysis
AD3	36,659 diagnosed	63,137	99.796	
BMI	-	-	681,275	GIANT consortium meta-analysis[2]
BMI male	-	-	374,756	GIANT consortium[3]
BMI female	-	-	434,794	
BMI male under 50	-	-	50,095	
BMI male over 50	-	-	93,021	
BMI female under 50	-	-	70,692	
BMI female over 50	-	-	106,497	
T2D	180,834	1,159,055	1,339,889	T2D genomics Initiative meta-analysis[4]
T2D male	41,846	383,767	425,613	T2D genomics Initiative[5]
T2D female	30,053	434,336	464,389	

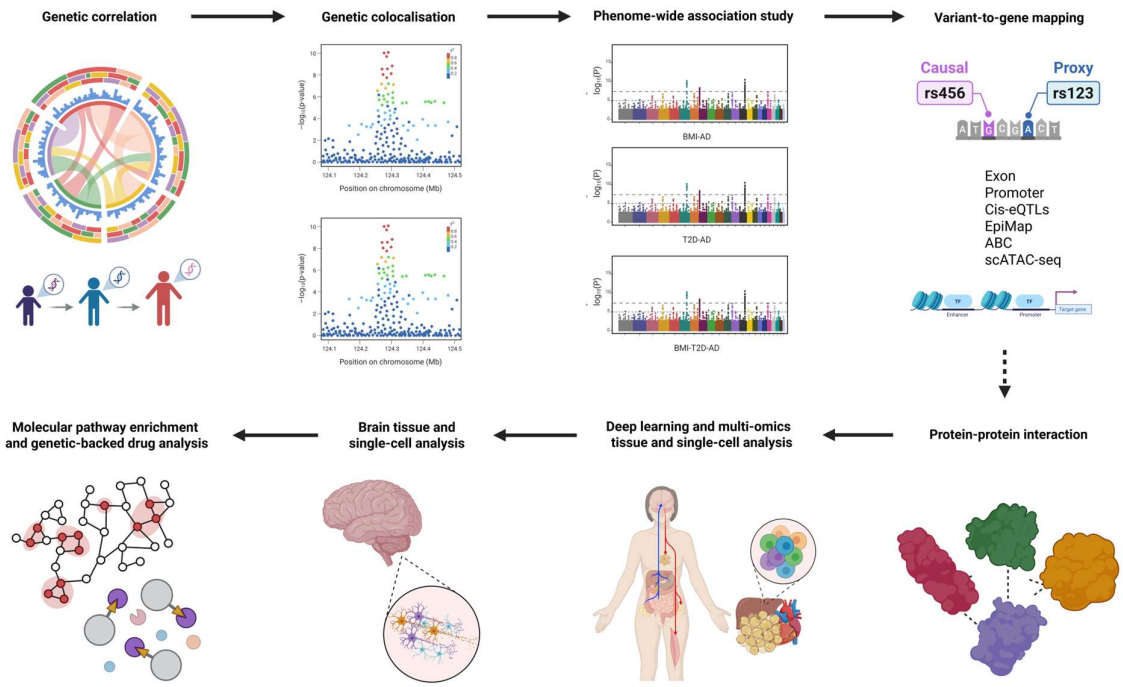

Fig. 1 | Schematic overview of the study. Created in BioRender.

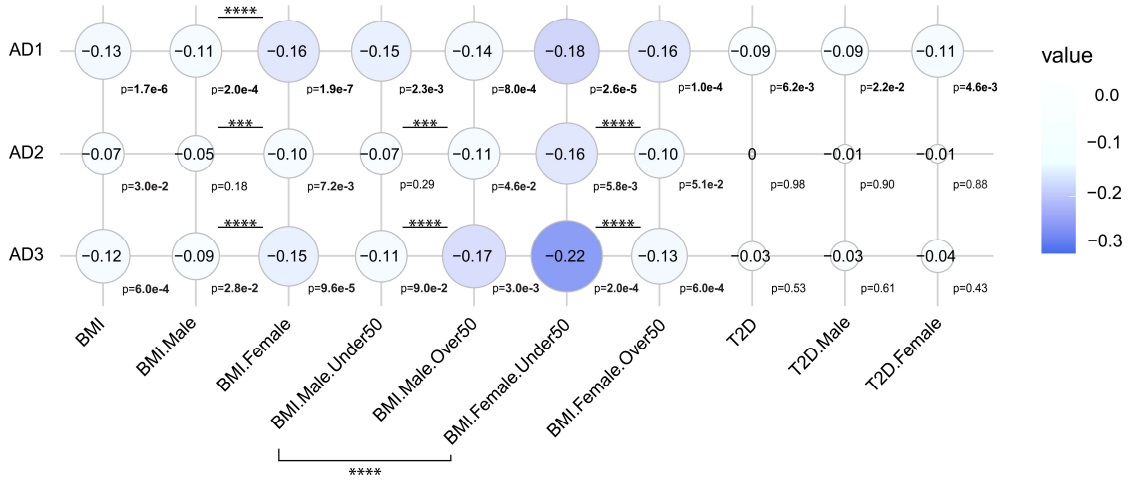

Fig. 2 | Cross-phenotype genetic correlation estimates. AD1: Includes AD proxy cases and non-age-matched controls. AD2: Excludes AD proxy cases, but retains non-age matched controls. AD3: Excludes AD proxy cases and non-age-matched controls. Sex-combined datasets: AD1, AD2, AD3, BMI, T2D. Sex and age-stratified datasets: BMI.Male, BMI.Female, BMI.Male.Under50, BMI.Male.Over50, BMI.Female.Under50, BMI.Female.Over50, T2D.Male, T2D.Female. The genetic correlation matrix was generated using the *corrplot* library in R (version 4.2.2). P-values are shown next to GC estimates. Statistical significance between genetic correlation estimates are stratified by p<0.05 (*); p<0.01 (**); p<0.001 (***); p<0.0001 (****) (**Table S1**).

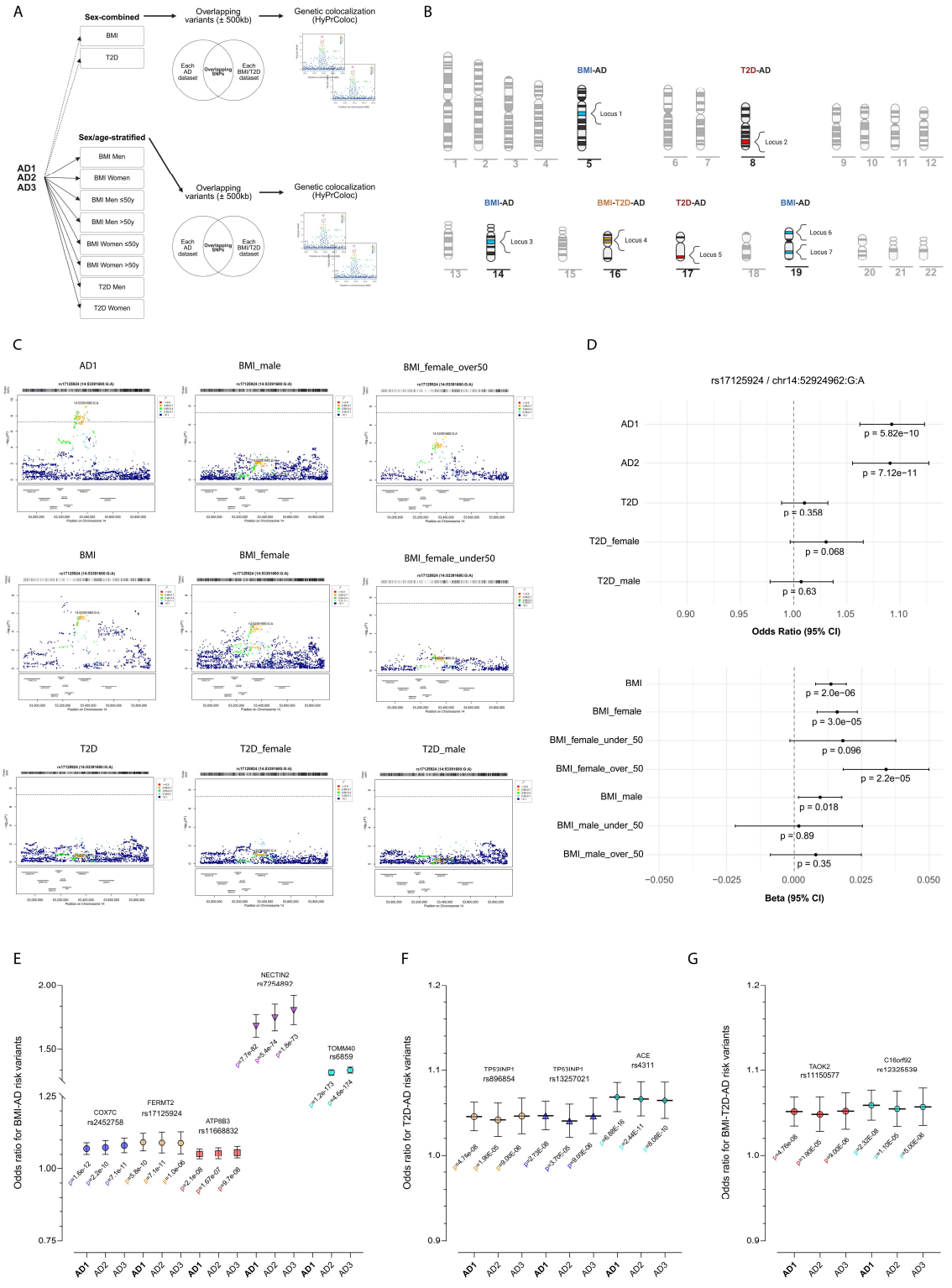

Fig. 3 | Genetic colocalization analysis. (**A**) Schematic overview of the multi-trait colocalized locus discovery pipeline. (**B**) Karyotype representation of the colocalized loci for BMI-AD (chr5, chr14, chr19), T2D-AD (chr8, chr17) and BMI-T2D-AD (chr16). (**C**) Locuszoom plots for the BMI-AD rs17125924 locus (GRCh37). The overlapped variant is circled in green (**Table S3**) while the colocalized variant is shown in yellow (rs17125924). Variants in linkage disequilibrium (R^2) are color-coded. (**D**) Forest plot for the

BMI-AD rs17125924 locus showcasing odds ratio for dichotomous traits (AD and T2D) and effect size (beta) for the continuous trait (BMI). P-values are shown under each odds ratio/beta estimate. Odds ratio and p-values for (E) BMI-AD, (F) T2D-AD and (G) BMI-T2D-AD risk variants across AD datasets (AD1, AD2 and AD3).

Table 2 | Novel sex and age-specific loci associated with BMI-AD, T2D-AD and BMI-T2D-AD (**Table S3**).

Traits	Effect direction	Colocalized SNP	Closest Gene	PPC	Chr	Pos	EA (↑ AD)	NEA	EAF (%)	Beta (SE)	P
BMI-AD											
AD2	+	rs2452758	COX7C	0.569	5	86885886	G	A	76.0	0.07 (0.010)	$2.2x10^{-10}$
BMI_female	+								78.0	0.01 (0.003)	$1.6x10^{-5}$
AD1	+	rs17125924	FERMT2	0.793	14	52924962	G	A	9.0	0.09 (0.014)	$5.8x10^{-10}$
BMI_female	+								8.0	0.02 (0.004)	$3.0x10^{-5}$
BMI_female_over50	+								7.0	0.03 (0.008)	$2.2x10^{-5}$
AD1	+	rs11668832	**ATP8B3**	0.853	19	1812683	A	G	4.6	0.05 (0.009)	$2.1x10^{-8}$
BMI	-								4.6	-0.01 (0.002)	$7.5x10^{-15}$
AD1	+	rs7254892	TOMM40	0.999	19	44886339	G	A	9.7	0.52 (0.027)	$7.7x10^{-82}$
BMI	-								9.6	-0.03 (0.005)	$4.0x10^{-9}$
AD2	+	rs6859	NECTIN2	0.552	19	44878777	A	G	4.5	0.270 (0.009)	$1.2x10^{-173}$
BMI	-								4.1	-0.009 (0.002)	$4.6x10^{-7}$
T2D-AD											
AD1	+	rs13257021	TP53INP1	0.888	8	94953467	G	A	5.3	0.045 (0.008)	$2.7x10^{-8}$
T2D	-								5.1	-0.049 (0.006)	$3.1x10^{-14}$
AD1	+	rs13257021	TP53INP1	0.888	8	94953467	G	A	5.3	0.045 (0.008)	$2.7x10^{-8}$
T2D_female	-								5.1	-0.050 (0.009)	$3.2x10^{-7}$
AD1	+	rs896854	TP53INP1	0.870	8	94948283	C	T	5.1	0.044 (0.008)	$4.8x10^{-8}$
T2D_male	-								5.0	-0.053 (0.009)	$3.4x10^{-10}$
AD1	+	rs4311	ACE	0.566	17	63483402	C	T	5.2	0.066 (0.008)	$6.9x10^{-16}$
T2D	-								5.2	-0.028 (0.007)	$1.8x10^{-5}$
AD1	+	rs4311	ACE	0.566	17	63483402	C	T	5.2	0.066 (0.008)	$6.9x10^{-16}$
T2D_male	-								5.3	-0.040 (0.009)	$3.0x10^{-6}$
AD2	+	rs4311	ACE	0.566	17	63483402	C	T	5.1	0.064 (0.009)	$2.4x10^{-11}$
T2D_male	-								5.3	-0.040 (0.009)	$3.0x10^{-6}$
BMI-T2D-AD											
AD1	+	rs12325539	C16orf92	0.987	16	30022312	T	C	6.2	0.057 (0.008)	$1.2x10^{-11}$
T2D	-								6.0	-0.041 (0.007)	$2.7x10^{-10}$
AD1	+	rs11150577	TAOK2	0.321	16	29975204	G	A	5.7	0.050 (0.008)	$1.4x10^{-9}$
BMI_female	-								5.4	-0.022 (0.002)	$2.6x10^{-21}$
BMI_female_over50	-								5.2	-0.023 (0.005)	$9.0x10^{-6}$
T2D_female	-								5.5	-0.035 (0.010)	$2.9x10^{-4}$
AD1	+	rs12325539	C16orf92	0.962	16	30022312	T	C	6.2	0.057 (0.008)	$1.2x10^{-11}$
T2D_male	-								6.0	-0.043 (0.009)	$9.3x10^{-7}$

Effect direction: aligned to the risk increasing allele for AD. **Colocalized**: SNP identified by HyPrColoc to drive the same genetic signal in both traits. **SNP**: Single nucleotide polymorphism. **PPC**: Posterior Probability of Colocalization. **Chr**: Chromosome. **Pos**: Position in hg38. **EA**: Effect allele aligned to the risk increasing allele for AD. **NEA**: Non-effect allele. **LD**: Linkage disequilibrium. **NEAF**: Non-effect allele frequency. **Beta (SE)**: effect size (standard error). **P**: p-value.

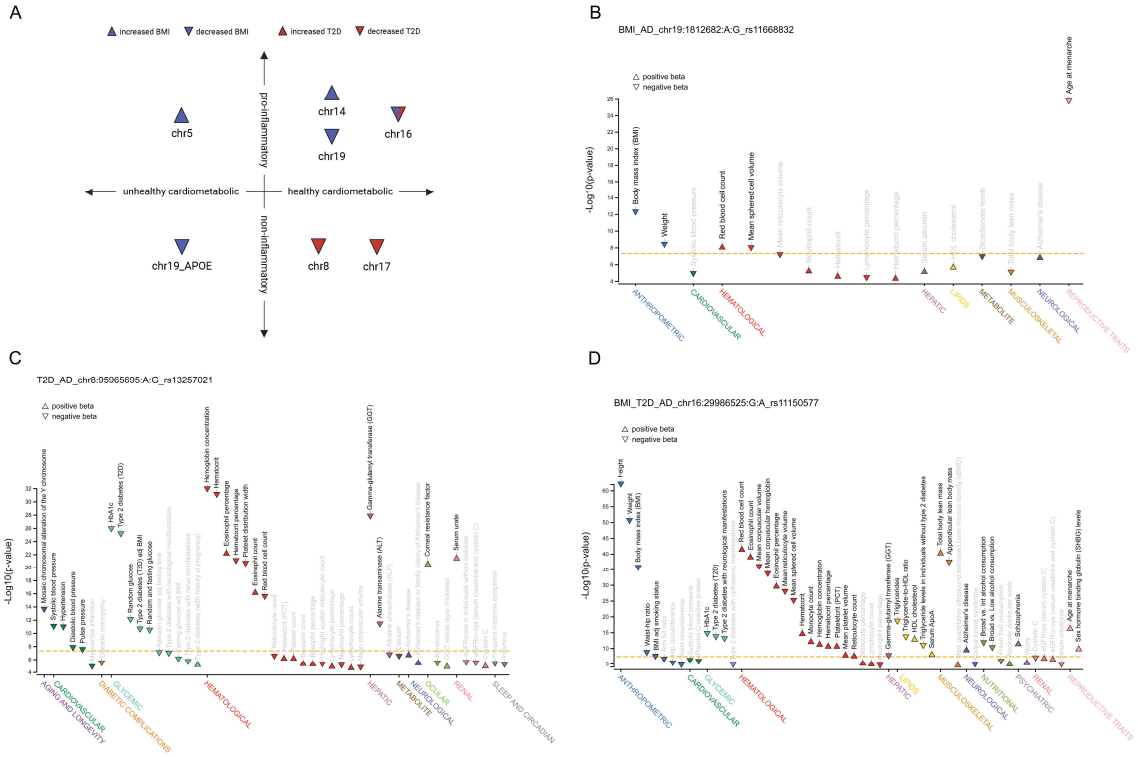

Fig. 4 | Phenome wide association study (PheWAS) analyses. (**A**) Summary of PheWAS associations of inflammatory and cardiometabolic profiles. PheWAS profile of the (**B**) rs11668832 BMI-AD locus (ATP8B3) in chr19, (**C**) rs13257021 T2D-AD locus (TP53INP1) in chr8 and (**D**) rs11150577 BMI-T2D-AD locus (TAOK2) in chr16. PheWAS p-value is set at a Bonferroni corrected threshold of 4.3×10^{-5} (orange dotted line). All PheWAS results are aligned to the risk-increasing allele for AD. Position in hg19.

Table 3 | Genes with functional evidence across colocalized shared loci (all variants in the same credible set with the colocalized variant). The closest gene and those with coding evidence (exon or promoter) are shown in bold. Genes in each locus are ranked by mapping confidence from cS2G (**Table S5**).

Colocalized variant Locus (± 500kb)	**Gene**	**AD**	**Phenotype pair**	**Credible set**	**Coloc. variant**
				cS2G Annotation	**GTEx-sQTL**
BMI-AD					
rs2452758 chr5:86385886-87385886	**COX7C**	Reported	Novel	**Closest,** ABC	-
rs17125924 chr14:52424962-53424962	**FERMT2**	Reported	Reported[6]	**Exon**, **Promoter**, **Closest**, GTEx-eQTL, EpiMap, ABC,	sQTL
rs11668832 chr19:1312683-2312683	**ATP8B3**	Reported	Novel	**Promoter**, **Closest**, GTEx-eQTL, EpiMap, ABC	sQTL
	REXO1	Reported	Novel	**Promoter**, GTEx-eQTL, EpiMap, ABC	-
	ABHD17A	Reported	Novel	eQTLGen	sQTL
	ADAT3	Novel	Novel	EpiMap	-
	SCAMP4	Novel	Novel	EpiMap	-
rs7254892 chr19:44386339-45386339	**NECTIN2 (PVRL2)**	Reported	Novel	**Exon**, **Closest**, GTEx-eQTL, EpiMap	-
rs6859 chr19:44378777-45378777	**TOMM40**	Reported	Novel	**Exon**, **Closest**	-
	APOC1	Reported	Novel	EpiMap	-
T2D-AD					
rs13257021 chr8:94453467-95453467	**TP53INP1**	Reported	Reported[7]	**Exon**, **Promoter**, **Closest**, eQTLGen, GTEx-eQTL, Cicero, EpiMap, ABC	-
	INTS8	Novel	Novel	**Exon**, eQTLGen, EpiMap, ABC	sQTL
rs896854 chr8:94448283-95448283	**NDUFAF6**	Reported	Reported[8]	**Promoter**, GTEx-eQTL, Cicero	sQTL
	CCNE2	Reported	Novel	eQTLGen, GTEx-eQTL, EpiMap, ABC	-
	PLEKHF2	Novel	Novel	Cicero	-
rs4311 chr17:62983402-6398.402	**ACE**	Reported	Reported[8,9]	**Exon**, **Promoter**, **Closest**, eQTLGen, GTEx-eQTL, EpiMap, ABC	sQTL
	KCNH6	Novel	Novel	GTEx-eQTL, EpiMap	sQTL
	DCAF7	Novel	Novel	GTEx-eQTL	-
BMI-T2D-AD					
rs11150577 chr16:29475204-30475204 **rs12325539** chr16:29522312-30522312	**TAOK2**	Novel	Novel	**Exon**, **Promoter**, **Closest**, EpiMap, ABC,	sQTL
	TMEM219	Reported	Novel	**Exon**, **Promoter**, ABC	-
	DOC2A	Reported	Reported T2D-AD[8]	**Exon**, **Promoter**, GTEx-eQTL, ABC	sQTL
	TLCD3B	Novel	Novel	**Promoter**, GTEx-eQTL, EpiMap, ABC	sQTL
	TBX6	Reported	Novel	**Exon**	sQTL
	C16orf92	Reported	Novel	Cicero, **Closest**	-
	INO80E	Reported	Novel	eQTLGen, GTEx-eQTL, ABC	sQTL
	PPP4C	Reported	Novel	eQTLGen, EpiMap, ABC	-
	MAPK3	Reported	Novel	eQTLGen, EpiMap	-
	KCTD13	Reported	Novel	eQTLGen, EpiMap,	sQTL
	YPEL3	Reported	Novel	GTEx-eQTL, EpiMap	sQTL
	GDPD3	Reported	Novel	GTEx-eQTL	-
	MVP	Novel	Reported T2D-AD[10]	EpiMap	sQTL
	SPN	Reported	Novel	EpiMap	-
	MAZ	Reported	Novel	EpiMap	-
	C16orf54	Novel	Novel	EpiMap	-
	HIRIP3	Reported	Novel	ABC	-

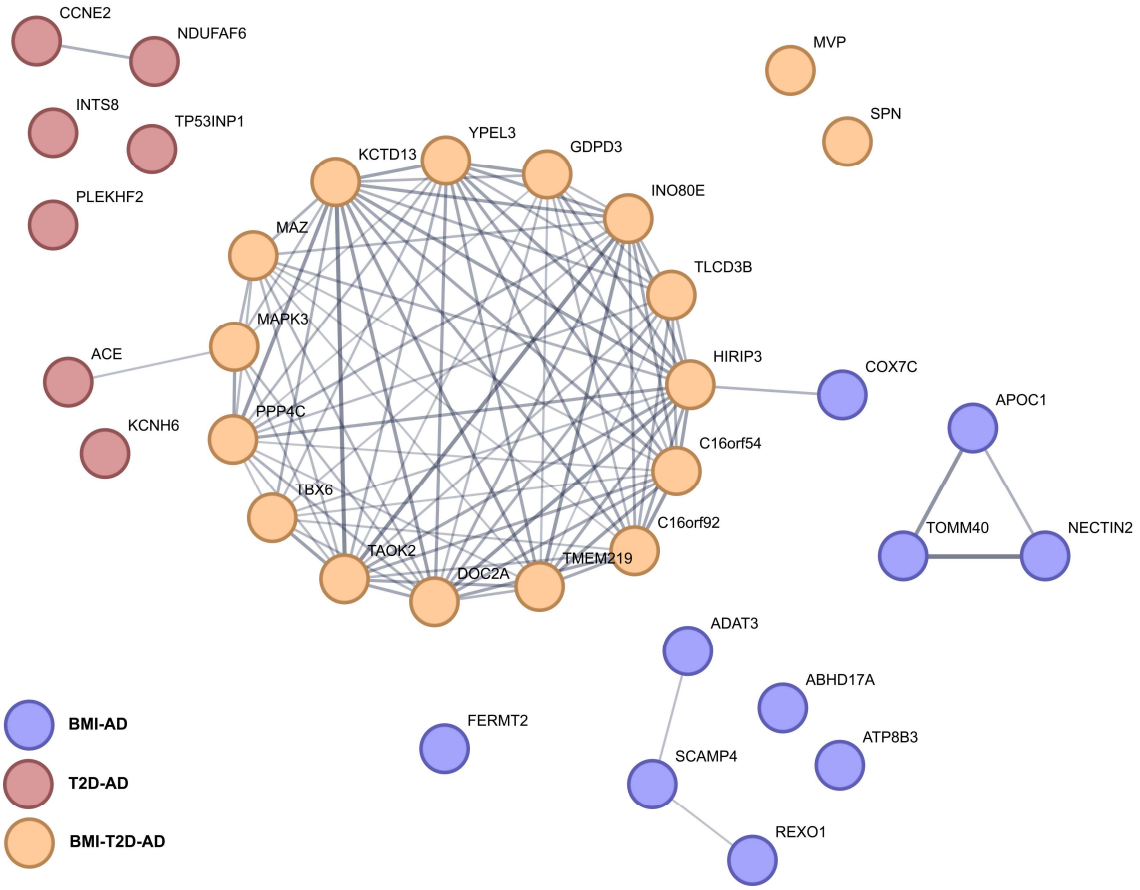

Fig. 5 | Protein-protein interaction (PPI) analysis. Genes from **Table 3** were included. Analysis performed in STRING (version 12.0), indicating both functional and physical protein associations with sufficient confidence (0.4) including data from text mining, experiments, databases, co-expression, neighborhood, gene fusion and co-occurrence. Line thickness indicates the strength of data support.

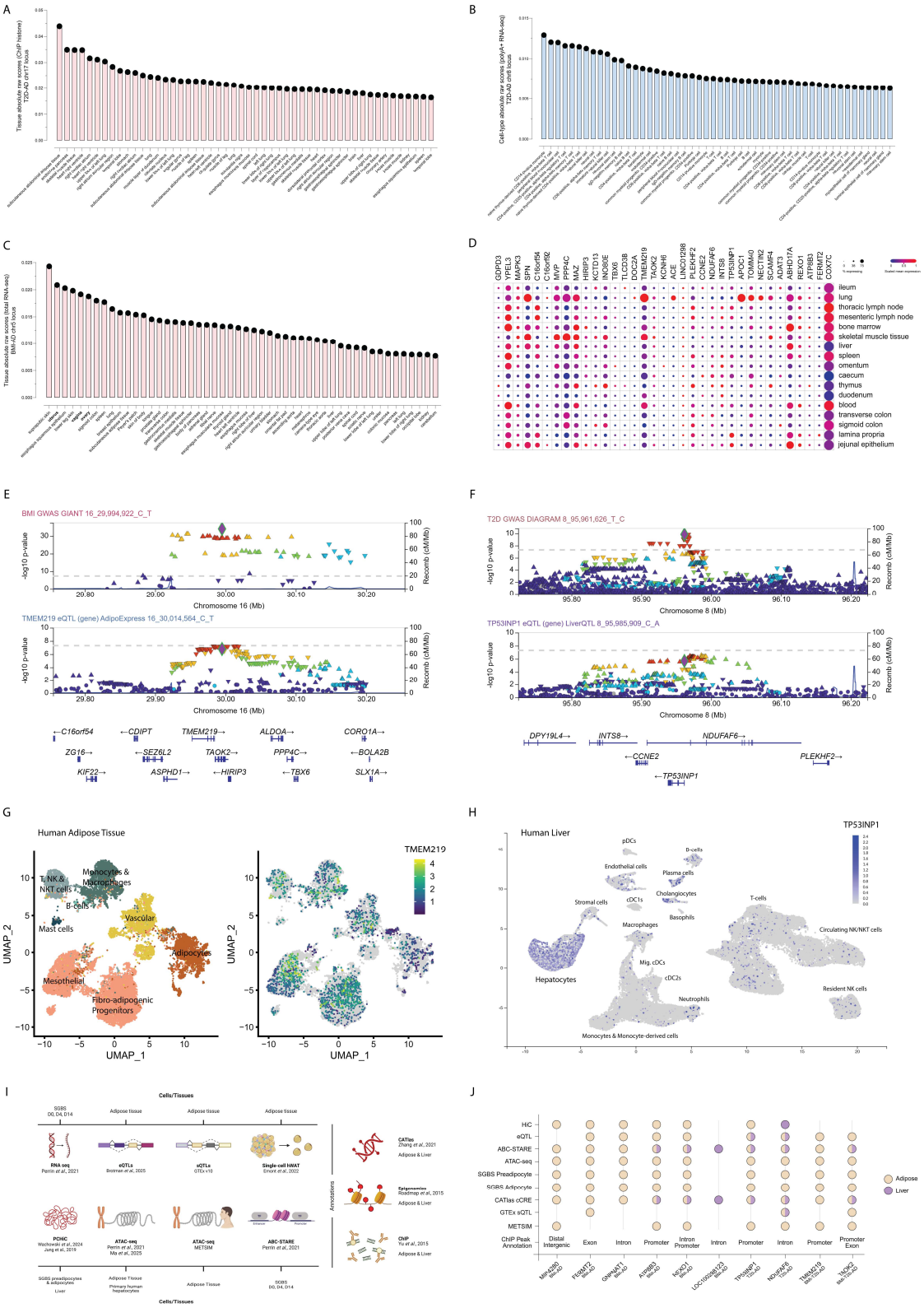

Fig. 6 | Immune and metabolic tissue association analyses.
(**A**) AlphaGenome *in silico* perturbation prediction of the colocalized risk variant (rs4311) in the T2D-AD chr17 locus. The graph showcases the tissues where histone modifications (predicted from chromatin

immunoprecipitation data) are most affected by perturbing the rs4311 variant. (**B**) AlphaGenome *in silico* perturbation prediction of the colocalized risk variant (rs13257021) in the T2D-AD chr8 locus. The graph showcases the cell-types where gene expression (predicted from poly(A) tail-containing RNA sequencing data) is most affected by perturbing the rs13257021 variant. (**C**) AlphaGenome *in silico* perturbation prediction of the colocalized risk variant (rs2452758) in the BMI-AD chr5 locus. The graph showcases the tissues where gene expression (predicted from total RNA sequencing data) is most affected by perturbing the rs2452758 variant. (**D**) Individual gene expression and % of expressing cells within the immune compartment of 17 peripheral tissues. (**E**) GWAS-eQTL colocalization locuszoom (LZ) region plot for BMI and TMEM219 eQTL in adipose tissue. (**F**) GWAS-eQTL colocalization LZ region plot for T2D and TP53INP1 eQTL in liver. (**G**) Human adipose tissue single-cell expression of TMEM219. (**H**) Human liver single-cell expression of TP53INP1. (**I**) Schematic overview of enhancer-to-gene (E2G) in adipose tissue and liver. (**J**) Summary associations of prioritized genes by E2G in adipose tissue and liver.

Table 4 | Summary table of colocalized GWAS-eQTL pairs (build 37) in metabolic tissues, including adipose, pancreatic islets, liver and muscle.

Colocalized variant Locus (± 100kb)	**GWAS trait**	**eQTL gene**	**eQTL tissue**	**PPC**
BMI-AD				
rs11668832 chr19:1712682-1912682	HC	ATP8B3	adipose	0.96
	HC	ABHD17A	adipose	0.69
	WC	ATP8B3	adipose	0.94
	WC	ABHD17A	adipose	0.73
rs7254892 chr19:45289596-45489596 **rs6859** chr19:45282034-45482034	HDL	APOC4-APOC2	adipose	0.98
	HDL	APOC2	adipose	1.00
	HDL	APOC4	adipose	0.98
	LDL	APOE	adipose	1.00
	LDL	APOC1P1	adipose	1.00
	logTG	APOE	adipose	1.00
	logTG	APOC1P1	adipose	1.00
	nonHDL	APOE	adipose	1.00
	nonHDL	APOC1P1	adipose	1.00
	TC	APOE	adipose	1.00
	TC	APOC1P1	adipose	0.93
T2D-AD				
rs13257021 chr8:95865695-96065695 **rs896854** chr8:95860511-96060511	FG	TP53INP1	liver	0.84
	T2D	TP53INP1	liver	0.88
	FG	NDUFAF6	adipose	0.91
	T2D	NDUFAF6	adipose	0.67
	T2D	CCNE2	adipose	0.63
rs4311 chr17:61460763-61660763	DBP	ACE	adipose	0.98
	DBP	ACE	adipose	0.98
BMI-T2D-AD				
rs11150577 chr16:29933633-30133633 **rs12325539** chr16:29886525-30086525	BMI	INO80E	liver	0.68
	HDL	INO80E	liver	0.84
	T2D	INO80E	liver	0.88
	WC	INO80E	liver	0.92
	WHR	INO80E	liver	0.95
	logTG	INO80E	liver	0.94
	BMI	DOC2A	adipose	0.90
	BMI	TMEM219	adipose	0.96
	BMI	RP11-455F5.3	adipose	0.60
	HC	KCTD13	adipose	0.96
	HDL	DOC2A	adipose	0.90
	HDL	HIRIP3	adipose	0.66
	HDL	TMEM219	adipose	0.94
	logTG	TMEM219	adipose	0.75
	T2D	PPP4C	adipose	0.75
	T2D	DOC2A	adipose	0.86
	T2D	HIRIP3	adipose	0.63
	T2D	TMEM219	adipose	0.88
	T2D	RP11-455F5.3	adipose	0.88
	WC	KCTD13	adipose	0.81
	WC	DOC2A	adipose	0.82
	WC	TMEM219	adipose	0.92
	WHR	DOC2A	adipose	0.97
	WHR	TMEM219	adipose	0.97
	WHR	HIRIP3	adipose	0.88
	T2D	INO80E	muscle	0.70
	T2D	ALDOA	islet	0.56
	T2D	INO80E	islet	0.72

PPC: Posterior Probability of Colocalization**, HC**: Hip circumference, **WC**: Waist circumference, **HDL**: High-density lipoprotein cholesterol, **LDL**: Low-density lipoprotein cholesterol, **logTG**: Log-transformed triglycerides, **nonHDL**: Non-high-density lipoprotein cholesterol, **TC**: Total cholesterol, **FG**: Fasting glucose, **T2D**: Type 2 diabetes, **DBP**: Diastolic blood pressure, **BMI**: Body mass index, **WHR**: Waist-to-hip ratio

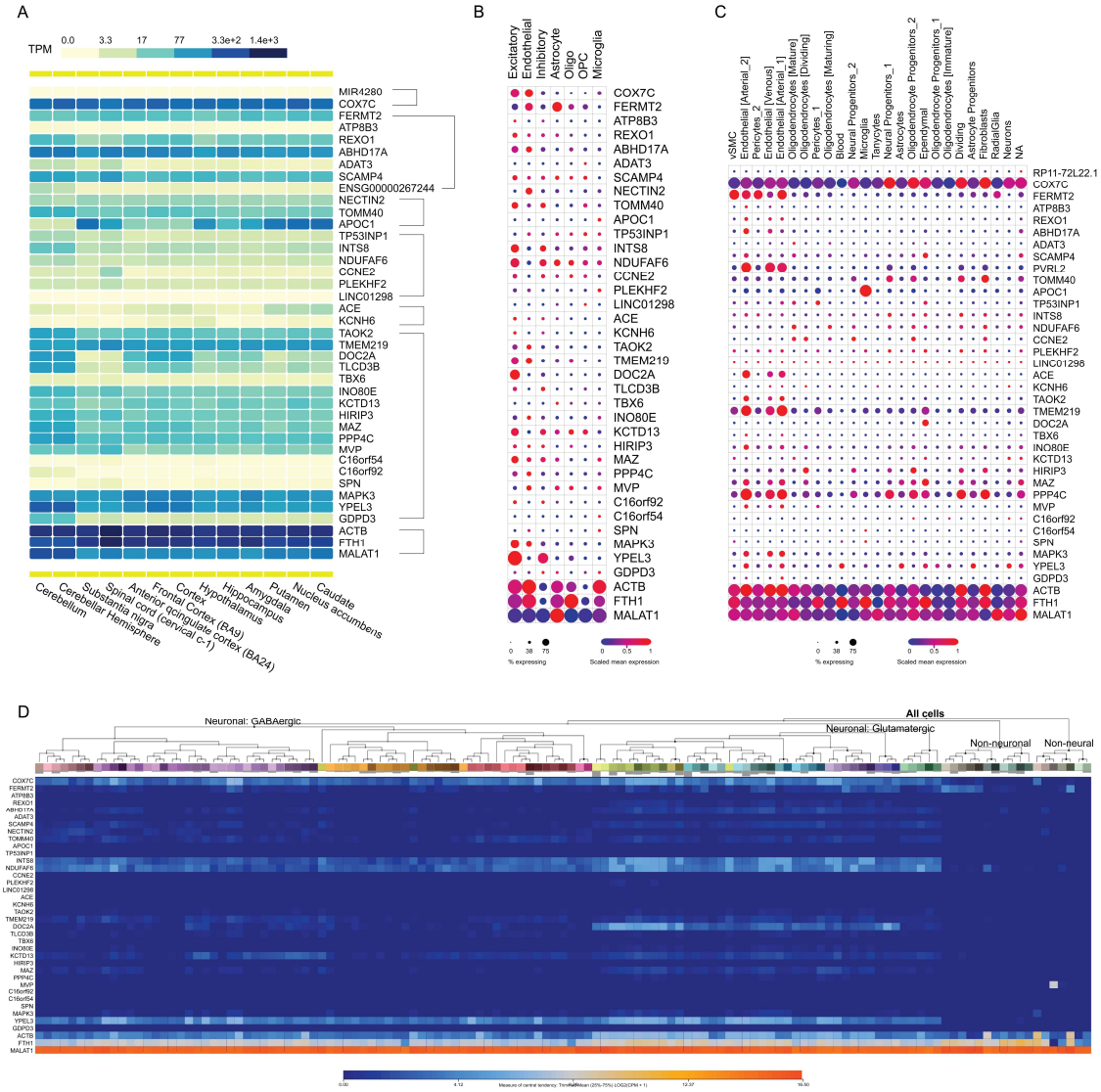

Fig. 7 | Regional and single-cell neural expression of high likelihood effector risk genes across colocalized loci. (**A**) Bulk tissue expression from multiple regions across the neurotypical brain (GTEx). (**B**) Single-cell gene expression in the neurotypical prefrontal cortex (PFC). (**C**) Single-cell gene expression in the neurotypical hypothalamus. (**D**) Single-cell gene expression in the middle temporal gyrus (MTG) of individuals with AD. ACTB, FTHI1 and MALAT1 were used as reference genes due to their high and ubiquitous expression levels across brain regions and cell-types[11].

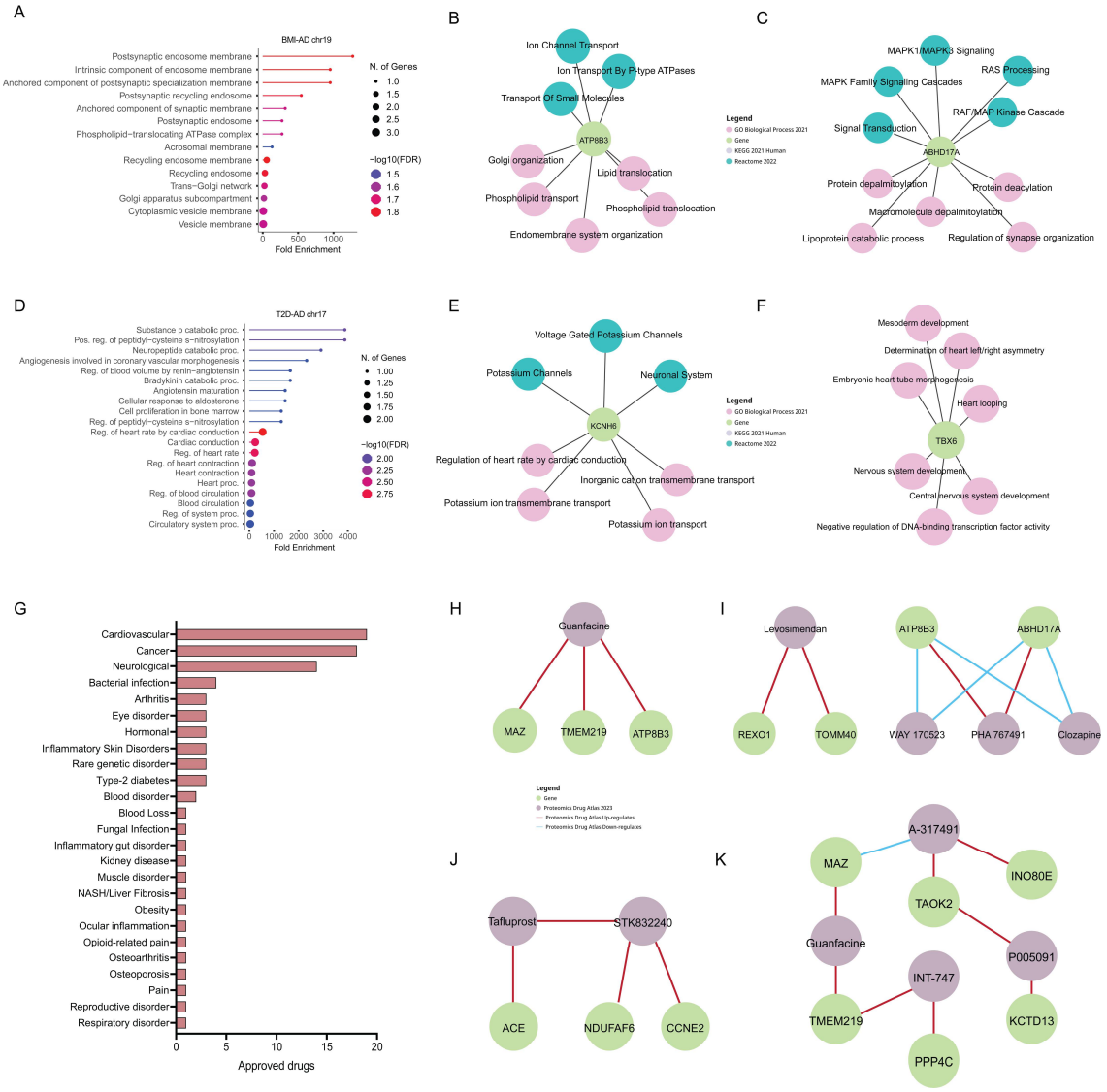

Fig. 8 | Enrichment and proteomic-based drug targeting analyses. (**A**) GO cellular components enrichment analysis for all genes with functional annotation in the BMI-AD chr19 locus. (**B**) Individual gene enrichment analysis for ATP8B3. (**C**) Individual gene enrichment analysis for ABHD17A. (**D**) GO cellular components enrichment analysis for genes with coding annotation in the T2D-AD chr17 locus. (**E**) Individual gene enrichment analysis for KCNH6. (**F**) Individual gene enrichment analysis for TBX6. (**G**) Summary of compound categories based on proteomic drug atlas hits for all effector genes. Proteomic drug atlas enrichment analysis for (**H**) all effector genes (minimum 3 links per drug target); (**I**) BMI-AD effector genes; (**J**) T2D-AD effector genes; BMI-T2D-AD effector genes. Enrichment analyses' false discovery rate (FDR) was set at 0.05.

Table 5 | Therapeutic programmes targeting effector genes driving shared BMI, T2D and AD genetics.

Gene	Status	Indication
ACE	Multiple approved drugs[12] Phase 3[13]	Hypertension, cardiovascular disease, heart failure, dyslipidemia, kidney disease
MAPK3	Preclinical[14]	Drug resistance, triple-negative breast cancer, solid tumors
NECTIN2	Preclinical[15]	Ovarian cancer immunotherapy
TAOK2	Preclinical[16,17]	Cancer
TMEM219	Preclinical[18,19]	Liver fibrosis, gastrointestinal autoimmune disorders
ATP8B3	Preclinical[20]	Colon adenocarcinoma immunotherapy
CCNE2	Preclinical[21,22]	Breast cancer
ABHD17A	Preclinical[23]	NRAS-mutant cancers
GDPD3	Preclinical[24]	Hepatic steatosis
TP53INP1	Preclinical[25]	Castration-resistant prostate cancer
FERMT2	Preclinical[26]	Prostate cancer
COX7C	Preclinical[27]	Stroke, mitochondrial disorders
MVP	Preclinical[28]	Pancreatic adenocarcinoma
PPP4C	Preclinical[29]	Ovarian cancer

TABLE AND FIGURE REFERENCES

1. Bellenguez, C. *et al.* New insights into the genetic etiology of Alzheimer's disease and related dementias. *Nat Genet* **54**, 412-436 (2022).
2. Pulit, S.L. *et al.* Meta-analysis of genome-wide association studies for body fat distribution in 694 649 individuals of European ancestry. *Hum Mol Genet* **28**, 166-174 (2019).
3. Winkler, T.W. *et al.* The Influence of Age and Sex on Genetic Associations with Adult Body Size and Shape: A Large-Scale Genome-Wide Interaction Study. *PLoS Genet* **11**, e1005378 (2015).
4. Mahajan, A. *et al.* Multi-ancestry genetic study of type 2 diabetes highlights the power of diverse populations for discovery and translation. *Nat Genet* **54**, 560-572 (2022).
5. Mahajan, A. *et al.* Fine-mapping type 2 diabetes loci to single-variant resolution using high-density imputation and islet-specific epigenome maps. *Nat Genet* **50**, 1505-1513 (2018).
6. Broce, I.J. *et al.* Dissecting the genetic relationship between cardiovascular risk factors and Alzheimer's disease. *Acta Neuropathol* **137**, 209-226 (2019).
7. Wang, X.F. *et al.* Linking Alzheimer's disease and type 2 diabetes: Novel shared susceptibility genes detected by cFDR approach. *Journal of the Neurological Sciences* **380**, 262-272 (2017).
8. Hardy, J., de Strooper, B. & Escott-Price, V. Diabetes and Alzheimer's disease: shared genetic susceptibility? *Lancet Neurol* **21**, 962-964 (2022).
9. Yuan, X. *et al.* The common genes involved in the pathogenesis of Alzheimer's disease and type 2 diabetes and their implication for drug repositioning. *Neuropharmacology* **223**, 109327 (2023).
10. Chung, Y., Lee, H. & the Alzheimer's Disease Neuroimaging, I. Correlation between Alzheimer's disease and type 2 diabetes using non-negative matrix factorization. *Sci Rep* **11**, 15265 (2021).
11. McKenzie, A.T. *et al.* Brain Cell Type Specific Gene Expression and Co-expression Network Architectures. *Sci Rep* **8**, 8868 (2018).
12. Zheng, W. *et al.* Small molecule angiotensin converting enzyme inhibitors: A medicinal chemistry perspective. *Front Pharmacol* **13**, 968104 (2022).
13. Heerspink, H.J.L. *et al.* Sparsentan in patients with IgA nephropathy: a prespecified interim analysis from a randomised, double-blind, active-controlled clinical trial. *Lancet* **401**, 1584-1594 (2023).
14. Xiao, H. *et al.* A first-in-class selective inhibitor of ERK1/2 and ERK5 overcomes drug resistance with a single-molecule strategy. *Signal Transduct Target Ther* **10**, 70 (2025).
15. Sim, Y.H., Um, Y.J., Park, J.Y., Seo, M.D. & Park, S.G. A Novel Antibody-Drug Conjugate Targeting Nectin-2 Suppresses Ovarian Cancer Progression in Mouse Xenograft Models. *Int J Mol Sci* **23**(2022).
16. Piala, A.T. *et al.* Discovery of novel TAOK2 inhibitor scaffolds from high-throughput screening. *Bioorg Med Chem Lett* **26**, 3923-7 (2016).
17. Koo, C.Y. *et al.* Targeting TAO Kinases Using a New Inhibitor Compound Delays Mitosis and Induces Mitotic Cell Death in Centrosome Amplified Breast Cancer Cells. *Mol Cancer Ther* **16**, 2410-2421 (2017).
18. Amabile, G. *et al.* Targeting of the IGFBP3/TMEM219 pathway restores intestinal stem cells capability of healing mucosa in gastrointestinal autoimmune disorders. *Pharmacol Res* **219**, 107901 (2025).
19. Mokhtariye, A., Varshosaz, J., Mohammadalipour, A., Hashemnia, M. & Mofid, M.R. Xanthosomes loaded with recombinant TMEM219 for targeting IGFBP-3: A novel approach for targeted drug delivery to ameliorate liver fibrosis. *Life Sci* **377**, 123748 (2025).
20. Zhang, W. *et al.* The aminophospholipid transporter, ATP8B3, as a potential biomarker and target for enhancing the therapeutic effect of PD-L1 blockade in colon adenocarcinoma. *Genomics* **116**, 110907 (2024).
21. Caldon, C.E. *et al.* Cyclin E2 overexpression is associated with endocrine resistance but not insensitivity to CDK2 inhibition in human breast cancer cells. *Mol Cancer Ther* **11**, 1488-99 (2012).
22. Abdel-Magid, A.F. Potential of Cyclin-Dependent Kinase Inhibitors as Cancer Therapy. *ACS Med Chem Lett* **12**, 182-184 (2021).
23. Decker, M. *et al.* In vivo and In vitro Chemical Synthetic Lethality of ABHD17 and MEK Inhibition in NRAS-Mutant Acute Myeloid Leukemia. *Blood* **144**, 5808-5809 (2024).
24. Key, C.C. *et al.* Human GDPD3 overexpression promotes liver steatosis by increasing lysophosphatidic acid production and fatty acid uptake. *J Lipid Res* **61**, 1075-1086 (2020).
25. Giusiano, S. *et al.* TP53INP1 as new therapeutic target in castration-resistant prostate cancer. *Prostate* **72**, 1286-94 (2012).
26. Bialkowska, K. *et al.* Role of Kindlin 2 in prostate cancer. *Sci Rep* **14**, 19809 (2024).
27. Jia, J. *et al.* Effect of Dl-3-n-butylphthalide on mitochondrial Cox7c in models of cerebral ischemia/reperfusion injury. *Front Pharmacol* **14**, 1084564 (2023).
28. Wu, X. *et al.* Unraveling the role of Major Vault Protein as a novel immune-related biomarker that promotes the proliferation and migration in pancreatic adenocarcinoma. *Front Immunol* **15**, 1399222 (2024).
29. Raja, R. *et al.* PP4 inhibition sensitizes ovarian cancer to NK cell-mediated cytotoxicity via STAT1 activation and inflammatory signaling. *J Immunother Cancer* **10**(2022).

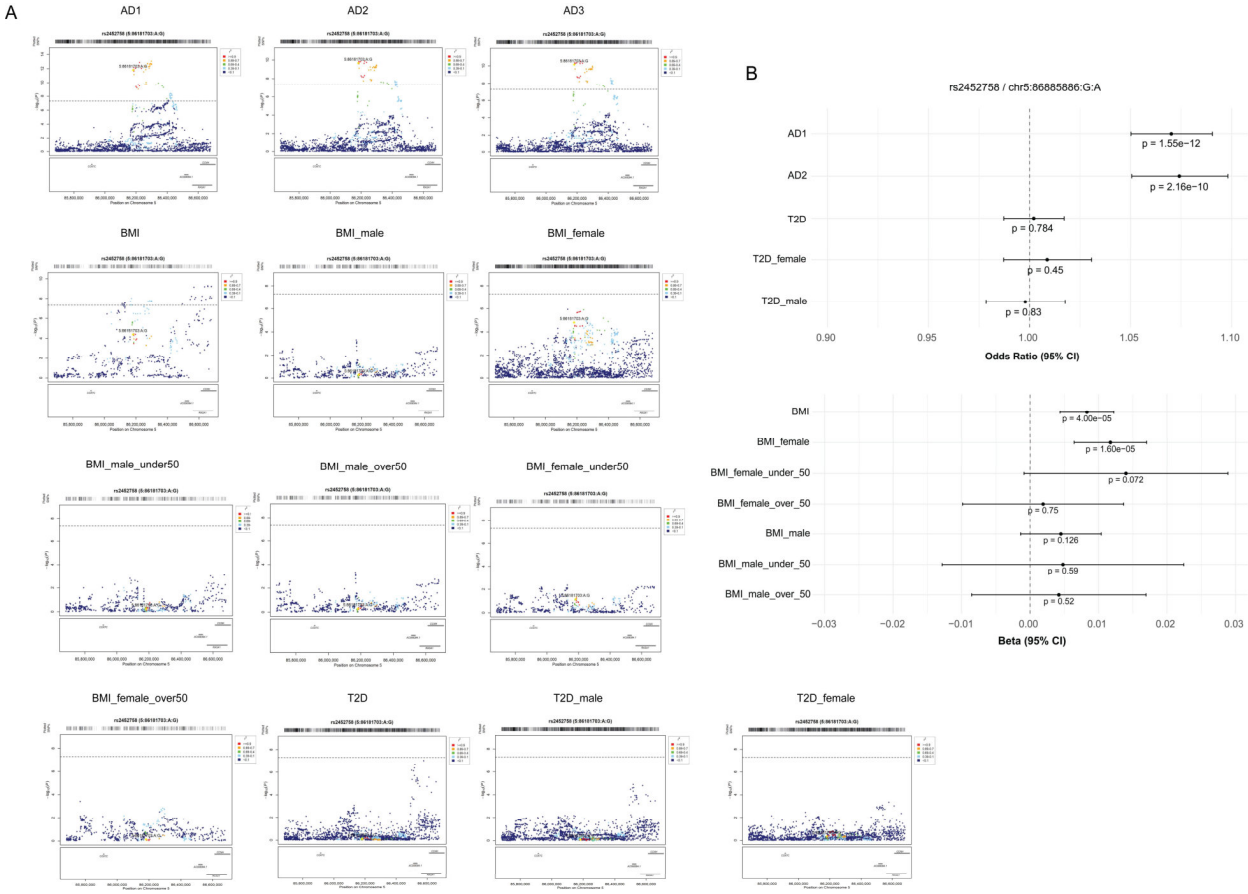

Fig. S1A | **Genetic colocalization analysis**. (**A**) Locuszoom plots for the BMI-AD rs2452758 locus (GRCh37). The overlapped variant is circled in green (**Table S3**) while the colocalized variant is shown in yellow (rs2452758). Variants in linkage disequilibrium (R^2) are color-coded. (**B**) Forest plot for the BMI-AD rs2452758 locus showcasing odds ratio for dichotomous traits (AD and T2D) and effect size (beta) for the continuous trait (BMI). P-values are shown under each odds ratio/beta estimate. Odds ratio and p-values for BMI-AD, T2D-AD and BMI-T2D-AD risk variants across AD datasets (AD1, AD2 and AD3).

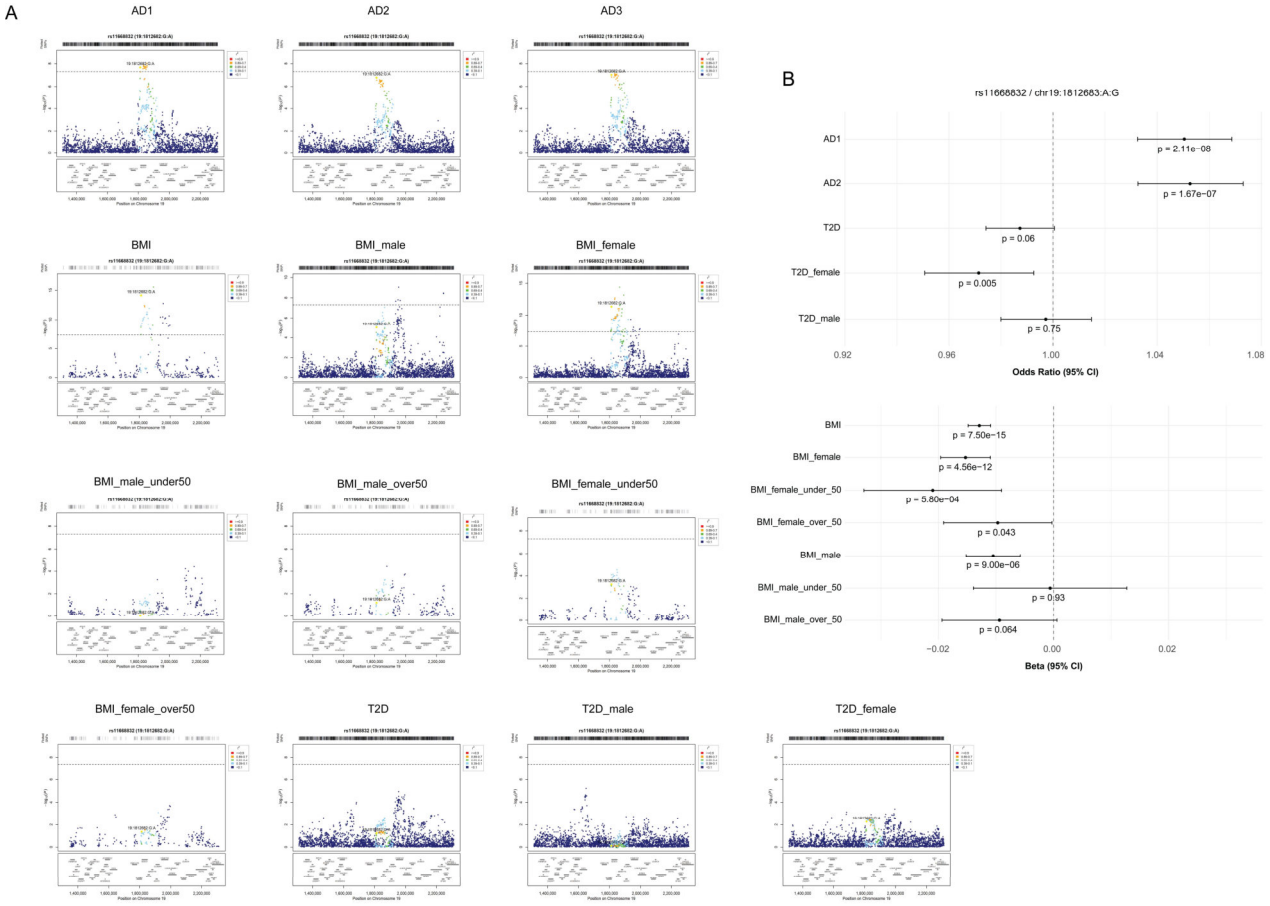

Fig. S1B | **Genetic colocalization analysis**. (**A**) Locuszoom plots for the BMI-AD rs11668832 locus (GRCh37). The overlapped variant is circled in green (**Table S3**) while the colocalized variant is shown in yellow (rs11668832). Variants in linkage disequilibrium (R^2) are color-coded. (**B**) Forest plot for the BMI-AD rs11668832 locus showcasing odds ratio for dichotomous traits (AD and T2D) and effect size (beta) for the continuous trait (BMI). P-values are shown under each odds ratio/beta estimate. Odds ratio and p-values for BMI-AD, T2D-AD and BMI-T2D-AD risk variants across AD datasets (AD1, AD2 and AD3).

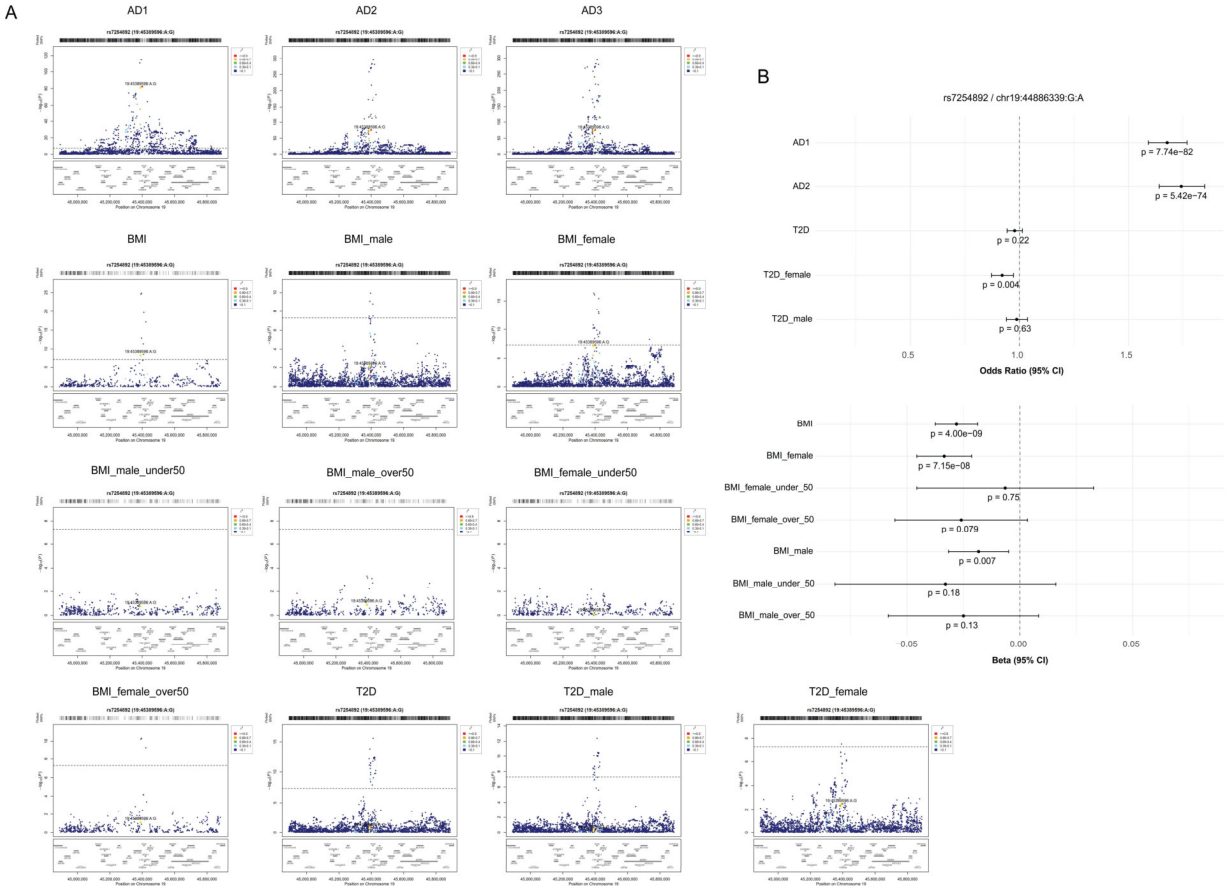

Fig. S1C | **Genetic colocalization analysis**. (**A**) Locuszoom plots for the BMI-AD rs7254892 locus (GRCh37). The overlapped variant is circled in green (**Table S3**) while the colocalized variant is shown in yellow (rs7254892). Variants in linkage disequilibrium (R^2) are color-coded. (**B**) Forest plot for the BMI-AD rs7254892 locus showcasing odds ratio for dichotomous traits (AD and T2D) and effect size (beta) for the continuous trait (BMI). P-values are shown under each odds ratio/beta estimate. Odds ratio and p-values for BMI-AD, T2D-AD and BMI-T2D-AD risk variants across AD datasets (AD1, AD2 and AD3).

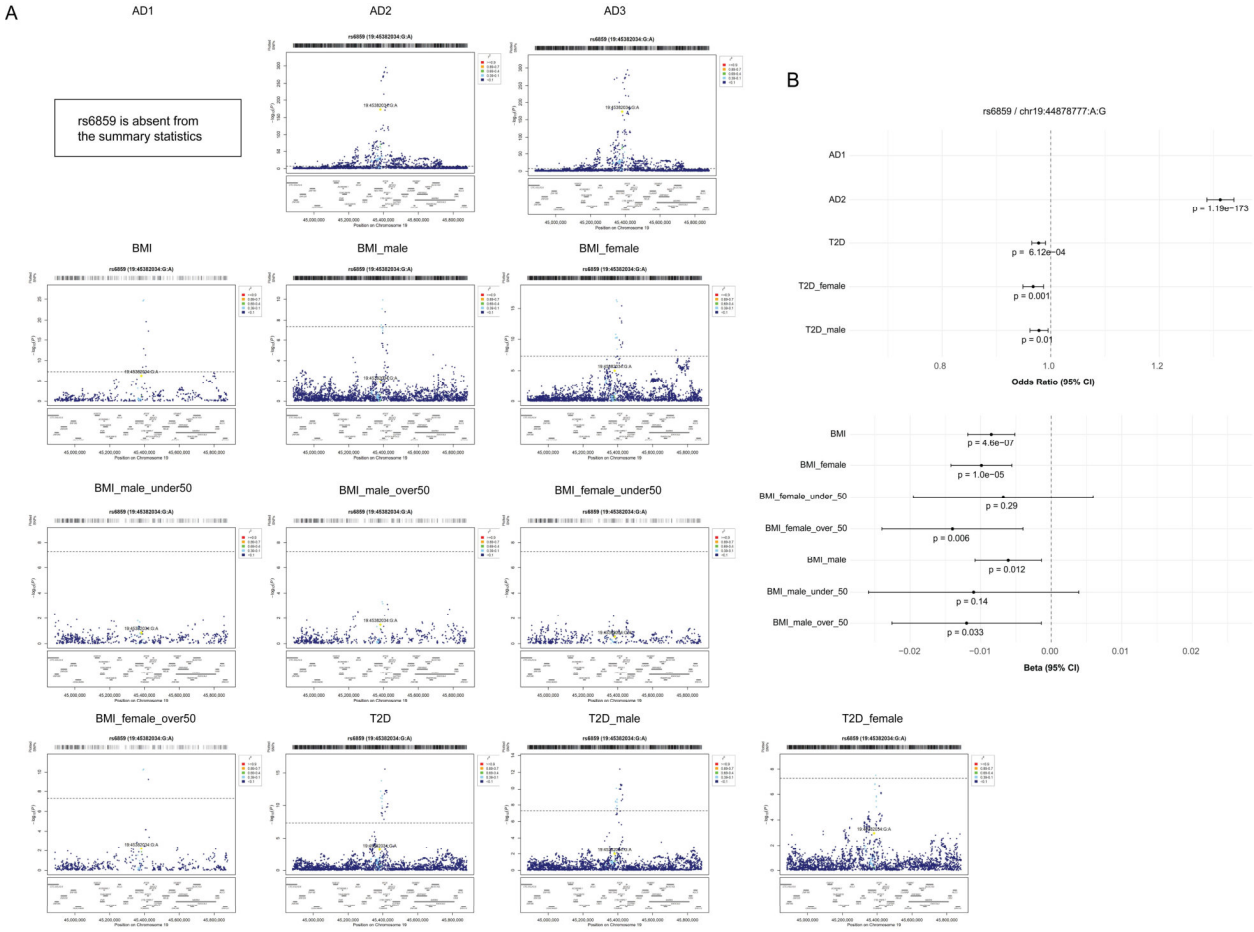

Fig. S1D | **Genetic colocalization analysis**. (**A**) Locuszoom plots for the BMI-AD rs6859 locus (GRCh37). The overlapped variant is circled in green (**Table S3**) while the colocalized variant is shown in yellow (rs6859). Variants in linkage disequilibrium (R^2) are color-coded. (**B**) Forest plot for the BMI-AD rs6859 locus showcasing odds ratio for dichotomous traits (AD and T2D) and effect size (beta) for the continuous trait (BMI). P-values are shown under each odds ratio/beta estimate. Odds ratio and p-values for BMI-AD, T2D-AD and BMI-T2D-AD risk variants across AD datasets (AD1, AD2 and AD3).

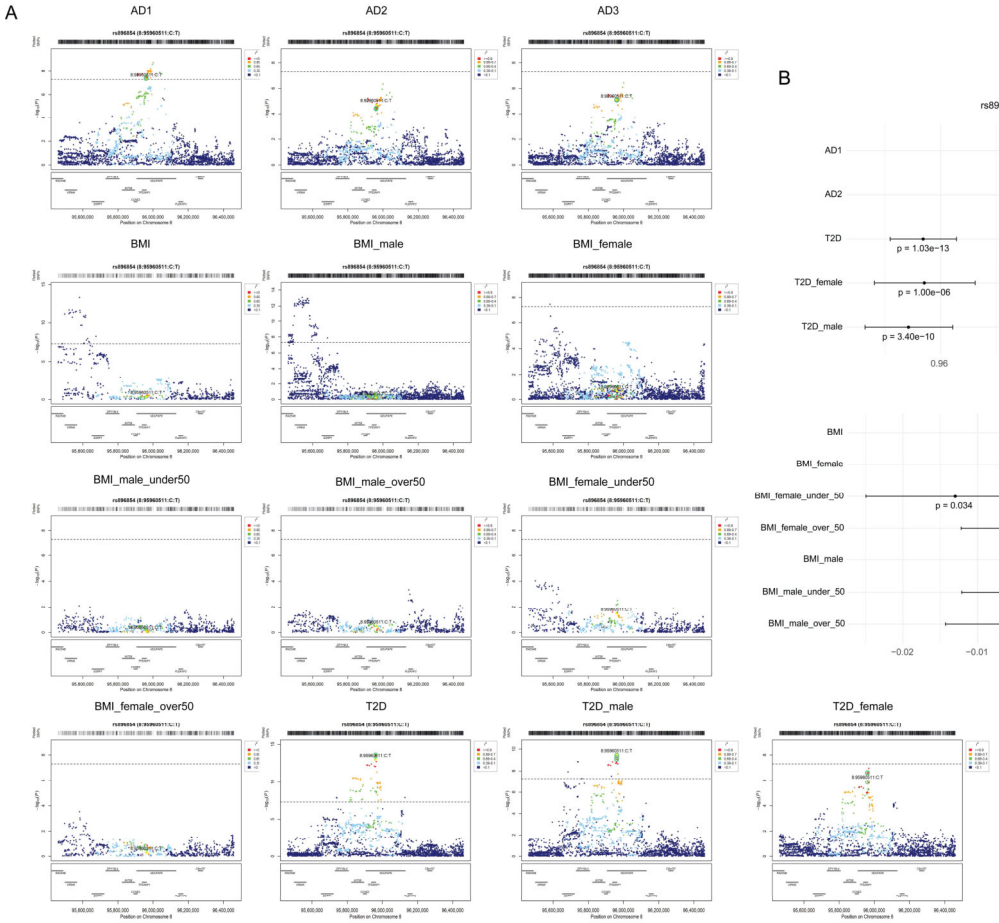

Fig. S1E | **Genetic colocalization analysis**. (**A**) Locuszoom plots for the T2D-AD rs896854 locus (GRCh37). The overlapped variant is circled in green (**Table S3**) while the colocalized variant is shown in yellow (rs896854). Variants in linkage disequilibrium (R^2) are color-coded. (**B**) Forest plot for the T2D-AD rs896854 locus showcasing odds ratio for dichotomous traits (AD and T2D) and effect size (beta) for the continuous trait (BMI). P-values are shown under each odds ratio/beta estimate. Odds ratio and p-values for BMI-AD, T2D-AD and BMI-T2D-AD risk variants across AD datasets (AD1, AD2 and AD3).

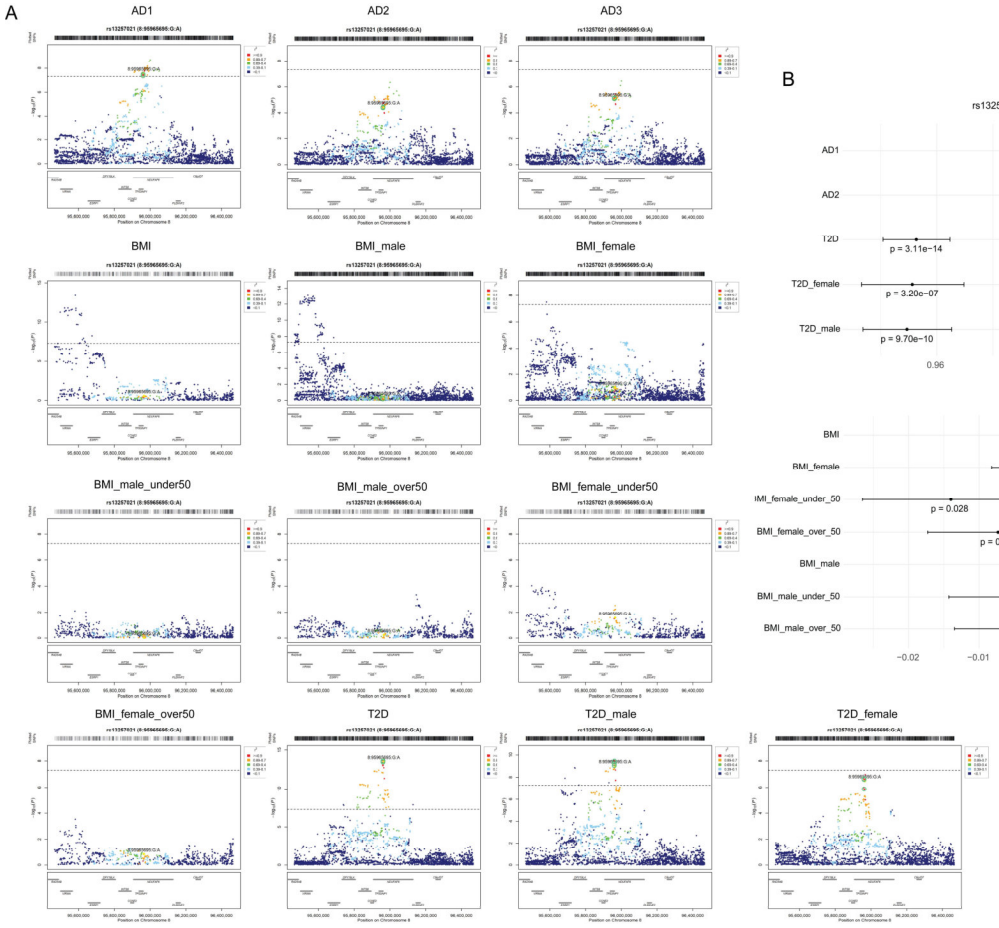

Fig. S1F | **Genetic colocalization analysis**. (**A**) Locuszoom plots for the T2D-AD rs13257021 locus (GRCh37). The overlapped variant is circled in green (**Table S3**) while the colocalized variant is shown in yellow (rs13257021). Variants in linkage disequilibrium (R^2) are color-coded. (**B**) Forest plot for the T2D-AD rs13257021 locus showcasing odds ratio for dichotomous traits (AD and T2D) and effect size (beta) for the continuous trait (BMI). P-values are shown under each odds ratio/beta estimate. Odds ratio and p-values for BMI-AD, T2D-AD and BMI-T2D-AD risk variants across AD datasets (AD1, AD2 and AD3).

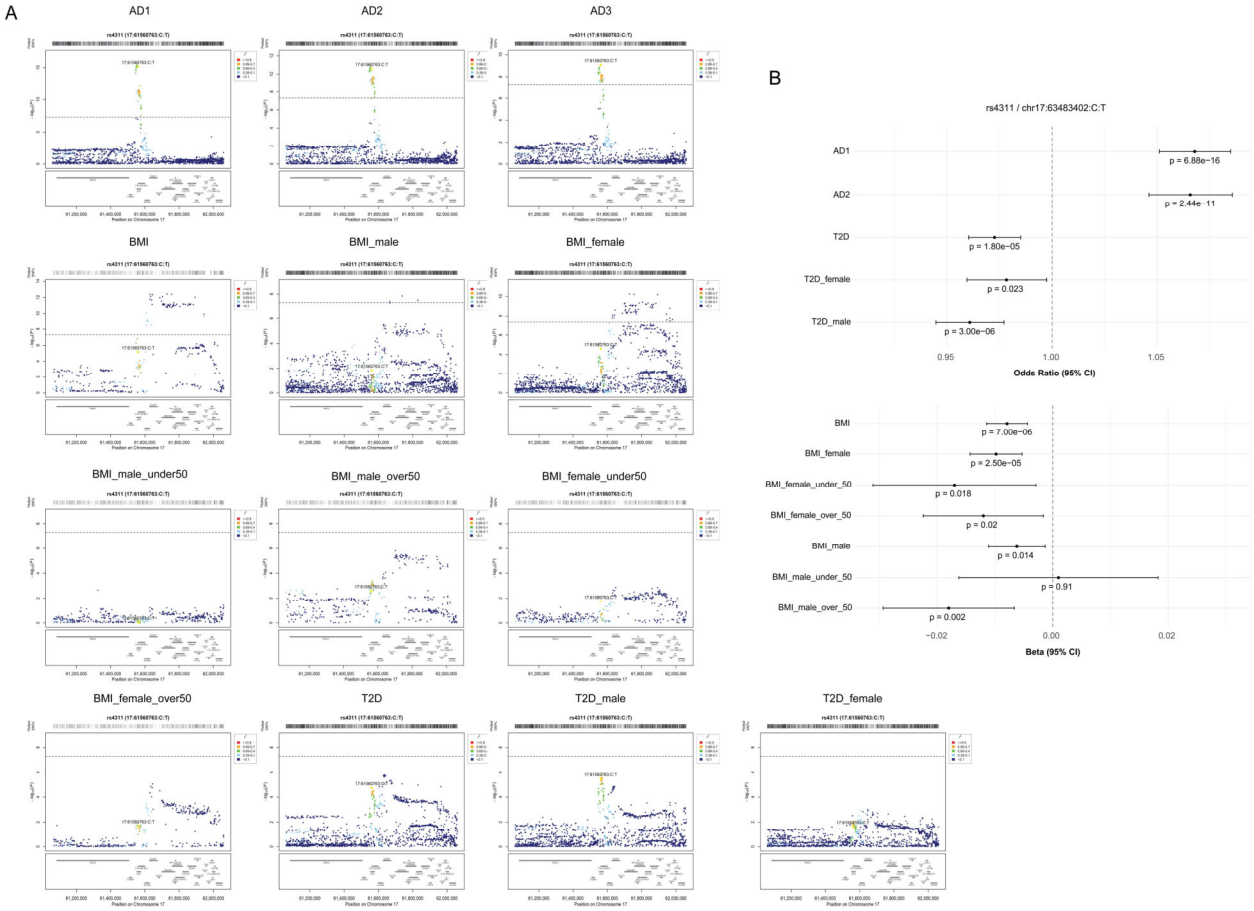

Fig. S1G | **Genetic colocalization analysis**. (**A**) Locuszoom plots for the T2D-AD rs4311 locus (GRCh37). The overlapped variant is circled in green (**Table S3**) while the colocalized variant is shown in yellow (rs4311). Variants in linkage disequilibrium (R^2) are color-coded. (**B**) Forest plot for the T2D - AD rs4311 locus showcasing odds ratio for dichotomous traits (AD and T2D) and effect size (beta) for the continuous trait (BMI). P-values are shown under each odds ratio/beta estimate. Odds ratio and p-values for BMI-AD, T2D-AD and BMI-T2D-AD risk variants across AD datasets (AD1, AD2 and AD3).

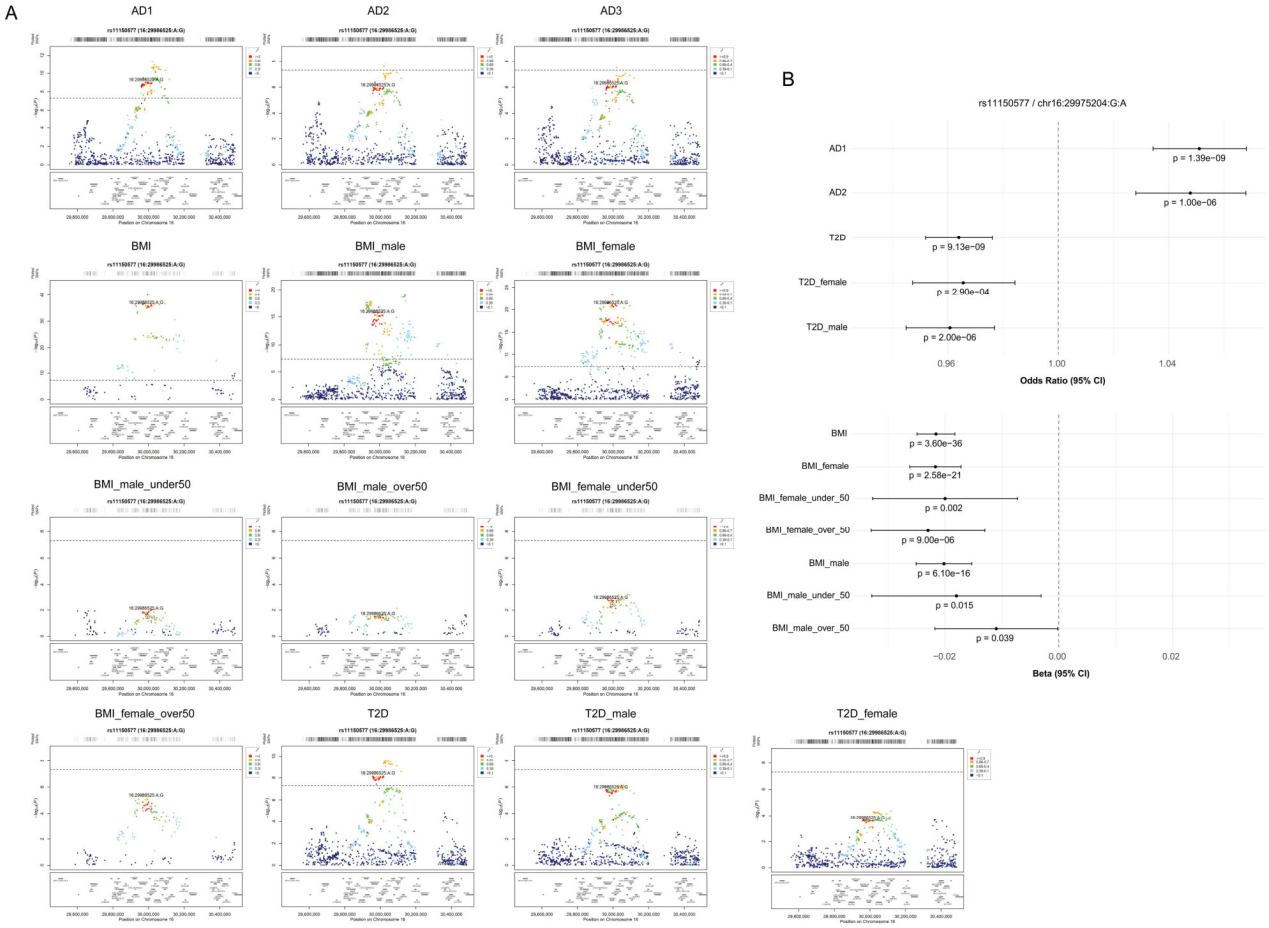

Fig. S1H | **Genetic colocalization analysis**. (**A**) Locuszoom plots for the BMI-T2D-AD rs11150577 locus (GRCh37). The overlapped variant is circled in green (**Table S3**) while the colocalized variant is shown in yellow (rs11150577). Variants in linkage disequilibrium (R^2) are color-coded. (**B**) Forest plot for the BMI-T2D-AD rs11150577 locus showcasing odds ratio for dichotomous traits (AD and T2D) and effect size (beta) for the continuous trait (BMI). P-values are shown under each odds ratio/beta estimate. Odds ratio and p-values for BMI-AD, T2D-AD and BMI-T2D-AD risk variants across AD datasets (AD1, AD2 and AD3).

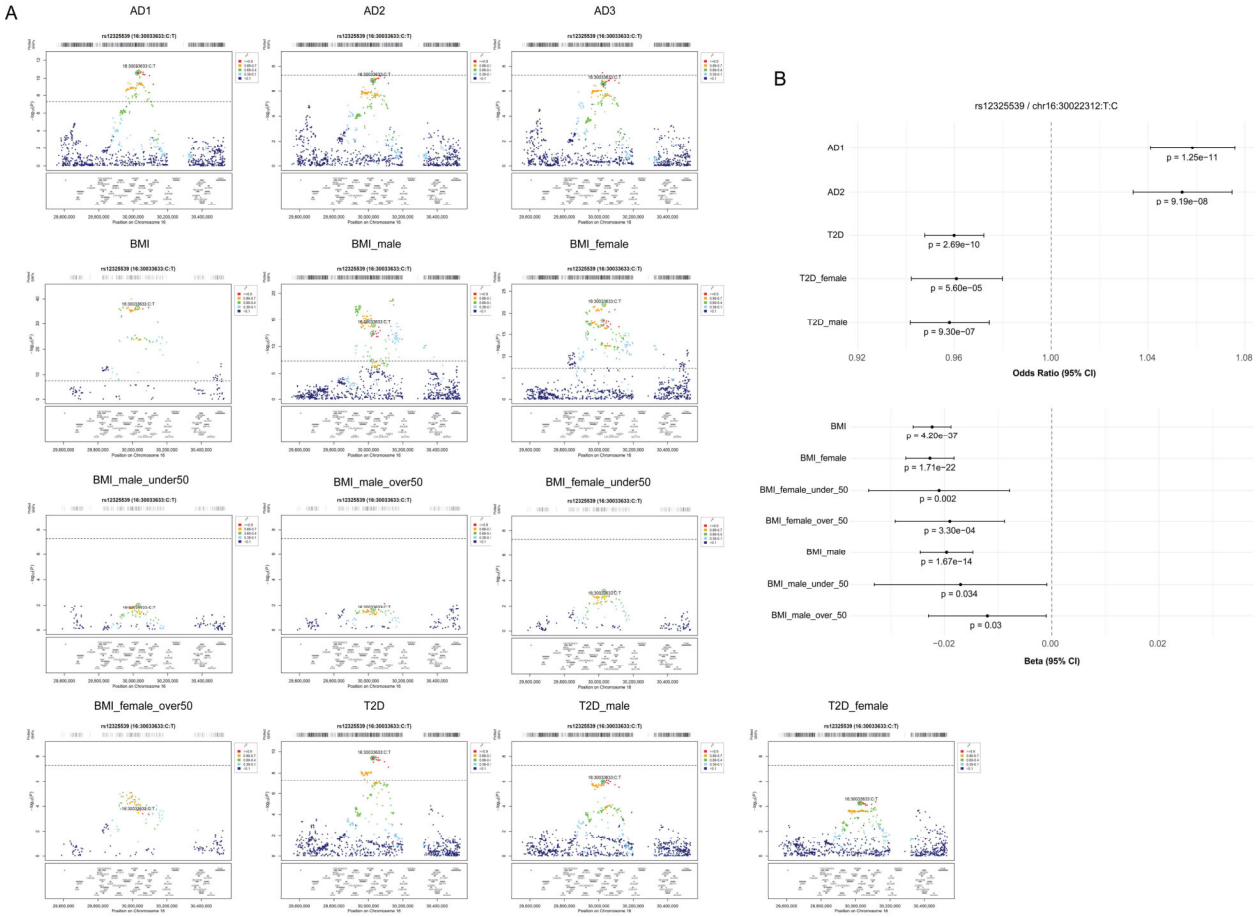

Fig. S1l | **Genetic colocalization analysis**. (**A**) Locuszoom plots for the BMI-T2D-AD rs12325539 locus (GRCh37). The overlapped variant is circled in green (**Table S3**) while the colocalized variant is shown in yellow (rs12325539). Variants in linkage disequilibrium (R^2) are color-coded. (**B**) Forest plot for the BMI-T2D-AD rs12325539 locus showcasing odds ratio for dichotomous traits (AD and T2D) and effect size (beta) for the continuous trait (BMI). P-values are shown under each odds ratio/beta estimate. Odds ratio and p-values for BMI-AD, T2D-AD and BMI-T2D-AD risk variants across AD datasets (AD1, AD2 and AD3).

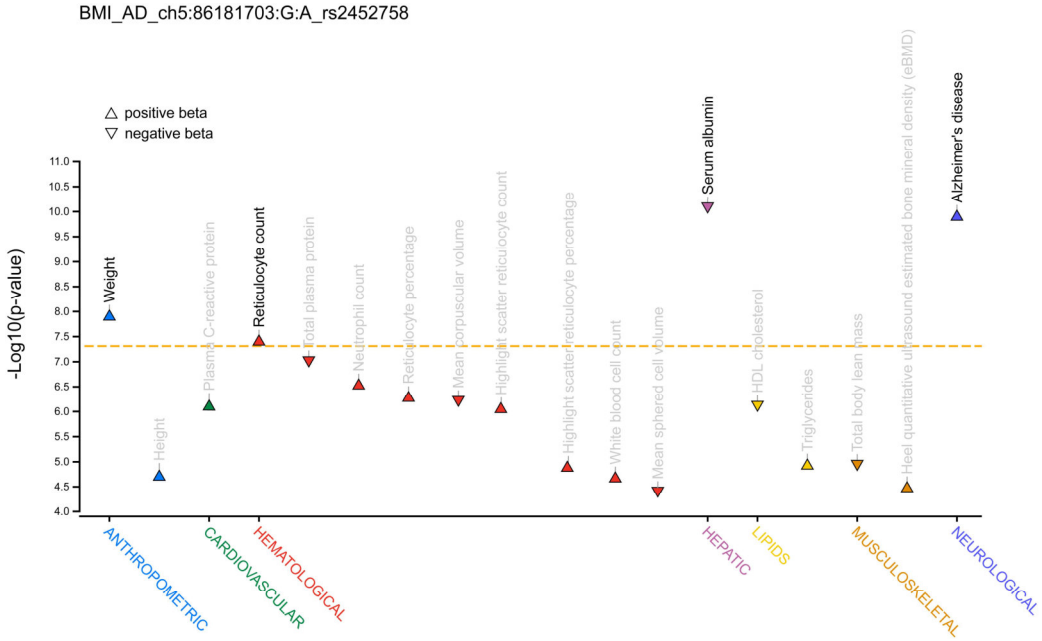

Fig. S2A | **Phenome wide association study (PheWAS)**. Results are aligned to the risk-increasing allele for AD. Position in hg19.

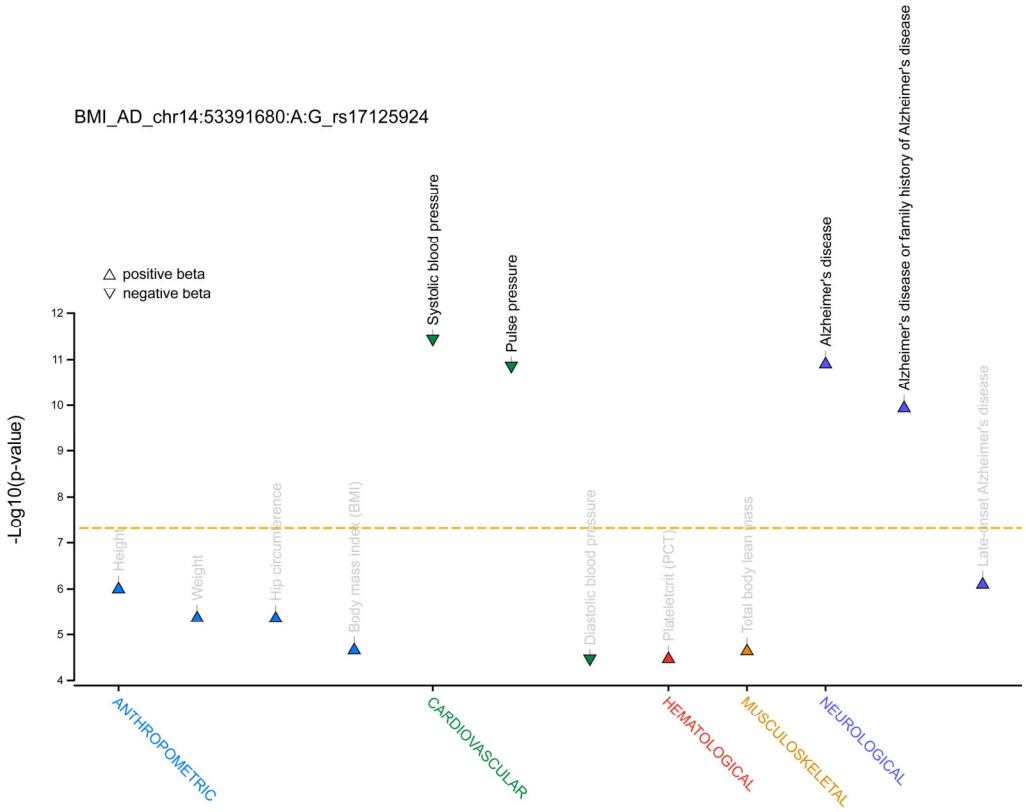

Fig. S2B | **Phenome wide association study (PheWAS)**. Results are aligned to the risk-increasing allele for AD. Position in hg19.

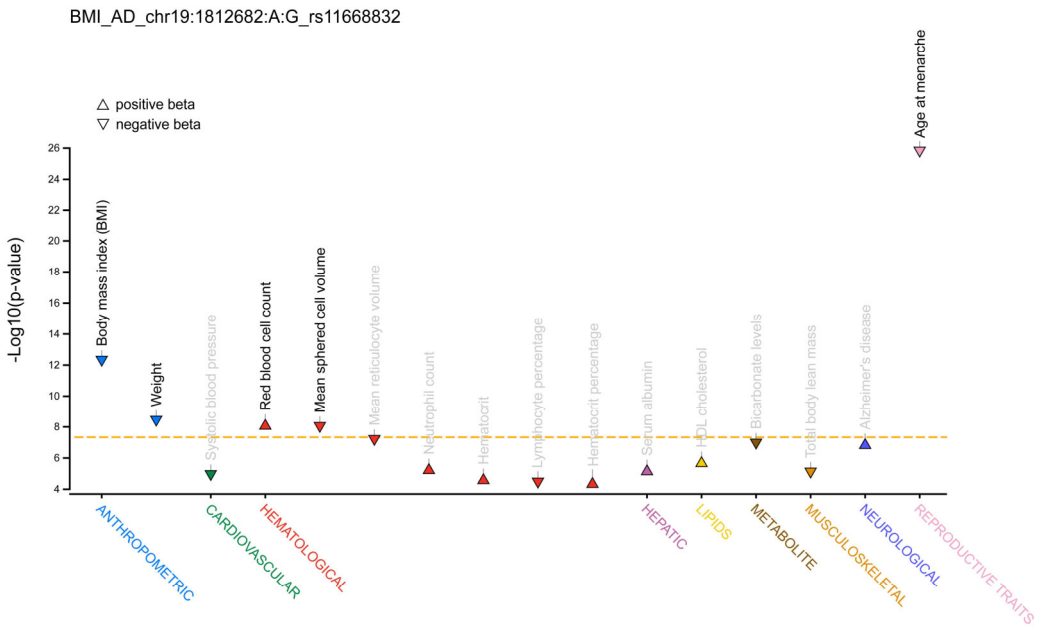

Fig. S2C | **Phenome wide association study (PheWAS)**. Results are aligned to the risk-increasing allele for AD. Position in hg19.

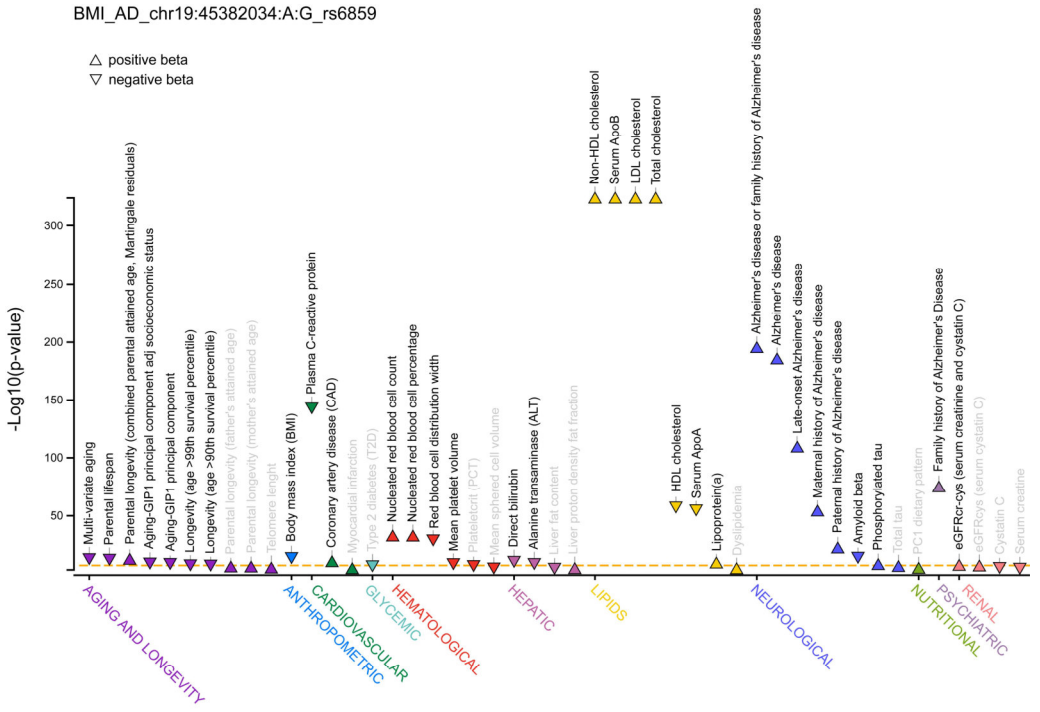

Fig. S2D | **Phenome wide association study (PheWAS)**. Results are aligned to the risk-increasing allele for AD. Position in hg19.

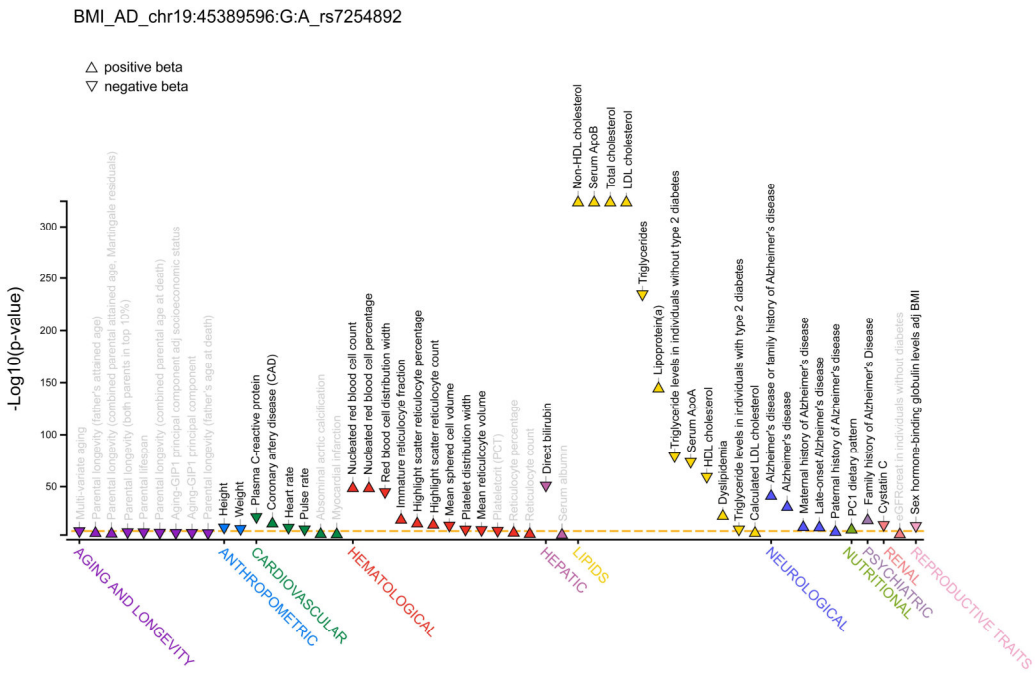

Fig. S2E | **Phenome wide association study (PheWAS)**. Results are aligned to the risk-increasing allele for AD. Position in hg19.

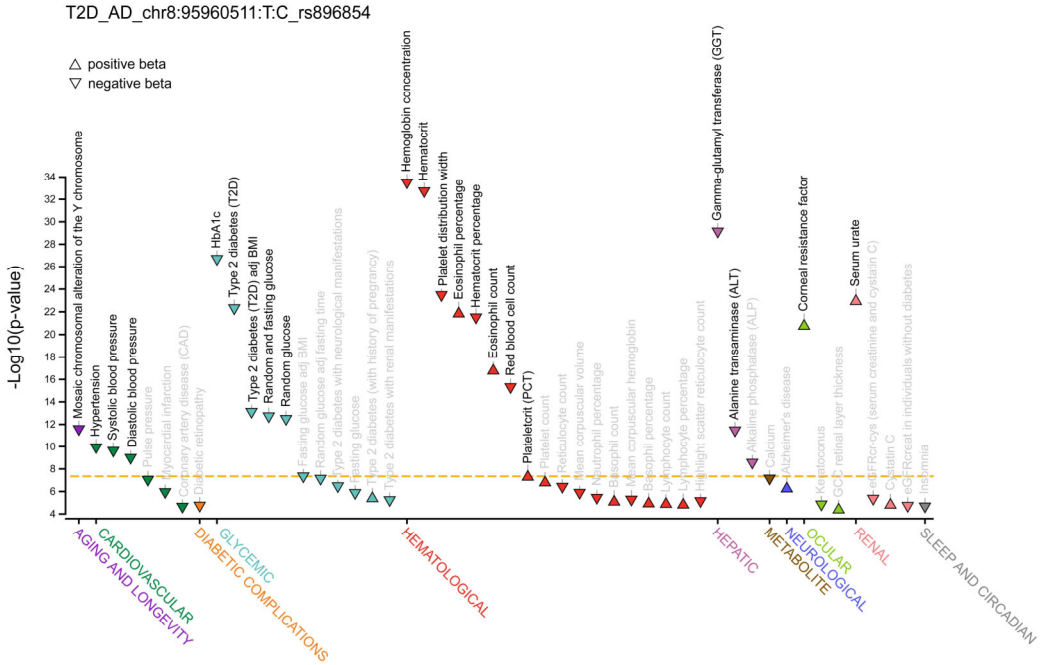

Fig. S2F | **Phenome wide association study (PheWAS)**. Results are aligned to the risk-increasing allele for AD. Position in hg19.

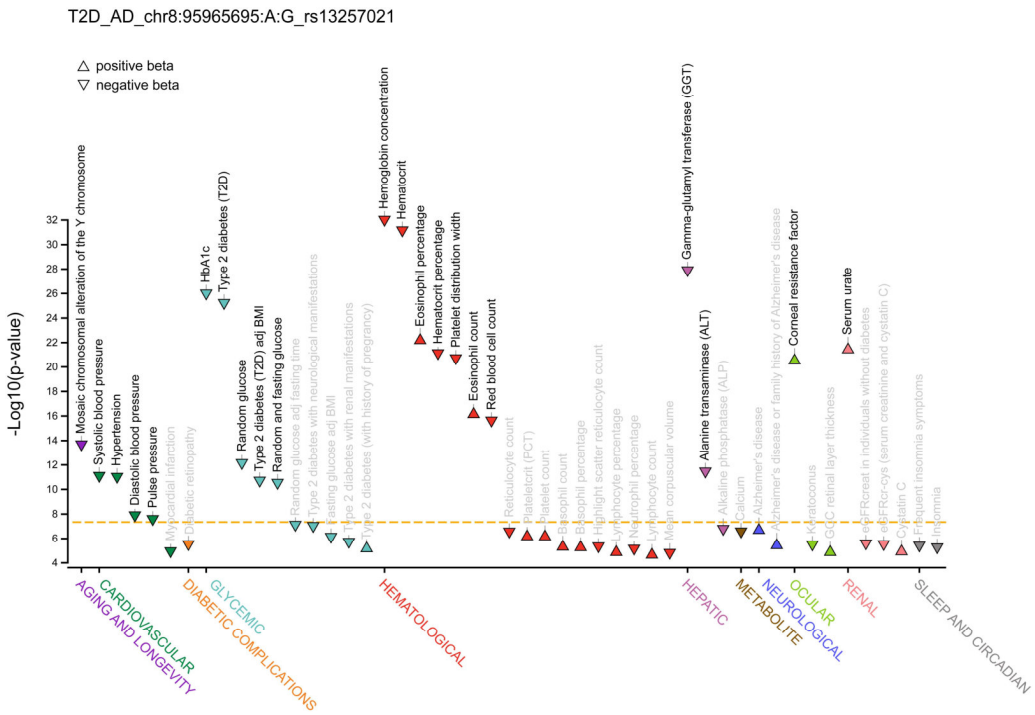

Fig. S2G | **Phenome wide association study (PheWAS)**. Results are aligned to the risk-increasing allele for AD. Position in hg19.

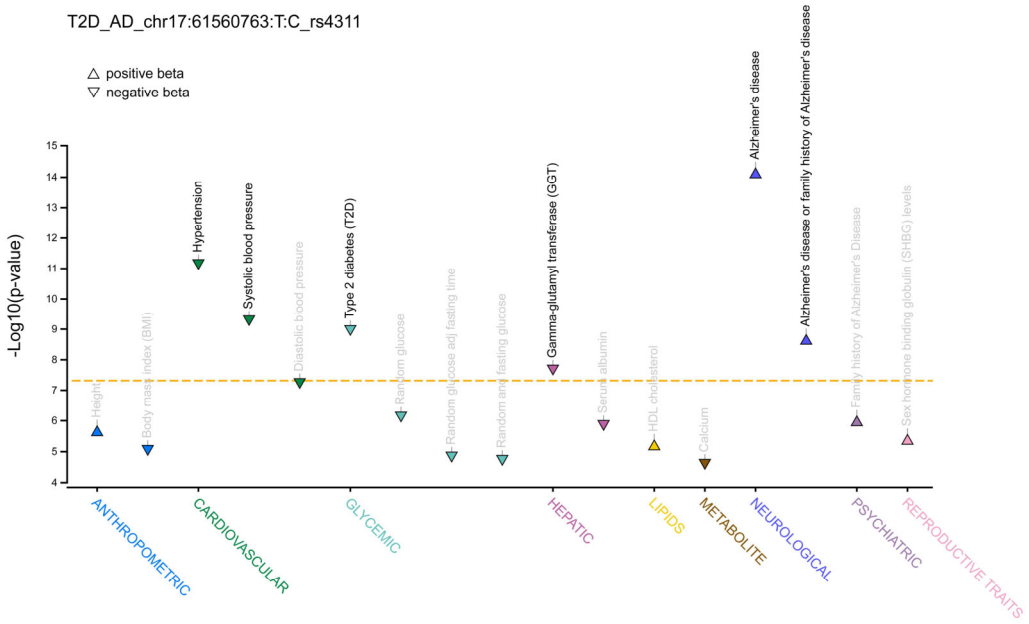

Fig. S2H | **Phenome wide association study (PheWAS)**. Results are aligned to the risk-increasing allele for AD. Position in hg19.

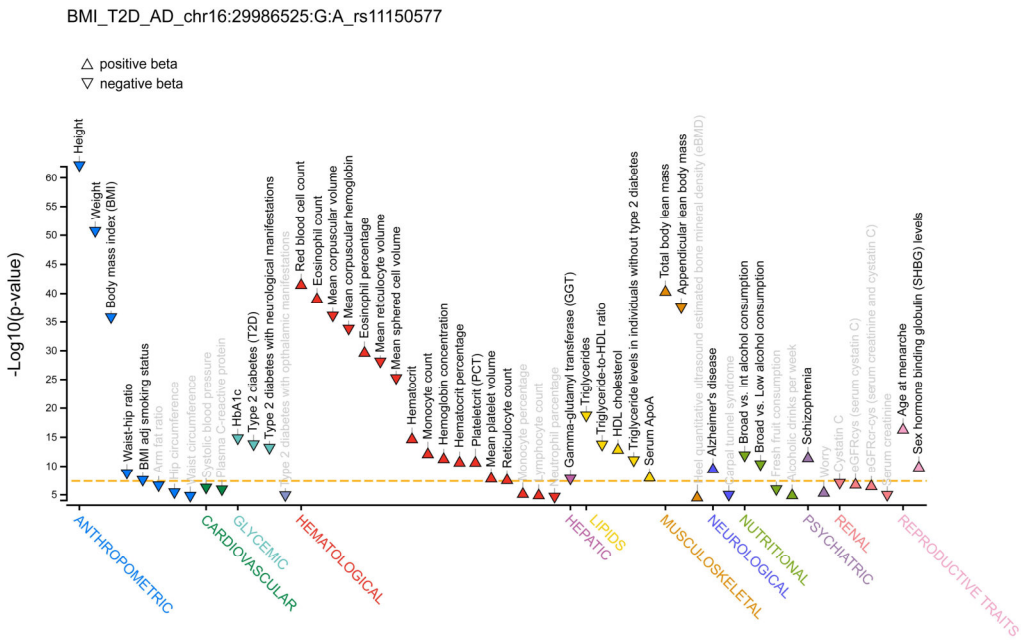

Fig. S2I | **Phenome wide association study (PheWAS)**. Results are aligned to the risk-increasing allele for AD. Position in hg19.

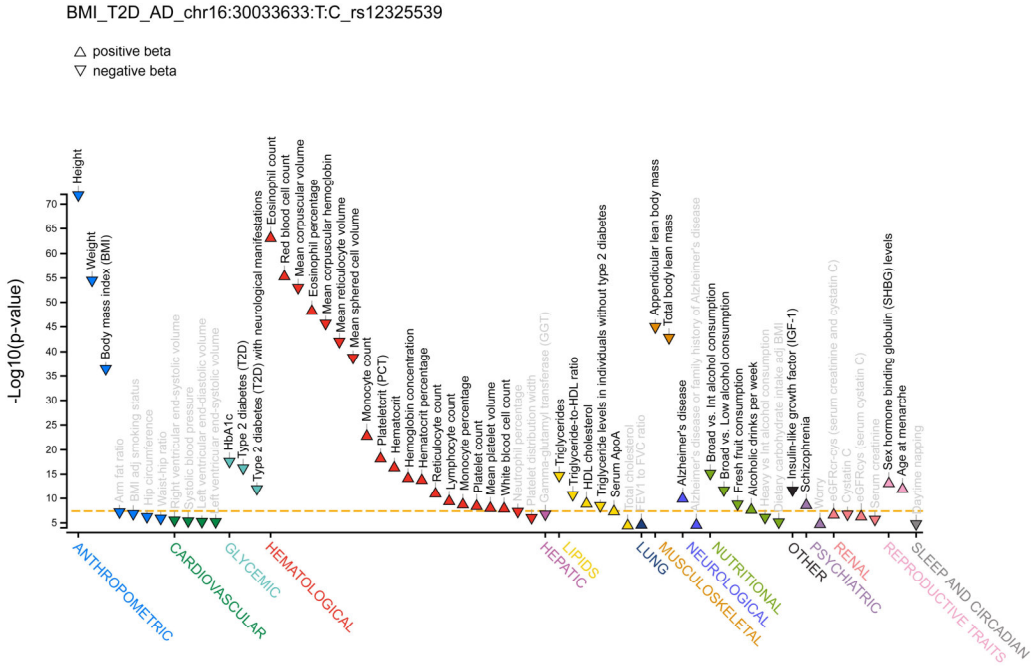

Fig. S2J | **Phenome wide association study (PheWAS)**. Results are aligned to the risk-increasing allele for AD. Position in hg19.

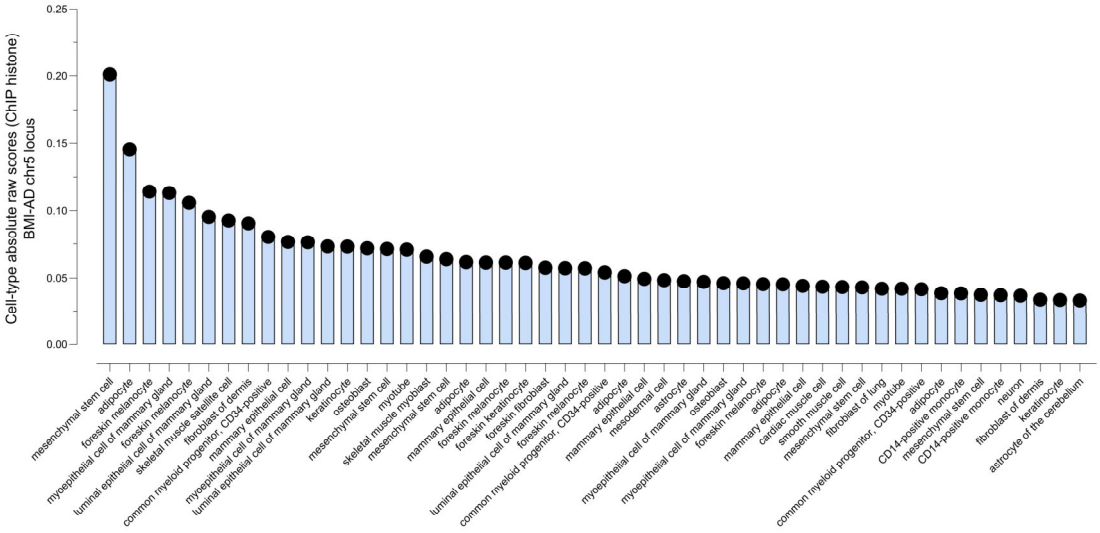

Fig. S3A | **AlphaGenome**. Top cell-type predictions for the effects of rs2452758 in histone modifications.

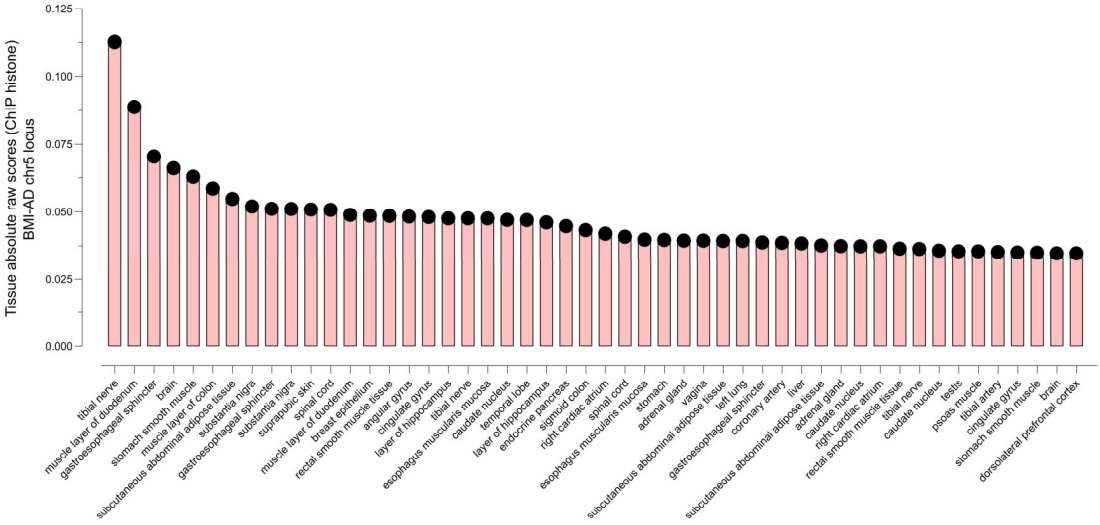

Fig. S3B | **AlphaGenome**. Top tissue predictions for the effects of rs2452758 in histone modifications.

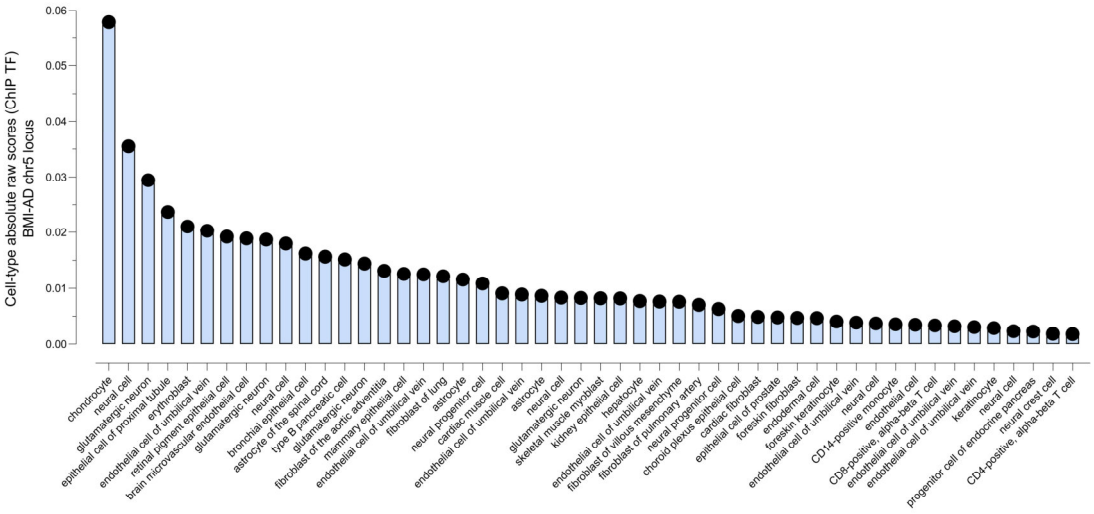

Fig. S3C | **AlphaGenome**. Top cell-type predictions for the effects of rs2452758 in transcription factor binding.

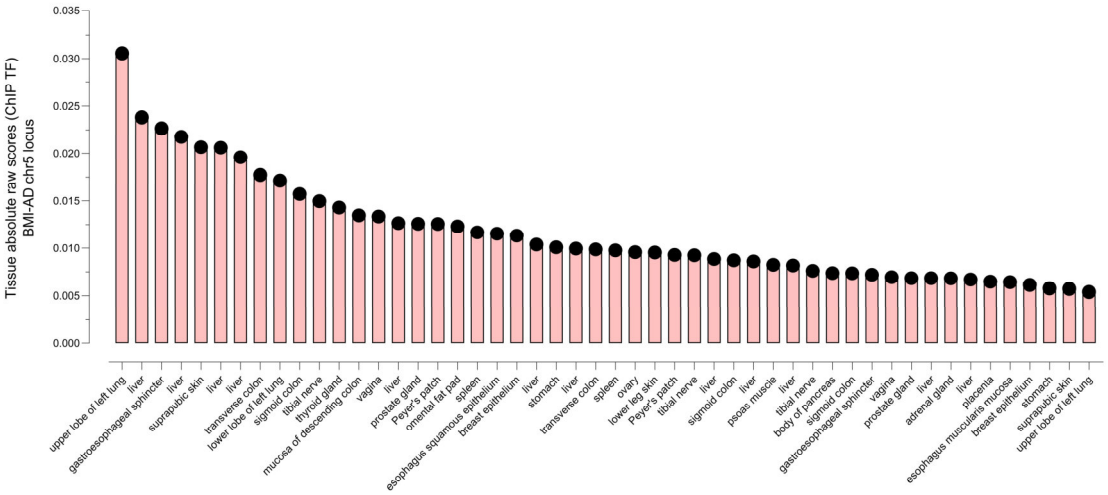

Fig. S3D | **AlphaGenome**. Top tissue predictions for the effects of rs2452758 in transcription factor binding.

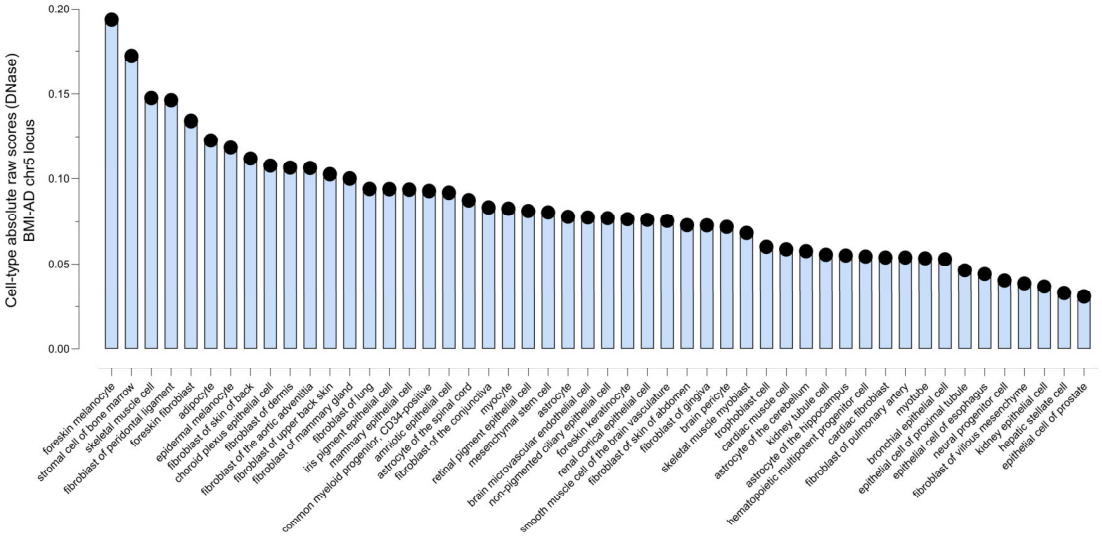

Fig. S3E | **AlphaGenome**. Top cell-type predictions for the effects of rs2452758 in chromatin accessibility assessed by DNase.

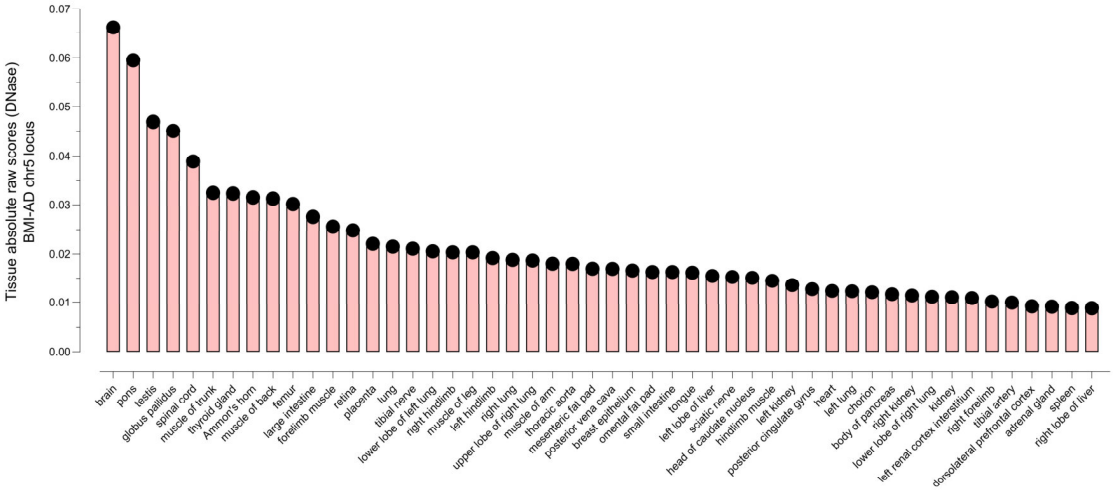

Fig. S3F | **AlphaGenome**. Top tissue predictions for the effects of rs2452758 in chromatin accessibility assessed by DNase.

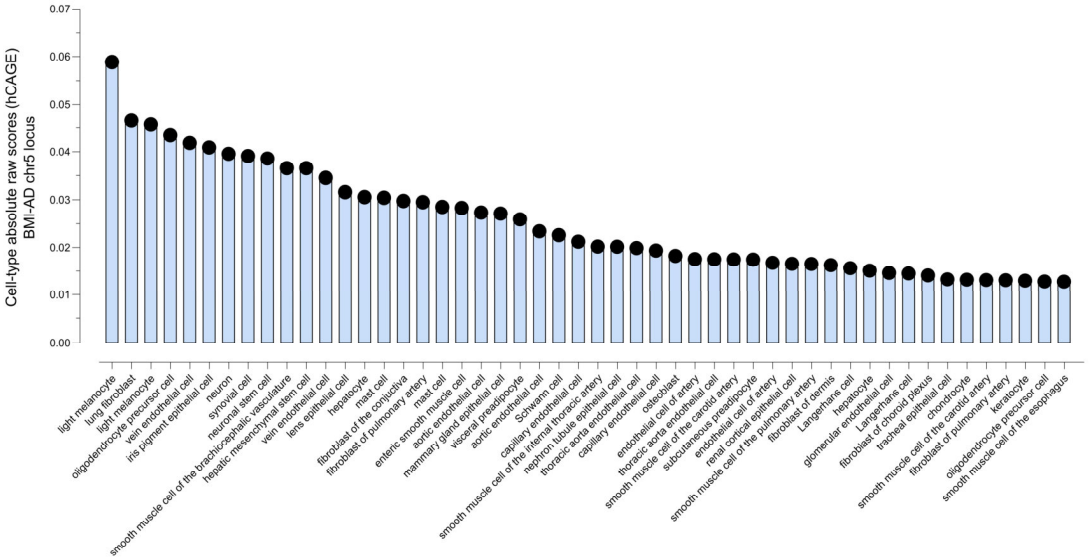

Fig. S3G | **AlphaGenome**. Top cell-type predictions for the effects of rs2452758 in gene expression assessed by hCAGE.

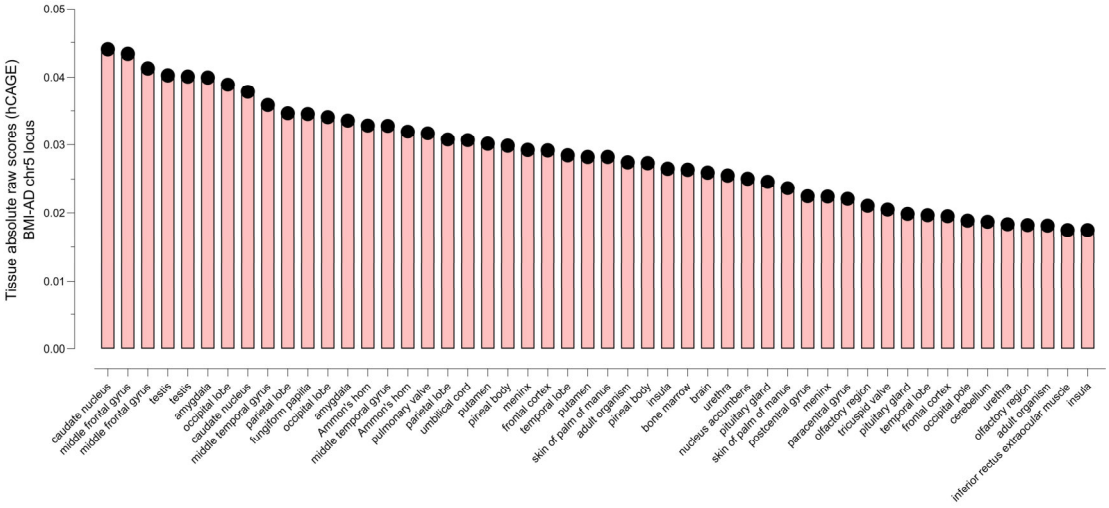

Fig. S3H | **AlphaGenome**. Top tissue predictions for the effects of rs2452758 in gene expression assessed by hCAGE.

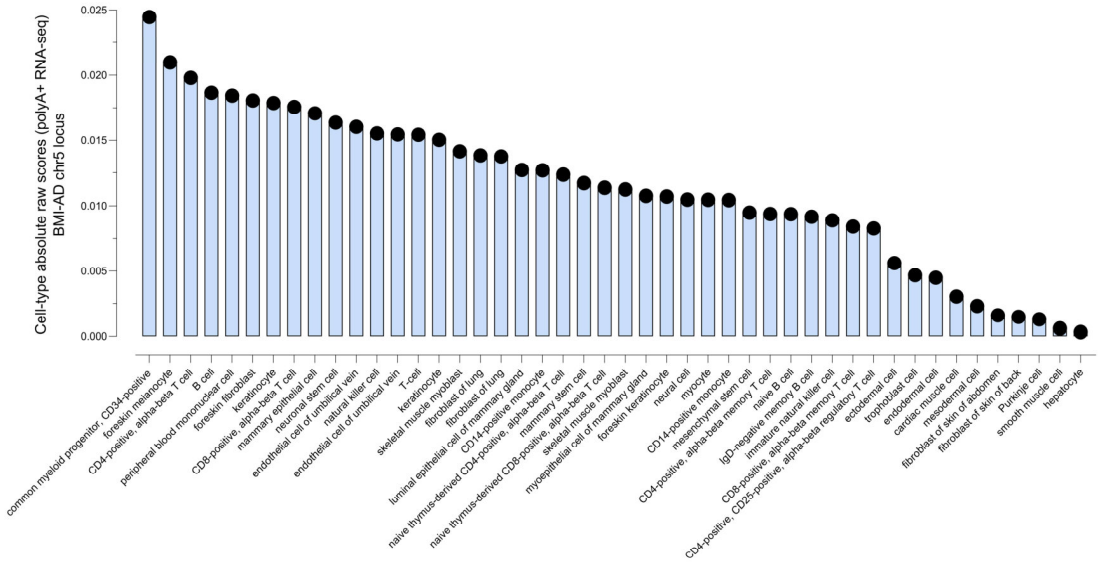

Fig. S3I | **AlphaGenome**. Top tissue predictions for the effects of rs2452758 in gene expression assessed by polyA+ RNA-seq.

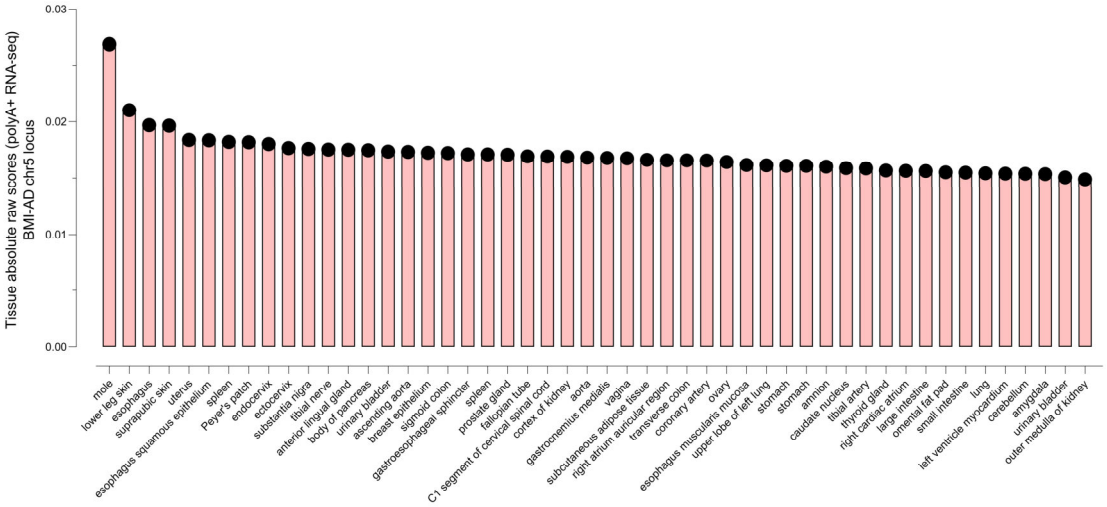

Fig. S3J | **AlphaGenome**. Top cell-type predictions for the effects of rs2452758 in gene expression assessed by polyA+ RNA-seq.

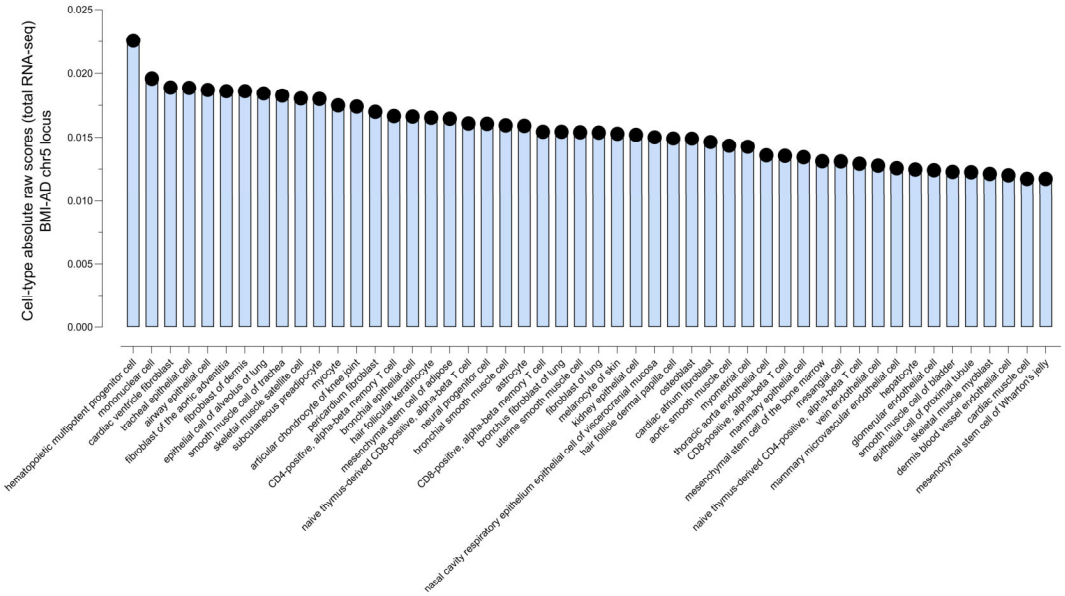

Fig. S3K | **AlphaGenome**. Top tissue predictions for the effects of rs2452758 in gene expression assessed by total RNA-seq.

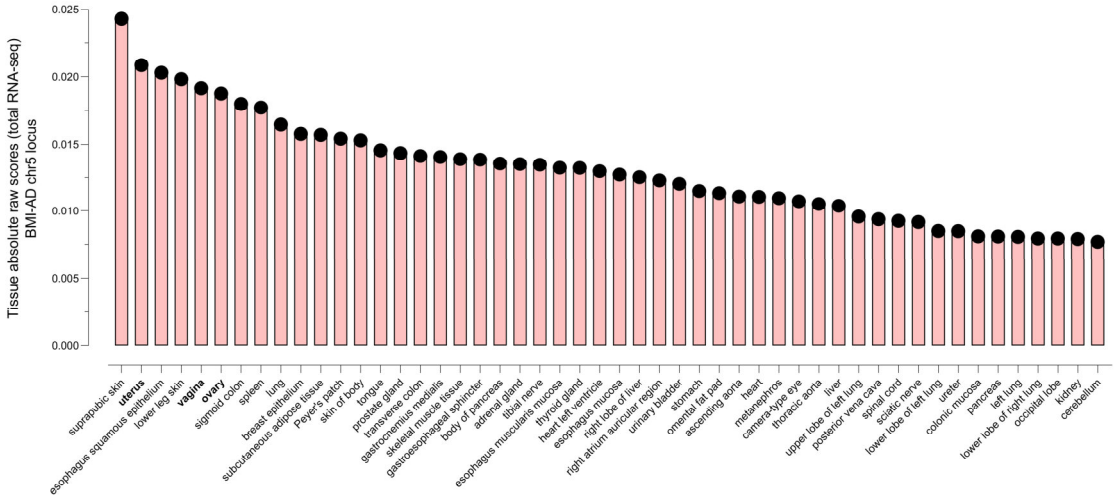

Fig. S3L | **AlphaGenome**. Top tissue predictions for the effects of rs2452758 in gene expression assessed by total RNA-seq.

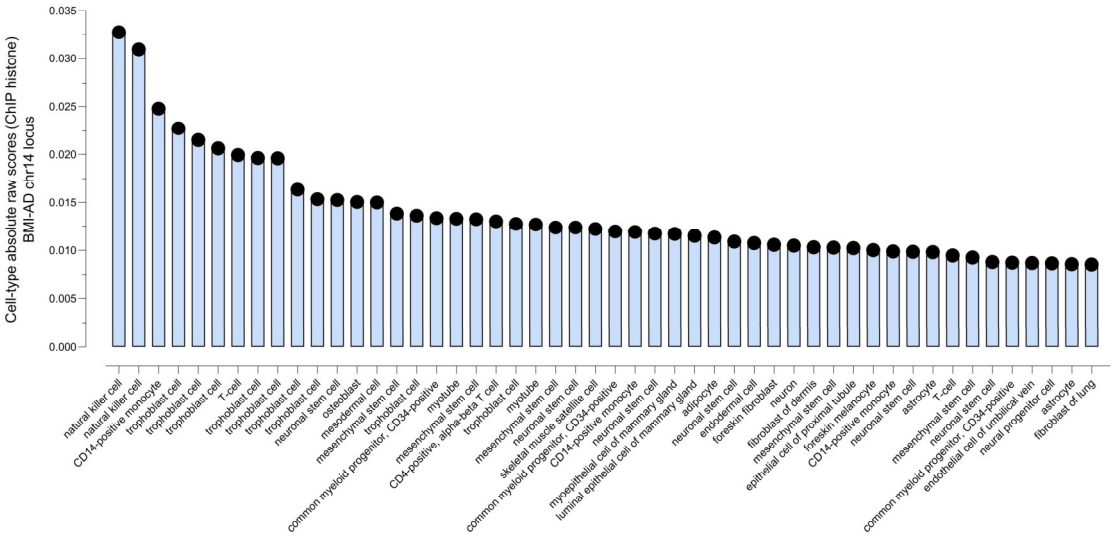

Fig. S3M | **AlphaGenome**. Top cell-type predictions for the effects of rs17125924 in histone modifications.

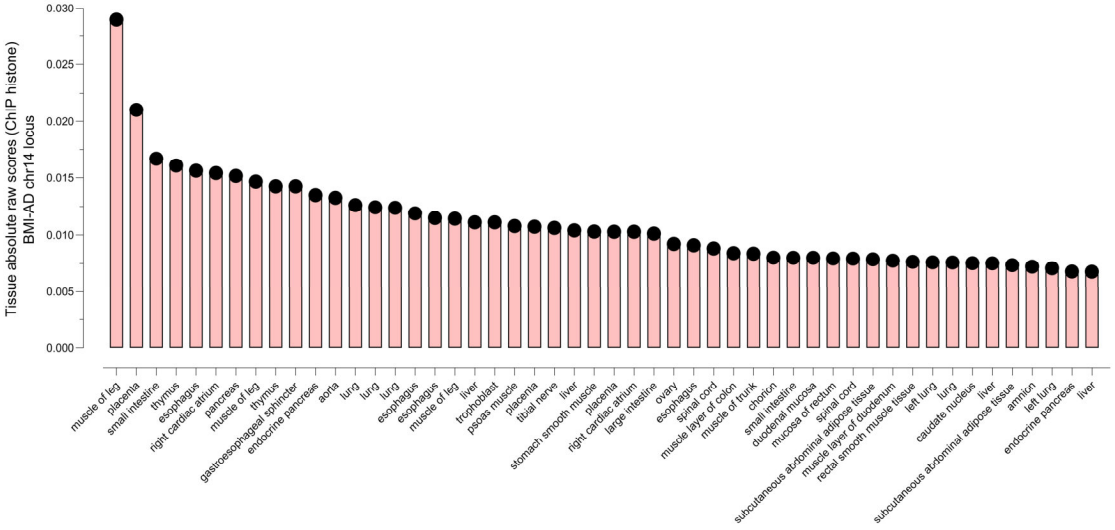

Fig. S3N | **AlphaGenome**. Top tissue predictions for the effects of rs17125924 in histone modifications.

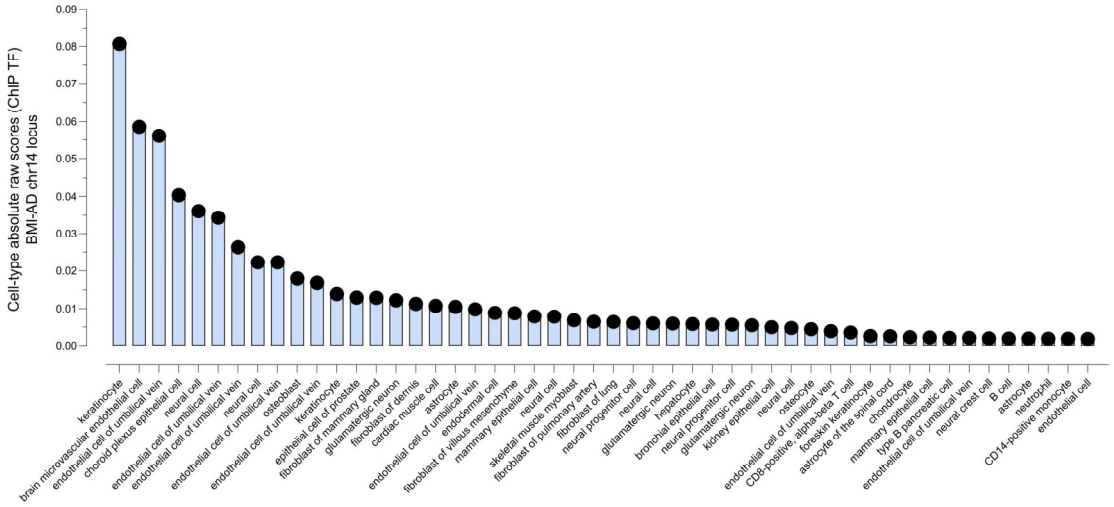

Fig. S3O | **AlphaGenome**. Top cell-type predictions for the effects of rs17125924 in transcription factor binding.

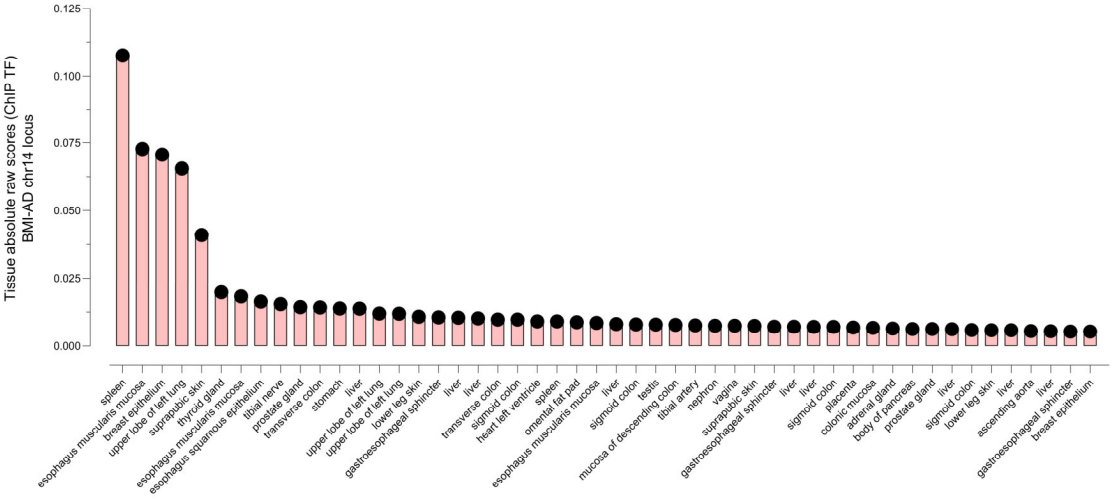

Fig. S3P | **AlphaGenome**. Top tissue predictions for the effects of rs17125924 in transcription factor binding.

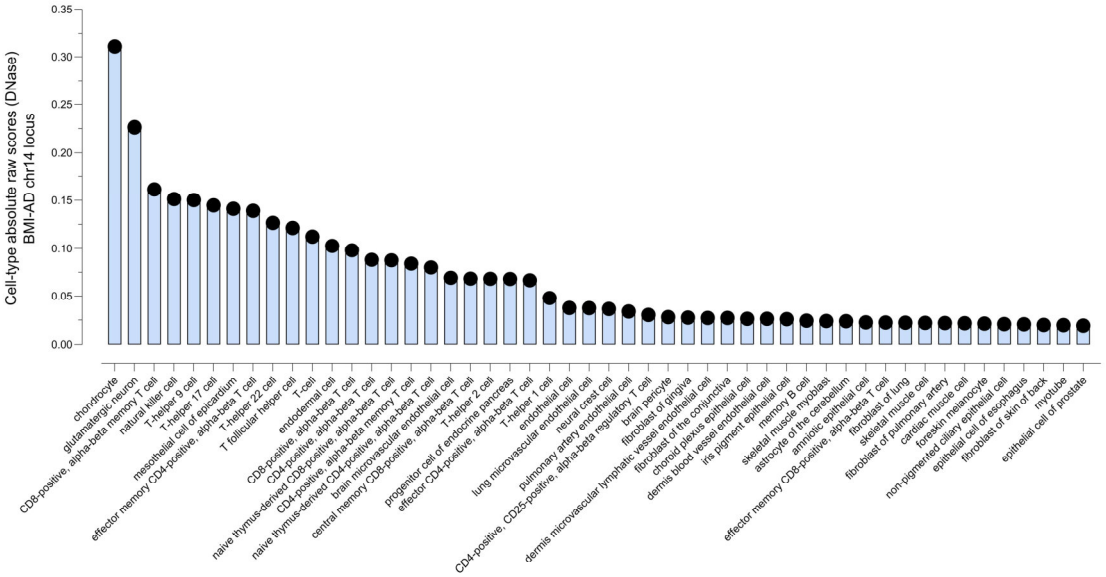

Fig. S3Q | **AlphaGenome**. Top cell-type predictions for the effects of rs17125924 in chromatin accessibility assessed by DNase.

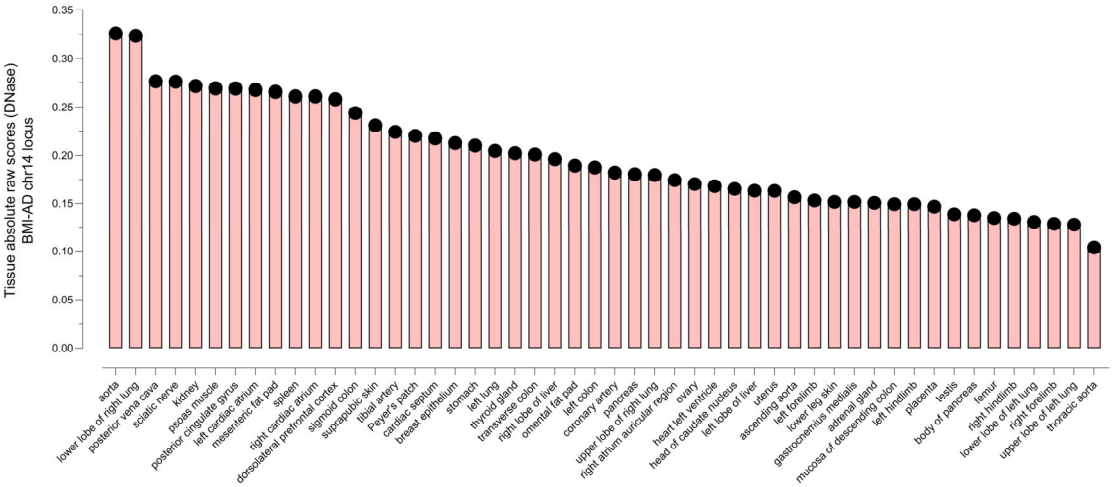

Fig. S3R | **AlphaGenome**. Top tissue predictions for the effects of rs17125924 in chromatin accessibility assessed by DNase.

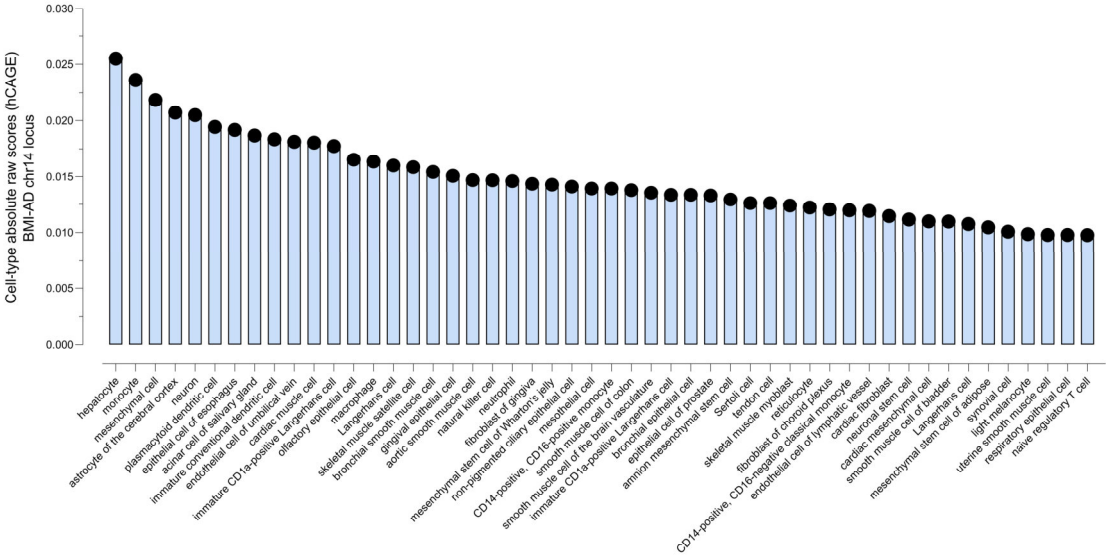

Fig. S3S | **AlphaGenome**. Top cell-type predictions for the effects of rs17125924 in gene expression assessed by hCAGE.

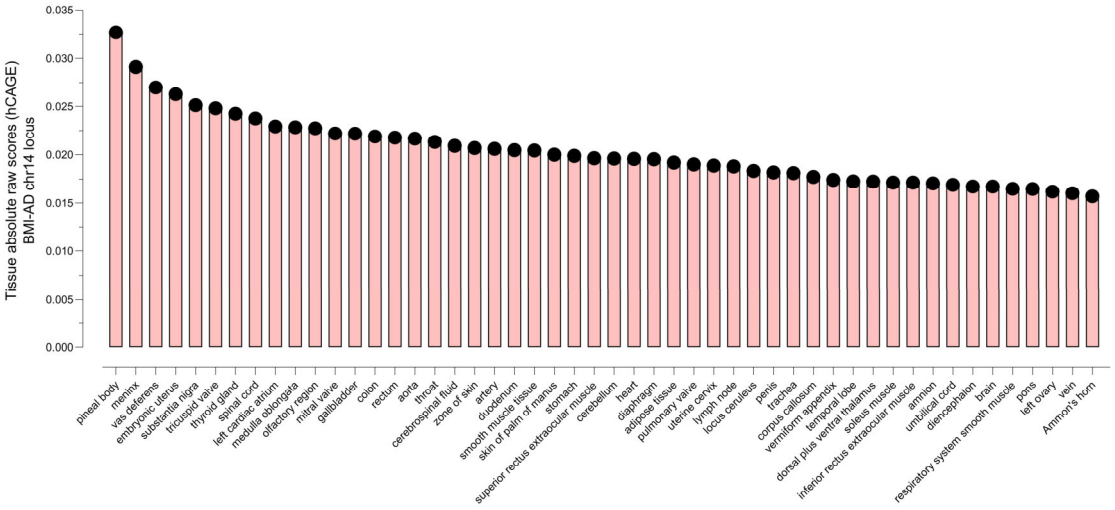

Fig. S3T | **AlphaGenome**. Top tissue predictions for the effects of rs17125924 in gene expression assessed by hCAGE.

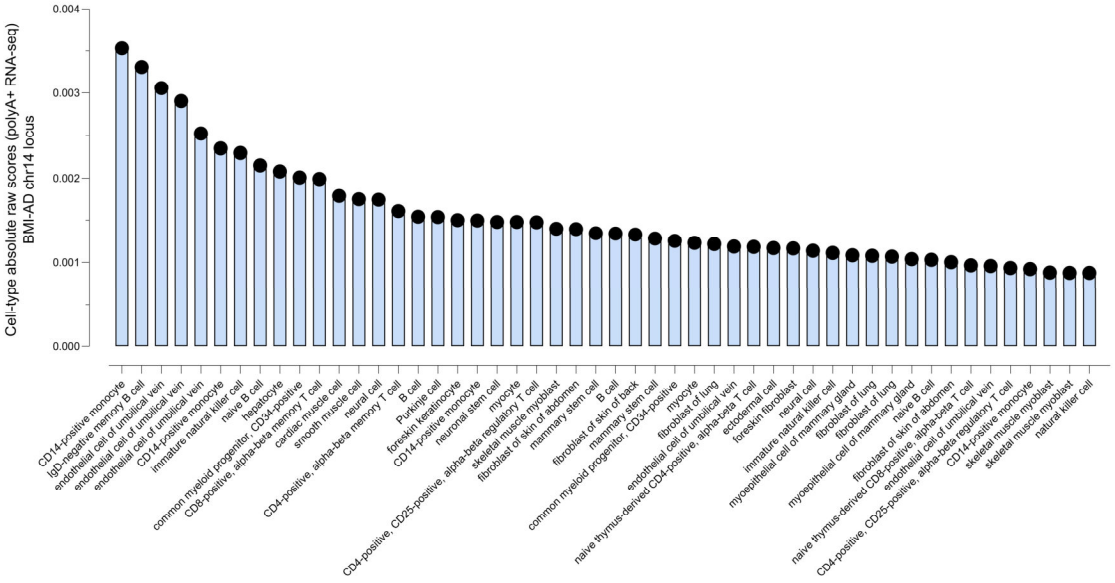

Fig. S3U | **AlphaGenome**. Top cell-type predictions for the effects of rs17125924 in gene expression assessed by polyA+ RNA-seq.

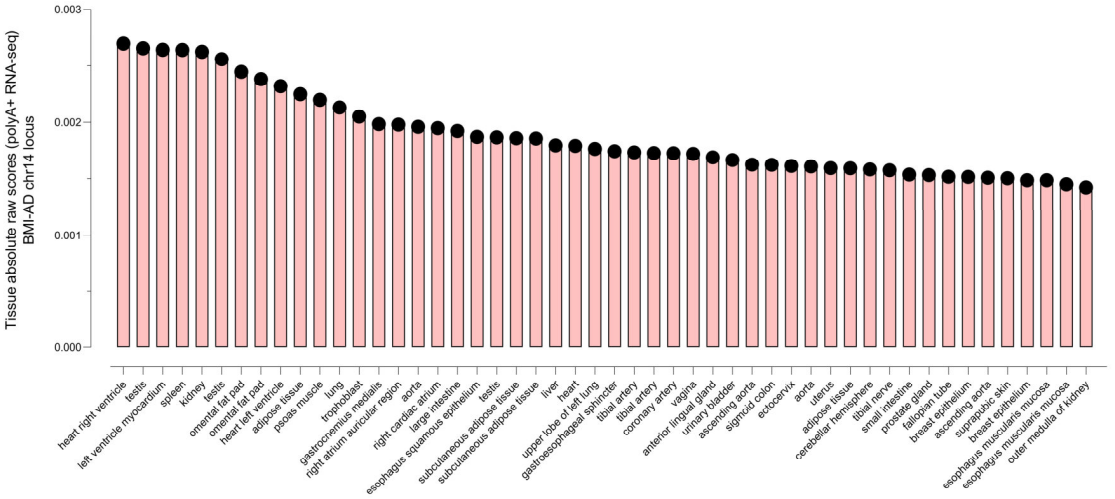

Fig. S3V | **AlphaGenome**. Top tissue predictions for the effects of rs17125924 in gene expression assessed by polyA+ RNA-seq.

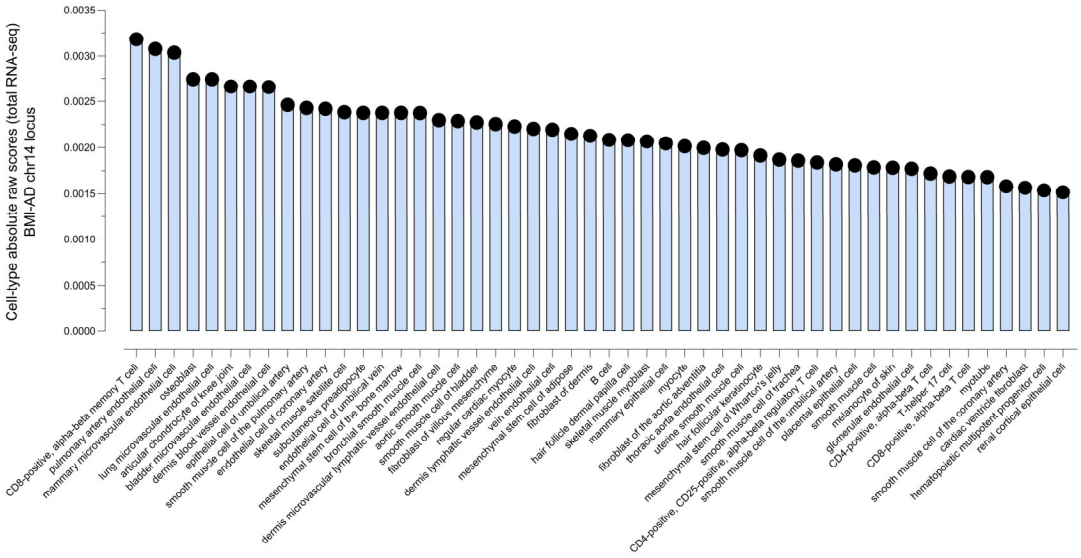

Fig. S3W | **AlphaGenome**. Top cell-type predictions for the effects of rs17125924 in gene expression assessed by total RNA-seq.

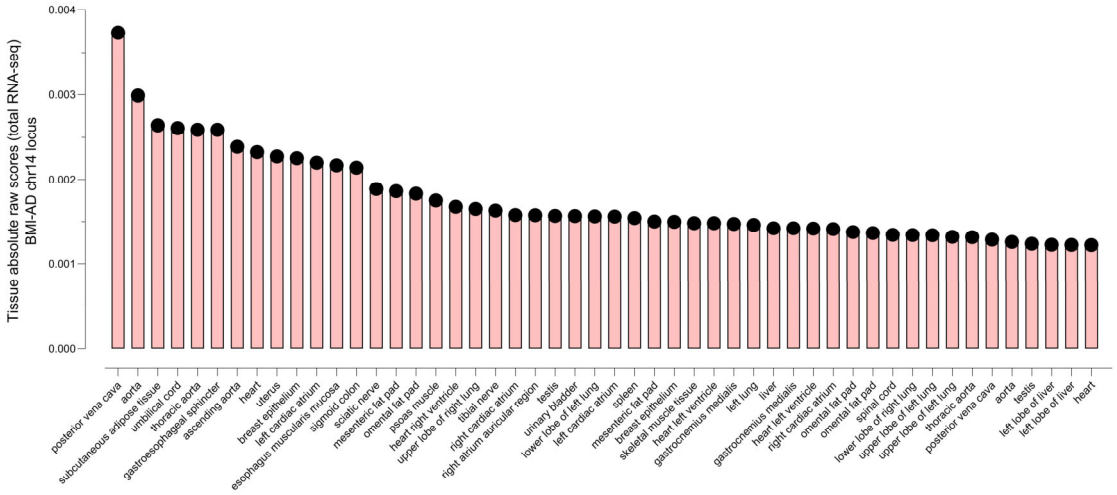

Fig. S3X | **AlphaGenome**. Top tissue predictions for the effects of rs17125924 in gene expression assessed by total RNA-seq.

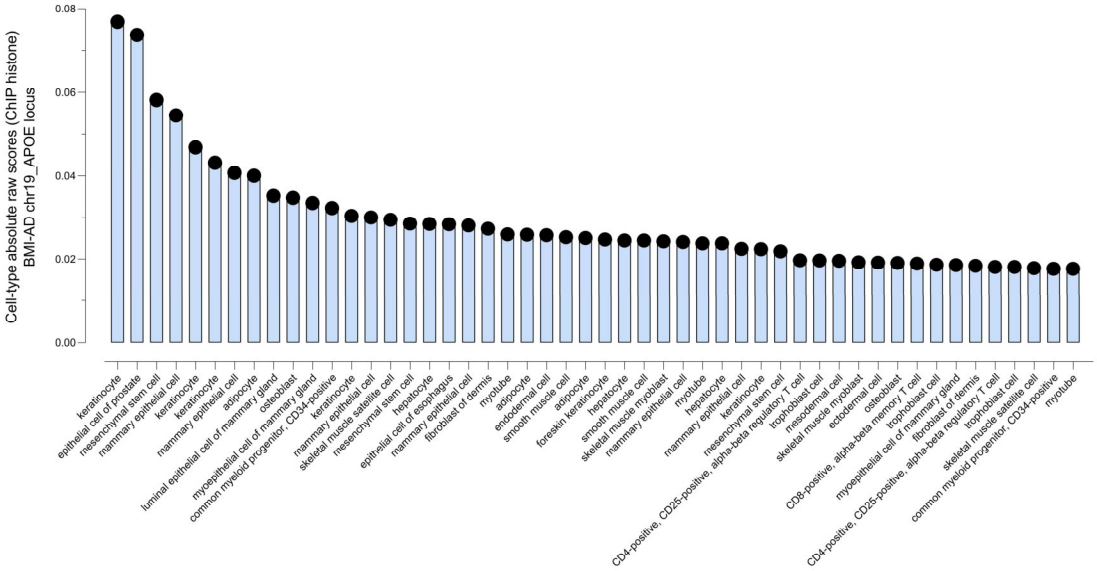

Fig. S3Y | **AlphaGenome**. Top cell-type predictions for the effects of rs7254892 in histone modifications.

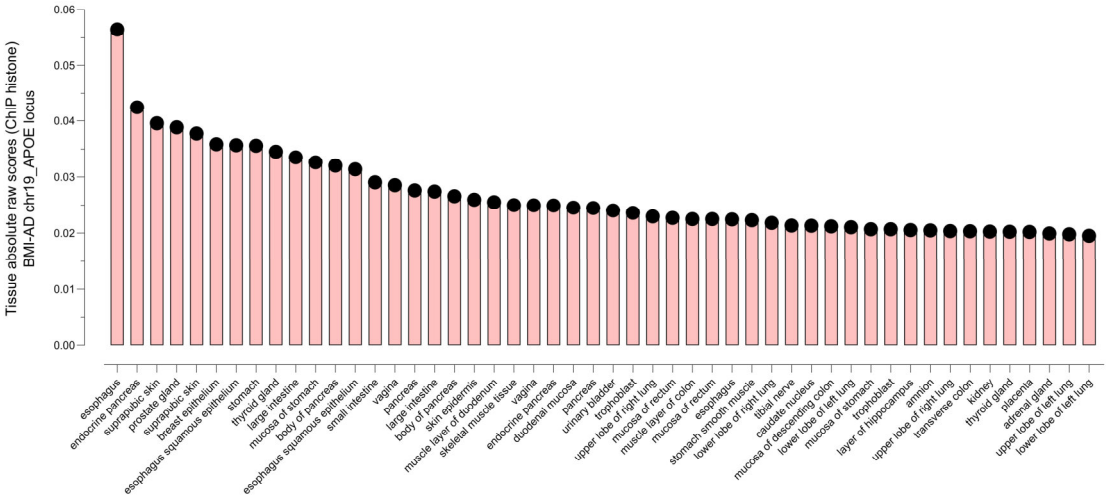

Fig. S3Z | **AlphaGenome**. Top tissue predictions for the effects of rs7254892 in histone modifications.

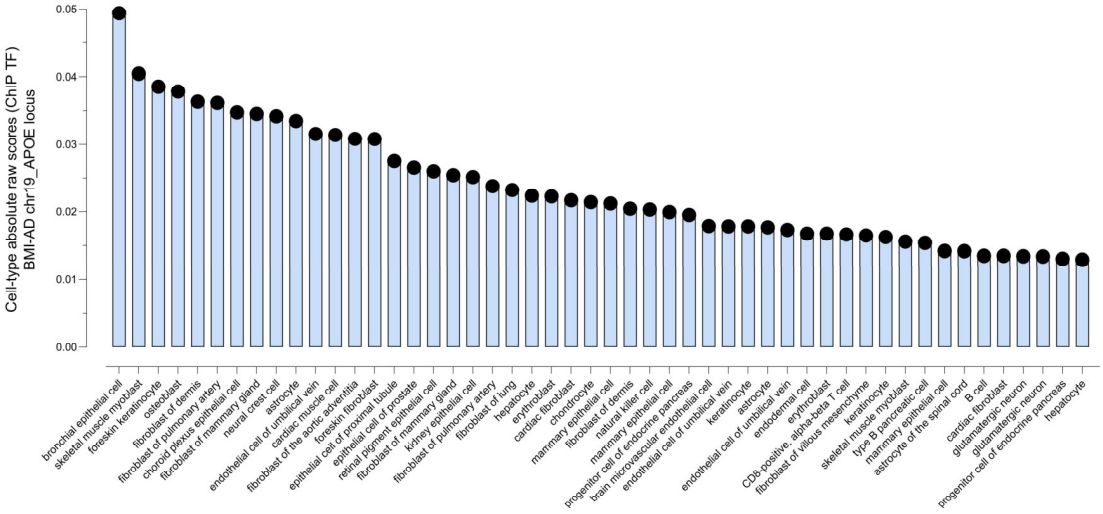

Fig. S3A1 | **AlphaGenome**. Top cell-type predictions for the effects of rs7254892 in transcription factor binding.

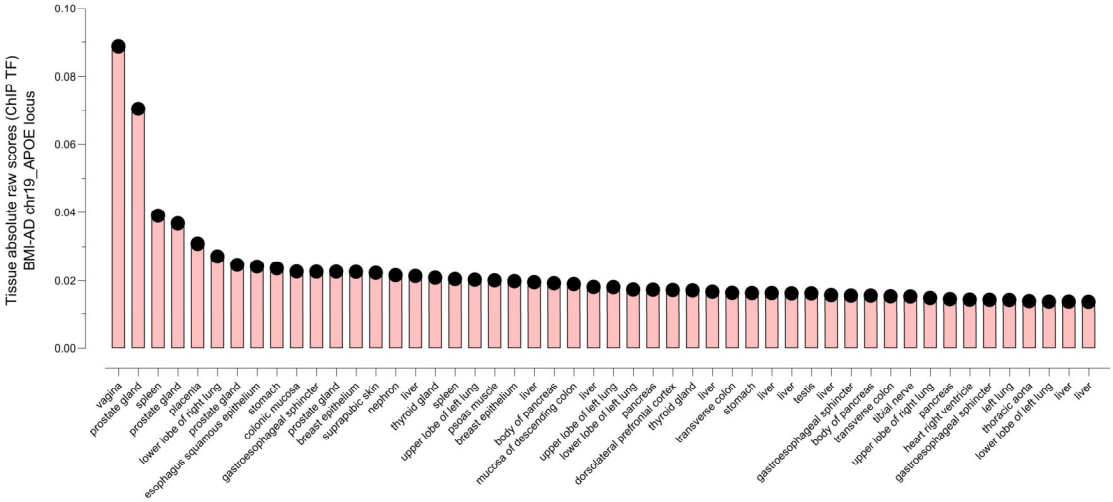

Fig. S3B1 | **AlphaGenome**. Top tissue predictions for the effects of rs7254892 in transcription factor binding.

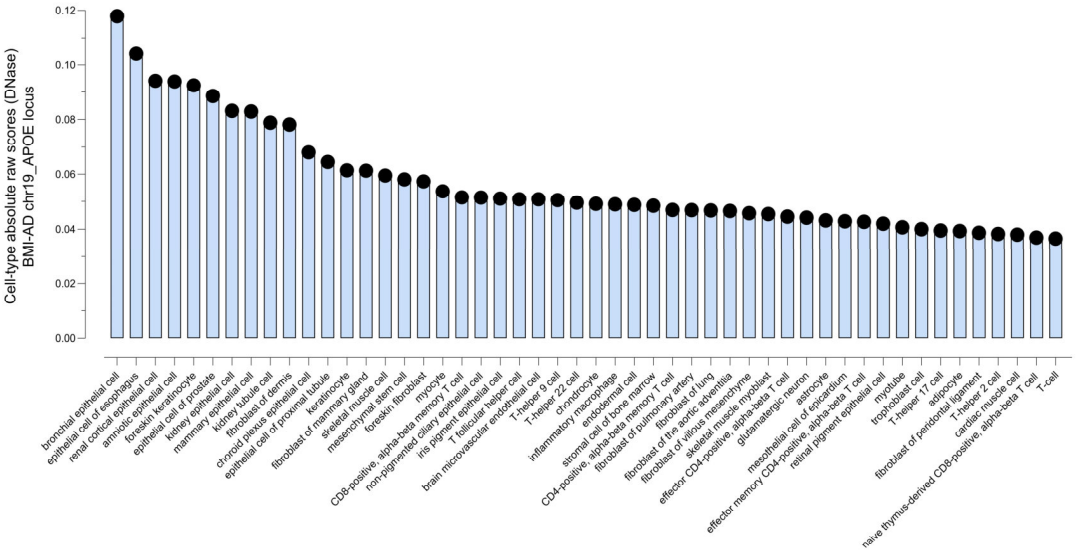

Fig. S3C1 | **AlphaGenome**. Top cell-type predictions for the effects of rs7254892 in chromatin accessibility assessed by DNase.

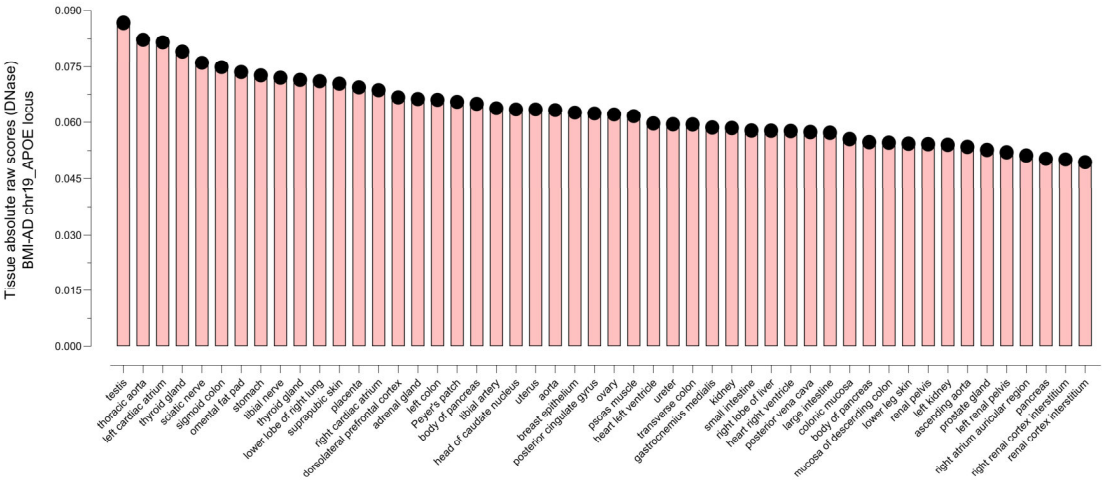

Fig. S3D1 | **AlphaGenome**. Top tissue predictions for the effects of rs7254892 in chromatin accessibility assessed by DNase.

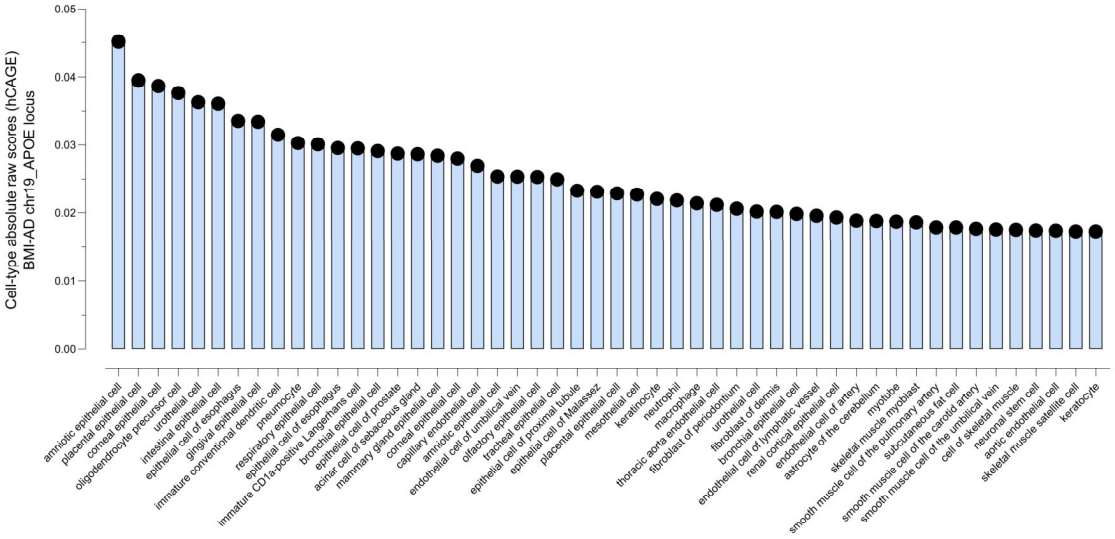

Fig. S3E1 | **AlphaGenome**. Top cell-type predictions for the effects of rs7254892 in gene expression assessed by hCAGE.

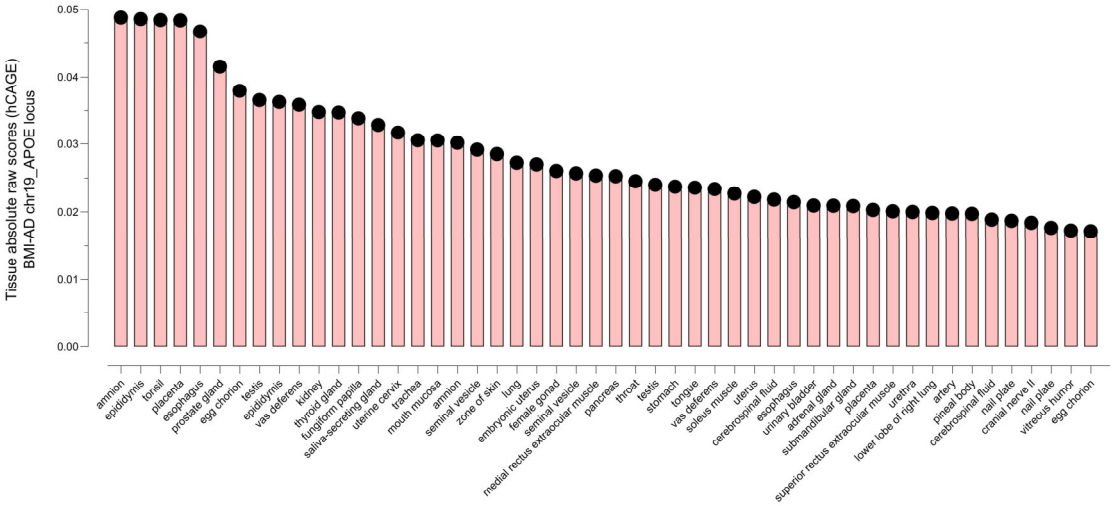

Fig. S3F1 | **AlphaGenome**. Top tissue predictions for the effects of rs7254892 in gene expression assessed by hCAGE.

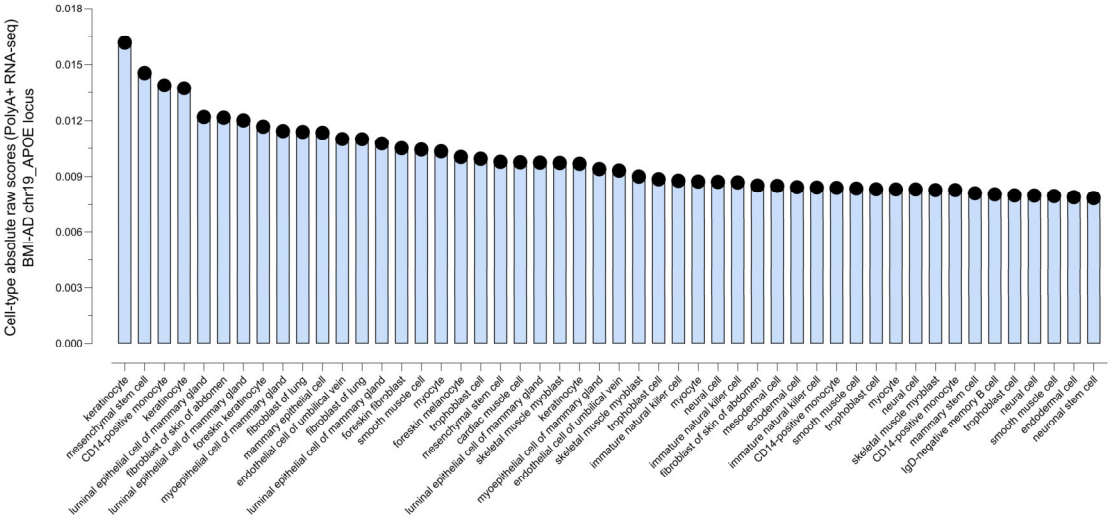

Fig. S3G1 | **AlphaGenome**. Top cell-type predictions for the effects of rs7254892 in gene expression assessed by polyA+ RNA-seq.

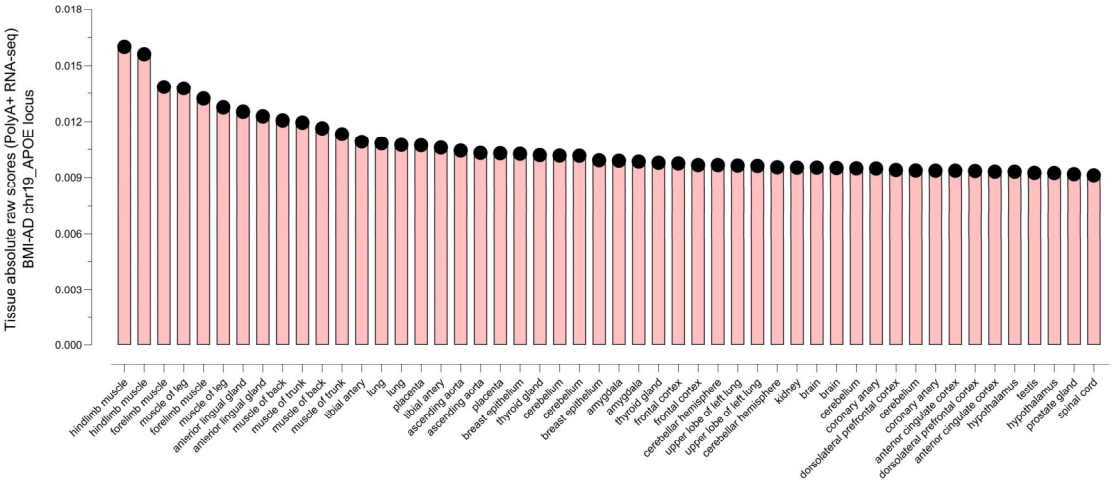

Fig. S3H1 | **AlphaGenome**. Top tissue predictions for the effects of rs7254892 in gene expression assessed by polyA+ RNA-seq.

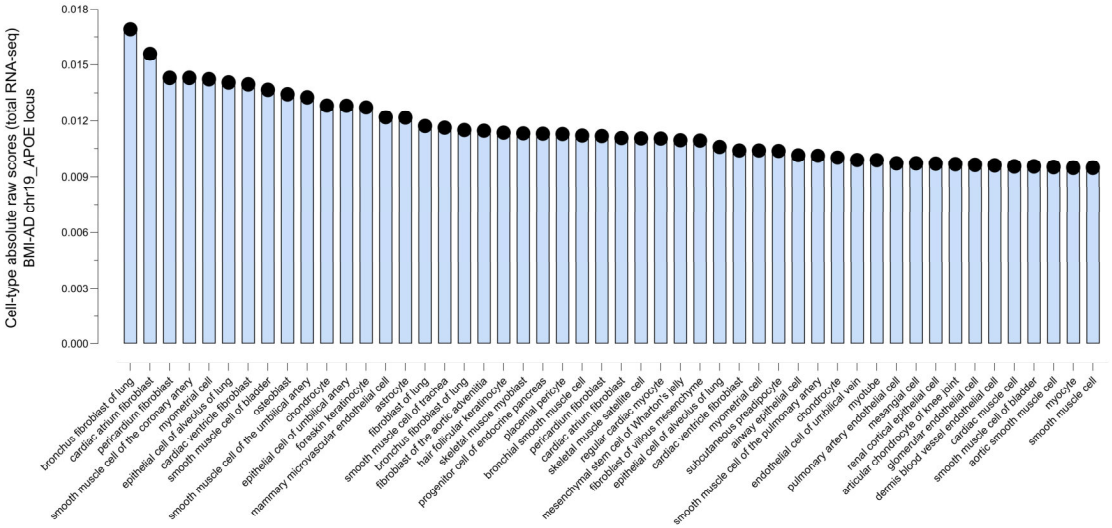

Fig. S3I1 | **AlphaGenome**. Top cell-type predictions for the effects of rs7254892 in gene expression assessed by total RNA-seq.

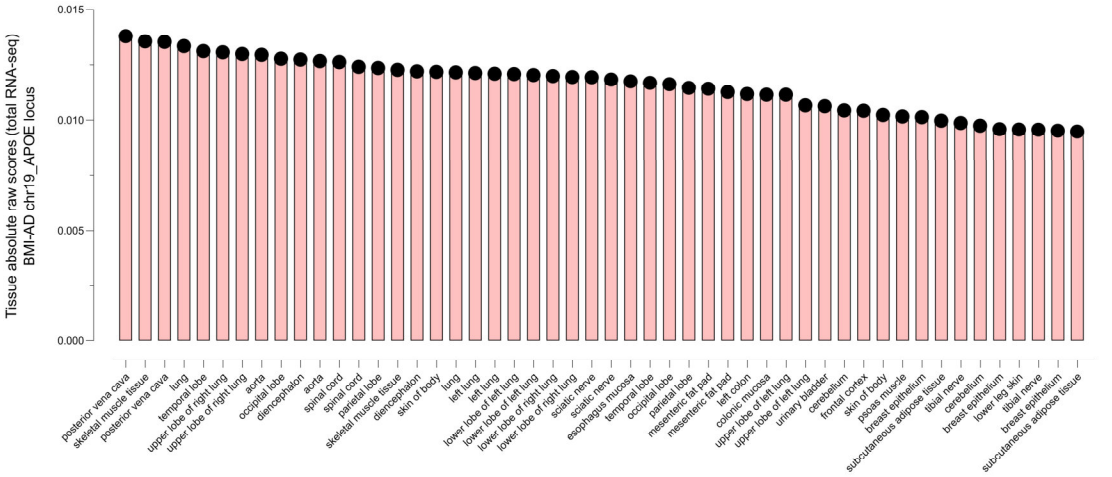

Fig. S3J1 | **AlphaGenome**. Top tissue predictions for the effects of rs7254892 in gene expression assessed by total RNA-seq.

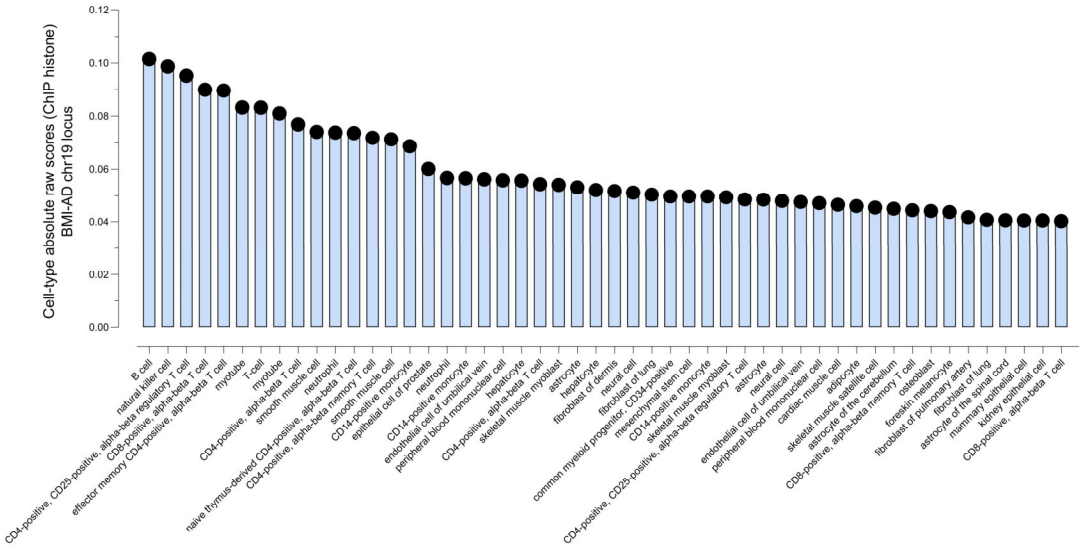

Fig. S3K1 | **AlphaGenome**. Top cell-type predictions for the effects of rs11668832 in histone modifications.

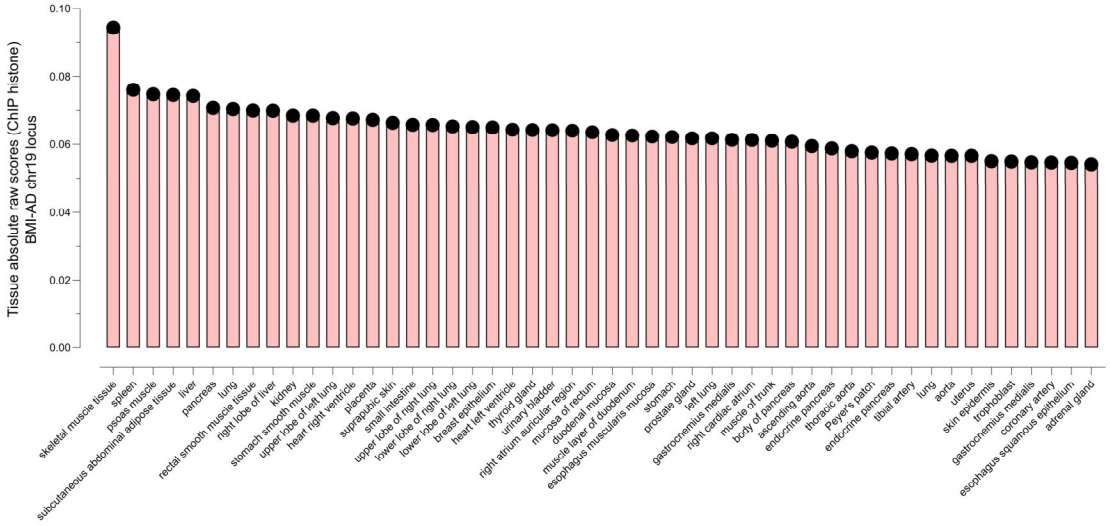

Fig. S3L1 | **AlphaGenome**. Top tissue predictions for the effects of rs11668832 in histone modifications.

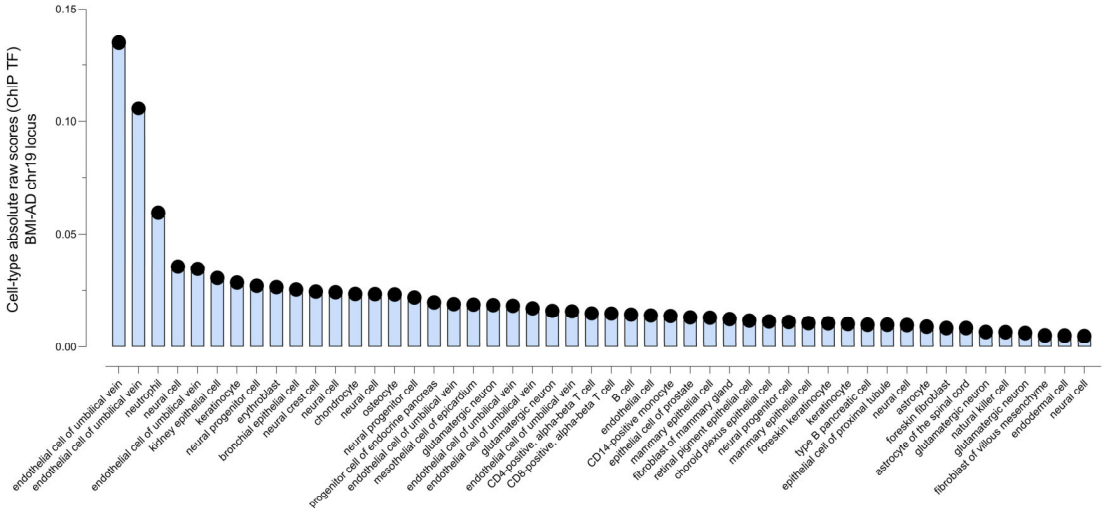

Fig. S3M1 | **AlphaGenome**. Top cell-type predictions for the effects of rs11668832 in transcription factor binding.

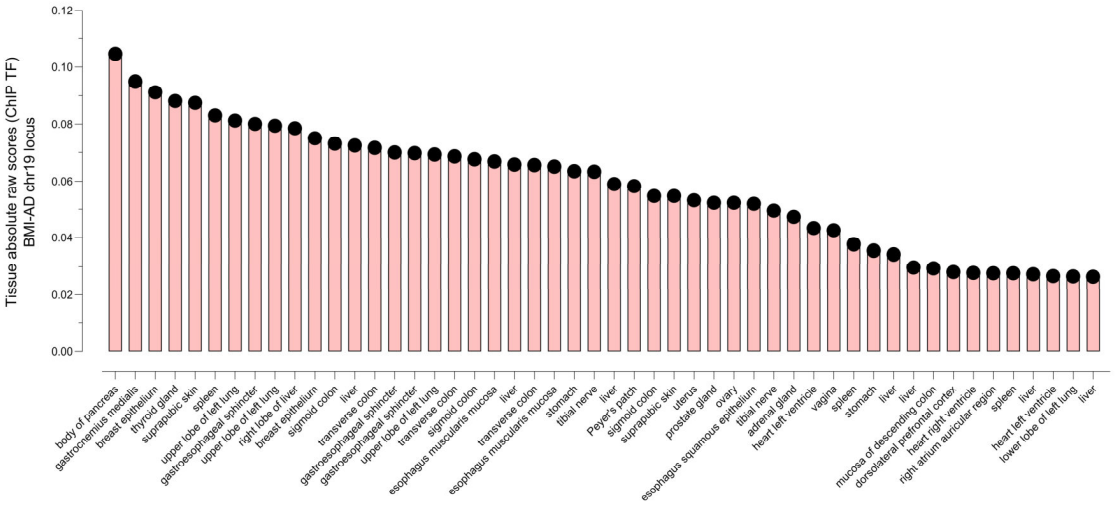

Fig. S3N1 | **AlphaGenome**. Top tissue predictions for the effects of rs11668832 in transcription factor binding.

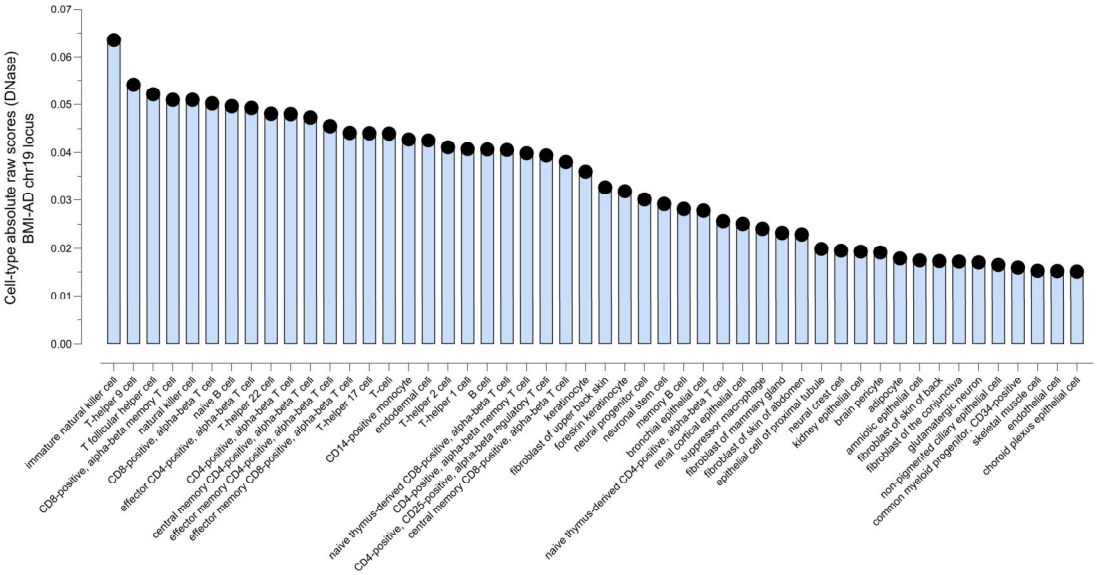

Fig. S3O1 | **AlphaGenome**. Top cell-type predictions for the effects of rs11668832 in chromatin accessibility assessed by DNase.

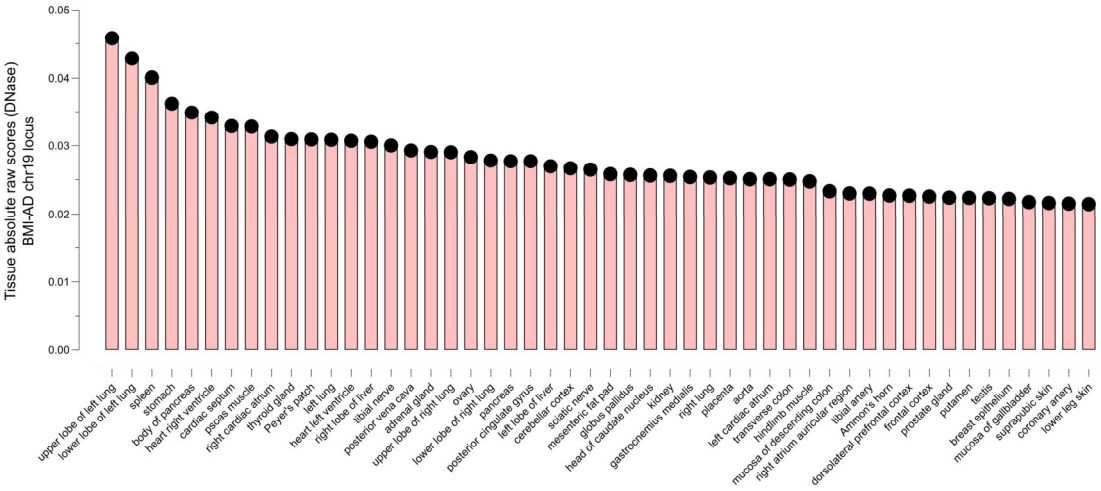

Fig. S3P1 | **AlphaGenome**. Top tissue predictions for the effects of rs11668832 in chromatin accessibility assessed by DNase.

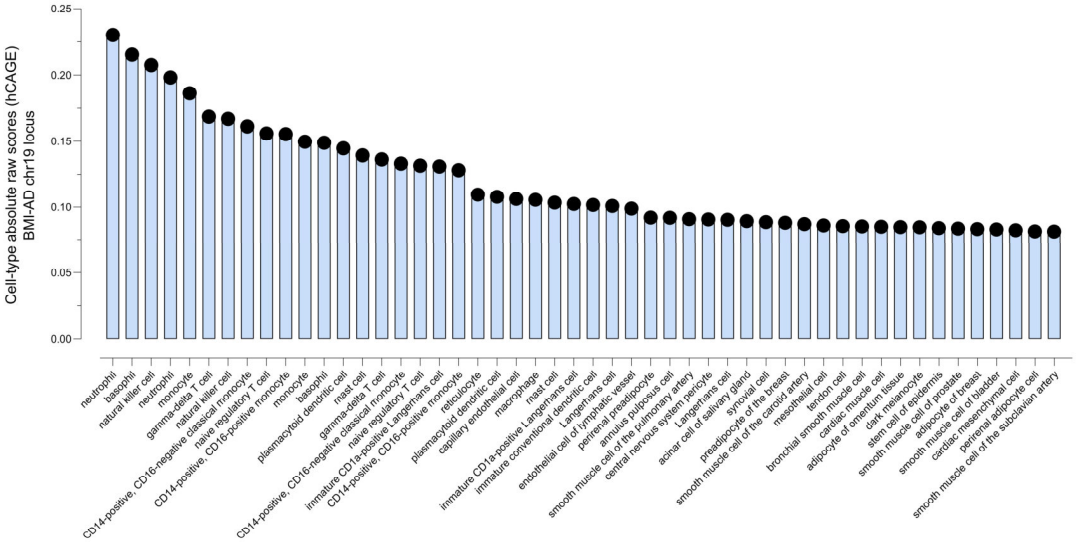

Fig. S3Q1 | **AlphaGenome**. Top cell-type predictions for the effects of rs11668832 in gene expression assessed by hCAGE.

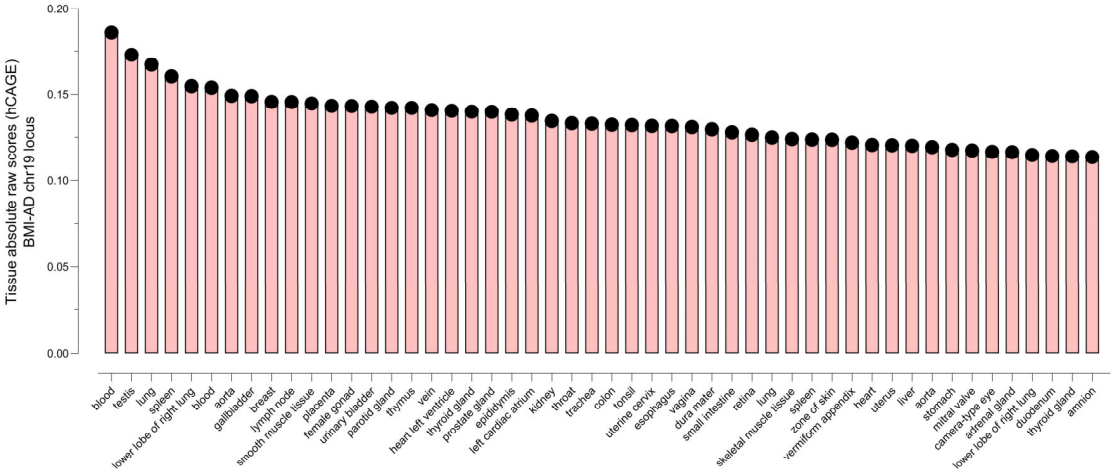

Fig. S3R1 | **AlphaGenome**. Top tissue predictions for the effects of rs11668832 in gene expression assessed by hCAGE

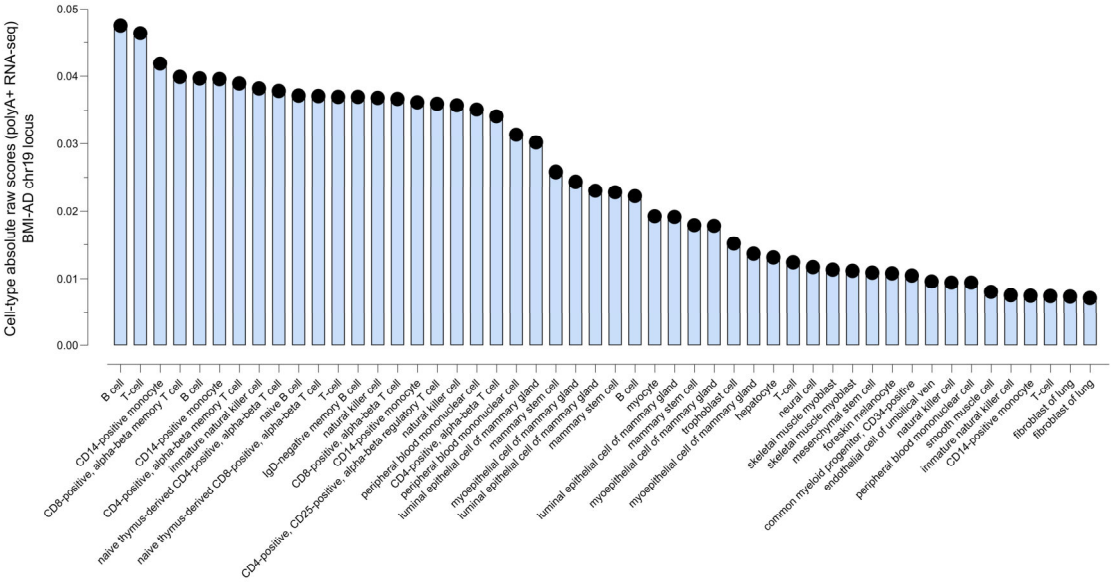

Fig. S3S1 | **AlphaGenome**. Top cell-type predictions for the effects of rs11668832 in gene expression assessed by polyA+ RNA-seq.

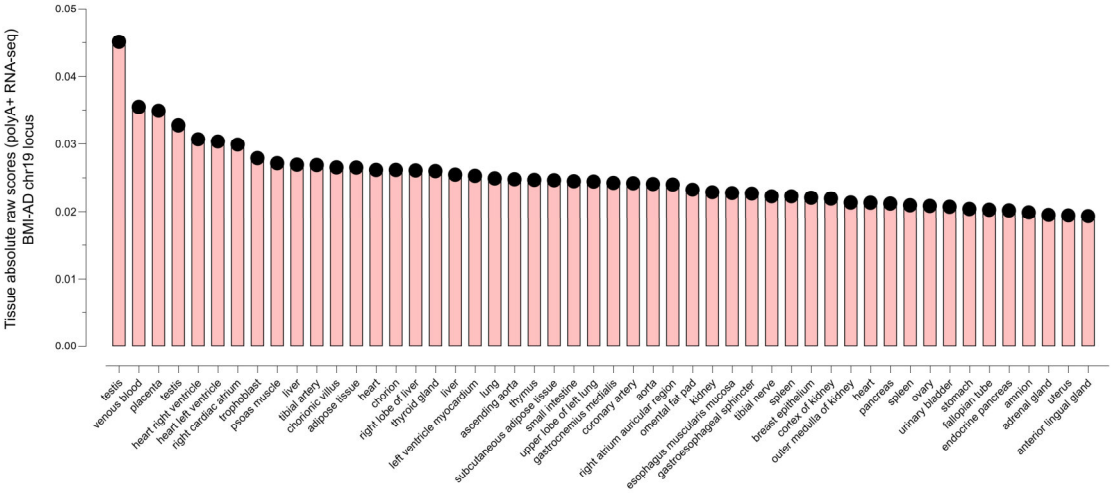

Fig. S3T1 | **AlphaGenome**. Top tissue predictions for the effects of rs11668832 in gene expression assessed by polyA+ RNA-seq.

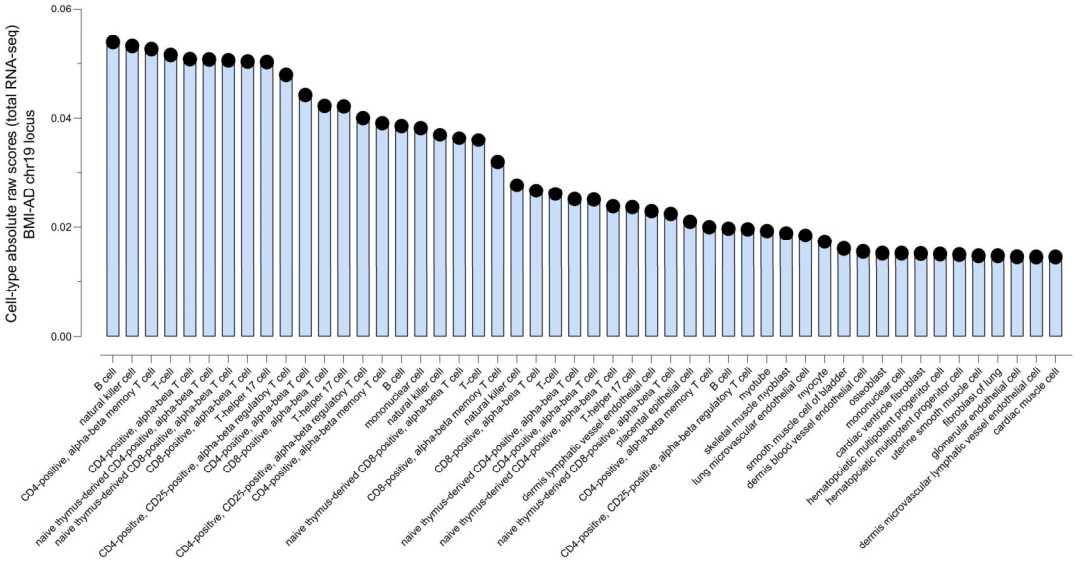

Fig. S3U1 | **AlphaGenome**. Top cell-type predictions for the effects of rs11668832 in gene expression assessed by total RNA-seq.

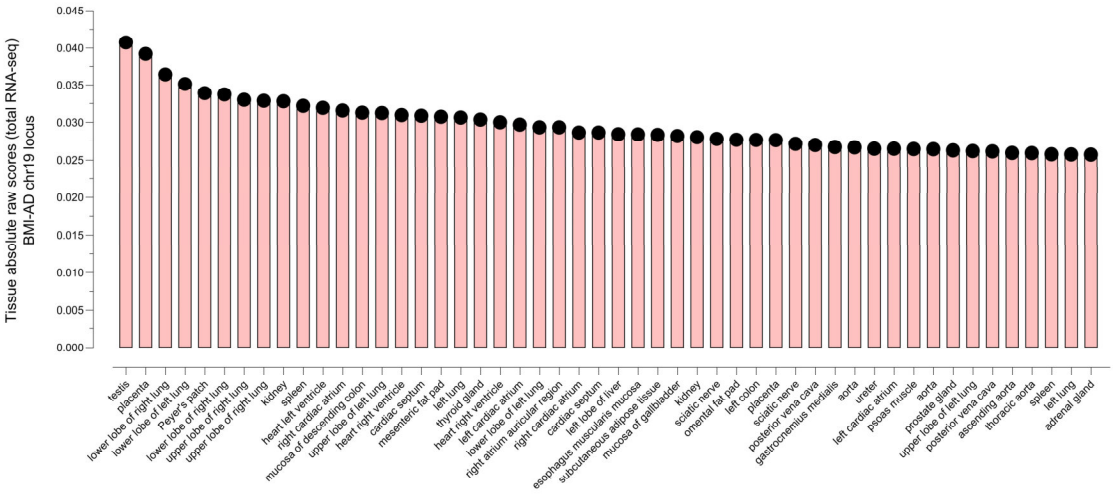

Fig. S3U1 | **AlphaGenome**. Top tissue predictions for the effects of rs11668832 in gene expression assessed by total RNA-seq.

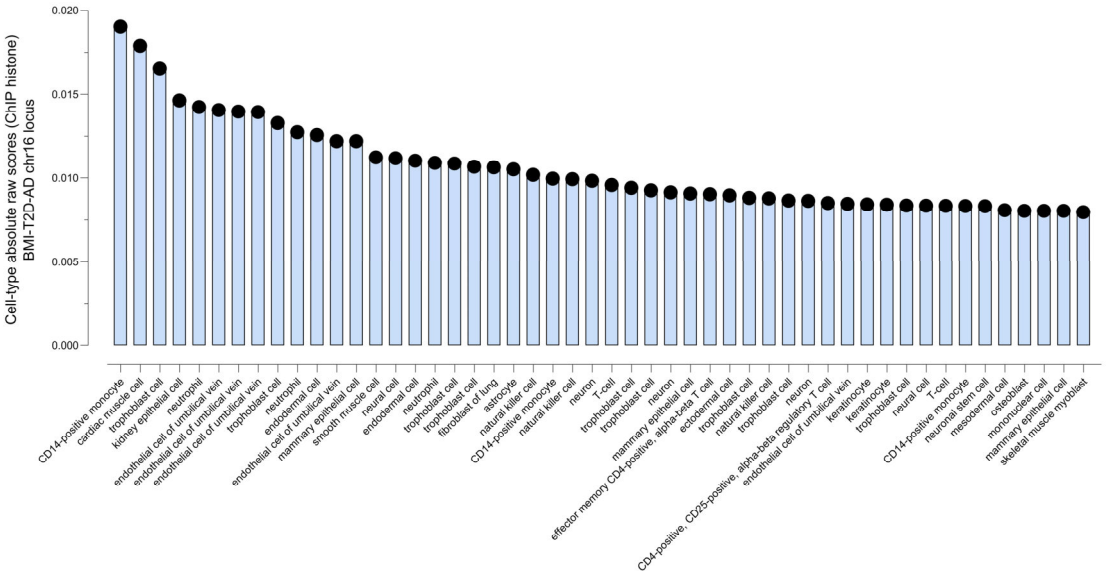

Fig. S3V1 | **AlphaGenome**. Top cell-type predictions for the effects of rs11150577 in histone modifications.

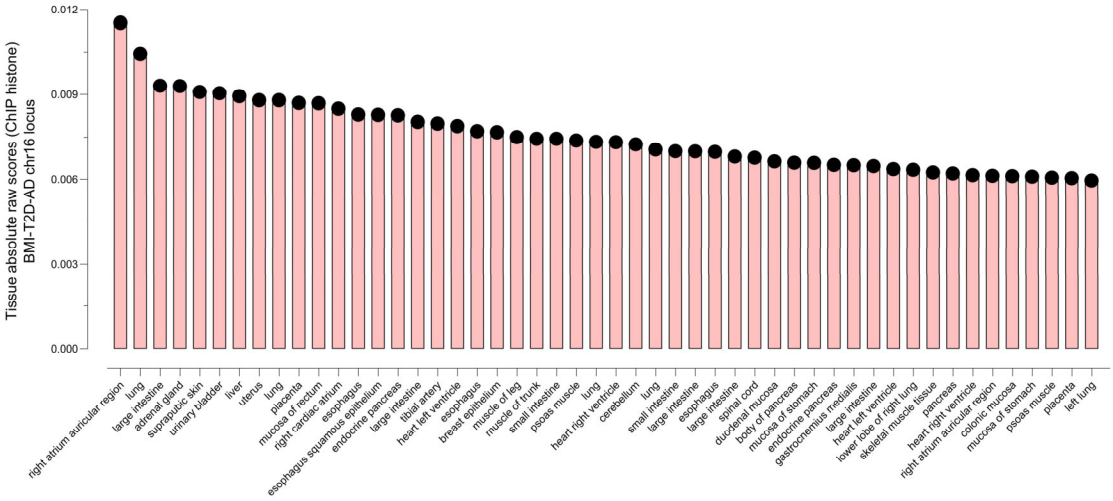

Fig. S3W1 | **AlphaGenome**. Top tissue predictions for the effects of rs11150577 in histone modifications.

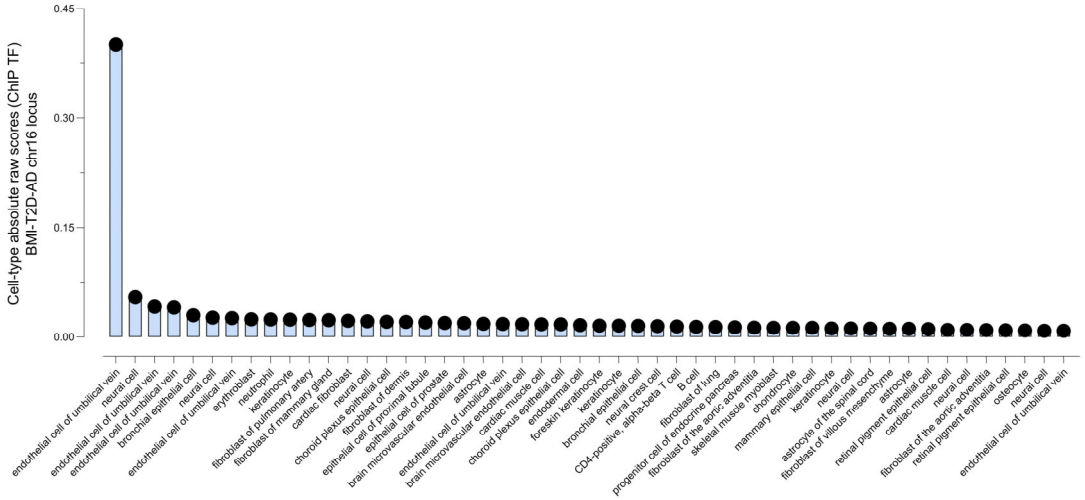

Fig. S3X1 | **AlphaGenome**. Top cell-type predictions for the effects of rs11150577 in transcription factor binding.

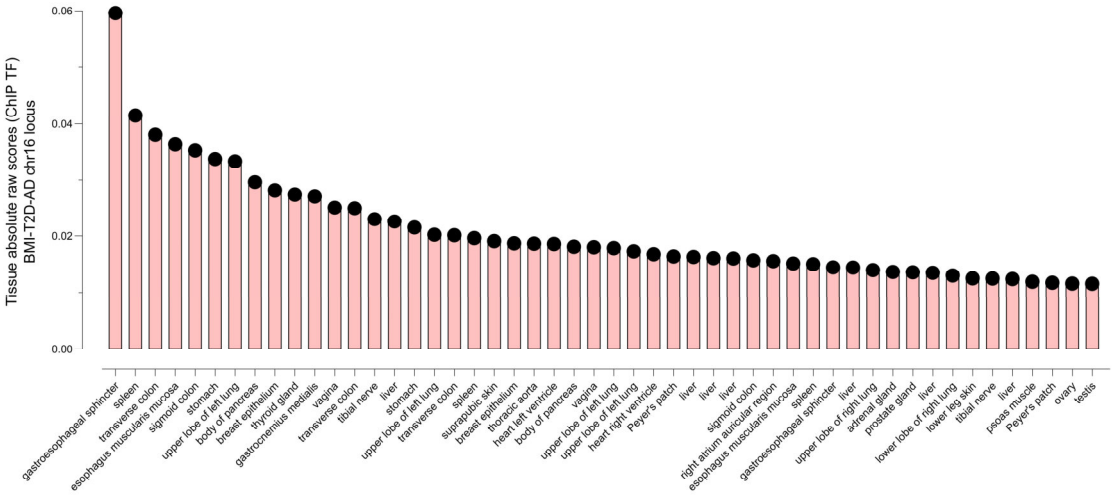

Fig. S3Y1 | **AlphaGenome**. Top cell-type predictions for the effects of rs11150577 in transcription factor binding.

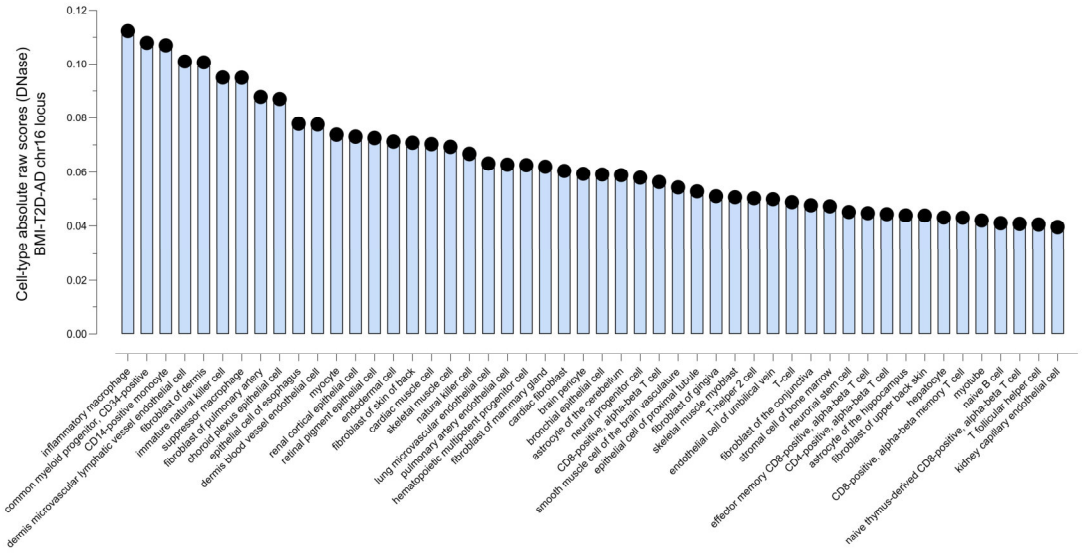

Fig. S3Z1 | **AlphaGenome**. Top cell-type predictions for the effects of rs11150577 in chromatin accessibility assessed by DNase.

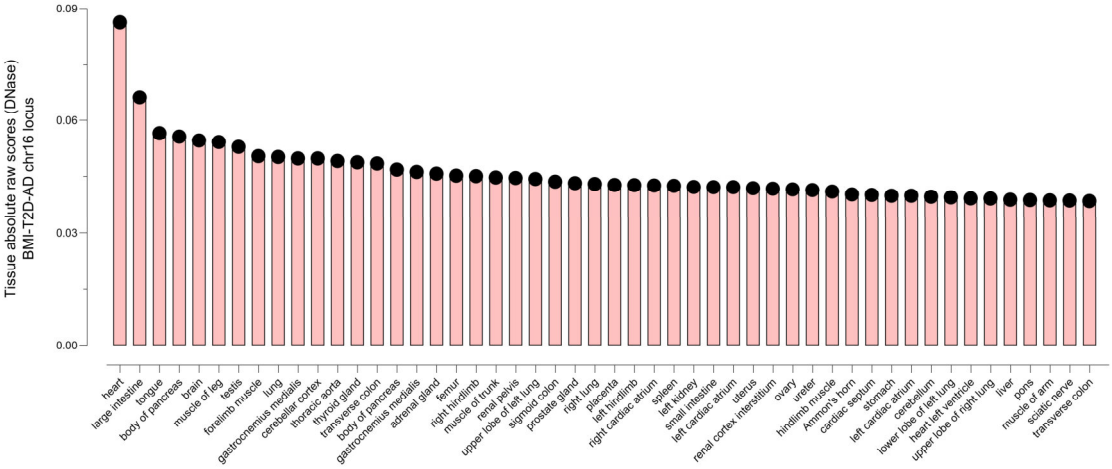

Fig. S3A2 | **AlphaGenome**. Top tissue predictions for the effects of rs11150577 in chromatin accessibility assessed by DNase.

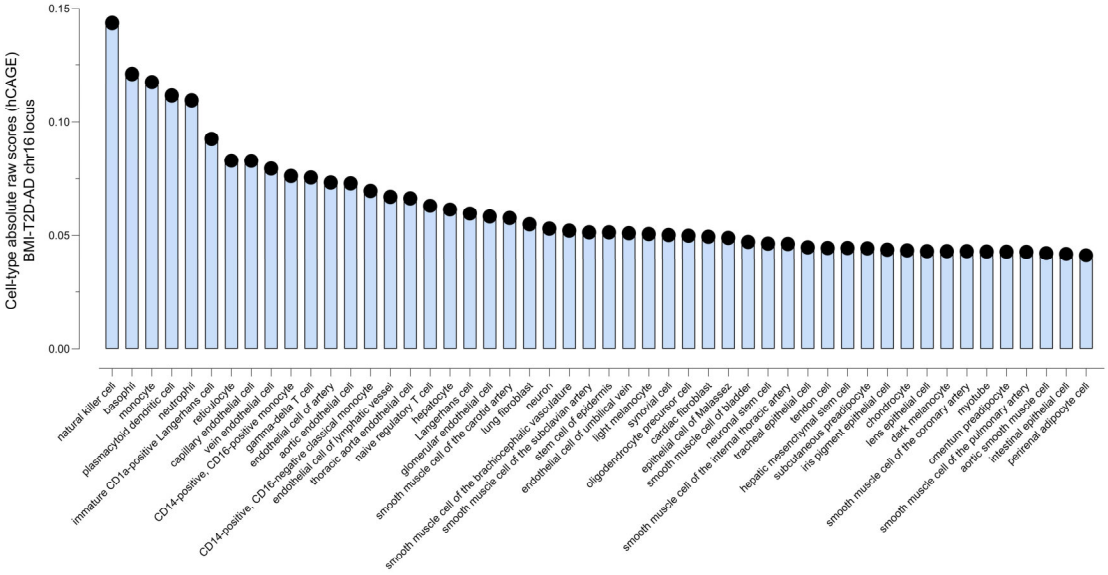

Fig. S3B2 | **AlphaGenome**. Top cell-type predictions for the effects of rs11150577 in gene expression assessed by hCAGE.

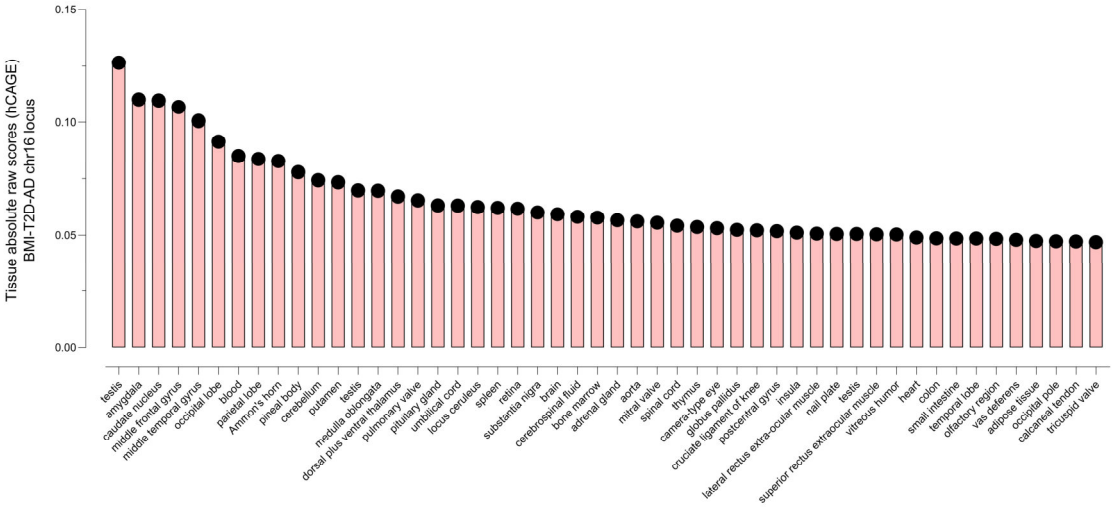

Fig. S3C2 | **AlphaGenome**. Top tissue predictions for the effects of rs11150577 in gene expression assessed by hCAGE.

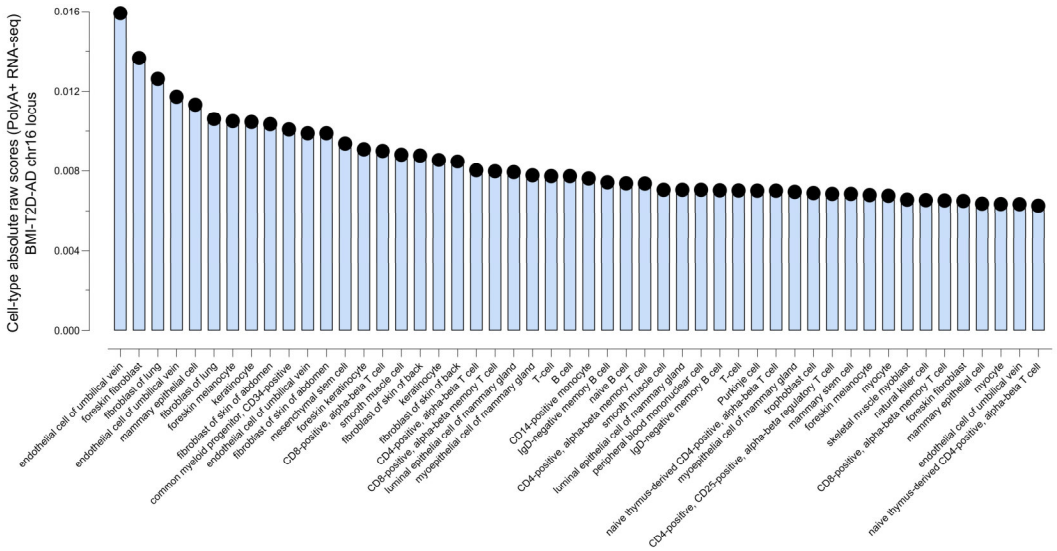

Fig. S3D2 | **AlphaGenome**. Top cell-type predictions for the effects of rs11150577 in gene expression assessed by polyA+ RNA-seq.

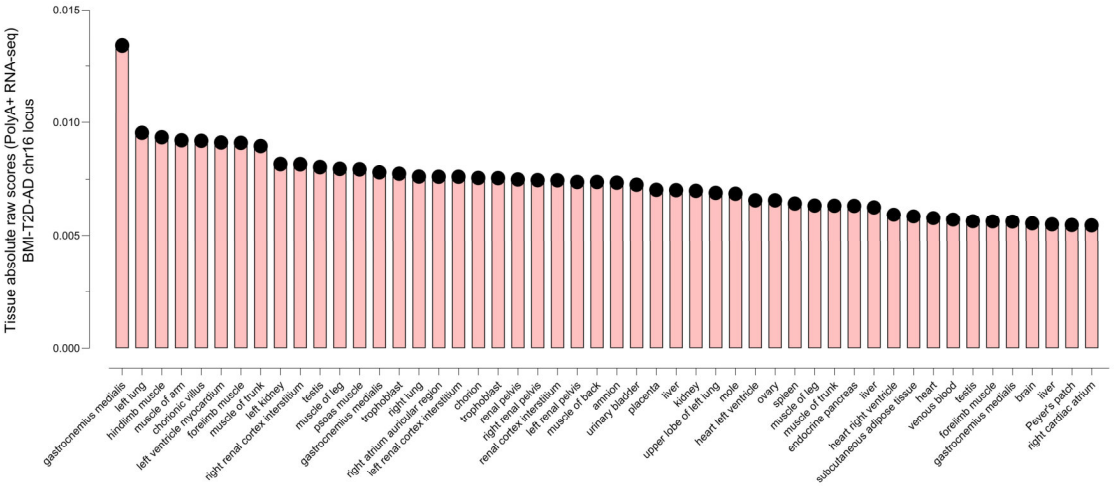

Fig. S3E2 | **AlphaGenome**. Top tissue predictions for the effects of rs11150577 in gene expression assessed by polyA+ RNA-seq.

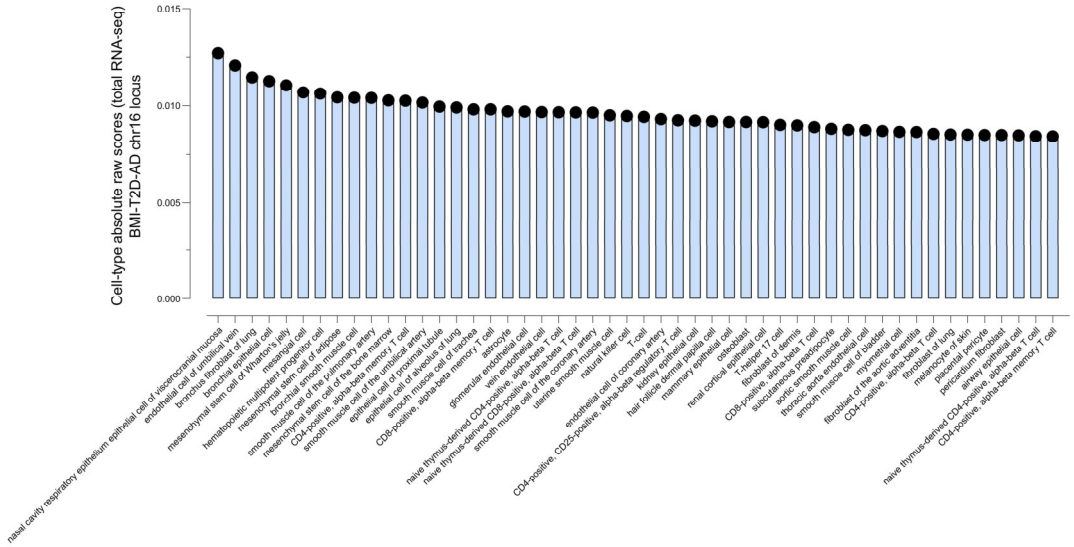

Fig. S3F2 | **AlphaGenome**. Top cell-type predictions for the effects of rs11150577 in gene expression assessed by total RNA-seq.

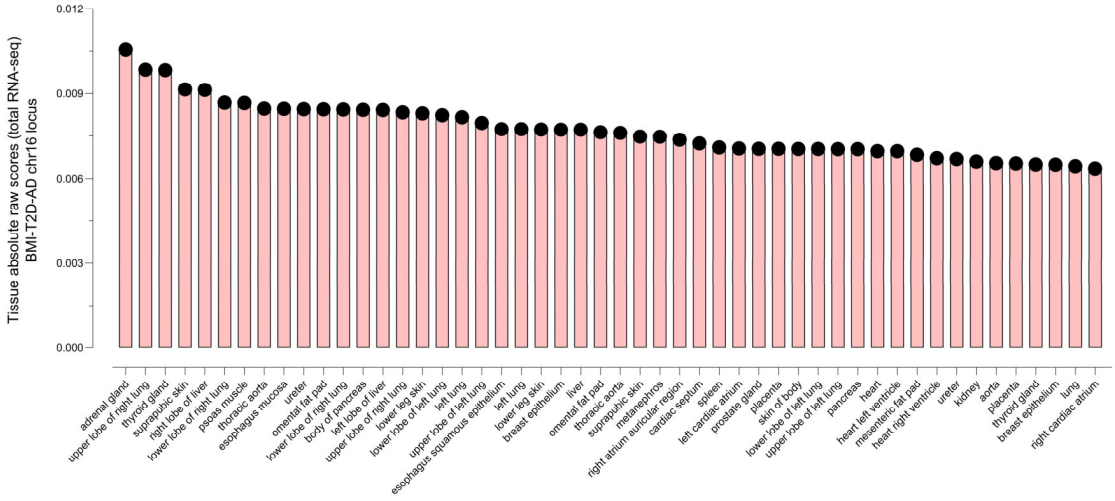

Fig. S3G2 | **AlphaGenome**. Top tissue predictions for the effects of rs11150577 in gene expression assessed by total RNA-seq.

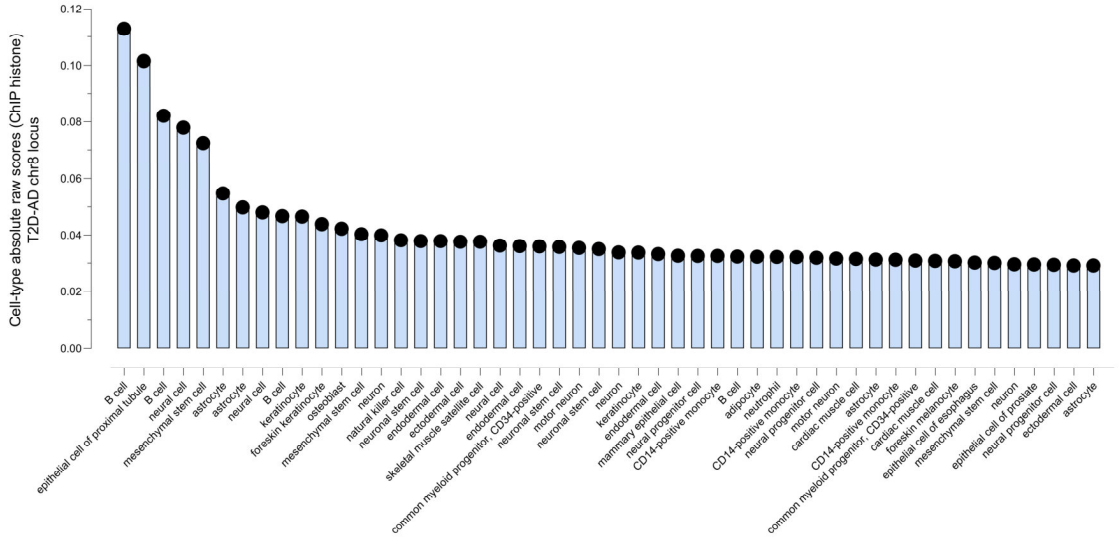

Fig. S3H2 | **AlphaGenome**. Top cell-type predictions for the effects of rs13257021 in histone modifications.

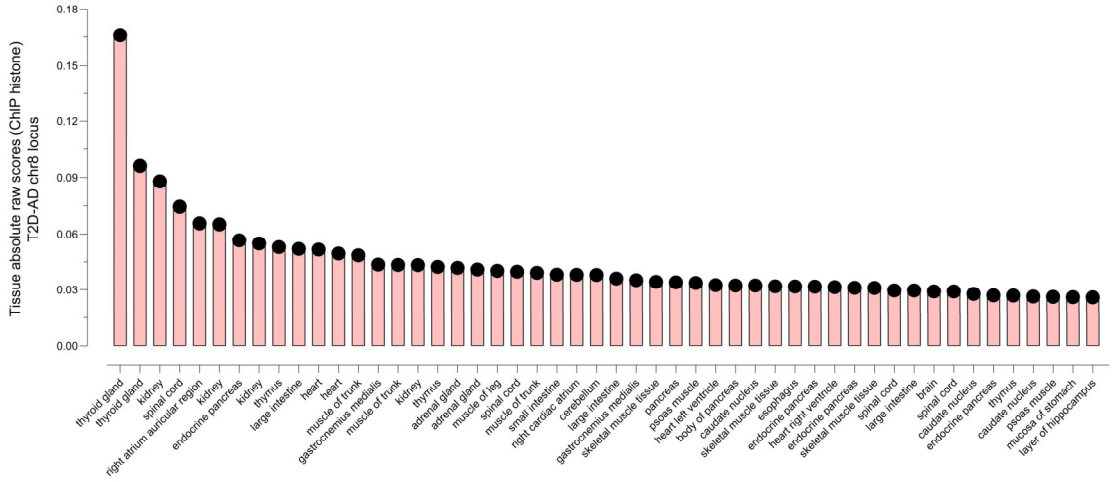

Fig. S3I2 | **AlphaGenome**. Top tissue predictions for the effects of rs13257021 in histone modifications.

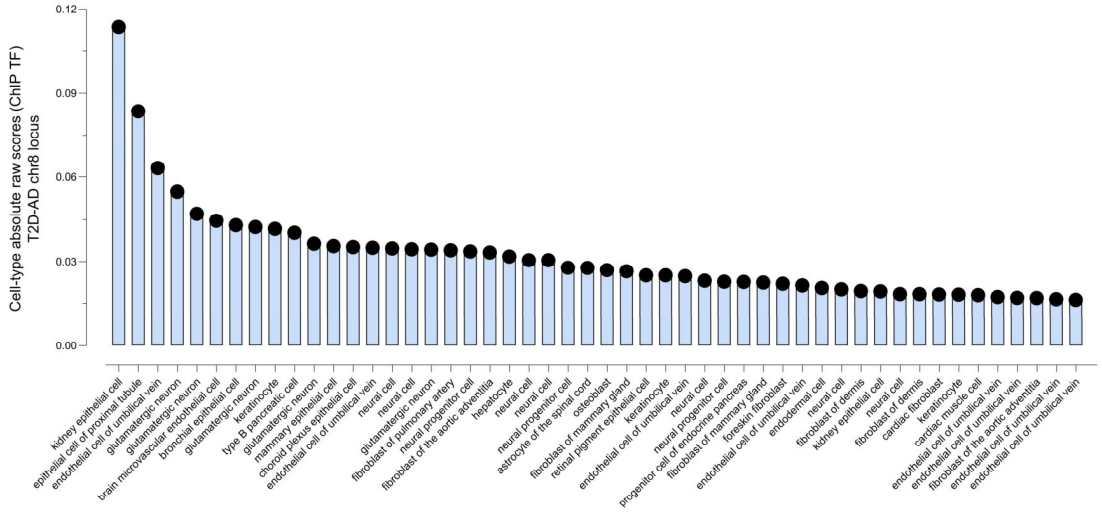

Fig. S3J2 | **AlphaGenome**. Top cell-type predictions for the effects of rs13257021 in transcription factor binding.

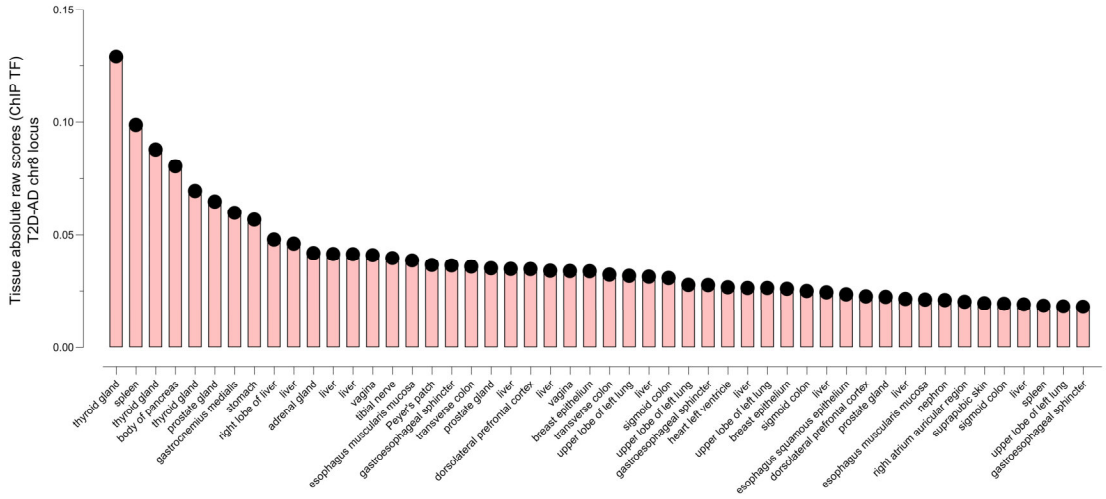

Fig. S3K2 | **AlphaGenome**. Top tissue predictions for the effects of rs13257021 in transcription factor binding.

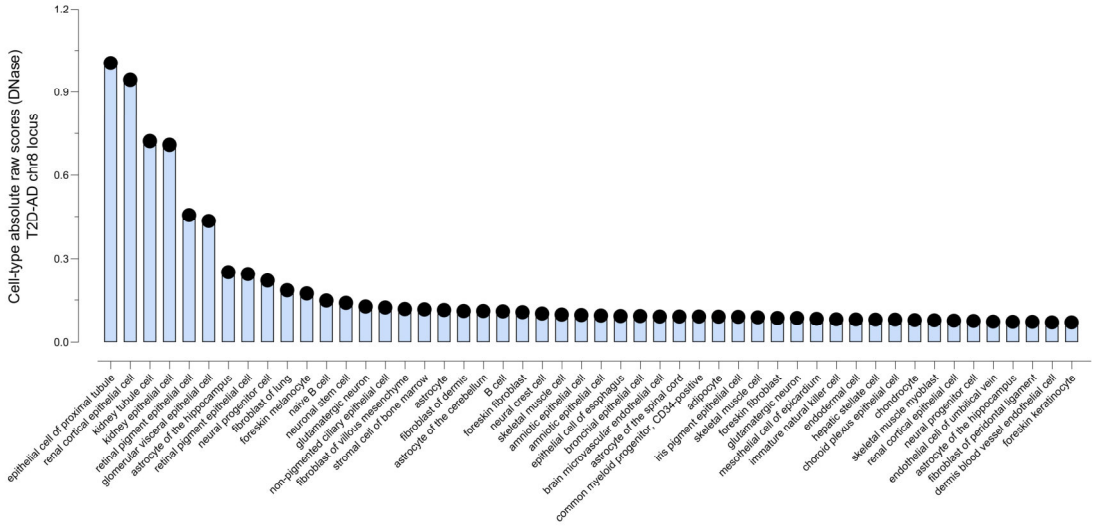

Fig. S3L2 | **AlphaGenome**. Top cell-type predictions for the effects of rs13257021 in chromatin accessibility assessed by DNase.

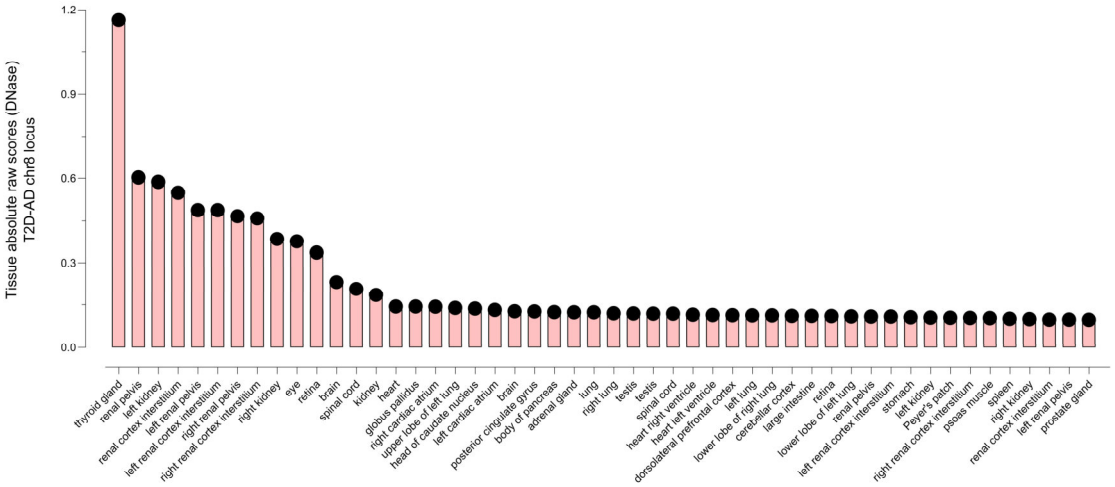

Fig. S3M2 | **AlphaGenome**. Top tissue predictions for the effects of rs13257021 in chromatin accessibility assessed by DNase.

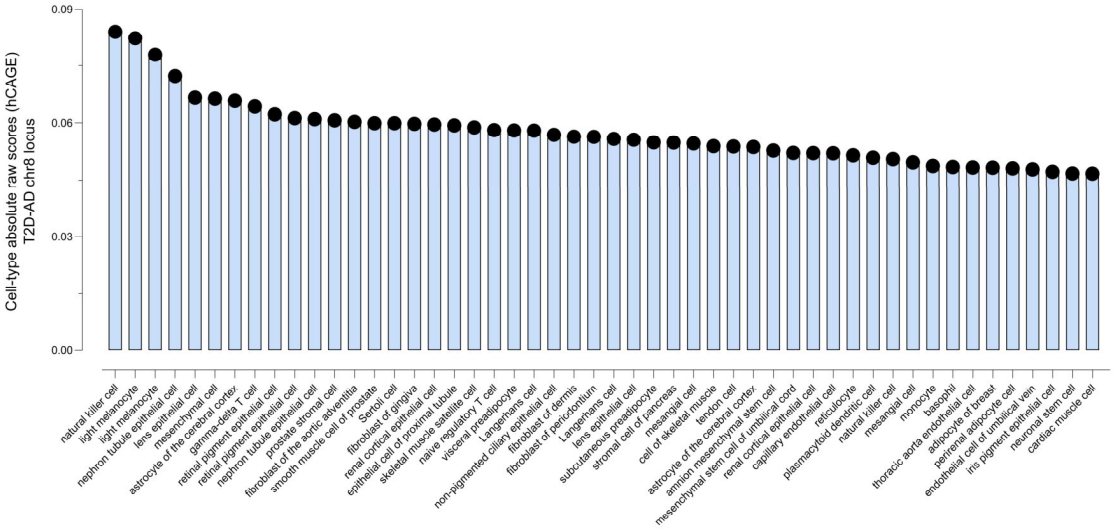

Fig. S3N2 | **AlphaGenome**. Top cell-type predictions for the effects of rs13257021 in gene expression assessed by hCAGE.

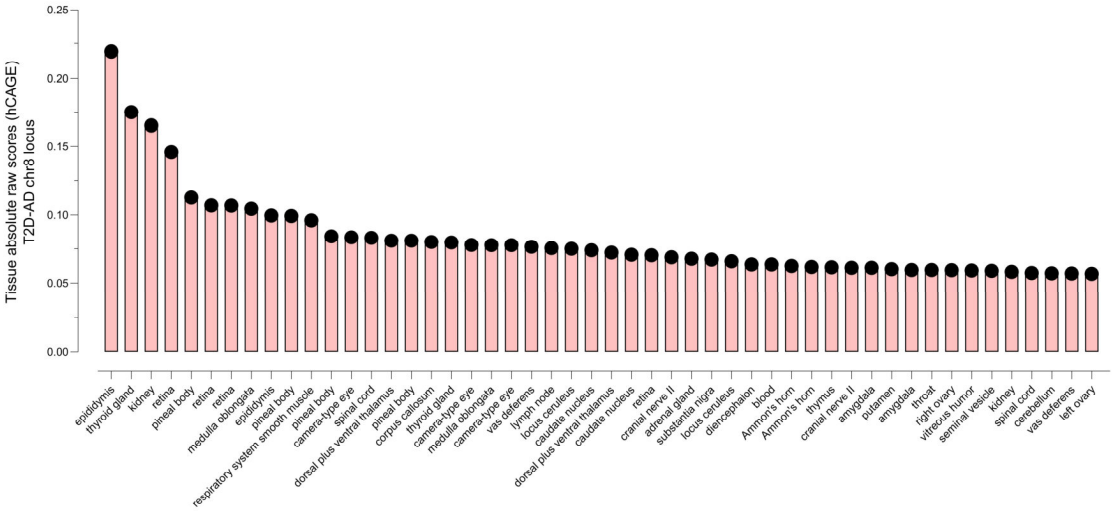

Fig. S3O2 | **AlphaGenome**. Top tissue predictions for the effects of rs13257021 in gene expression assessed by hCAGE.

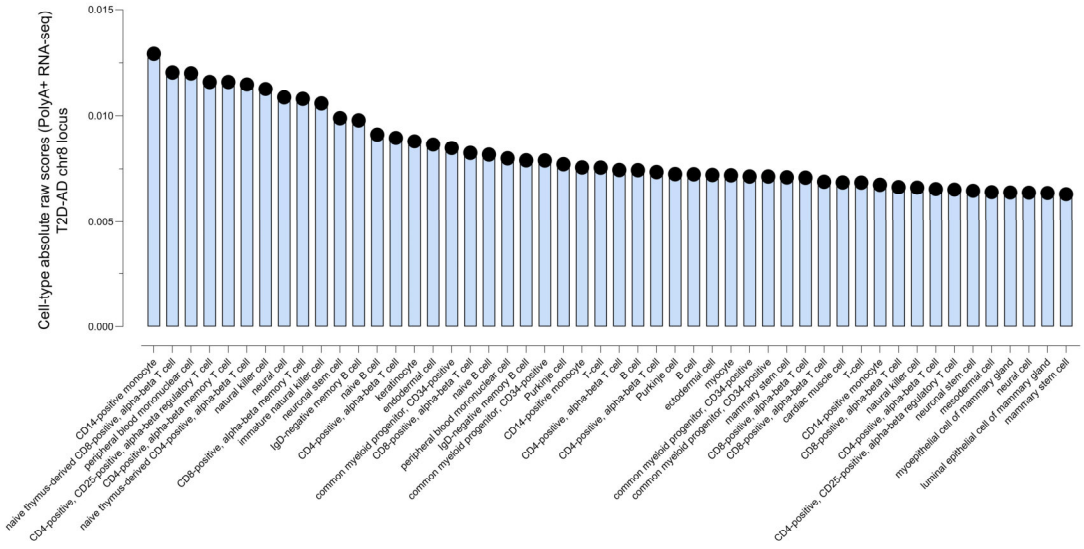

Fig. S3P2 | **AlphaGenome**. Top cell-type predictions for the effects of rs13257021 in gene expression assessed by polyA+ RNA-seq.

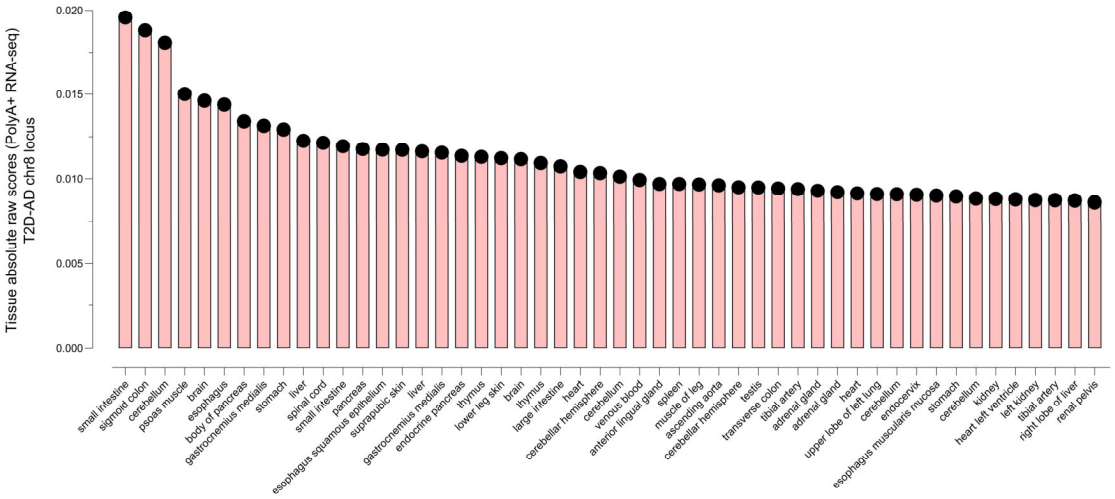

Fig. S3Q2 | **AlphaGenome**. Top tissue predictions for the effects of rs13257021 in gene expression assessed by polyA+ RNA-seq.

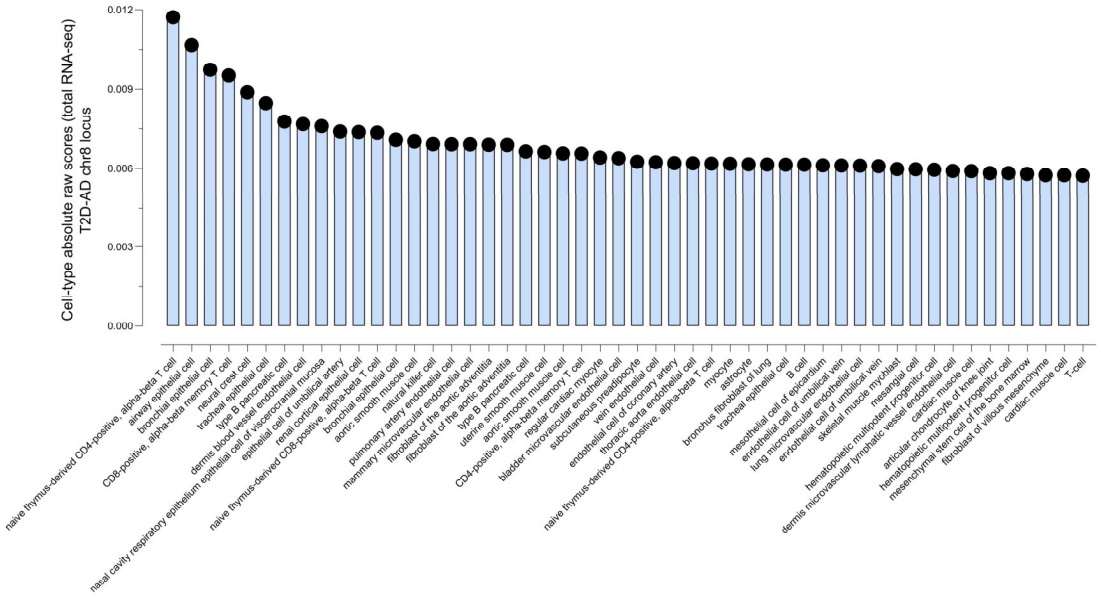

Fig. S3R2 | **AlphaGenome**. Top cell-type predictions for the effects of rs13257021 in gene expression assessed by total RNA-seq.

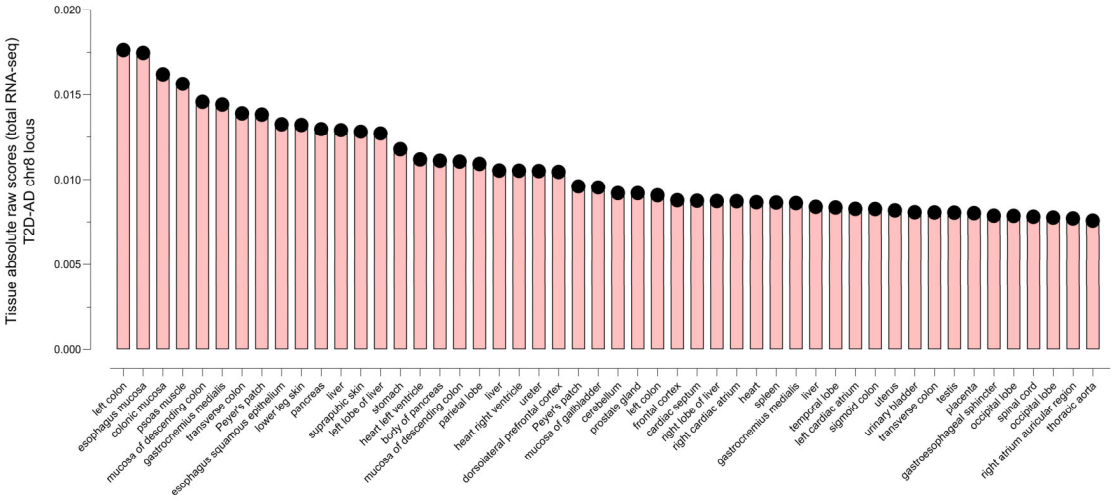

Fig. S3S2 | **AlphaGenome**. Top tissue predictions for the effects of rs13257021 in gene expression assessed by total RNA-seq.

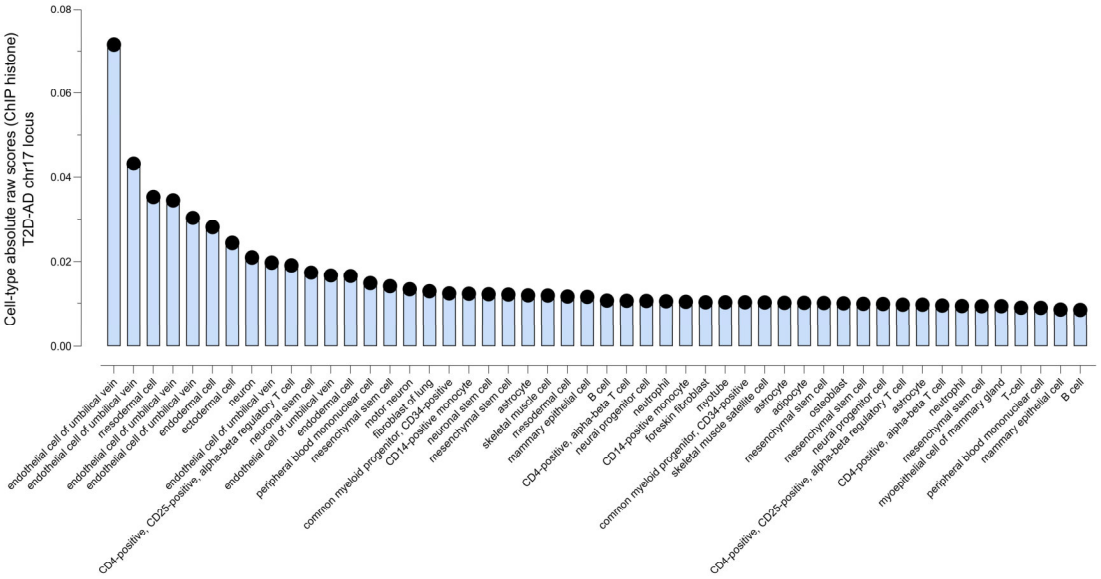

Fig. S3T2 | **AlphaGenome**. Top cell-type predictions for the effects of rs4311 in histone modifications.

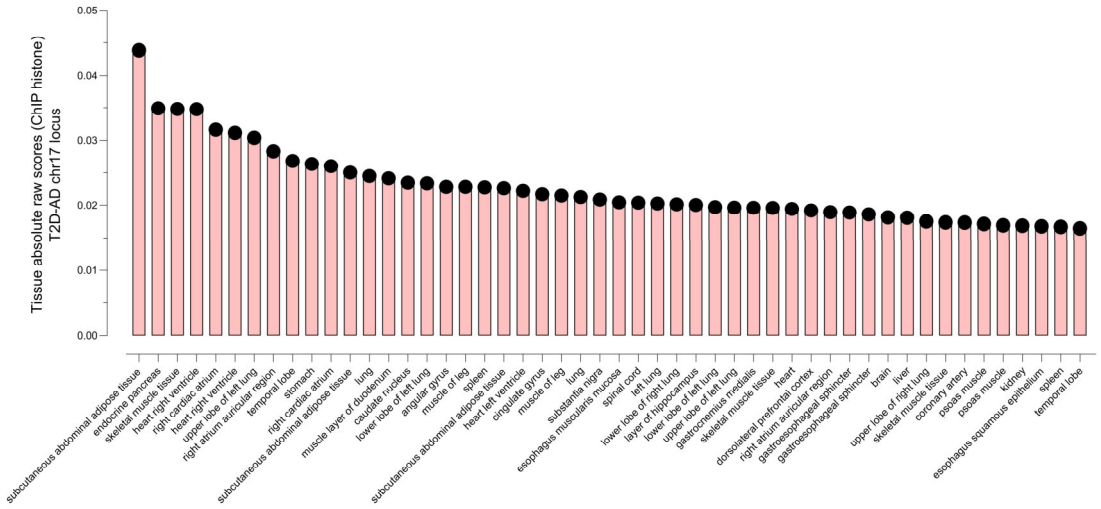

Fig. S3U2 | **AlphaGenome**. Top tissue predictions for the effects of rs4311 in histone modifications.

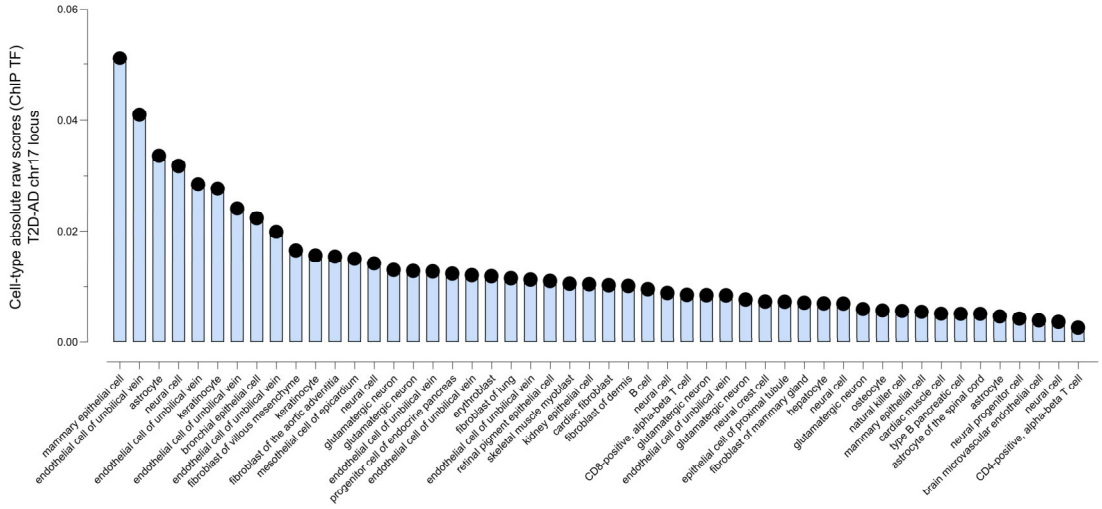

Fig. S3V2 | **AlphaGenome**. Top cell-type predictions for the effects of rs4311 in transcription factor binding.

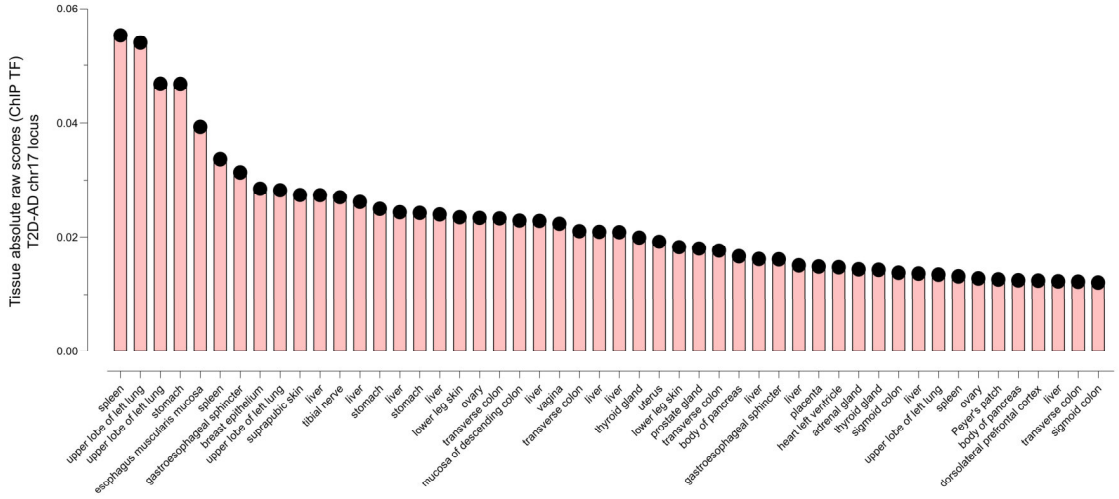

Fig. S3W2 | **AlphaGenome**. Top tissue predictions for the effects of rs4311 in transcription factor binding.

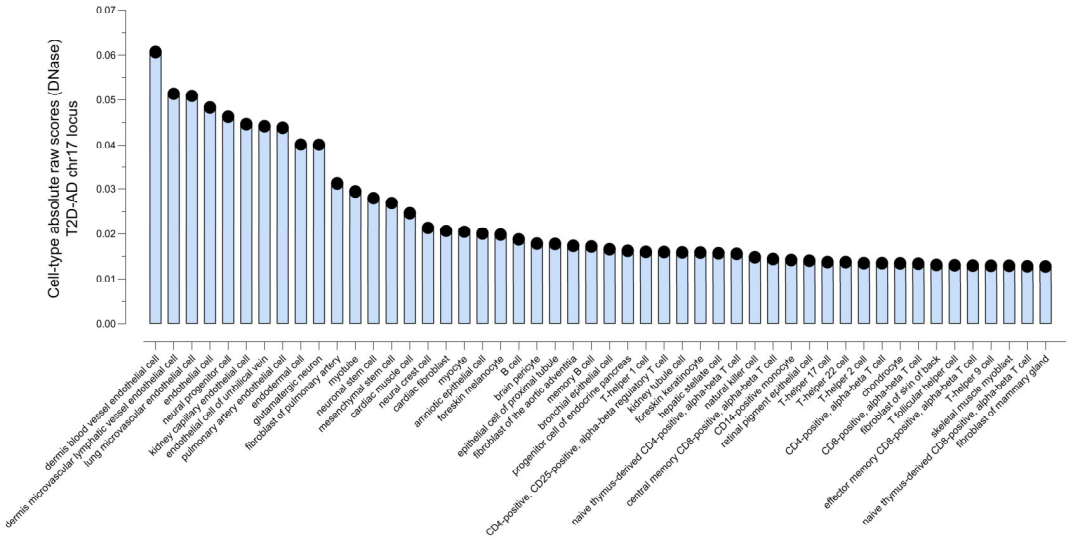

Fig. S3X2 | **AlphaGenome**. Top cell-type predictions for the effects of rs4311 in chromatin accessibility assessed by DNase.

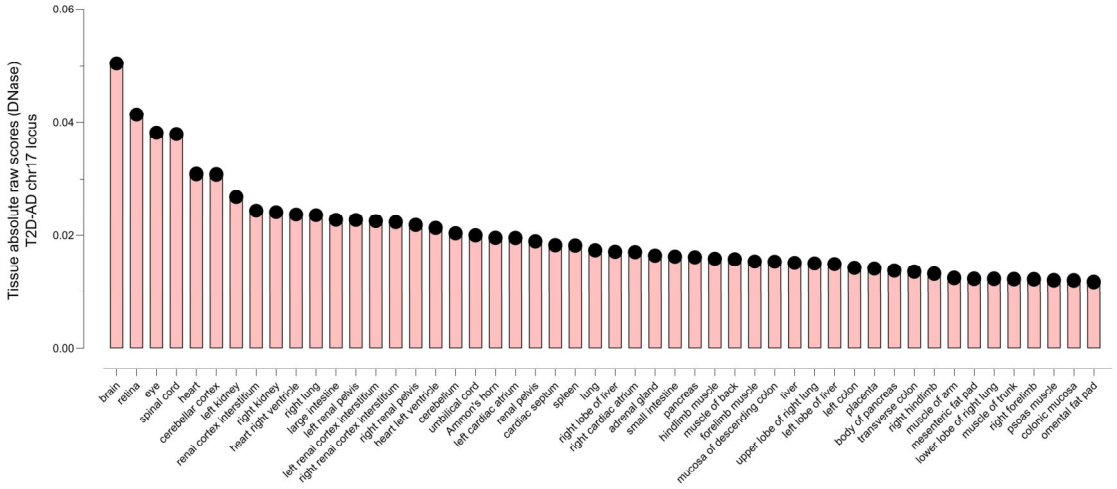

Fig. S3Y2 | **AlphaGenome**. Top tissue predictions for the effects of rs4311 in chromatin accessibility assessed by DNase.

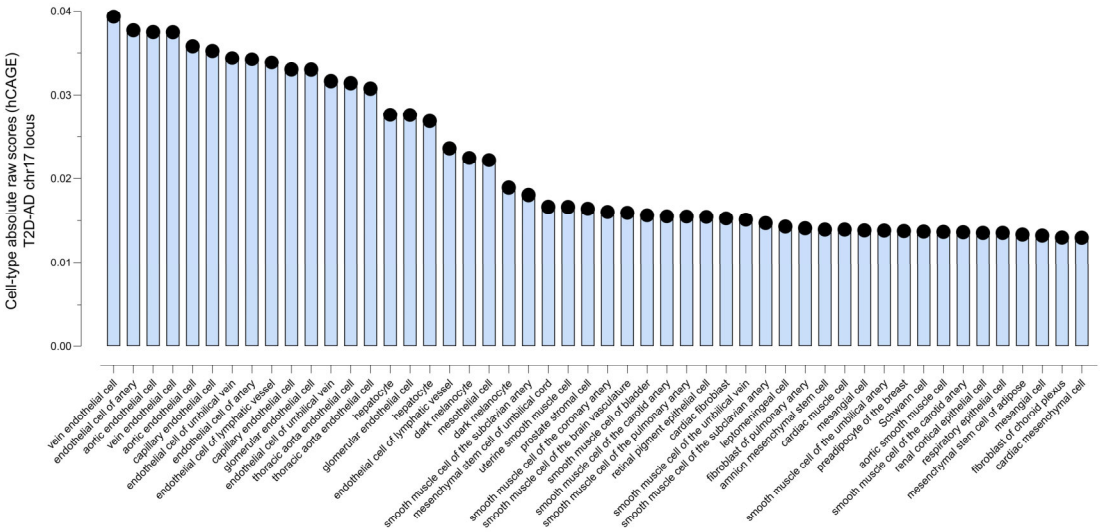

Fig. S3Z2 | **AlphaGenome**. Top cell-type predictions for the effects of rs4311 in gene expression assessed by hCAGE.

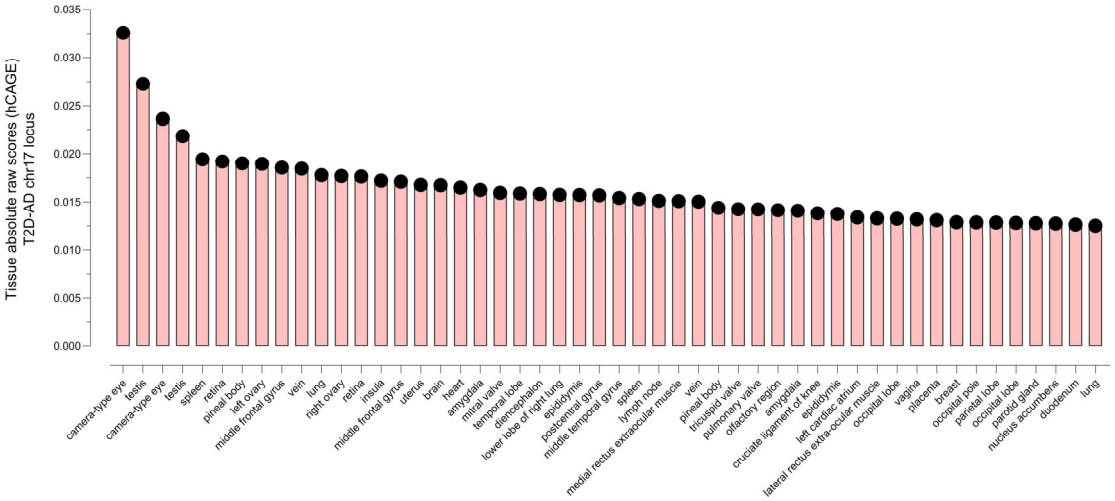

Fig. S3A3 | **AlphaGenome**. Top tissue predictions for the effects of rs4311 in gene expression assessed by hCAGE.

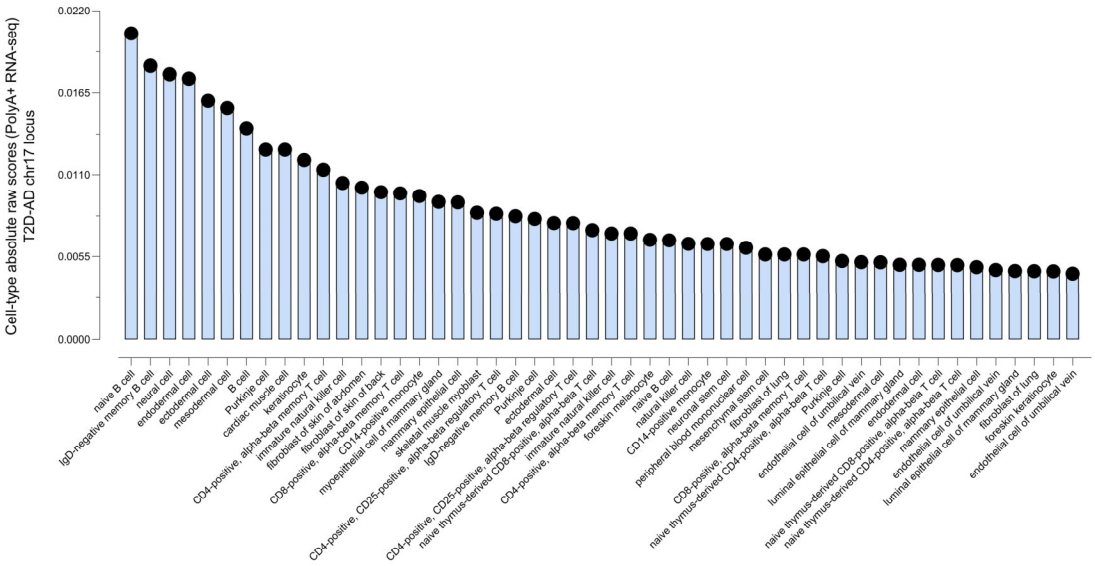

Fig. S3B3 | **AlphaGenome**. Top cell-type predictions for the effects of rs4311 in gene expression assessed by polyA+ RNA-seq.

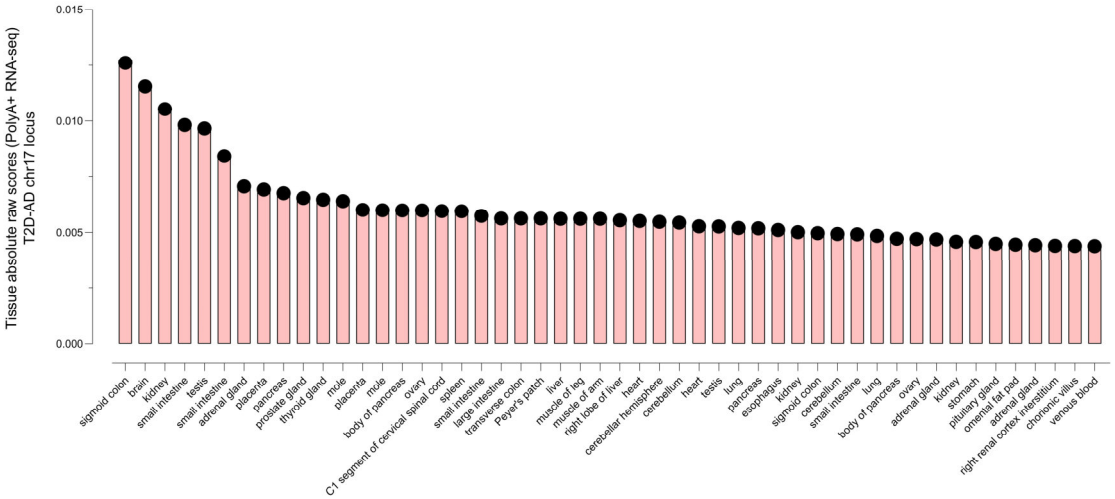

Fig. S3C3 | **AlphaGenome**. Top tissue predictions for the effects of rs4311 in gene expression assessed by polyA+ RNA-seq.

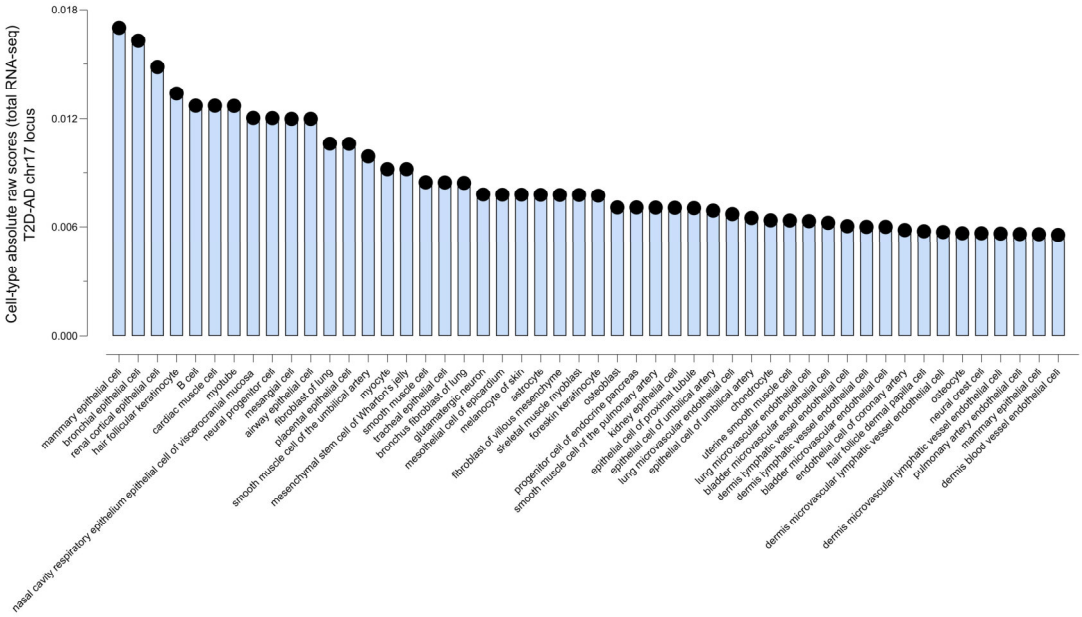

Fig. S3D3 | **AlphaGenome**. Top cell-type predictions for the effects of rs4311 in gene expression assessed by total RNA-seq.

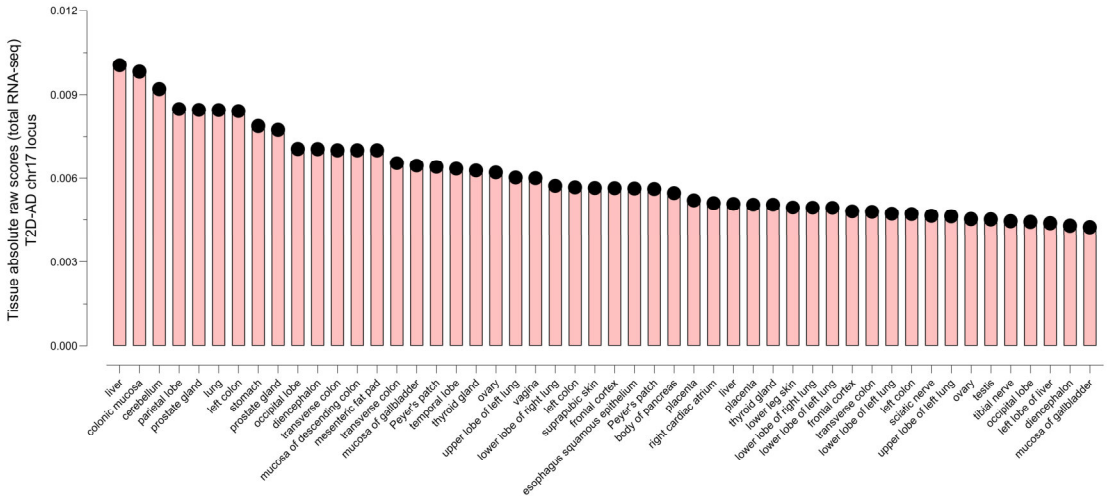

Fig. S3E3 | **AlphaGenome**. Top tissue predictions for the effects of rs4311 in gene expression assessed by total RNA-seq.

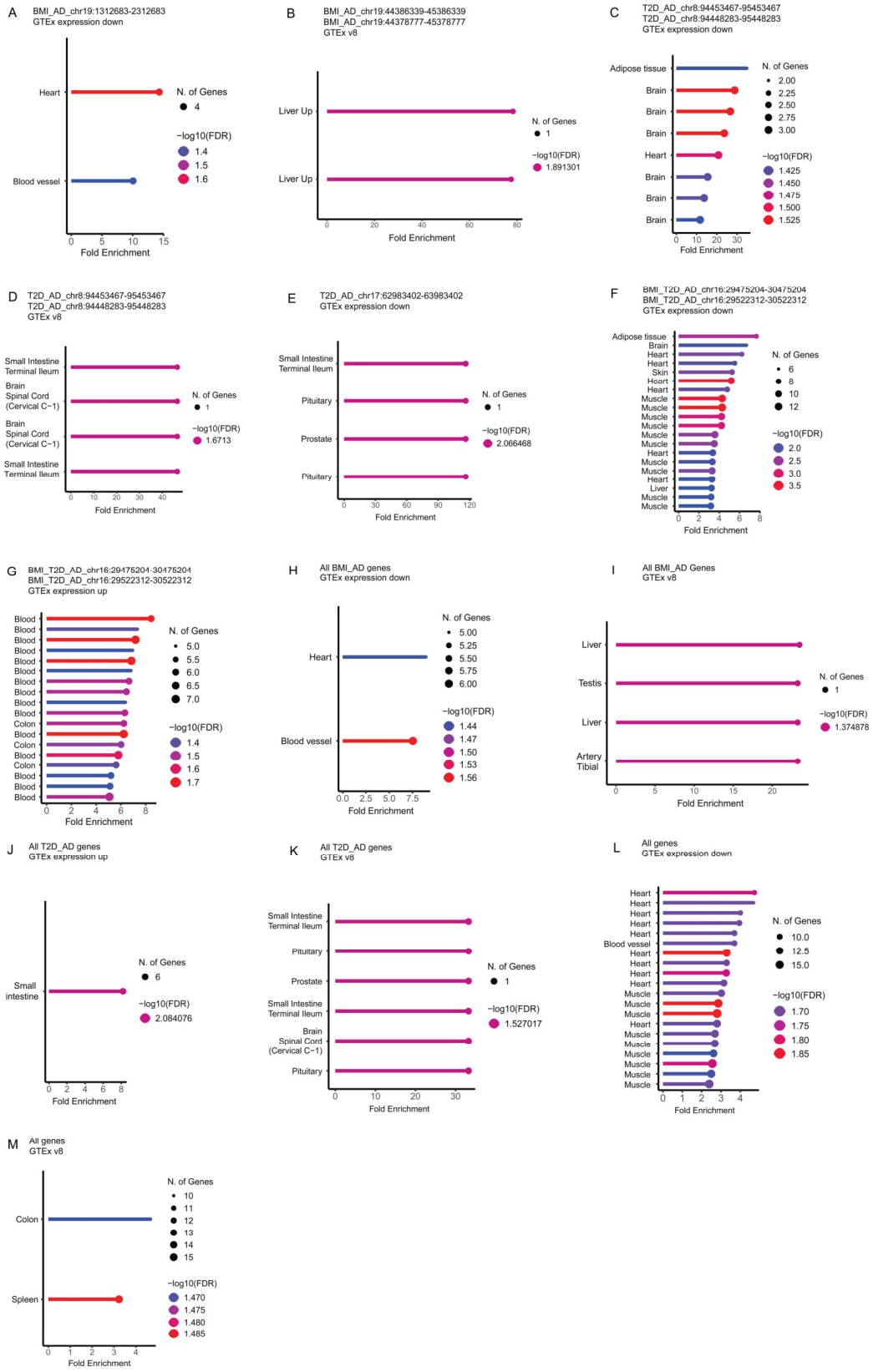

Fig. S4 | GTEx enrichment analyses.

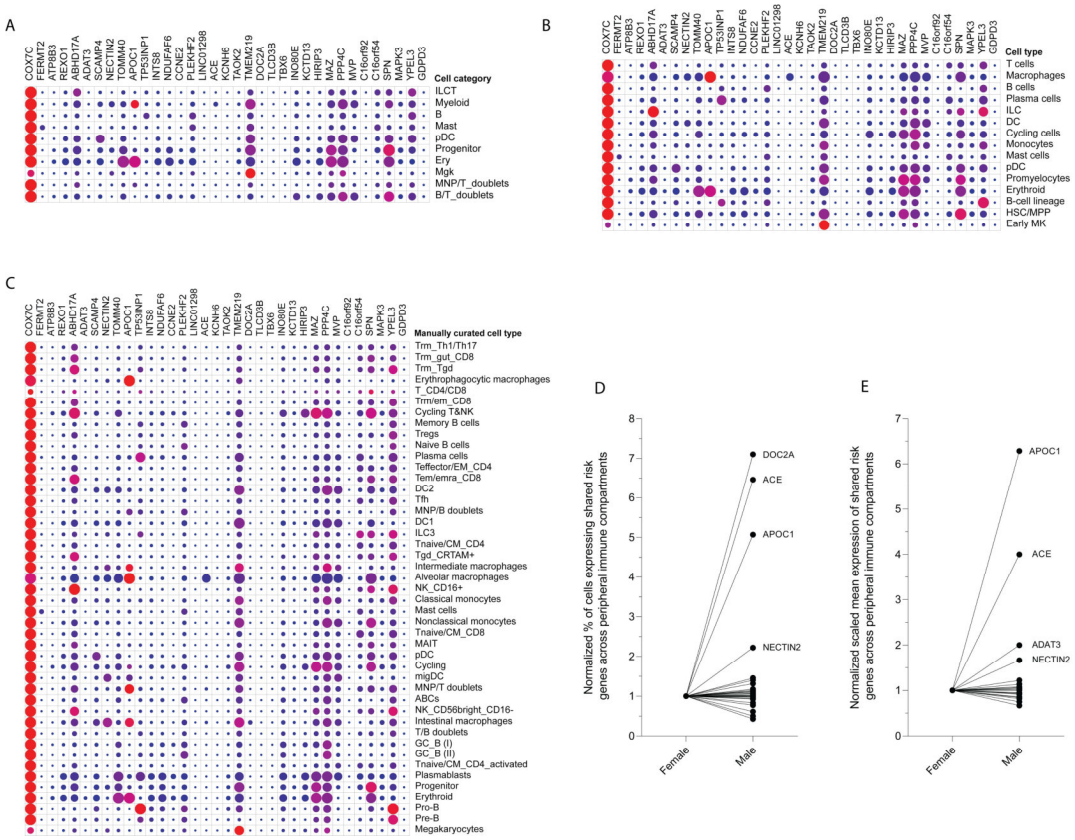

Fig. S5 | (**A-C**) Individual gene expression and % of expressing cell-types in the immune niches of 17 peripheral tissues. (**D-E**) Sex-stratified individual gene expression and % of expressing cells. Results are normalized to females.

(A) **rs11668832** - chr19:1712682-1912682

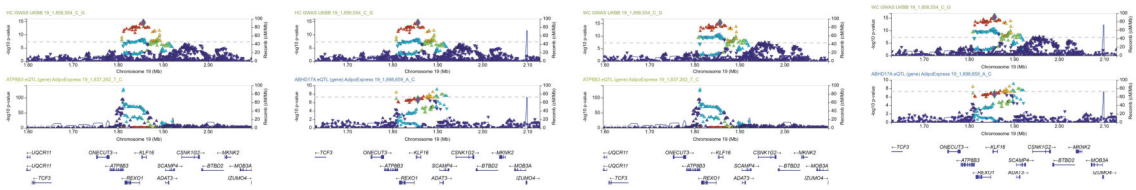

(B) **rs7254892** - chr19:45289596-45489596 / **rs6859** - chr19:45282034-45482034

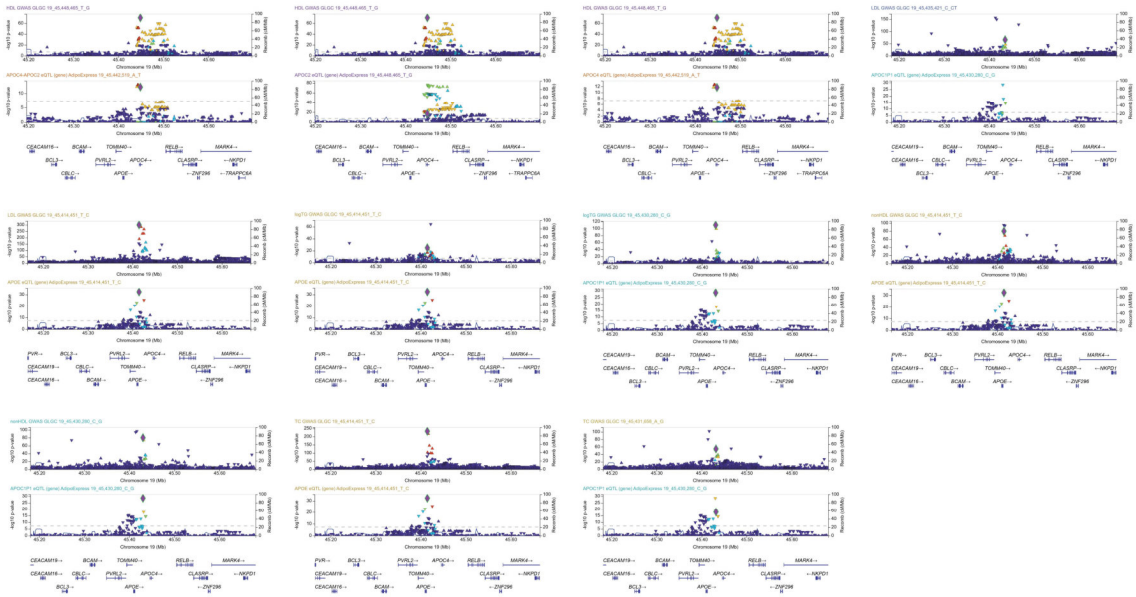

(C) **rs13257021** - chr8:95865695-96065695 / **rs896854** - chr8:95860511-96060511

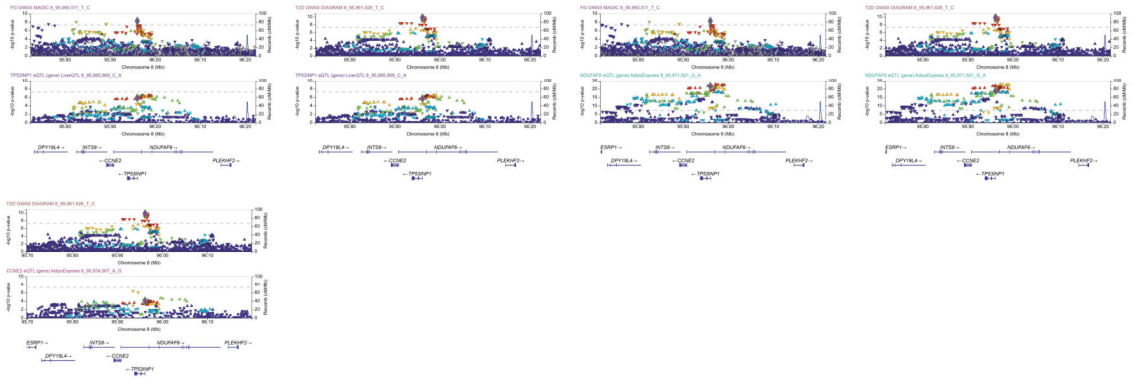

(D) **rs4311** - chr17:61460763-61660763

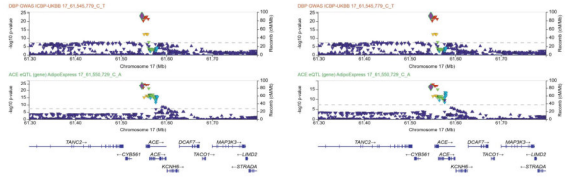

(E) **rs11150577** - chr16:29933633-30133633 / **rs12325539** - chr16:29886525-30086525

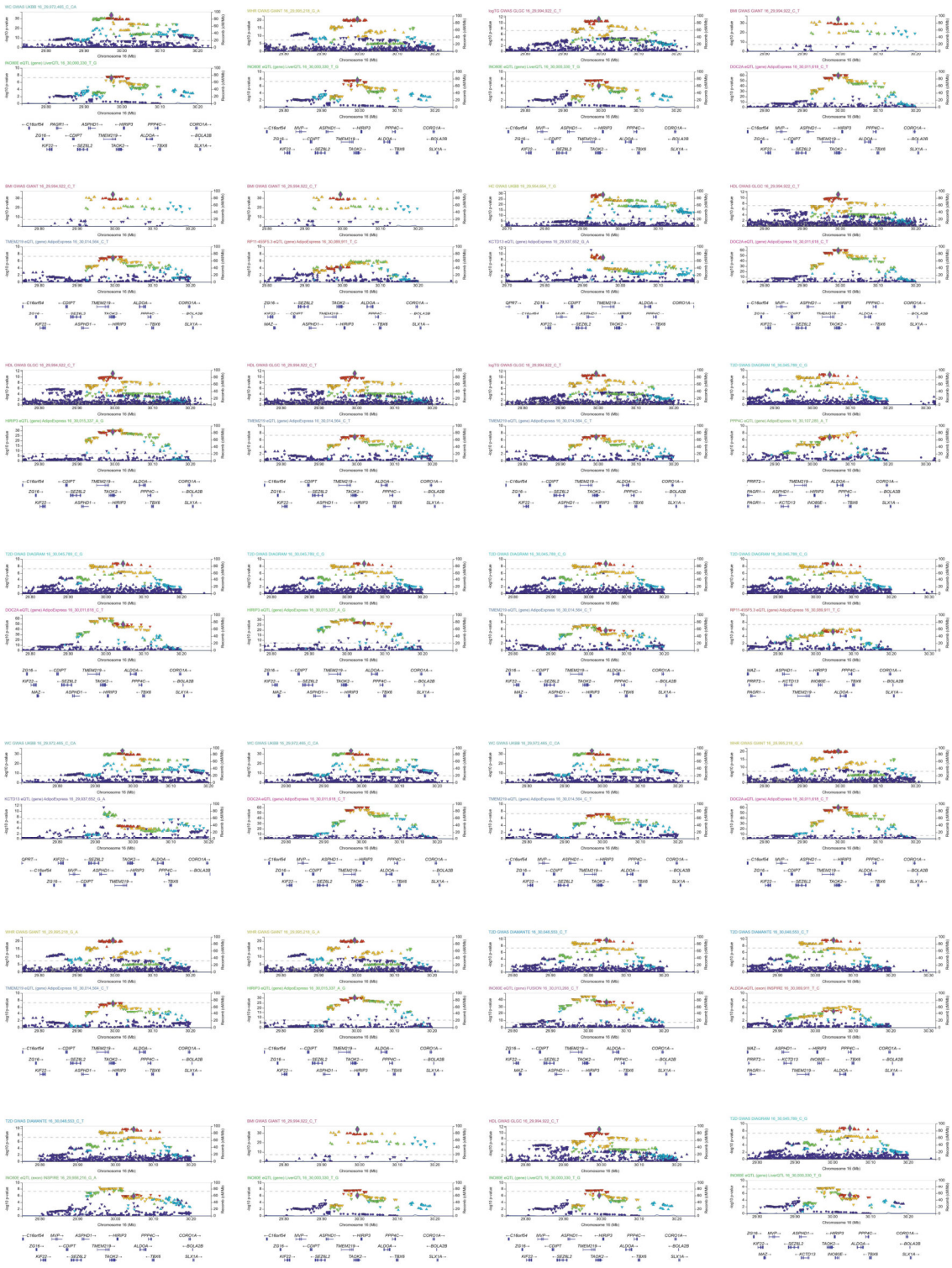

Fig. S6 | GWAS-eQTL colocalization locuszoom region plots.

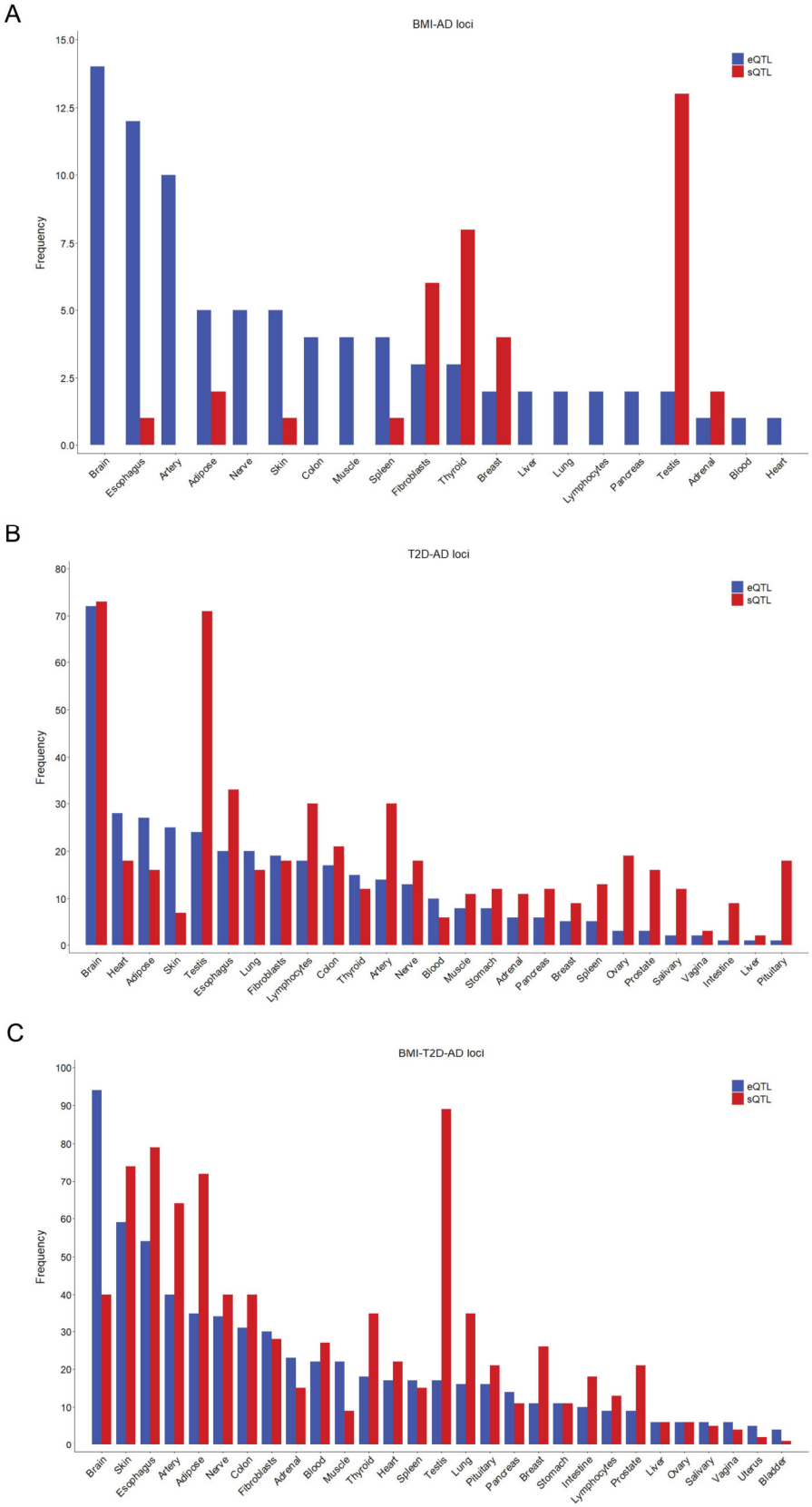

Fig. S7 | eQTL and sQTL frequency.

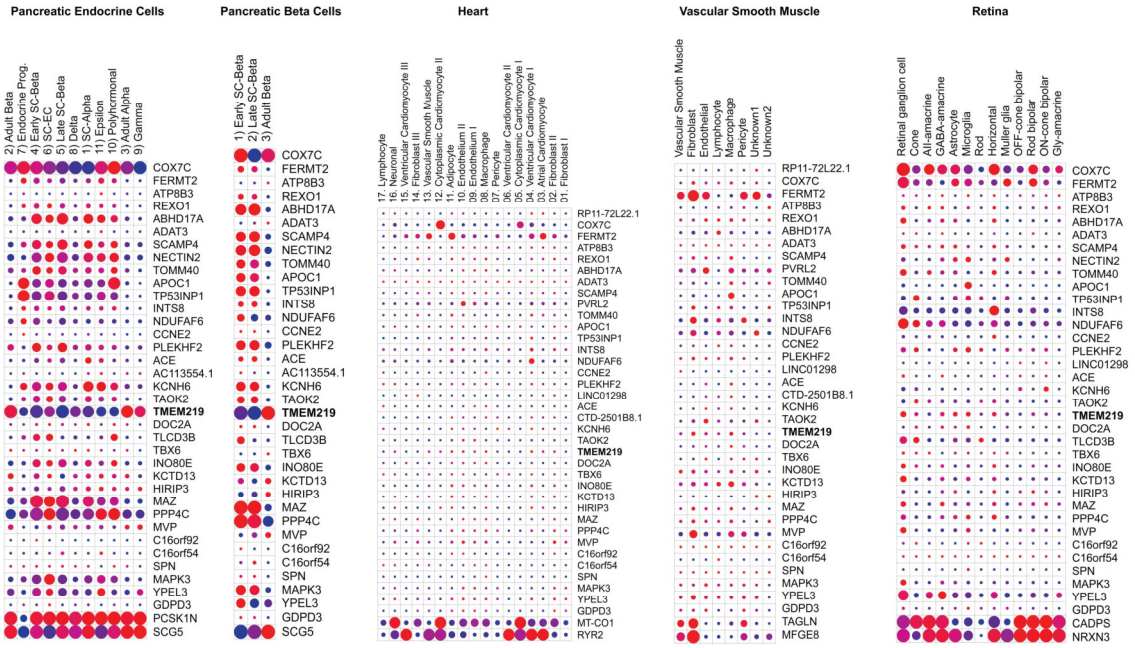

Fig. S8 | Single-cell transcriptomics analysis of pancreatic endocrine cells, pancreatic beta cells, heart, vascular smooth muscle and retina.

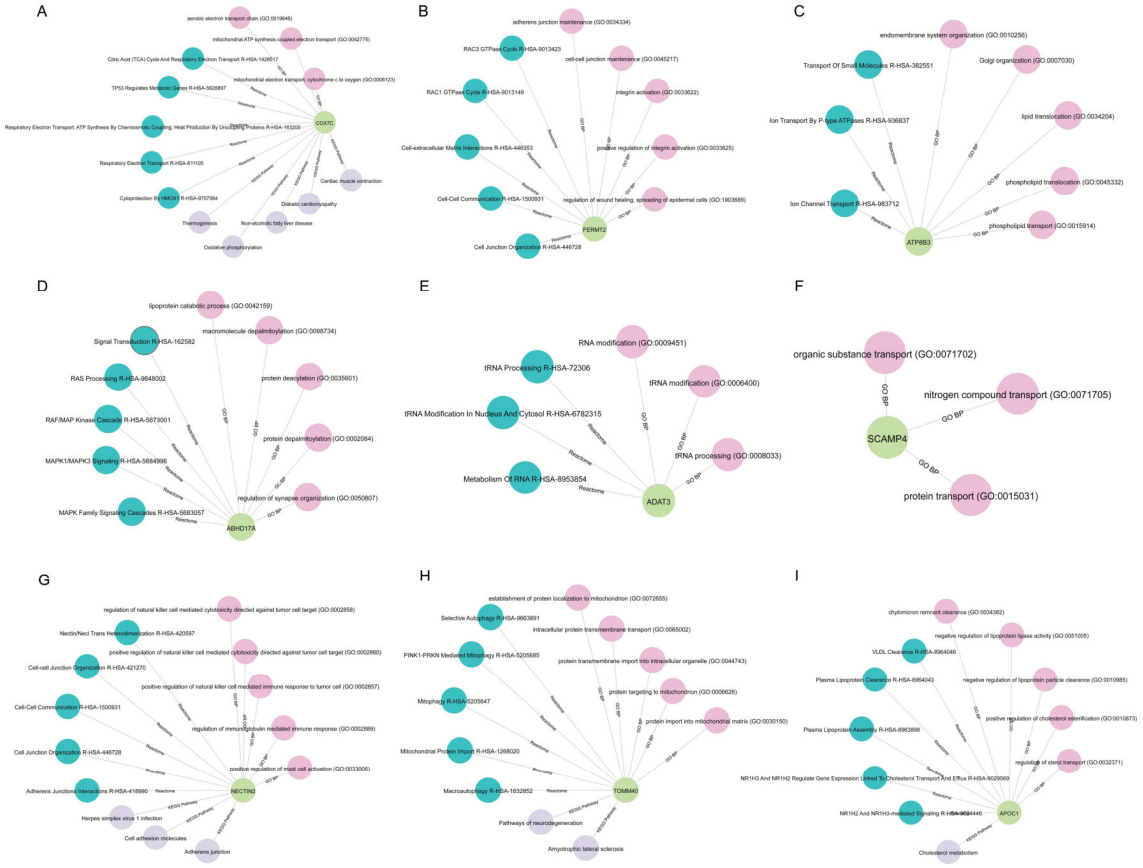

Fig. S9A | **Enrichment results using GO terms, KEGG and Reactome pathways for BMI-AD effector genes.**

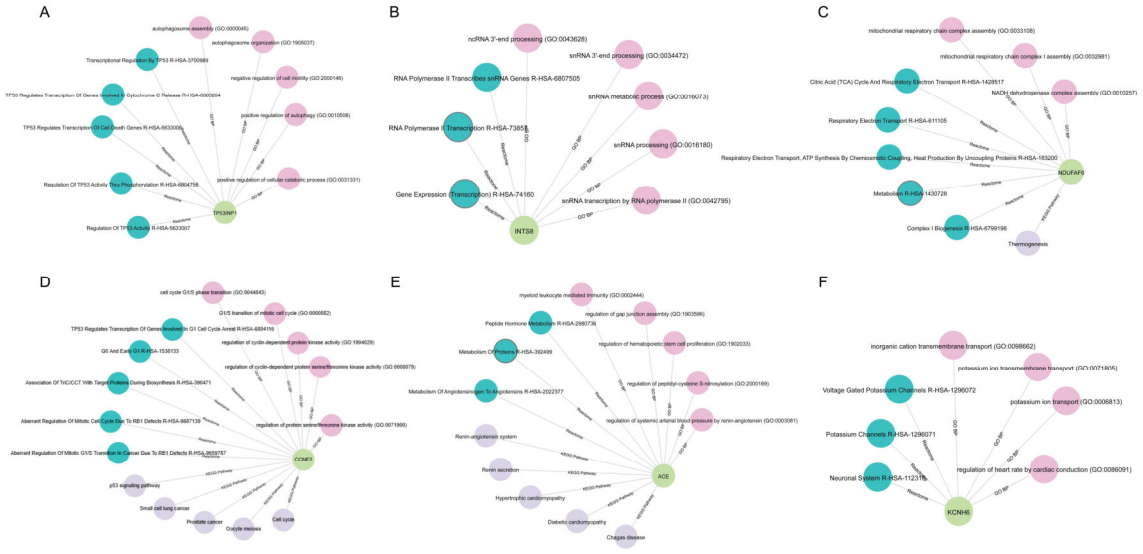

Fig. S9B | **Enrichment results using GO terms, KEGG and Reactome pathways for T2D-AD effector genes.**

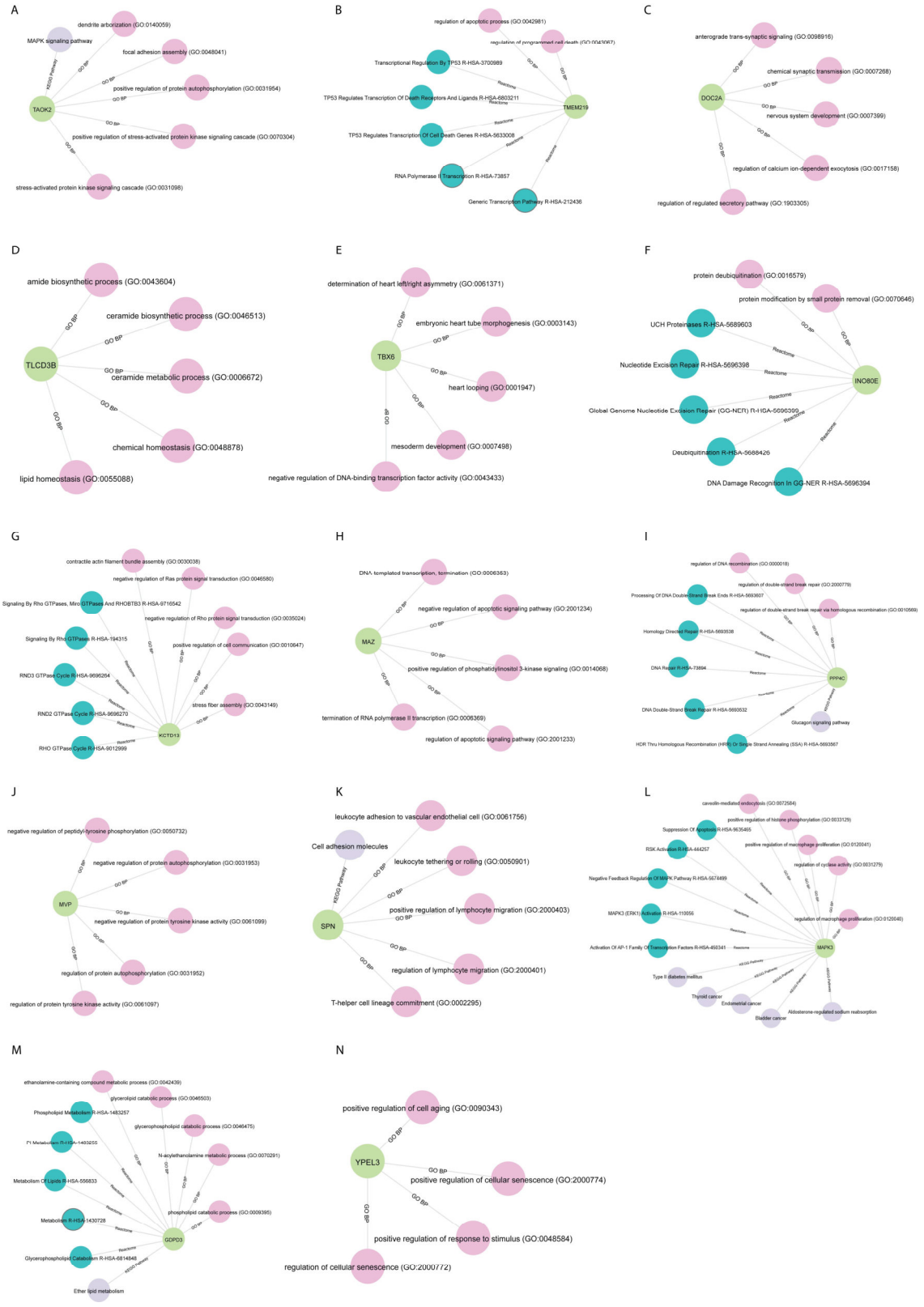

Fig. S9C | Individual enrichment results using GO terms, KEGG and Reactome pathways for BMI-T2D-AD effector genes.

GWAS cohort descriptions and acknowledgements.

Table of Content

1. GWAS Cohort descriptions and acknowledgements 1

1.1 European Alzheimer & Dementia Biobank (EADB-TOPMed) 1

1.2 FinnGen 7

1.3 UK Biobank (UKB) 8

1.4 GR@CE 9

1.5 European Alzheimer's Disease Initiative (EADI) Consortium 9

1.6 Genetic and Environmental Risk in AD (GERAD) Consortium 10

1.7 Bonn studies 11

1. GWAS Cohort descriptions and acknowledgements

1.1 European Alzheimer & Dementia Biobank (EADB-TOPMed)

EADB-France. In the France node, samples were collected from nine countries (39 centers/studies), and after quality controls (QCs), we obtained 13,867 AD cases and 15,310 controls. All these samples were genotyped at the Centre National de Recherche en Génomique Humaine (CNRGH, Evry, France).
Belgium: The participants were part of a large prospective cohort (PMID: 29589097) of Belgian AD patients and healthy elderly control individuals. The patients were ascertained at the memory clinic of Middelheim and Hoge Beuken (Hospital Network Antwerp, Belgium) and at the memory clinic of the University Hospitals of Leuven, Belgium. The control individuals were the partners of the patients or volunteers from the Belgian community. The study protocols were approved by the ethics committees of the Antwerp University Hospital and the participating neurological centers at the different hospitals of the BELNEU consortium and by the University of Antwerp.
Czech Republic: The Czech Brain Aging Study (CBAS) (PMID: 31857299) is a longitudinal memory-clinic–based study recruiting subjects at risk of dementia (subjects referred for cognitive complaints-SCD, MCI). The CBAS+ study is a cross-sectional study of patients in the early stages of dementia. All subjects signed informed consent and both studies were approved by the local ethics committee.
Denmark: The Copenhagen General Population Study (CGPS) is a prospective study of the Danish general population initiated in 2003 and still recruiting. Individuals were selected randomly based on the national Danish Civil Registration System to reflect the adult Danish population aged 20-100. Data were obtained from a self-administered questionnaire reviewed together with an investigator at the day of attendance, a physical examination, and from blood samples including DNA extraction (PMID: 33022702). The study is approved by the regional ethics committee and by the Steering Committee of the CGPS.
Finland: *The ADGEN cohort (PMID: 25807283):* clinic-based collection of AD patients from Eastern and Northern Finland examined in the Department of Neurology in Kuopio University Hospital and the Department of Neurology in Oulu University Hospital. All the patients were diagnosed with probable AD according to the criteria of the National Institute of Neurological and Communicative Disorders and Stroke and the Alzheimer's disease and Related Disorders Association (NINCDS–ADRDA). The study was approved by the ethics committee of Kuopio University Hospital, Finland (420/2016). *The FINGER study* (PMID: 25771249): a Finnish multi-domain lifestyle RCT enrolling 1,260 older adults with an increased risk of dementia from the general population. The intensive lifestyle intervention lasted for two years, and follow-up extends currently up to seven years. The FINGER study was approved by the coordinating ethics committee of the Hospital District of Helsinki and Uusimaa (94/13/03/00/2009 and HUS/1204/2017), and all the participants gave written informed consent.
France: *The BALTAZAR multicenter (23 memory centers) prospective study* (PMID: 29458036): 1,040 participants from September 2010 to April 2015. They were classified as AD cases (n = 501) according to DSM IV-TR and NINCDS–ADRDA criteria as well as amnestic mild cognitive impairment (MCI) cases (a MCI, n = 417) and non-amnestic MCI cases (na MCI, n = 122) according to Petersen's criteria. A comprehensive battery of cognitive tests was performed, including MMSE, verbal fluency, and FCSRT. All the participants or their legal guardians gave written informed consent. The study was approved by the Paris ethics committee (CPP Ile de France IV Saint Louis Hospital). MEMENTO: a clinic-based study (PMID: 28851447) aimed at better understanding the natural history of AD, dementia, and related diseases. Between 2011 and 2014, 2,323 individuals presenting either recently diagnosed MCI or isolated cognitive complaints were enrolled in 26 memory centers in France. This study was performed in accordance with the guidelines of the Declaration of Helsinki. The MEMENTO study protocol has been approved by the local ethics committee (Comité de Protection des Personnes Sud-Ouest et Outre Mer III; approval number 2010-A01394-35). All the participants provided written informed consent. The CNRMAJ-Rouen study (PMID: 26242991): early onset AD patients (n = 870). The patients or their legal guardians provided written informed consent. This study was approved by the ethics committee of CPP Ile de France II.
Italy: The AD cases and controls were collated through Italy in different centers: Brescia, Cagliari, Florence, Milan, Rome, Pertugia, San Giovani Rotondo and Torino. AD cases were diagnosed according to DSM III-R,IV and NINCDS–ADRDA criteria. Controls were defined a minima as subjects without DMS-III-R dementia criteria and with integrity of their cognitive functions (MMS>25).
Spain: *The Dementia Genetic Spanish Consortium (DEGESCO)* is a national consortium comprising 23 research centers and hospitals across the country, that holds the institutional coverage of The Network Center for Biomedical Research in Neurodegenerative Diseases (CIBERNED). Created in 2013, DEGESCO's

objective is the promotion and conduction of genetic studies aimed at understanding the genetic architecture of neurodegenerative dementias in the Spanish population and participates in coordinated actions in national and international frameworks. All DNA samples are in compliance with the Law of Biomedical Research (Law 14/2007) and the Royal Decree on Biobanks (RD 1716/2011). Patients included in the present study met clinical criteria for probable or possible disease established by the National Institute of Neurological and Communication Disorders and Stroke and the Alzheimer Disease and Related Disorders Association (NINCDS-ADRDA). Cognitively healthy controls were unrelated individuals who had a documented MMSE in the normal range. Contributing centers in the France node genotyping were Centro de Biología Molecular Severo Ochoa (CSIC-UAM (Madrid), the Institute Biodonostia, University of Basque Contry (EHU-UPV, San Sebastián), Institut de Biomedicina de Valencia CSIC (València), and Sant Pau Biomedical Research Institute (Barcelona).

Sweden: *Uppsala.* The Swedish AD patients were ascertained at the Memory Disorder Unit at Uppsala University Hospital. For all patients, the diagnosis was established according to the National Institute on Neurological Disorders and Stroke, and the Alzheimer's Disease and Related Disorders Association (NINDS-ADRDA) guidelines (PMID: 6610841). Healthy control subjects were recruited from the same geographic region following advertisements in local newspapers and displayed no signs of dementia upon Mini Mental State Examination (MMSE). *Karolinska Institutet, Stockholm*. AD patients were ascertained at the Memory Clinic at Karolinska University Hospital - Huddinge, Stockholm Sweden. For all patients, the diagnosis was established according to the National Institute on Neurological Disorders and Stroke, and the Alzheimer's Disease and Related Disorders Association (NINDS-ADRDA) guidelines (PMID: 6610841) and if available supported by CSF beta-amyloid and phospho-tau biomarker analyses. As controls, DNA from participants in the *Swedish National Study on Aging and Care in Kungsholmen* (SNAC-K) data was collected. The original SNAC-K population consisted of 4590 living and eligible persons who lived on the island of Kungsholmen in Central Stockholm, belonged to pre-specified age strata, and were randomly selected to take part in the study. Between 2001 and 2004, 3363 persons participated in the baseline assessment. They belonged to the age cohorts 60, 66, 72, 78, 81, 84, 87, 90, 93, and 96 years and 99 years and older. The examination consists of three parts: a nurse interview, a medical examination, and a neuropsychological testing session. Altogether, the examination takes about six hours. The participants are reexamined each time they reach the next age cohort. All parts of the SNAC-K project have been approved by the ethical committee at Karolinska Institutet or the regional ethical review board. Informed consent was collected from all the participants or, if the person was severely cognitively impaired, from their next of kin.

The UK: MRC. The sample set comprises individuals with AD and healthy controls recruited across the MRC Centre for Neuropsychiatric Genetics and Genomics, Cardiff University, Cardiff, UK; Institute of Psychiatry, London, UK; University of Cambridge, Cambridge, UK. The collection of the samples was through multiple channels, including specialist NHS services and clinics, research registers and Join Dementia Research (JDR) platform. The participants were assessed at home or in research clinics along with an informant, usually a spouse, family member or close friend, who provided information about and on behalf of the individual with dementia. Established measures were used to ascertain the disease severity: Bristol activities of daily living (BADL), Clinical Dementia Rating scale (CDR), Neuropsychiatric Inventory (NPI) and Global Deterioration Scale (GIDS). Individuals with dementia completed the Addenbrooke's Cognitive Examination (ACE-r), Geriatric Depression Scale (GeDS) and National Adult Reading Test (NART) too. Control participants were recruited from GP surgeries and by means of self-referral (including existing studies and Joint Dementia Research platform). For all other recruitment, all AD cases met criteria for either probable (NINCDS-ADRDA, DSM-IV) or definite (CERAD) AD. All elderly controls were screened for dementia using the Mini Mental State Examination (MMSE) or ADAS-cog, were determined to be free from dementia at neuropathological examination or had a Braak score of 2.5 or lower. Control samples were chosen to match case samples for age, gender, ethnicity and country of origin. Informed consent was obtained for all study participants, and the relevant independent ethical committees approved study protocols. SOTON, University of Southampton, Southampton, UK. All AD cases met criteria for either probable (NINCDS-ADRDA, DSM-IV) or definite (CERAD) AD. All elderly controls were screened for dementia using the MMSE or ADAS-cog, were determined to be free from dementia at neuropathological examination or had a Braak score of 2.5 or lower. Nottingham and Manchester, University of Nottingham, Nottingham, UK and Manchester Brain Bank. All AD cases met criteria for either probable (NINCDS-ADRDA, DSM-IV) or definite (CERAD) AD. All elderly controls were screened for dementia using the MMSE or ADAS-cog, were determined to be free from dementia at neuropathological examination or had a Braak score of 2.5 or lower. KCL, London Neurodegenerative Diseases Brain Bank. All AD cases met criteria for either probable (NINCDS-ADRDA, DSM-IV) or definite (CERAD) AD. All elderly controls were screened for dementia using the MMSE or ADAS-cog, were determined to be free from dementia at neuropathological examination or had a Braak score of 2.5 or lower. PRION, All

AD cases met criteria for either probable (NINCDS-ADRDA, DSM-IV) or definite (CERAD) AD. All elderly controls were screened for dementia using the MMSE or ADAS-cog, were determined to be free from dementia at neuropathological examination or had a Braak score of 2.5 or lower. CFAS Wales, The Cognitive Function and Ageing Study Wales (CFAS-Wales) is a longitudinal population-based study of people aged 65 years and over in rural and urban areas of Wales that aims to investigate physical and cognitive health in older age and examine the interactions between health, social networks, activity, and participation. Individuals aged 65 years and over were randomly sampled from general medical practice lists between 2011 and 2013, stratified by age to ensure equal numbers in two age groups, 65-74 years and 75 and over. The baseline sample included 3593 older people and included those living in care homes as well as those living at home. Those who provided written consent to join the study were interviewed in their own homes by trained interviewers and could choose to have the interview conducted through the medium of either English or Welsh. Participants were followed up 2 years later. All AD cases met criteria for either probable (NINCDS-ADRDA, DSM-IV) or definite (CERAD) AD. All elderly controls were screened for dementia using the MMSE or CAMCOG, and were determined to be free from dementia. UCL-DRC. the UCL Alzheimer's disease cohort of the Dementia Research Centre (UCL - EOAD DRC) included patients seen at the Cognitive Disorders Clinics at The National Hospital for Neurology and Neurosurgery (Queen Square), or affiliated hospitals. Individuals were assessed clinically and diagnosed as having probable Alzheimer's disease based on contemporary clinical criteria in use at the time, including imaging and neuropsychological testing where appropriate.

EADB-Germany. In the German node, samples were collected from seven countries (11 centers/studies) and after QCs, we obtained 4,159 AD cases and 4,545 controls. All these samples were genotyped at Life&brain (Bonn, Germany).

Germany: *DELCODE (the multicenter DZNE-Longitudinal Cognitive Impairment and Dementia Study)*. This is an observational longitudinal memory clinic-based multicenter study in Germany comprising 400 subjects with Subjective cognitive decline (SCD), 200 mild cognitive impairment (MCI) patients, 100 AD dementia patients, 200 control subjects without subjective or objective cognitive decline, and 100 first-degree relatives of patients with a documented diagnosis of AD dementia. All patient groups (SCD, MCI, AD) are referrals, including self-referrals, to the participating memory centers. The control group and the relatives of AD dementia patients are recruited by standardized public advertisement. Ten university-based memory centers are participating, all being collaborators of local DZNE sites. All patient groups (SCD, MCI, AD) were assessed clinically at the respective memory centers before entering DELCODE. The assessments include medical history, psychiatric and neurological examination, neuropsychological testing, blood laboratory work-up, cerebrospinal fluid (CSF) biomarkers, and routine MRI, all according to the local standards. The Consortium to Establish a Registry for Alzheimer's Disease (CERAD) neuropsychological test battery was applied at all memory centers to measure cognitive function. German age, sex, and education-adjusted norms of the CERAD neuropsychological battery are available online (www.memoryclinic.ch). Detail description is of recruitment protocol is reported elsewhere. *The VOGEL study*: The VOGEL study is a prospective, observational, long-term follow-up study with three time points of investigation within 6–8 years. This cohort includes dementia and healthy subjects. Residents of the city of Würzburg born between 1936 and 1941 were recruited. Every participant underwent physical, psychiatric, and laboratory examinations and performed intense neuropsychological testing as well as VSEP and NIRS according to the published procedures. A total of 604 subjects were included. *The Heidelberg/Mannheim memory clinic sample*: This cohort includes 61 subjects from whom 40 MCI patients were recruited and assessed between 2012 and 2016. Some of those patients converted to dementia by AD or other dementias. *The PAGES study*: This study includes 301 subjects. AD patients were recruited at the memory clinic of the Department of Psychiatry, University of Munich, Germany. Participants in whom dementia associated with AD was diagnosed fulfilled the criteria for probable AD according to the NINCDS–ADRDA. The control group included participants who were randomly selected from the general population of Munich. Controls who had central nervous system diseases or psychotic disorders or who had first-degree relatives with psychotic disorders were excluded. *The Technische Universität München study*: This cohort includes 359 healthy, AD, and other dementias patients recruited from the Centre for Cognitive Disorders. All the participants provided written informed consent. A biobank was submitted to the ethics committee of the Technical University of Munich, School of Medicine (Munich, Germany), which raised no objections and approved the biobank (reference number 347-14*). The Göttingen Universität study*: This study includes 111 in- and outpatients with a healthy or AD dementia status from the Department of Psychiatry of the University of Göttingen. The study's ethical statement was provided locally at the Göttingen University Medical Centre. *The German Dementia Competence Network (DCN) cohort*: Individuals from the DCN cohort were recruited from 14 university hospital memory clinics across Germany between 2003 and 2005 (PMID: 19339779). The study was approved by the respective ethics committees, and written informed consent was obtained from all the participants prior to inclusion. *The German Study on Aging, Cognition, and Dementia (AgeCoDe)*: The

AgeCoDe study is a general practice (GP) registry-based longitudinal study in elderly individuals that recruited patients aged 75 years and above in six German cities from 2003 to 2004 (PMID: 17848793). The study was approved by the respective ethics committees, and written informed consent was obtained from all the participants prior to inclusion.
Greece: the HELIAD study, comprising 49 AD cases and 1,150 controls. HELIAD is a population-based, multidisciplinary, collaborative study designed to estimate, in the Greek population over the age of 64 years, the prevalence and incidence of MCI, AD, other forms of dementia, and other neuropsychiatric conditions of aging and to investigate associations between nutrition and cognitive dysfunction or age-related neuropsychiatric diseases. The participants were selected through random sampling from the records of two Greek municipalities, Larissa and Marousi. All the participants signed informed consent in Greek.
This study was supported by the following grants: IIRG-09-133014 from the Alzheimer's Association; 189 10276/8/9/2011 from the ESPA-EU program Excellence Grant (ARISTEIA), which is co-funded by the European Social Fund and Greek National Resources; and DY2b/oik.51657/14.4.2009 from the Ministry for Health and Social Solidarity(Greece).
Portugal: the Lisbon study from Portugal, totalling 78 AD cases and 74 controls. This cohort was recruited in 2008–2009 to investigate the connections between oxidative stress and lipid dyshomeostasis in AD. The project includes 190 subjects and was approved by the local ethics committee, and all the participants provided written informed consent. This study includes healthy and dementia-by-AD subjects.
Spain: Those samples are part of DEGESCO. DEGESCO Centers from whom DNA samples were genotyped in the German node (1,778 cases and 470 controls) were the Alzheimer Research Center and Memory Clinic, Fundació ACE, Institut Català de Neurociències Aplicades (Barcelona), the Neurology Service at University Hospital Marqués de Valdecilla (Santander), the Alzheimer's disease and other cognitive disorders, Neurology Department, at Hospital Clínic, IDIBAPS (Barcelona), the Molecular Genetics Laboratory, at the Hospital Universitario Central de Asturias (Oviedo), and Fundació Docència i Recerca Mútua de Terrassa and Movement Disorders Unit, Department of Neurology, University Hospital Mútua de Terrassa (Barcelona).
Switzerland: Two datasets from Switzerland and Austria were combined, totaling 182 AD cases and 388 controls. The Lausanne study: This study includes 137 community-dwelling participants aged 55+ years with cognitive impairment (memory clinic patients with MCI, dementia) or normal cognition (recruited by advertisement, word of mouth). The study's ethical statement was provided locally at the Department of Psychiatry, Geneva University Centre, Switzerland. The VITA study: This is a longitudinal study of 606 individuals (Vienna, Austria) who were 75 years old in 2000, followed up every 30–90 months. This cohort includes dementia and healthy subjects. All the participants gave written informed consent. The study conformed to the latest version of the Declaration of Helsinki and was approved by the ethics committee of the City of Vienna, Austria.
EADB-Netherlands. In the Dutch node, samples were collected from six organizations in the Netherlands and after QCs, we obtained 2,438 AD cases and 2,389 controls. All these samples were genotyped at the Erasmus Medical University (Rotterdam, The Netherlands). The Medical Ethics Committee (METC) of the local institutes approved the studies. All the participants and/or their legal guardians gave written informed consent for participation in the clinical and genetic studies. Samples from the following institutes were included. 1) *Erasmus Medical Center*: most individuals were selected from population studies from the epidemiology department and accounted for most of the controls, while a smaller subset of samples originated from the neurology department, where AD was diagnosed according to the National Institute of Neurological and Communicative Disorders and Stroke-Alzheimer's Disease and Related Disorders Association (NINCDS-ADRDA) criteria for AD (PMID: 21514250). 2) *The Amsterdam Dementia Cohort (ADC)* (PMID: 29562540): This cohort comprises patients who visit the memory clinic of the VU University Medical Centre, the Netherlands. The diagnosis of probable AD is based on the clinical criteria formulated by the NINCDS–ADRDA and based on the NIA–AA. Diagnosis of MCI was made according to Petersen and NIA-AA. Controls presented with subjective cognitive decline at the memory clinic, but performed within normal limits on all clinical investigations. 3) *The 100-Plus study*: This study includes Dutch-speaking individuals who (i) can provide official evidence for being aged 100 years or older, (ii) self-report to be cognitively healthy, which is confirmed by a proxy, (iii) consent to the donation of a blood sample, (iv) consent to (at least) two home visits from a researcher, and (v) consent to undergo an interview and neuropsychological test battery (PMID: 30362018). 4) *Parelsnoer Institute*: a collaboration between 8 Dutch University Medical Centers in which clinical data and biomaterials from patients suffering from chronic diseases (so called "Pearls") are collected according to harmonized protocols. The Pearl Neurodegenerative Diseases (PMID: 25551191) includes individuals diagnosed with dementia, mild cognitive impairment, and controls with subjective memory complaints. 5) *The Netherlands Brain Bank*: a non-profit organization that collects human brain tissue of donors with a variety of neurological and psychiatric disorders, but also of non-diseased donors. A clinical diagnosis of AD is based on the clinical criteria of probable AD

(PMID: 6610841, PMID: 17616482). The selected AD patients for this study all received a definitive diagnosis which was based on autopsy. 6) *Maastricht University Medical Center*: a subset of individuals that were referred to the memory clinic for cognitive complaints were included if they participated in the BioBank-Alzheimer Centrum Limburg (BB-ACL). Diagnosis of MCI was made according to the criteria of Petersen, and diagnosis of AD-type dementia was made according to the criteria of the DSM-4, and the NINCDS-ADRDA (PMID: 6610841).

Genotyping. EADB genomic DNA samples were transferred to 3 genotyping centers and samples that passed the DNA QC were genotyped with the Illumina Infinium Global Screening Array. Raw probe intensities were shared with the CNRGH, which performed the genotype calling on all samples using the same custom cluster file. During the genotyping QC process, three genotyping batches were considered: (1) 49 genotyping chips were identified as possibly problematic and thus were considered as a separate batch, (2) a batch of samples was genotyped and processed after all other samples and (3) the main batch including all other samples. Further details are available in *Bellenguez et al 2022*.

Additional support for EADB cohorts was provided by: The work for this manuscript was further supported by the CoSTREAM project (www.costream.eu) and funding from the European Union's Horizon 2020 research and innovation programme under grant agreement No 667375. Italian Ministry of Health (Ricerca Corrente); Ministero dell'Istruzione, dell'Università e della Ricerca–MIUR project “Dipartimenti di Eccellenza 2018–2022” to Department of Neuroscience “Rita Levi Montalcini”, University of Torino (IR), and AIRAlzh Onlus-ANCC-COOP (SB); Partly supported by “Ministero della Salute”, I.R.C.C.S. Research Program, Ricerca Corrente 2018-2020, Linea n. 2 “Meccanismi genetici, predizione e terapie innovative delle malattie complesse” and by the “5 x 1000” voluntary contribution to the Fondazione I.R.C.C.S. Ospedale “Casa Sollievo della Sofferenza”; and RF-2018-12366665, Fondi per la ricerca 2019 (Sandro Sorbi). Karolinska Institutet AD cohort: Dr. Graff and co-authors of the Karolinska Institutet AD cohort report grants from Swedish Research Council (VR) 2015-02926, 2018-02754, 2015-06799, Swedish Alzheimer Foundation, Stockholm County Council ALF and resarch school, Karolinska Institutet StratNeuro, Swedish Demensfonden, and Swedish brain foundation, during the conduct of the study. ADGEN: This work was supported by Academy of Finland (grant numbers 307866); Sigrid Jusélius Foundation; the Strategic Neuroscience Funding of the University of Eastern Finland; EADB project in the JPNDCO-FUND program (grant number 301220). CBAS: Supported by the project no. LQ1605 from the National Program of Sustainability II (MEYS CR), Supported by Ministry of Health of the Czech Republic, grant nr. NV19-04-00270 (All rights reserved), Grant Agency of Charles University Grants No. 693018 and 654217; the Ministry of Health, Czech Republic—conceptual development of research organization, University Hospital Motol, Prague, Czech Republic Grant No. 00064203; the Czech Ministry of Health Project AZV Grant No. 16—27611A; and Institutional Support of Excellence 2. LF UK Grant No. 699012. CNRMAJ-Rouen: This study received fundings from the Centre National de Référence Malades Alzheimer Jeunes (CNRMAJ). The Finnish Geriatric Intervention Study for the Prevention of Cognitive Impairment and Disability (FINGER) data collection was supported by grants from the Academy of Finland, La Carita Foundation, Juho Vainio Foundation, Novo Nordisk Foundation, Finnish Social Insurance Institution, Ministry of Education and Culture Research Grants, Yrjö Jahnsson Foundation, Finnish Cultural Foundation South Osthrobothnia Regional Fund, and EVO/State Research Funding grants of University Hospitals of Kuopio, Oulu and Turku, Seinäjoki Central Hospital and Oulu City Hospital, Alzheimer's Research & Prevention Foundation USA, AXA Research Fund, Knut and Alice Wallenberg Foundation Sweden, Center for Innovative Medicine (CIMED) at Karolinska Institutet Sweden, and Stiftelsen Stockholms sjukhem Sweden. FINGER cohort genotyping was funded by EADB project in the JPND CO-FUND (grant number 301220). Research at the Belgian EADB site is funded in part by the Alzheimer Research Foundation (SAO-FRA), The Research Foundation Flanders (FWO), and the University of Antwerp Research Fund. FK is supported by a BOF DOCPRO fellowship of the University of Antwerp Research Fund. SNAC-K is financially supported by the Swedish Ministry of Health and Social Affairs, the participating County Councils and Municipalities, and the Swedish Research Council. BDR Bristol: We would like to thank the South West Dementia Brain Bank (SWDBB) for providing brain tissue for this study. The SWDBB is part of the Brains for Dementia Research programme, jointly funded by Alzheimer’s Research UK and Alzheimer’s Society and is supported by BRACE (Bristol Research into Alzheimer’s and Care of the Elderly) and the Medical Research Council. BDR Manchester: We would like to thank the Manchester Brain Bankfor providing brain tissue for this study. The Manchester Brain Bank is part of the Brains for Dementia Research programme, jointly funded by Alzheimer’s

Research UK and Alzheimer's Society. BDR KCL: Human post-mortem tissue was provided by the London Neurodegenerative Diseases Brain Bank which receives funding from the UK Medical Research Council and as part of the Brains for Dementia Research programme, jointly funded by Alzheimer's Research UK and the Alzheimer's Society. The CFAS Wales study was funded by the ESRC (RES-060-25-0060) and HEFCW as 'Maintaining function and well-being in later life: a longitudinal cohort study', (Principal Investigators: R.T Woods, L.Clare, G.Windle, V. Burholt, J. Philips, C. Brayne, C. McCracken, K. Bennett, F. Matthews). We are grateful to the NISCHR Clinical Research Centre for their assistance in tracing participants and in interviewing and in collecting blood samples, and to general practices in the study areas for their cooperation. MRC: We thank all individuals who participated in this study. Cardiff University was supported by the Alzheimer's Society (AS; grant RF014/164) and the Medical Research Council (MRC; grants G0801418/1, MR/K013041/1, MR/L023784/1) (R. Sims is an AS Research Fellow). Cardiff University was also supported by the European Joint Programme for Neurodegenerative Disease (JPND; grant MR/L501517/1), Alzheimer's Research UK (ARUK; grant ARUK-PG2014-1), the Welsh Assembly Government (grant SGR544:CADR), Brain's for dementia Research and a donation from the Moondance Charitable Foundation. Cardiff University acknowledges the support of the UK Dementia Research Institute, of which J. Williams is an associate director. Cambridge University acknowledges support from the MRC. Patient recruitment for the MRC Prion Unit/UCL Department of Neurodegenerative Disease collection was supported by the UCLH/UCL Biomedical Centre and NIHR Queen Square Dementia Biomedical Research Unit. The University of Southampton acknowledges support from the AS. King's College London was supported by the NIHR Biomedical Research Centre for Mental Health and the Biomedical Research Unit for Dementia at the South London and Maudsley NHS Foundation Trust and by King's College London and the MRC. ARUK and the Big Lottery Fund provided support to Nottingham University. Alfredo Ramirez: Part of the work was funded by the JPND EADB grant (German Federal Ministry of Education and Research (BMBF) grant: 01ED1619A). German Study on Ageing, Cognition and Dementia in Primary Care Patients (AgeCoDe): This study/publication is part of the German Research Network on Dementia (KND), the German Research Network on Degenerative Dementia (KNDD; German Study on Ageing, Cognition and Dementia in Primary Care Patients; AgeCoDe), and the Health Service Research Initiative (Study on Needs, health service use, costs and health-related quality of life in a large sample of oldestold primary care patients (85+; AgeQualiDe)) and was funded by the German Federal Ministry of Education and Research (grants KND: 01GI0102, 01GI0420, 01GI0422, 01GI0423, 01GI0429, 01GI0431, 01GI0433, 01GI0434; grants KNDD: 01GI0710, 01GI0711, 01GI0712, 01GI0713, 01GI0714, 01GI0715, 01GI0716; grants Health Service Research Initiative: 01GY1322A, 01GY1322B, 01GY1322C, 01GY1322D, 01GY1322E, 01GY1322F, 01GY1322G). In addition, this publication was supported by the German Federal Ministry of Education and Research (Grant numbers: PreADAPT project 01ED2007A and DESCARTES project 01EK2102B to Alfredo Ramirez, 01EK2102A to Anja Schneider, and 01EK2102C to Michael Wagner. VITA study: The support of the Ludwig Boltzmann Society and the AFI Germany have supported the VITA study. The former VITA study group should be acknowledged: W. Danielczyk, G. Gatterer, K Jellinger, S Jugwirth, KH Tragl, S Zehetmayer. Vogel Study: This work was financed by a research grant of the ''Vogelstiftung Dr. Eckernkamp''. HELIAD study: This study was supported by the grants: IIRG-09-133014 from the Alzheimer's Association, 189 10276/8/9/2011 from the ESPA-EU program Excellence Grant (ARISTEIA) and the ΔΥ2β/οικ.51657/14.4.2009 of the Ministry for Health and Social Solidarity (Greece). Biobank Department of Psychiatry, UMG: Prof. Jens Wiltfang is supported by an Ilídio Pinho professorship and iBiMED (UID/BIM/04501/2013), and FCT project PTDC/DTP_PIC/5587/2014 at the University of Aveiro, Portugal. Lausanne study: This work was supported by grants from the Swiss National Research Foundation (SNF 320030_141179). PAGES study: Harald Hampel is an employee of Eisai Inc. During part of this work he was supported by the AXA Research Fund, the "Fondation partenariale Sorbonne Université" and the "Fondation pour la Recherche sur Alzheimer", Paris, France. Mannheim, Germany Biobank: Department of geriatric Psychiatry, Central Institute for Mental Health, Mannheim, University of Heidelberg, Germany. Genotyping for the Swedish Twin Studies of Aging was supported by NIH/NIA grant R01 AG037985. Genotyping in TwinGene was supported by NIH/NIDDK U01 DK066134. WvdF is recipient of Joint Programming for Neurodegenerative Diseases (JPND) grants PERADES (ANR-13-JPRF-0001) and EADB (733051061). Gothenburg Birth Cohort (GBC) Studies: We would like to thank UCL Genomics for performing the genotyping analyses. The studies were supported by The Stena Foundation, The Swedish Research Council (2015-02830, 2013-8717), The Swedish Research Council for Health, Working Life and Wellfare (2013-1202, 2005-0762, 2008-1210, 2013-2300, 2013- 2496, 2013-0475), The Brain Foundation, Sahlgrenska

University Hospital (ALF), The Alzheimer's Association (IIRG-03-6168), The Alzheimer's Association Zenith Award (ZEN-01-3151), Eivind och Elsa K:son Sylvans Stiftelse, The Swedish Alzheimer Foundation. Clinical AD, Sweden: We would like to thank UCL Genomics for performing the genotyping analyses. Barcelona Brain Biobank: Brain Donors of the Neurological Tissue Bank of the Biobanc-Hospital Clinic-IDIBAPS and their families for their generosity. Hospital Clínic de Barcelona Spanish Ministry of Economy and Competitiveness-Instituto de Salud Carlos III and Fondo Europeo de Desarrollo Regional (FEDER), Unión Europea, "Una manera de hacer Europa" grants (PI16/0235 to Dr. R. Sánchez-Valle and PI17/00670 to Dr. A.Antonelli). AA is funded by Departament de Salut de la Generalitat de Catalunya, PERIS 2016-2020 (SLT002/16/00329). Work at JP-T laboratory was possible thanks to funding from Ciberned and generous gifts from Consuelo Cervera Yuste and Juan Manuel Moreno Cervera. Sydney Memory and Ageing Study (Sydney MAS): We gratefully acknowledge and thank the following for their contributions to Sydney MAS: participants, their supporters and the Sydney MAS Research Team (current and former staff and students). Funding was awarded from the Australian National Health and Medical Research Council (NHMRC) Program Grants (350833, 568969, 109308). AddNeuroMed consortium was led by Simon Lovestone, Bruno Vellas, Patrizia Mecocci, Magda Tsolaki, Iwona Kłoszewska, Hilkka Soininen. This work was supported by InnoMed (Innovative Medicines in Europe), an integrated project funded by the European Union of the Sixth Framework program priority (FP6-2004- LIFESCIHEALTH-5). Oviedo: This work was partly supported by Grant from Fondo de Investigaciones Sanitarias-Fondos FEDER EuropeanUnion to Victoria Alvarez PI15/00878. Pascual Sánchez-Juan is supported by CIBERNED and Carlos III Institute of Health, Spain (PI08/0139, PI12/02288, and PI16/01652), jointly funded by Fondo Europeo de Desarrollo Regional (FEDER), Unión Europea, "Una manera de hacer Europa". Project MinE: The ProjectMinE study was supported by the ALS Foundation Netherlands and the MND association (UK) (Project MinE, www.projectmine.com). The SPIN cohort: We are indebted to patients and their families for their participation in the "Sant Pau Initiative on Neurodegeneration cohort", at the Sant Pau Hospital (Barcelona). This is a multimodal research cohort for biomarker discovery and validation that is partially funded by Generalitat de Catalunya (2017 SGR 547 to JC), as well as from the Institute of Health Carlos III-Subdirección General de Evaluación and the Fondo Europeo de Desarrollo Regional (FEDER- "Una manera de Hacer Europa") (grants PI11/02526, PI14/01126, and PI17/01019 to JF; PI17/01895 to AL), and the Centro de Investigación Biomédica en Red Enfermedades Neurodegenerativas programme (Program 1, Alzheimer Disease to AL). We would also like to thank the Fundació Bancària Obra Social La Caixa (DABNI project) to JF and AL; and Fundación BBVA (to AL), for their support in funding this follow-up study. Adolfo López de Munain is supported by Fundación Salud 2000 (PI2013156), CIBERNED and Diputación Foral de Gipuzkoa (Exp.114/17).

1.2 FinnGen

Current FinnGen Acknowledgment Statement

We want to acknowledge the participants and investigators of the FinnGen study. The FinnGen project is funded by two grants from Business Finland (HUS 4685/31/2016 and UH 4386/31/2016) and the following industry partners: AbbVie Inc., AstraZeneca UK Ltd, Biogen MA Inc., Bristol Myers Squibb Inc. (and Celgene Corporation & Celgene International II Sàrl), Genentech Inc., Merck Sharp & Dohme LCC, Pfizer Inc., GlaxoSmithKline Intellectual Property Development Ltd., Sanofi US Services Inc., Maze Therapeutics Inc., Johnson&Johnson Innovative Medicine Inc., Novartis AG, Boehringer Ingelheim International GmbH and Bayer AG. Following biobanks are acknowledged for delivering biobank samples to FinnGen: Auria Biobank (www.auria.fi/biopankki), THL Biobank (www.thl.fi/biobank), Helsinki Biobank (www.helsinginbiopankki.fi), Biobank Borealis of Northern Finland (https://www.ppshp.fi/Tutkimus-ja-opetus/Biopankki/Pages/Biobank-Borealis-briefly-in-English.aspx), Finnish Clinical Biobank Tampere (www.tays.fi/en-US/Research_and_development/Finnish_Clinical_Biobank_Tampere), Biobank of Eastern Finland (www.ita-suomenbiopankki.fi/en), Central Finland Biobank (www.ksshp.fi/fi-FI/Potilaalle/Biopankki), Finnish Red Cross Blood Service Biobank (www.veripalvelu.fi/verenluovutus/biopankkitoiminta), Terveystalo Biobank (www.terveystalo.com/fi/Yritystietoa/Terveystalo-Biopankki/Biopankki/) and Arctic Biobank

(https://www.oulu.fi/en/university/faculties-and-units/faculty-medicine/northern-finland-birth-cohorts-and-arctic-biobank). All Finnish Biobanks are members of BBMRI.fi infrastructure (https://www.bbmri-eric.eu/national-nodes/finland/). Finnish Biobank Cooperative -FINBB (https://finbb.fi/) is the coordinator of BBMRI-ERIC operations in Finland. The Finnish biobank data can be accessed through the Fingenious® services (https://site.fingenious.fi/en/) managed by FINBB.

FinnGen R11 ethics statement and materials & methods

Study subjects in FinnGen provided informed consent for biobank research, based on the Finnish Biobank Act. Alternatively, separate research cohorts, collected prior the Finnish Biobank Act came into effect (in September 2013) and start of FinnGen (August 2017), were collected based on study-specific consents and later transferred to the Finnish biobanks after approval by Fimea (Finnish Medicines Agency), the National Supervisory Authority for Welfare and Health. Recruitment protocols followed the biobank protocols approved by Fimea. The Coordinating Ethics Committee of the Hospital District of Helsinki and Uusimaa (HUS) statement number for the FinnGen study is Nr HUS/990/2017.

The FinnGen study is approved by Finnish Institute for Health and Welfare (permit numbers: THL/2031/6.02.00/2017, THL/1101/5.05.00/2017, THL/341/6.02.00/2018, THL/2222/6.02.00/2018, THL/283/6.02.00/2019, THL/1721/5.05.00/2019 and THL/1524/5.05.00/2020), Digital and population data service agency (permit numbers: VRK43431/2017-3, VRK/6909/2018-3, VRK/4415/2019-3), the Social Insurance Institution (permit numbers: KELA 58/522/2017, KELA 131/522/2018, KELA 70/522/2019, KELA 98/522/2019, KELA 134/522/2019, KELA 138/522/2019, KELA 2/522/2020, KELA 16/522/2020), Findata permit numbers THL/2364/14.02/2020, THL/4055/14.06.00/2020, THL/3433/14.06.00/2020, THL/4432/14.06/2020, THL/5189/14.06/2020, THL/5894/14.06.00/2020, THL/6619/14.06.00/2020, THL/209/14.06.00/2021, THL/688/14.06.00/2021, THL/1284/14.06.00/2021, THL/1965/14.06.00/2021, THL/5546/14.02.00/2020, THL/2658/14.06.00/2021, THL/4235/14.06.00/2021, Statistics Finland (permit numbers: TK-53-1041-17 and TK/143/07.03.00/2020 (earlier TK-53-90-20) TK/1735/07.03.00/2021, TK/3112/07.03.00/2021) and Finnish Registry for Kidney Diseases permission/extract from the meeting minutes on 4th July 2019.

The Biobank Access Decisions for FinnGen samples and data utilized in FinnGen Data Freeze 11 include: THL Biobank BB2017_55, BB2017_111, BB2018_19, BB_2018_34, BB_2018_67, BB2018_71, BB2019_7, BB2019_8, BB2019_26, BB2020_1, BB2021_65, Finnish Red Cross Blood Service Biobank 7.12.2017, Helsinki Biobank HUS/359/2017, HUS/248/2020, HUS/430/2021 §28, §29, HUS/150/2022 §12, §13, §14, §15, §16, §17, §18, §23, §58 and §59, Auria Biobank AB17-5154 and amendment #1 (August 17 2020) and amendments BB_2021-0140, BB_2021-0156 (August 26 2021, Feb 2 2022), BB_2021-0169, BB_2021-0179, BB_2021-0161, AB20-5926 and amendment #1 (April 23 2020) and it´s modification (Sep 22 2021), BB_2022-0262, BB_2022-0256, Biobank Borealis of Northern Finland_2017_1013, 2021_5010, 2021_5018, 2021_5015, 2021_5015 Amendment, 2021_5023, 2021_5023 Amendment, 2021_5017, 2022_6001, 2022_6006 Amendment, BB22-0067, 2022_0262, Biobank of Eastern Finland 1186/2018 and amendment 22§/2020, 53§/2021, 13§/2022, 14§/2022, 15§/2022, 27§/2022, 28§/2022, 29§/2022, 33§/2022, 35§/2022, 36§/2022, 37§/2022, 39§/2022, 7§/2023, Finnish Clinical Biobank Tampere MH0004 and amendments (21.02.2020 & 06.10.2020), 8§/2021, 9§/2021, §9/2022, §10/2022, §12/2022, 13§/2022, §20/2022, §21/2022, §22/2022, §23/2022, 28§/2022, 29§/2022, 30§/2022, 31§/2022, 32§/2022, 38§/2022, 40§/2022, 42§/2022, 1§/2023, Central Finland Biobank 1-2017, BB_2021-0161, BB_2021-0169, BB_2021-0179, BB_2021-0170, BB_2022-0256, and Terveystalo Biobank STB 2018001 and amendment 25th Aug 2020, Finnish Hematological Registry and Clinical Biobank decision 18th June 2021, Arctic biobank P0844: ARC_2021_1001.

1.3 UK Biobank (UKB)

The UK Biobank is comprised of environmental, lifestyle, and genetic data for 500,000 participants. Cases and controls for this analysis were included based on similar criteria to what was used for the FinnGen cohort. AD cases included participants with an ICD10 code of F00 or G30 (UKB codes p130836 and p131036). Controls included participants that did not have an algorithmically defined AD diagnosis as assigned by UKB (UKB code p42020) or any ICD10 code of A81, F01, F02, G31, F03, or I673 (UKB codes p130136, p130838, p130840, p131038, p130842 or p41270). Controls were also filtered for participants currently over 60 years of age to approximate the age distribution of the cases. Cases and controls were filtered for Caucasian ancestry and related individuals removed.

UKB genetic data was genotyped and underwent quality control as described elsewhere (PMID: 30305743). For this manuscript, data imputed using the TOPMed reference panel was used for determining *APOE* genotype and for all subsequent analyses. Data was accessed and analysed on the UKB Research Analysis Platform (RAP) under UK Biobank application ID 33601.

1.4 GR@CE

The GR@ACE study (PMID: 31473137) recruited Alzheimer's disease (AD) patients from Fundació ACE, Institut Català de Neurociències Aplicades (Catalonia, Spain), and control individuals from three centers: Fundació ACE (Barcelona, Spain), Valme University Hospital (Seville, Spain), and the Spanish National DNA Bank–Carlos III (University of Salamanca, Spain) (http://www.bancoadn.org). At all sites, AD diagnosis was established by a multidisciplinary working group—including neurologists, neuropsychologists, and social workers—according to the DSM-IV criteria for dementia and the National Institute on Aging and Alzheimer's Association's (NIA–AA) 2011 guidelines for diagnosing AD. In our study, we considered as AD cases any individuals with dementia diagnosed with probable or possible AD at any point in their clinical course. Genotyping was conducted using the Axiom 815K Spanish biobank array (Thermo Fisher) at the Spanish National Centre for Genotyping (CeGEN, Santiago de Compostela, Spain). The genotyping array not only is an adaptation of the Axiom biobank genotyping array but also contains rare population-specific variations observed in the Spanish population.

The Genome Research @ Fundació ACE project (GR@ACE) is supported by Grifols SA, Fundación bancaria 'La Caixa', Fundació ACE, and CIBERNED (Centro de Investigación Biomédica en Red Enfermedades Neurodegenerativas (Program 1, Alzheimer Disease to MB and AR)). A.R. and M.B. receive support from the European Union/EFPIA Innovative Medicines Initiative Joint undertaking ADAPTED and MOPEAD projects (grant numbers 115975 and 115985, respectively). M.B. and A.R. are also supported by national grants PI13/02434, PI16/01861, PI17/01474 and PI19/01240. Acción Estratégica en Salud is integrated into the Spanish National R + D + I Plan and funded by ISCIII (Instituto de Salud Carlos III)–Subdirección General de Evaluación and the Fondo Europeo de Desarrollo Regional (FEDER–'Una manera de hacer Europa'). Some control samples and data from patients included in this study were provided in part by the National DNA Bank Carlos III (www.bancoadn.org, University of Salamanca, Spain) and Hospital Universitario Virgen de Valme (Sevilla, Spain); they were processed following standard operating procedures with the appropriate approval of the Ethical and Scientific Committee.

1.5 European Alzheimer's Disease Initiative (EADI) Consortium

EADI is composed of several case-control studies and one population-based cohort, the 3C study (PMID: 14598854, PMID: 19734903). Case-control studies are comprised of AD cases and cognitively normal controls across France. The population-based cohort, the 3C study, is a prospective study of the relationship between vascular factors and dementia carried out in the three French cities Bordeaux, Montpellier and Dijon. The AD status was defined based on 12 years follow-up for Dijon participants, 14-15 years follow-up for Montpellier participants and 17-18 years follow-up for Bordeaux participants. All other non demented subjects of 3C were included as controls. All AD cases, both in the case-control studies and the 3C study, were ascertained by neurologists and the clinical diagnosis of probable AD was established according to the DSM-III-R and NINCDS-ADRDA criteria. Samples that passed DNA quality control were genotyped with Illumina Human 610-Quad BeadChips.

This work has been developed and supported by the LABEX (laboratory of excellence program investment for the future) DISTALZ grant (Development of Innovative Strategies for a Transdisciplinary approach to ALZheimer's disease) including funding from MEL (Metropole européenne de Lille), ERDF (European Regional Development Fund) and Conseil Régional Nord Pas de Calais. This work was supported by INSERM, the National Foundation for Alzheimer's disease and related disorders, the Institut Pasteur de Lille and the Centre National de Recherche en Génomique Humaine, CEA, the JPND PERADES, the Laboratory of Excellence GENMED (Medical Genomics) grant no. ANR-10-LABX-0013 managed by the National Research Agency (ANR) part of the Investment for the Future program, and the FP7 AgedBrainSysBio. The Three-City Study was performed as part of collaboration between the Institut National de la Santé et de la Recherche Médicale (Inserm), the Victor Segalen Bordeaux II University and Sanofi-Synthélabo. The Fondation pour la Recherche Médicale funded the preparation and initiation of the study. The 3C Study was also funded by the Caisse Nationale Maladie des Travailleurs Salariés, Direction Générale de la Santé, MGEN, Institut de la Longévité,

Agence Française de Sécurité Sanitaire des Produits de Santé, the Aquitaine and Bourgogne Regional Councils, Agence Nationale de la Recherche, ANR supported the COGINUT and COVADIS projects. Fondation de France and the joint French Ministry of Research/INSERM "Cohortes et collections de données biologiques" programme. Lille Génopôle received an unconditional grant from Eisai. The Three-city biological bank was developed and maintained by the laboratory for genomic analysis LAG-BRC - Institut Pasteur de Lille.

1.6 Genetic and Environmental Risk in AD (GERAD) Consortium

Genetic and Environmental Risk in AD (GERAD) Consortium/Defining Genetic, Polygenic, and Environmental Risk for Alzheimer's Disease (PERADES) Consortium

The GERAD/PERADES sample comprises 3,177 Alzheimer's disease cases and 7,277 controls with available age and gender data (PMID: 19734902). Cases and elderly screened controls were recruited by the Medical Research Council (MRC) Genetic Resource for Alzheimer's disease (Cardiff University; Institute of Psychiatry, London; Cambridge University; Trinity College Dublin), the Alzheimer's Research Trust (ART) Collaboration (University of Nottingham; University of Manchester; University of Southampton; University of Bristol; Queen's University Belfast; the Oxford Project to Investigate Memory and Ageing (OPTIMA), Oxford University); Washington University, St Louis, United States; MRC PRION Unit, University College London; London and the South East Region Alzheimer's disease project (LASER-AD), University College London; Competence Network of Dementia (CND) and Department of Psychiatry, University of Bonn, Germany; the National Institute of Mental Health (NIMH) Alzheimer's disease Genetics Initiative. 6129 population controls were drawn from large existing cohorts with available GWAS data, including the 1958 British Birth Cohort (1958BC) (http://www.b58cgene.sgul.ac.uk), the KORA F4 Study and the Heinz Nixdorf Recall Study. All Alzheimer's disease cases met criteria for either probable (NINCDS-ADRDA, DSM-IV) or definite (CERAD) Alzheimer's disease. All elderly controls were screened for dementia using the MMSE or ADAS-cog, were determined to be free from dementia at neuropathological examination or had a Braak score of 2.5 or lower. Genotypes from all cases and 4617 controls were previously included in the AD GWAS by Harold and colleagues (PMID: 19734902). Genotypes for the remaining 2660 population controls were obtained from WTCCC2.

We thank all individuals who participated in this study. Cardiff University was supported by the Wellcome Trust, Alzheimer's Society (AS; grant RF014/164), the Medical Research Council (MRC; grants G0801418/1, MR/K013041/1, MR/L023784/1), the European Joint Programme for Neurodegenerative Disease (JPND, grant MR/L501517/1), Alzheimer's Research UK (ARUK, grant ARUK-PG2014-1), Welsh Assembly Government (grant SGR544:CADR), a donation from the Moondance Charitable Foundation, UK Dementia's Platform (DPUK, reference MR/L023784/1), and the UK Dementia Research Institute at Cardiff. Cambridge University acknowledges support from the MRC. ARUK supported sample collections at the Kings College London, the South West Dementia Bank, Universities of Cambridge, Nottingham, Manchester and Belfast. King's College London was supported by the NIHR Biomedical Research Centre for Mental Health and Biomedical Research Unit for Dementia at the South London and Maudsley NHS Foundation Trust and Kings College London and the MRC. Alzheimer's Research UK (ARUK) and the Big Lottery Fund provided support to Nottingham University. Ulster Garden Villages, AS, ARUK, American Federation for Aging Research, NI R&D Office and the Royal College of Physicians/Dunhill Medical Trust provided support for Queen's University, Belfast. The University of Southampton acknowledges support from the AS. The MRC and Mercer's Institute for Research on Ageing supported the Trinity College group. DCR is a Wellcome Trust Principal Research fellow. The South West Dementia Brain Bank acknowledges support from Bristol Research into Alzheimer's and Care of the Elderly. The Charles Wolfson Charitable Trust supported the OPTIMA group. Washington University was funded by NIH grants, Barnes Jewish Foundation and the Charles and Joanne Knight Alzheimer's Research Initiative. Patient recruitment for the MRC Prion Unit/UCL Department of Neurodegenerative Disease collection was supported by the UCLH/UCL Biomedical Research Centre and their work was supported by the NIHR Queen Square Dementia BRU, the Alzheimer's Research UK and the Alzheimer's Society. LASER-AD was funded by Lundbeck SA. The AgeCoDe study group was supported by the German Federal Ministry for Education and Research grants 01 GI 0710, 01 GI 0712, 01 GI 0713, 01 GI 0714, 01 GI 0715, 01 GI 0716, 01 GI 0717. Genotyping of the Bonn case-control sample was funded by the German centre for Neurodegenerative Diseases (DZNE), Germany. The GERAD Consortium also used samples ascertained by the NIMH AD Genetics Initiative. HH was supported by a grant of the Katharina-Hardt-Foundation, Bad

Homburg vor der Höhe, Germany. The KORA F4 studies were financed by Helmholtz Zentrum München; German Research Center for Environmental Health; BMBF; German National Genome Research Network and the Munich Center of Health Sciences. The Heinz Nixdorf Recall cohort was funded by the Heinz Nixdorf Foundation (Dr. Jur. G.Schmidt, Chairman) and BMBF. We acknowledge use of genotype data from the 1958 Birth Cohort collection and National Blood Service, funded by the MRC and the Wellcome Trust which was genotyped by the Wellcome Trust Case Control Consortium and the Type-1 Diabetes Genetics Consortium, sponsored by the National Institute of Diabetes and Digestive and Kidney Diseases, National Institute of Allergy and Infectious Diseases, National Human Genome Research Institute, National Institute of Child Health and Human Development and Juvenile Diabetes Research Foundation International. The project is also supported through the following funding organisations under the aegis of JPND - www.jpnd.eu (United Kingdom, Medical Research Council (MR/L501529/1; MR/R024804/1) and Economic and Social Research Council (ES/L008238/1)) and through the Motor Neurone Disease Association. This study represents independent research part funded by the National Institute for Health Research (NIHR) Biomedical Research Centre at South London and Maudsley NHS Foundation Trust and King's College London. Prof Jens Wiltfang is supported by an Ilídio Pinho professorship and iBiMED (UID/BIM/04501/2013), at the University of Aveiro, Portugal.

1.7 Bonn studies

The Bonn group would like to thank Dr. Heike Koelsch for her scientific support.
The Bonn samples are part of the German Dementia Competence Network (DCN) and the German Research Network on Degenerative Dementia (KNDD, AgeCoDe study group), which are funded by the German Federal Ministry of Education and Research (BMBF): grants DCN: 01G10102, 01GI0420, 01GI0422, 01GI0423, 01GI0429, 01GI0431, 01GI0433, 04GI0434, 01GI0711; grants KNDD: 01GI1007A, 01GI0710, 01GI0711, 01GI0712, 01GI0713, 01GI0714, 01GI0715, 01GI0716, 01GI0717, 01ET1006B. Controls for the Bonn samples were also obtained from the Heinz Nixdorf Recall cohort that was funded by the Heinz Nixdorf Foundation (Dr. Jur. G.Schmidt, Chairman) and BMBF. Genotyping of the Bonn case-control sample was funded by the German Centre for Neurodegenerative Diseases (DZNE), Germany. Markus M Nöthen and Alfredo Ramirez are members of the German Research Foundation (DFG) cluster of excellence ImmunoSensation.

Bonn OMNI cohort: the Bonn OMNI cohort consists of AD patients and controls derived from a larger German GWAS cohort which was recruited from the following three sources: (i) the German Dementia Competence Network; (ii) the German study on Aging, Cognition, and Dementia in primary care patients (AgeCoDe); and (iii) the interdisciplinary Memory Clinic at the University Hospital of Bonn. The control sample comprised of individuals from the population-based study Heinz Nixdorf Recall (HNR) study cohort. This sample was previously used for replication in Lambert et al.[33]. *The German study on aging, cognition and dementia (AgeCoDe)*: see description above. *The German competence network cohort (DCN)*: The DCN cohort includes 1,095 patients with mild cognitive impairment (MCI) and 648 cases with mild Alzheimer's disease (AD) clinical dementia syndrome that were recruited from 14 university hospital memory clinics across Germany between 2003 and 2005[9]. Exclusion criteria were substance abuse or dependence, insufficient German language skills, multi-morbidity, comorbid condition with excess mortality, circumstances that would have made regular attendance at follow-up visits questionable and lack of an informant. The diagnosis of mild dementia according to ICD-10 criteria required a decline of cognitive ability (at least 1 SD) from a previous level in at least 2 domains as evidenced by age-corrected standardized tests, impairment in activities of daily living (i.e. B-ADL > 6), changes in personality, drive, social behavior or control of emotion but no clouding of consciousness. These changes must have persisted for at least 3 months. The etiological diagnosis of AD was assigned according to NINCDS-ADRDA criteria[8]. *Memory clinic Bonn*: The interdisciplinary Memory Clinic of the Department of Psychiatry and Department of Neurology at the University Hospital in Bonn provided further patients. Diagnoses were assigned according the NINCDS/ADRDA criteria[8] and on the basis of clinical history, physical examination, neuropsychological testing (using the CERAD neuropsychological battery, including the MMSE), laboratory assessments, and brain imaging. *Control sample:* In the Heinz Nixdorf Recall (Risk Factors, Evaluation of Coronary Calcification, and Lifestyle) study, participants were randomly sampled in three cities in Germany. The study design has previously been described[34,35]. Briefly, 4814 participants aged 45 to 75 years were enrolled between 2000 and 2003 (t0, baseline). Cognitive performance of participants was evaluated at follow up scheduled 5 years after baseline (t1, n = 4157, 2005–2008) and then again at follow up 5 years after t1 (t2, n = 3087, 2010–2015). Controls sample was selected if participant did not present cognitive

impairment as reported at the last available evaluation. Cognitive evaluation has been described extensively previously[36,37]. Herein, cognitive impairment at t1 was defined as a performance of one standard deviation (SD) below the age- and education-adjusted mean except for the clock-drawing test, where a performance ≥3 was rated as impaired (for a detailed description, see the study by Winkler et al.[36]). The study was approved by the University of Duisburg-Essen Institutional Review Board and followed established guidelines of good epidemiological practice.